SEPARATION, PRECONCENTRATION AND DETERMINATION OF RARE EARTH ELEMENTS BY INDUCTIVELY COUPLED PLASMA EMISSION SPECTROSCOPY

A thesis submitted to the
UNIVERSITY OF CAPE TOWN
in fulfilment of the requirements for the degree of
MASTER OF SCIENCE

by

R H CRACKNELL B.Sc. (Hons.) (Cape Town)

Department of Analytical Science
University of Cape Town
Rondebosch
7700
Republic of South Africa

January 1988

CONTENTS

ACKNOWLEDGEMENTS 1

1. ABSTRACT 2

2. INTRODUCTION 4

2.1 Determination of Rare Earths 5

2.2 Interferences 7

2.2.1 Effect of Easily Ionizable Elements 7

2.2.2 Matrix Effects 10

2.2.3 Spectral Interferences 12

2.3 Preconcentration Techniques 16

2.3.1 Ion-Exchange Separations 16

2.3.2 Liquid-Liquid Extraction Techniques 20

2.4 Decomposition Methods 25

2.5 Research Objectives 28

3. EXPERIMENTAL 29

3.1 Chemicals, Reagents and Glassware 29

3.2 Preparation of Standards 30

3.3 Operating Conditions used with the ICP 34

3.4 Decomposition Methods 37

3.5 Methods for Determination of REE in Rock Samples 38

4. RESULTS AND DISCUSSION 39

4.1 Spectroscopic Method Development 39

4.1.1 Optimization of ICP Parameters 39

4.1.1.1 Torch Power 40

4.1.1.2 Nebulizer Driving Pressure 43

4.1.1.3 Plasma Gas Flow Rates 48

4.1.1.4 Sample Aspiration Rate (Pump Rate) 48

4.1.1.5 Torch Observation Height 51

4.1.1.6 Pump Delay and Settling Time 53

4.1.1.7 Line Selection 54

4.1.1.8 Matrix and Calibration Effects 65

4.2 Optimization of Group Separation of the Rare Earth Elements from Matrix Elements 73

4.2.1 Chromatography 1 75

4.2.2 Chromatography 2 77

4.2.3 Chromatography 3 79

4.2.4 Chromatography 4 81

4.2.5 Chromatography 5 83

4.2 6 Chromatography 6 85

4.2.7 Chromatography 7 87

4.2.8 Chromatography 8 91

4.2.9 Chromatography 9 96

4.2.10 Chromatography 10 100

4.2.11 Chromatography 11 102

4.2.12 Chromatography 12 105

4.2.13 Chromatography 13 107

4.2.14 Chromatography 14 110

4.3 Determination of REE in NIM-G and SS-18 113

4.4 Liquid-Liquid Extraction of REE 119

4.4.1 Extraction with AcAc and MIBK 119

4.4.2 Extraction of REE using HHFA and HTPB with Quinoline in CCl_4 122

4.4.3 Extraction of REE with HHFA and Quinoline in $CHCl_3$ 124

4.5 Crystal Structures of 3.5-Diacetyl 1.4-Dihydro-2.6-Dimethyl Pyridine 127

5. CONCLUSIONS 149

APPENDICES

Appendix 1 151

Appendix 2 152

Appendix 3 153

Appendix 4 154

Appendix 5 156

Appendix 6 159

REFERENCES 168

ACKNOWLEDGEMENTS

I should sincerely like to thank

-my supervisor, Professor M J Orren, for his expert guidance and encouragement during the course of this work.

-Dr K R Koch for assistance and advice on spectroscopic analysis of Hexac and Hexsub, and use of the adapted microwave oven.

-Associate Professor J P Willis for advice and help with the final draft of this thesis.

-Tony Jutzen and Fred Smith for their ever willing and assistance in the laboratory.

-Lindsay for the many hours of proof reading and moral support.

-Mike for his assistance with the X-ray crystallographic analysis of Hexac and Hexsub and computer work.

-Marius and Dan for their assistance with the diagrams.

-Lynda and Anne for typing this thesis.

1. ABSTRACT

ABSTRACT

Rare earth elements, (REE), at ug g^{-1} levels are used for studies of petrogenisis of different geological materials. For these studies, the REE must be determined precisely.

An analytical program was established using an IL 200 Inductively Coupled Plasma, (ICP), spectrometer for the determination of the REE in various matrices, taking into consideration both matrix and spectral interferences, which were found to be severe in some cases.

Dissolution of the sample, (0.4-1.0 g), was carried out using two methods; a microwave heated dissolution using a modified commercial microwave oven and a conventional oven heated closed pressure digestion vessel method. The results of these two methods were compared to determine the viability of using the more rapid microwave heated method.

Separation of the REE from matrix elements was investigated using three cation exchange resins; Amberlite IR 120 (H), Zeocarb 225 and Dowex 50-W-X8. A gradient acid elution method was established using a 15 cm by 20 mm Zeocarb 225 column. The sample was eluted with 140 ml of a 1.5 M H^+ solution containing 0.75 M Cl^- and 0.75 M NO_3^-, this fraction containing all the matrix elements. The REE were then eluted from the resin with 100 ml of 3 M HNO_3. The REE containing fraction was then reduced to 5 ml, diluted to 10 ml, and analysed for REE content.

Liquid-liquid extraction methods for the separation of REE from matrix elements were investigated. It was found that the REE could be extracted synergistically from various buffered aqueous acidic media into chloroform, ($CHCl_3$), by hexafluoroacetylacetone, (HHFA), and quinoline.

Acetylacetone, (AcAc), was found to react with hexamethylenetetramine, (hexamine), when hexamine was used to buffer the aqueous phase during extraction procedures. The product of this reaction, 3.5-diacetyl-1.4-dihydro-2.6-dimethyl pyridine, was identified using X-ray crystallography.

2. INTRODUCTION

CHAPTER 2

2. INTRODUCTION

The Rare Earth Elements (REE) trace their origin to the accidental discovery by a Swedish Army Lieutenant, C A Arrhenius, of an unusual black mineral specimen in a quarry at Ytterby in Stockholm in 1787. In 1794 Johan Gadolin, a Finnish chemist at the University of Abo separated 38% of a previously undescribed "earth" (an oxide) from samples of this mineral, and thus set a basis for a series of investigations that continue to the present [1].

REE are all predominantly trivalent, and have closely similar chemical properties, showing a progressive decrease in ionic radii from 1,04 Å for La^{3+} to 0,861 Å for Lu^{3+}. This leads to preferential uptake by some minerals of the heavy REE relative to light REE, or vice-versa, while the predominantly trivalent Ce^{3+} may be oxidized to Ce^{4+} and Eu^{3+} reduced to Eu^{2+}. Jarvis and Jarvis concluded that this chemical behaviour could, potentially, prove a valuable guide to the mineralogical and diagenic history of sedimentary rocks [2]. Early workers, Goldberg *et al* [3], Haskin and Haskin [4], and Haskin *et al* [5], have emphasised similarities in REE distributions of different lithologies, and between samples of different areas from different ages. Wildeman and Haskin [6], and McLennan *et al* [7,8] have studied precambian sediments and demonstrated that they display small but significant differences in stratigraphical trends, which have been used to

elucidate the chemical evolution of the earths crust.

Fassel [9], and Dalvi *et al* [10] state that the analysis of the REE has become important in the nuclear industry, as products of the fission reactions of plutonium and uranium include rare earths which have a detrimental effect on the propogation of the chain reaction. Olmez and Gordon [11] have reported the analysis of REE on fine airborne particles, and found REE concentrations to be distorted from crustal abundance patterns in areas influenced by emissions from oil-fired plants, largely due to the presence of REE in zeolite catalysts used in oil refining. These rare earth ratios are used to determine movement and histories of various air masses.

2.1 DETERMINATION OF RARE EARTHS

Many instrumental methods have been employed for the determination of REE. These include neutron activation analysis [11 - 15], atomic absorption spectroscopy [16,17], optical fluorescent spectroscopy [18,19], X-ray fluorescence spectroscopy [20,21], capacitively coupled microwave plasma optical emission spectroscopy [22], direct current plasma atomic emmission spectroscopy [10,23,24], ultraviolet spectrophotometry [25 - 28], infra-red spectroscopy [29], osmometry [30], densitometry [31] and adsorptive stripping voltametry [32]. Other methods of analysis include inductively

coupled plasma source mass spectrometry [33 - 37], inductively coupled plasma excited ionic fluorescent spectroscopy [100] and inductively coupled plasma optical emission spectroscopy (ICP OES) [2,38-52].

In general the spectroscopic determination of REE in geological samples is a complex problem. Although neutron activation analysis and isotope dilution procedures [53] yield excellent precision, both methods are tedious and time consuming [54] and few laboratories possess the necessary analytical equipment. ICP - OES is suitable for the analysis of the rare earths due to the sensitivity of the method, speed, and multi-element capability. Problems encountered with analysis include:

1) Low concentration of REE in some matrices, necessitating sample preconcentration.

2) High relative concentrations of major matrix elements such as Al, Fe, Mg, Mn, Na, K, Ca, Si, Ti and Zr which frequently give rise to spectral inteferences.

3) A lack of "accepted" values of analyte concentrations present in standard rocks for REE [55].

These limitations in the analysis of REE may be overcome to some extent by some form of sample pretreatment before analysis. However, lengthy sample pretreatment procedures may severely limit sample through-put, a major consideration for laboratories involved in high volume routine

analysis [55]. Methods of pretreatment include cation-exchange chromatography [12,21,54-60] anion-exchange chromatography [19,61,62] thin layer chromatography [31], precipitation [17,63] and solvent extraction [10,14,15,24-28,30,64-71].

2.2 INTERFERENCES

2.2.1 EFFECT OF EASILY IONIZABLE ELEMENTS

A literature survey of the study of effects of excess of an easily ionizable element (EIE) such as Na, K or Cs as concomitant on analyte emission intensity is a study in confusion. Virtually every spectroscopist has studied the effect of this matrix, as they exist in almost every type of matrix that is likely to be analysed, including animal and plant materials, seawater and geological materials [72]. In analytical flame spectroscopy the effect has been well charcterised, and depends upon whether an atom or ion line has been chosen for analysis. Differences may be rationalised on the basis of a shift in the ionization equilibrium of the analyte (A),

$$A \rightleftharpoons A^{+} + e^{-}$$

An increase in electron density causes a shift towards the neutral atom, enhancing atom line emission or absorption [73], the magnitude of the effect being related to the ionization potential of the EIE [74] in the sequence:

Cs > Rb > K > Na > Sr > Li > Mg, etc.

The opposite effect is observed in the arc discharge source, where increased electron density increases conductivity, and hence a reduction in arc temperature, causing longer analyte resident times as described by Boumans [75].

Observations by Boumans [76] and Larson [77] have shown that the magnitude of the effect of EIEs in a plasma source is a function of the power, and a change in aerosol flow rate while Kornblum and De Galan [78] noticed changes in the influence of EIEs with changes in viewing heights. Boumans and De Boer [79], were able to separate the effects of EIEs into "nebulizer" or "desolvation" effects and "plasma effects", where plasma effects were found to cause a greater deviation in expected analyte emission intensity. General trends are difficult to determine with a wide variation in operating conditions as noted by Boumans [80]: "It has also become apparent that certain interferences can be deliberately evoked or surpressed by varying the analytical parameters, and that inconsistencies in the results can show up owing to very small changes in the analytical parameters of the ICP and in the critical variables of the torch." Possible mechanisms for the observed effects of EIEs on analyte emission intensity have been proposed by Blades and Horlick [72], and include:

1) Shifts in ionization equilibria.

2) Enhanced collision excitation.

3) Volatilization effects.

4) Ambipolar effects (the diffusion of charged

particles under the influence of an electric field).

5) Nebulizer effects.

These authors also noted that more than one of these mechanisms may occur in different regions of the plasma, where the influence of an EIE may cause enhancement in the lower regions of the plasma, but depression of analyte emission in higher regions of the plasma [72]. These effects were found to vary depending upon the type of analyte line emission under investigation [81].

In addition, Prell *et al* [82] established that effects of EIEs low in the ICP are due primarily to increased excitation, not atom formation. They proposed that since the analyte is normally present at low concentrations, it creates few ions and electrons, and has little interaction with the plasma, except by thermal excitation. However, addition of EIEs, a source of low energy electrons, increased exchange of these electrons with toroid electrons into the central channel of the plasma, increasing analyte excitation. Matousek *et al* [83] have studied the interferences due to EIE in a microwave induced plasma system and reported that enhancement or suppression of the analyte line emission is dependant upon the type of line used. They found that the EIE phenomena resulted from a combination of causes, some related to processes of volatilization and others from excitation processes. Skogerboe and Butcher [84] observed a difference in the size of droplets found when solutions of analyte and

concomitant EIE were aspirated separately or together. This would lead to variations in aerosol transport efficiencies, vapourization characteristics and spatial distributions of atom concentrations in the light path.

2.2.2 MATRIX EFFECTS

Greenfield *et al* [85] have studied the effects of acid concentration on net intensities obtained for solutions of Ni, Fe, Co, Cr and Cu in various organic and inorganic acids, and in methanol using a high power plasma source. Generally, acid viscosity changes produced the largest effect on net signal intensity. As the concentration of the acid is increased, the viscosity of the acid is increased, droplet formation mechanisms alter, and the nebulization yield is reduced, affecting net signal intensity. Changes in droplet size produced by the nebulizer have the following effects:

1) Larger drops; more material is lost to the drain.

2) With lower power, some of the drops may not be completely evaporated during their passage through the plasma.

Increasing acid or salt concentrations [85,86] usually results in a lowering of analyte emission intensity. However, solution viscosity and density cannot be the only factors contributing to acid or salt matrix interferences as the effect does not disappear in force-fed low power ICPs [86]. To overcome some of the problems associated

with complex matrices, Botto [87] has proposed the use of a hydrogen emission line, the intensity of which is dependant upon sample introduction rate, as well as the acid or salt concentration. This allows the use of a single set of dilute acid calibration standards, and reduces the need for matrix matched standards, especially if little is known about the sample matrix.

Boumans and De Boer [76] and Broekaert *et al* [88] have investigated the influence of high concentrations of other matrix concomitants likely to be present in samples after decomposition. Broekaert *et al* [88] reported the influence of sodium tetraborate on net emission intensities of the REE was minimised when aerosol gas flow rate was adjusted to give maximum net line intensity. The overall matrix effects due to $Na_2B_4O_7$ were mainly nebulizer effects. Also, high concentrations of alkali metal salts may influence the excitation behaviour of the analyte in the ICP, the degree of influence depending upon the operating conditions chosen. Introducing large amounts of $Na_2B_4O_7$ was found to reduce the excitation temperature of the plasma, hence reducing ion concentration, hence the degree of excitation. Broekaert *et al* [88] also observed that decreases in the emission intensity of EuII (420,5 nm) is mainly due to borate anions and their dissociation products, when comparing effects of $Na_2B_4O_7$ only, with a mixture of $Na_2B_4O_7$ and H_3BO_3, keeping total concentrations of added interferents equivalent. Brenner *et al* [40] noted that substitution of Li for Na in preparation of a standard reference material gave analytical results for REE within experimental error for

those obtained with Na. Ni-Chung *et al* [47] noted that the presence of a large excess of Y_2O_3 in the matrix caused depression of impurity line emission intensities requiring the preparation of matrix matched standards.

2.2.3 SPECTRAL INTERFERENCES

Larson and Fassel [89] have reported that spectral line broadening and radiative ion-electron recombination processes make significant contributions to spectral background levels. These are more easily identified in ICP sources due to the relatively small effects of analyte concomitants on net intensities, and the relatively stable background found in ICP sources. Wings of collisionally broadened peaks may be found at wavelengths some 10 nm from the parent line centre. They also found that for concentrations of 2500 µg cm^{-3} Al, radiative ion-electron recombination may increase backgrounds tenfold over the wavelengths 193 nm to 210 nm. Larson *et al* [90], have also studied the problems of stray light when determination of analytes close to their detection limits is required, as spectral background will be a large fraction of the measured signal. Stray light may cause large shifts in background intensity, depending upon the composition of the sample matrix. For example, with Ca and Al, where the shift in Al background at 394.40 nm and 396.15 nm in close proximity to the sensitive ion lines of Ca at 393.37 nm and 396.85 nm, upward shifts in the background under both Al lines is related to the increase in Ca concentration, and may be due to grating defects

producing near scatter, far scatter and ghosts, as well as defects in spectrometer design.

The most common problem found in the analysis of trace and ultra-trace elements in a complex matrix, is the degree and complexity of spectral interferences. Since most elements, especially REE in hot sources have many emission lines, it is usually possible to select an alternative line. However, one is often forced to trade sensitivity for precision [46,91]. Botto [92] proposed a dual spectrometer system, attaching two spectrometers to a single ICP. In this case one spectrometer was set up for simultaneous analysis, the other for simultaneous or manually controlled single element wavelength scans. The spectrometers were also of different resolutions. Since both spectrometers observed the same ICP source, a comparison of their spectral interference characteristics was possible. Botto found that they were not the same. Thus detection limits and degrees of spectral interference varied for each monochromator. The detection limits for REE in geological matrices depend on several factors:

1) Instrument sensitivity.

2) Instrument stability.

3) Reproducibility of sample preparation.

4) Dilution factors.

5) Matrix interferences.

The precision and accuracy of results obtained would also depend upon the amount of spectral

interference from concomitant emission. As spectral interference corrections are subject to error, there will always be some error introduced in determinations employing such techniques [55]. Forster *et al* [93] have characterised the argon spectrum between 2075 Å and 6005 Å with a view to clarifying some possible spectral interferences and identifying peaks to Ar rather that OH transitions. Anderson *et al* [94] classified the spectra of the alkaline earth elements noting variations in the type of spectra emitted when comparing DC arc derived spectra with ICP derived spectra. Farwell and Kagel [95] used an empirical line width ratio technique to detect spectral overlap while Burton and Blades [96] developed method of computer simulation of emission from analyte atoms and ions excited in the ICP to model potential spectral interferences from sample matrices of varying complexity. Boumans and Vrakking [97-99] have undertaken a number of studies of spectral interferences with "medium resolution" and "high resolution" monochromator conditions. They found that increasing practical resolving power generally increased the selectivity as a result of improved separation of analyte signal from those of interferents hence reducing "limits of determination." Thus lines which may not be acceptable for analytical use at medium resolution due to interferences may become acceptable at high resolution. However, this is complicated by changes in line profiles at high resolution due to different interactions of analyte concomitants in different matrices [97]. Problems may also be encountered with a high resolution spectrometer with the positioning of the grating, as small movements of the grating

will introduce errors in analysis [98]. The presence of OH emission bands is also a source of spectral interference [93] but an assessment of the degree of interference depends upon the relative line intensities, signal to background ratios of the OH band components, and the operating conditions of the ICP. A list of prominent lines which suffer from OH spectral overlap has appeared [99]. Spectral interferences were observed in the analysis of REE by a number of authors [2,38-41,43-49,55]. Of these, Iwasaki [45] compiled a list of concomitant REE interferences that were observed while analysing monazites and xenotimes.

Choot and Horlick [101-104] have recently undertaken a detailed study of mixed gas plasmas including Ar-N_2, Ar-O_2, Ar-Air and Ar-He mixtures. These plasmas have the advantage of reducing running costs, while expanding the overall capability of the ICP. Most of the mixed gas plasmas showed superior signal to noise ratios with 10% foreign gas: 90% argon used as the coolant gas, but this was found to be dependant upon observation heights [102]. Interferences are also found to exist in these plasmas, the effects being dependant upon concentration of interferent and observation height [103]. Analyte emission signals are found to increase in 10% foreign gas: 90% argon plasmas, indicating that mixed gas plasmas are more energetic than conventional argon plasma discharges [104].

Methods have been reported by Belchamber *et al* [105], Moore *et al* [106], Smith *et al* [107] and Werner and Friege [108] to remove matrix interferences by Simplex optimisation. This iterative process maximizes instrument parameters such as observation height, RF power, nebulizer pressure and argon flow rates. As a variety of working parameters need to be optimized these working conditions will lead to a compromise set of analytical conditions producing the best possible results. Belchamber *et al* [105] were able to remove matrix effects from most of their analytical lines without loss of sensitivity.

It is apparent that analysis of materials by ICP is complicated by a number of problems. However, it is an extremely powerful technique capable of producing high quality analytical data.

2.3 PRECONCENTRATION TECHNIQUES

2.3.1 ION-EXCHANGE SEPARATIONS

An increasing demand is being made for the analysis of REE in geological matrices at relatively low concentrations (chondritic levels) for studies in petrogenisis [55]. In general, determinations of REE in geological materials are characterised by complicating features discussed previously [55]. Preconcentration is thus almost always necessary. Ion-exchange separation and preconcentration procedures have the following advantages:

1) The total salt content of the solution is reduced, decreasing viscosity, which allows better nebulization characteristics and reduces memory effects in subsequent atomic spectroscopic determinations.

2) Separation reduces the total number of elements present thus minimising spectral interferences and so called matrix effects.

3) Detection limits of REE are usually reduced [55].

Extensive studies by Crock *et al* [58] show that it is possible to use both nitric acid and hydrochloric acid as eluents in gradient elution chromatography. They showed that quantitative recovery of all REE (and Y) was possible from a cation exchange resin eluted with 8 M nitric acid or 8 M hydrochloric acid. Major differences were observed in behaviour of the light REE, (represented by La and Ce), iron and the alkali earth metals. With elution using 8 M hydrochloric acid, elution patterns of light and heavy REE differed considerably while with 8 M nitric acid elution patterns of light and heavy REE were similar. Using gradient elution with hydrochloric acid both strontium and barium were found to elute with the REE but with nitric acid gradient elution this did not occur. A comparison of elution patterns with selected transition elements and aluminium shows that iron is eluted with the rare earth fractions when nitric acid is the eluent but is eluted with the transition elements when hydrochloric acid is the eluent. Zirconium was found to elute with the REE with both acids [58]. In a subsequent publication Crock *et al* [57] used

a gradient elution procedure using a combination of hydrochloric and nitric acids to separate the REE from the matrix. This has the advantage of removing iron from the REE fraction (using only nitric acid) as well as reducing the total volume of eluate required to carry out the separation, allowing increased sample though-put and a reduction in reagent blank. However, both strontium and barium were still eluted with the REE fractions [57]. Jarvis and Jarvis [2], Eby [21], Crock and Lichte [54], Brenner *et al* [40,56] and Walsh *et al* [60] have described methods using cation exchange separation and preconcentration using Dowex 50-W-X8 cation exchangers, while Crock and Lichte [54] used a second preconcentration step involving an anion exchange process to remove iron from the cation exchange eluates.

Korkish *et al* [109] have suggested various nitric acid-alcohol systems to separate the REE from less sorbable elements. Fritz and Greene [61] have reported separation of the REE from bismuth, lead and thorium using a nitrate form anion exchange resin and eluting with 1.5 M nitric acid in 85% isopropyl alcohol. With Amberlyst XN-1002, a highly porous anion exchange resin, better separations were obtained and equilibrium was reached more rapidly when compared with Dowex 1-X8 (100-200 mesh) resin. However, the distribution coefficient decreased with increasing atomic number of the REE, and hence poorer separations were achieved for the heavy REE. This was related to sample size, (amount of REE in solution), and the loading of the column. Jangida *et al* [62] reported a phosphate interference, due to low

solubilities of rare earth phosphates, and prior separation of phosphate ion was necessary. Metal ions were separated from phosphate on activated alumina, eluting with 2 M nitric acid. Roelandts [19] employed the strongly basic anion exchanger Dowex 1-X8 using a 95% methanol - 5% 7 M nitric acid (V/V) solution to carry the REE onto the resin bed. He found that the capacity for lanthanum was about 25 mg g^{-1} of resin, and therefore, the amount of REE that could be separated should not be more than 0.5 mequiv.

Miyazaki and Barnes [59] have reported the use of a poly(dithiocarbamate) chelating resin to preconcentrate the rare earth elements. Since alkali and alkali earth elements do not complex with this resin, separation of electrolytes and EIEs was achieved. The loaded resin was digested in 90% (V/V) 1:1 nitric acid-sulphuric acid, avoiding any precipitation due to hydrolysis of the resin. However, detection limits for metals in this digestate are poorer than those obtained with water or dilute nitric acid due to the increased viscosity of the solution causing poorer nebulization characteristics. Alternatively, the resin may be digested in successive amounts in concentrated nitric acid until a clear solution is obtained, followed by dilution with (3 + 1) nitric acid-water to appropriate volume. Optimum uptake of REE onto the resin was found to occur between pH 4 and pH 6. This method was found to work well with single and binary rare earth solutions, but no experiments were carried out with rock digestates. Hirose *et al* [12] have employed Chelex-100 to preconcentrate the REE and heavy

metals by selective elution, the REE being eluted with hot 1 M sodium carbonate and the heavy metals with 2 M nitric acid. Horvath and Barnes [110] have prepared and used a carboxymethylated polyethylenimine - polymethylenepolyphenylene isocyanate (CPPI) chelating resin. Rare earths could be extracted from solution between pH 5 and 8 in the presence of high salt containing matrices, and could be eluted with dilute strong acids such as 2 M HNO_3. CPPI is not as good a chelating resin as poly(dithiocarbamate) resins but does not need to be digested to return the loaded metals to solution. Huff [111] reported the use of neutral phosphorous chelators adsorbed onto a stationary phase to separate and preconcentrate REE, which are eluted from the column using 8.2 M HNO_3 with recoveries between 96.5% and 102.4%. Fuxing *et al* [112] have also carried out separations of REE with neutral organophosphorous chelators using reversed phase partition chromatography with 3 M HNO_3 as the medium. Merciny [113] described separation of REE into two groups based on decomplexation rates of LnDOTA (DOTA = 1,4,7,10 Tetraazocyclododecane N. N′.N″.N‴- tetraacetic acid) moieties attached to a sulphonate cation exchange column, while Massart and Bossaert [114] and Powell and Burkholder [115] have studied separations of individual rare earths.

2.3.2 LIQUID-LIQUID EXTRACTION TECHNIQUES

Woo *et al* [29] observed that synergistic extraction of several rare earths occured into an organic phase of thenoyltrifluoroacetylacetone,

$C_4H_3SCOCH_2COCF_3$ (HTTA) and acetylacetone, $CH_3COCH_2COCH_3$ (HAcAc) in benzene. The authors were able to identify the species $M(TTA)_3$ HAcAc, a mixed β-diketone chelate. This species is responsible for the synergistic extraction of rare earths with systems containing both HTTA and HAcAc. It is assumed that a mixed complex species is formed with M^{3+}, the overall distribution of the metal ion being given by the equilibrium:

$$M^{3+}_{(aq)} + aHTTA_{(o)} + bHAcAc_{(o)} \rightleftharpoons (MTTA_aAcAc_b)_{(o)} + cH^+_{(aq)}$$

where M^{3+} represents the rare earth metal ion and $MTTA_a$ $AcAc_b$ the mixed complex. Assuming that this is the only significant species formed by MTTA and HAcAc with the metal ion, the mixed equilibrium constant for the distribution is:

$$K^*_{ab} = \frac{[MTTA_a\ AcAc_b]_{(o)}[H+]^c_{(aq)}}{[M^{3+}]_{(aq)}\ [HTTA]^a_{(o)}[HAcAc]^b_{(o)}}$$

The distribution ratio D is assumed to be:

$$D = \frac{[MTTA_aAcAc_b]_{(o)}}{[M^{3+}]_{(aq)}}$$

then:

$$\log D = \log K^*_{ab} + a\log [MTTA]^a_{(o)} + b\log [HAcAc]_{(o)} - c\log [H^+]$$

and if the MTTA concentration and the pH of the aqueous phase is held constant:

$$\log D = b\log [HAcAc]_{(o)} + C$$

where $C = \log K^*_{ab} + a\log [MTTA]^a_{(o)} + c\log [H^+]$

A curve of slope b gives the formula of the mixed complex formed. The authors [29] found that with

various concentrations of MTTA, HAcAc and H^+, linear portions of curves plotted gave the dependance of extraction of europium on the first power of HAcAc and the third power of MTTA and H^+. The formation of the synergistic species is represented by:

$$Eu^{3+} + 3\ HTTA_{(o)} + HAcAc_{(o)} \rightleftharpoons EuTTA_3.HAcAc_{(o)} + 3H^+$$

Sekine and Dyrssen [68-71] also observed synergistic extraction of rare earths with addition of a neutral adduct forming ligand and chelating acids. They investigated the influence of methyl isobutyl ketone (Hexone) and tributylphosphate on extraction of chelate complexes of europium and thenoyltrifluoroacetyl-acetone and β-isopropyltropolone (IPT) [68]. In a separate publication [69] they found that the addition of neutral ligands enhanced the extraction of the EuIII - TTA into chloroform or carbon tetrachloride in the order: trioctylphosphine oxide > tributylphosphate > quinoline > coumarin > hexone > α-naphthol. They also studied the extraction behaviour of La^{3+}, Lu^{3+} and Sc^{3+} [70] while they observed that more than one mixed chelate species could be formed during the extraction process [71]. Mitchell and Banks [27] conducted an investigation into extraction of REE by fluorinated β-diketones which could be employed in inorganic gas liquid chromatography (GLC). They noted that the use of hexafluoro-acetylacetone, $CF_3COCH_2COCF_3$ (HHFA), as a solvent extraction agent is limited as extraction was reduced with increasing basicity of the rare earth cation. However with tributyl phosphate (TBP) and HHFA they achieved 98-100% extraction of the cation provided the ratio of TBP to HHFA was not

greater than 4:1. The effect of excess synergistic agents, which produces an antisynergistic effect on extraction has been studied by Healy *et al* [116]. They found that this was related to the water content of the organic phase and the destruction of the $M(TTA)_x.S_y$ anhydrous synergic species as water entered the complex, S being a neutral organophosphorous ester. Healy and Ferraro [64] noted that the extracted $REE(TTA)_x.S_y$ complexes remained as oils in the organic phase and did not solidify. Alstad *et al* [14] using methods described by Sekine and Dyrssen [68-71] obtained varying degrees of extraction for all the rare earths, and noted that their results differed from those of Pierce and Peck [117]. They proposed that these differences may be attribtued to fluctuations in the ionic strength of the aqueous medium which would effect the degree of extraction.

Du Preez and Preston [30] studied the influence of organophosphorous chelate structure on the extraction of REE from an aqueous nitrate media. They found that the electron density around the oxygen governed the degree of extraction, the greater the electron density the greater the degree of extraction, reaching a maximum with trialkylphosphine oxide reagents. Flavelle and Westland [24] employed a combination of solvent extraction with Alamine 336 and cation exchange chromatography while Khopkar and Mathur [67] studied extraction of REE with HTTA and Aliquat-336-S. Manchanda and Chang [26], Tang and Wai [15] and Preston [118] have studied extraction

with carboxylic acid based extractants, as alternatives to more established methods. Macrocyclic ligands described, [26], do not necessarily follow expected chemical behaviour in terms of extraction efficiencies, due to different mechanisms of extraction for the light REE and heavy REE. This was proposed as a possible method for separating the REE into various groups based on their different rates of reaction between the aqueous and organic phase.

Nebulization of organic solvents may be used in analytical spectroscopy in two ways: firstly, after solvent extraction procedures and secondly, when water soluble organics are to be analysed [119]. Botto [120] has outlined qualities of suitable organic solvents for ICP analysis, these include:

1) Ability to solubilise the entire sample.

2) Ability to form stable solutions and standards.

3) Low or moderate viscosity and volatility.

4) Little or no metal impurities.

5) Low toxicity.

6) Acceptable cost and availability.

Cresser [121] has published a review of theoretical aspects of organic solvent enhancement in atomic spectroscopy. Enhancement effects may be due to :

1) Differences in viscosity (relative to water) caused changes in aspiration rate and droplet size distribution.

2) Reduction in droplet size improved aerosol transport efficiency, desolvation and atomisation rates.

3) Increased solvent volatility increases nebulization efficiency.

4) Temperature effects.

5) Free radical effects (limited).

6) Atomizer geometry effects (limited).

Boorn and Browner [122] studied the effects of a number of organic solvents on ICP operating conditions. The authors noted that conditions will vary greatly depending upon the solvent and solvent volatility. Broekaert *et al* [123] analysed various metals in lubricating oils diluted with xylene, and directly aspirated into the ICP. Precision and detection limits were comparable with those produced using aqueous ICP analysis. Recent technological advances by Ng *et al* [124] and Nygaard *et al* [125] have increased the feasibility of analysis of organic solutions by ICP.

2.4 DECOMPOSITION METHODS

A number of different methods have been reported for dissolution of the rock matrix. The method

employed depends upon the rock type and the expected concentrations of elements to be determined. A lithium metaborate fusion method was proposed by Walsh [49] based on the original method introduced by Suhr and Ingamells [126]. However, problems may be encountered with this method: firstly, incomplete attack of refractory materials in the rock, and secondly, failure to produce a stable solution due to the formation of unstable colloidal silica suspensions. Walsh [49] proposes a second method of attack modified from Riley [127] involving hydrofluoric and perchloric acid attack. This allows preparation of more concentrated solutions due to removal of silica, a major rock component, as the volatile tetrafluoride. Casetta *et al* [128] used a teflon lined pressure digestion vessel technique using a mixture of HF, HNO_3 and HCl. Fries *et al* [43] preferred a dissolution procedure using polycarbonate bottles with different acid ratios to those of Casetta [128] to a digestion bomb method as residues formed by the later had to be removed by addition of 30% H_2O_2. Floyd *et al* [44] used a sodium hydroxide fusion method, the cooled fusion melt dissolved with concentrated HCl and diluted, with any hydrated silicon oxide formed centrifuged out. Brenner *et al* [40] have employed a number of dissolution procedures based on the expected concentrations of REE and the type of material to be dissolved. These included fusions with $LiBO_2$ or Na_2O_2 or acid attack with $HClO_4$ and HF. Bernas [16] developed a method for decomposition of silicates in a digestion bomb involving primarily hydrofluoric acid attack at 110°C for 40 minutes. Hartstein *et al* [129] used a similar vessel to digest coal samples with

fuming HNO_3, followed by attack with HF. Langmyhr and co-workers [130-132] have described methods of direct attack on silicate materials by HF. However, certain elemental fluorides were found to precipitate from solution [131] and these may be resolubilized by addition of a large volume of saturated boric acid [132].

Microwave heating has only recently gained acceptance in sample dissolution procedures due to a number of disadvantages, as reported by Jassie and Kingston [133]. These include development of vessels capable of withstanding the pressures involved, a fear of microwaves, and a lack of accepted procedures for analysis of a variety of trace elements. However, advantages of the method include:

1) More rapid dissolution.

2) More complete digestion.

3) Lower reagent blanks.

4) Multiple simultaneous sample preparation.

5) Determination of volatile elements is feasible.

Lamothe *et al* [134] noted that recoveries of 95% were obtained for most elements except when refractory mineral phases are present. However, as much as 100 samples could be prepared per day, while Nadkarni [135] reported complete sample dissolutions in three minutes. Fischer [136] notes that the nature of microwave heating facilitates attack of the sample matrix by the

acid, and when dissolution is carried out in pressurised containers, a reduced volume of high purity acid is required.

2.5 RESEARCH OBJECTIVES

Since the importance of REE analysis is increasing, both in the geochemical and nuclear fields, it was decided that there was a need to establish methods for analysis of REE. Objectives of this research project include:

1) To establish a working instrumental method using the IL 200 ICP with a view to optimising analytical conditions and minimising all possible spectral interferences.

2) To separate and preconcentrate the REE from a rock matrix, either by liquid-liquid extraction techniques or by ion-exchange chromatography, to reduce the number of analyte concomitants in ICP analysis, thus limiting the need for spectral interference corrections.

3) To establish a viable method for decomposing the rock matrix, either by 'conventional' or microwave heated dissolution techniques.

4) To analyse a number of rock matrices to check the applicability of the method.

3. EXPERIMENTAL

CHAPTER 3

3. EXPERIMENTAL

3.1 CHEMICALS, REAGENTS AND GLASSWARE

All chemicals and reagents used for experimental work were analytically pure. All rare earth oxides, 99.9% and 99.99% pure were obtained from Johnson Matthey Chemicals, England. Lanthanum and cerium nitrates were obtained from BDH Chemicals, England. HNO_3, HCl, HF, $HCLO_4$ and H_3BO_3 were obtained from E Merck Darmstadt. Ion-exchange resins, Amberlite IR 120 (H), (17-42 mesh) from BDH chemicals, Zeocarb 225 SRC 16 (200 mesh) from Permutit Chemicals, England and Dowex 50-W-X8 from Biorad laboratories were used in chromatographic experiments.

Hexafluoroacetylacetone, (HHFA), thenoyltrifluoro-acetylacetone, (HTFA), were obtained from Aldrich Chemicals, 2.2.6.6-tetramethyl-3.5-heptadione, 4.4.4-trifluoro-1-phenyl-1.3-butadione, (HTPB), were obtained from Sigma Chemicals, acetylacetone (AcAc), methyl isobutyl ketone (Hexone or MIBK), chloroform and carbon tetrachloride were obtained from E Merck Darmstadt. Quinoline, 8-hydroxyquinoline, tri-n-butyl phosphate and pyridine were obtained from BDH Chemicals and hexamethylenetetramine (Hexamine) from May and Baker Chemicals England.

Spectroscopically pure argon for the ICP was obtained from Air Products, Cape Town. High purity Milli-Q water was used throughout the experimental work for dilution purposes, in the preparation of standards, solvent extraction experiments, and column chromatography.

Glassware used in all preparations was B grade glassware. Columns used in chromatographic experiments were made of pyrex glass tubing of 20 mm internal diameter, fitted with a teflon tap and a number four glass sinter to act as a stationary phase support. Separation funnels used were all 100 cm^3 pyrex funnels fitted with teflon taps.

All glassware was cleaned by first soaking in a solution of 5% (v/v) contrad solution for at least four hours, followed by rinsing with distilled water, and then transfered to a 10% (v/v) nitric acid bath for one hour. All glassware was then rinsed twice with distilled water and twice with Milli-Q water before use.

3.2 PREPARATION OF STANDARDS

Rare earth oxides were used to prepare stock solutions of approximately 1000 ppm, except for cerium and lanthanum, where an additional standard was prepared from the nitrate. Most rare earth oxides exist only in the form Ln_2O_3, but there are exceptions to this with cerium, terbium and praesodymium [138]. Terbium forms oxides Tb_2O_3 and Tb_4O_7 while praesodymium forms oxides Pr_2O_3 and Pr_8O_{11}. Since not all oxides are stoichiometric, and are hydrophilic at room temperature, (see Table 3.1), it was decided to standardize all rare earth stock solutions chemically.

TABLE 3.1. Weight Variations of Selected Rare Earth Oxides Depending on Drying Method.

ELEMENT	WEIGHT[a] (g)	90 min[b]	5 day[c]	5 day[d]
Gd	0.1154	0.1109	0.1166	0.1128
Ho	0.1145	0.1130	0.1164	0.1144
Dy	0.1148	0.1093	0.1153	0.1135
Nd	0.1164	0.1134	0.1179	0.1158

a) Calculated weights to prepare a 1000 ppm stock solution from the oxide.

b) Weight of standard oxides after 90 minutes in an oven at 130° C followed by immediate weighing.

c) Weight of standard oxides after 5 days at 130° C followed by a 20 minute cooling period before weighing.

d) Weight of standard oxides after 5 days at 130° C followed by immediate weighing.

These weight variations due to the uptake of water and possibly CO_2 by the oxides made accurate standard preparation difficult. Following a method used by Lyle and Rahman [139], the stock solutions were standardized by titration with 0.001 M ethylenediamine tetracetic acid, (EDTA). The EDTA was first standardized using a solution of 0.001 M $MgSO_4.7H_2O$ using eriochrome black T as the indicator at pH 10. The rare earth solutions were then titrated with the standardized EDTA solutions

using xylenol orange as the indicator, with the addition of 4 g of hexamine as buffer. Concentrations of standards are given in appendix 1.

Synthetic rock solutions were prepared to match expected dissolution concentrations of REE and concomitants. All non-REE standards were prepared from 1000 ppm BDH 'spectrosol' standards. 100 ppm solutions of Si, Ca, Al, Fe, Cu, Zr, Na, K, Sr, Cr, Mn, Mg, Ba amd Zn were prepared as well as 50 ppm solutions of Ni, V and W. These solutions along with a series of REE standards of approximately 10 ppm were used to check potential spectral interferences between analytes and concomitants. A number of synthetic rock digests were prepared and used to verify line selection for REE. Concentrations of elements in these solutions is given in Appendix 2.

Matrix effects were found to be severe in analysis and two methods of separation and concentration of analytes were attempted; ion-exchange chromatography and liquid-liquid extraction techniques. Methods for chromatographic separations attempted will be given in Chapter 4. Resins were prepared for use in two different ways depending upon the resin used. Amberlite IR 120 (H) and Dowex 50-W-X8 were loaded into the column as an aquaeous slurry, and then washed with 2 M acid to remove any metal on the resin. The resin was then washed with Milli-Q water until the eluate was at pH 7. Zeocarb 225, which has a high affinity for iron [140], was washed with a warm solution of 1 M NaOH, followed by washing with a solution of 1 M EDTA. The resin was then loaded

into the column as an aqueous slurry and treated in the same manner as the other resins. To determine chromatographic elution behaviour a number of elements were selected as indicators, based on the method of Crock *et al* [57]. Operating conditions for these experiments are given in Appendix 3.

Liquid-liquid extraction techniques involved extracting a series of rare earths from aqueous media buffered between pH 1 and pH 5, with a combination of extracting species dissolved in Anala R carbon tetracholoride or chloroform. Details of these experiments are given in Chapter 4.

During an experiment involving liquid-liquid extraction of lanthanum with quinoline and acetyl acetone, the aqueous phase being buffered with hexamine, a yellow crystalline substance was observed to form after a six hour period in the aqueous phase. Experimental conditions in this case were as follows: 20 cm^3 of CCl_4 containing 0,07 M AcAc and 0,21 M quinoline with a 1 M acidic aqueous phase buffered with 2.0 g of hexamine. The crystals were filtered off and recrystallized from Anala R acetone and dried in a desiccator for 24 hours. The crystals were then analysed using proton and carbon - 13 nuclear magnetic resonance, infra-red and mass spectrometry, micro analysis and X-ray crystallography. A second set of crystals was prepared by sublimation recrystallization, where approximately 0.5 g was

placed in a schlink tube in a glycerol bath at 160° C for 3 days at a pressure of 4 mm Hg. Details of crystallographic analysis are given in Chapter 4.

3.3 OPERATING CONDITIONS USED WITH THE ICP

The instrument used was an Instrument Laboratory (IL) Plasma-200 spectrometer coupled to a Facit Dataroyal IPS 5000c on line printer and an Axiom EX 850 video printer. The component systems of the ICP include:

1) A RF power supply

2) A sample introduction system

3) A dual optical system consisting of a standard air monochromator and a vacuum ultraviolet monochromator.

These systems are all controlled by a built in microcomputer controlled by tape read-in system and user tapes. Schematic diagrams of the instrument are shown in Figures 3.1 and 3.2.

FIGURE 3.1 Schematic diagram of the IL 200 ICP

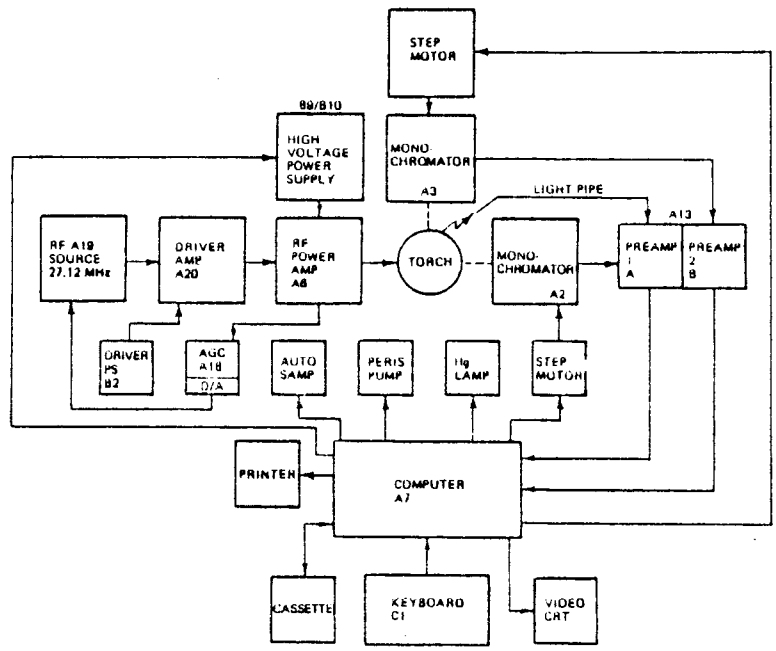

FIGURE 3.2 Double monochromator optical design

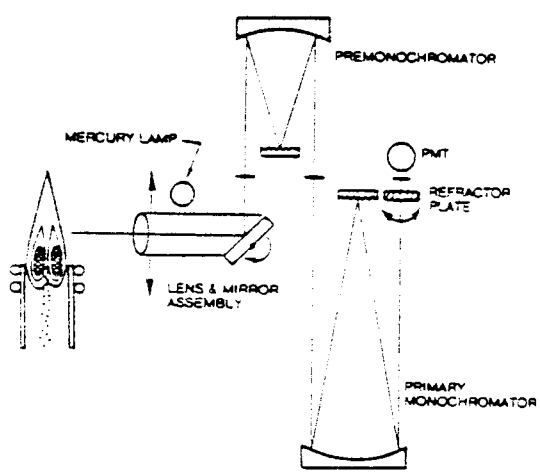

Operating variables are given in Table 3.2 below.

TABLE 3.2 Operating conditions of the IL Plasma 200

Power Supply	27.12 MHz,950-1750 W, selectable in power stages 0-6 inclusive
Optical system	Two double monochromators channels A and B (vacuum)
Primary Monochromator	1/3 M Erbert-Fastie
Premonochromator	1/6 M Erbert-Fastie
Resolution	0.02 nm (nominal)
1st Order	195 - 365 nm (A channel)
2nd Order	365 - 900 nm (A channel)
Peak Search Windows (User selectable)	0.033 nm (narrow) 0.067 nm (medium) 0.100 nm (wide)
Computer system	Intel 8080 up Forth Language
Sample Introduction	Polypropylene cross-flow nebulizer with synthetic saphire capillaries
Sample Flow Rate	Peristaltic Pump, controllable between 0.1 ml/m and 2.2 ml/m
Nebulizer Pressure	10 - 50 psi (0.75 - 3.5 kg/cm^2)
Plasma Gas Flow	13 - 18 dm^3/min, computer controlled depending on power
Torch Observation Height	0 - 48 mm in 2 mm increments above load coil

A number of analytical programs were set up on the instrument to determine spectral interferences and

elution patterns from ion-exchange experiments. Optimization of torch power, nebulizer pressure, observation height and pump rate will be discussed in Chapter 4, and details of instruments programs found in Appendix 4.

3.4 DECOMPOSITION METHODS

Several rock dissolution methods have been employed. A method based on that of Casetta *et al* [128] was used to dissolve samples of NIM-G and SS-18, (an Alenite). This involved weighing out approximately 0.4 g of the dry powdered sample into the teflon cup of a Parr digestion bomb, (teflon lined high pressure digestion vessel), to which 4 cm^3 of 38% HF and 2 cm^3 of concentrated HNO_3 were added. The bombs were then sealed and placed in an oven at 150° c for six hours. It was found that lower temperatures; 110° c and 130° c, yielded incomplete dissolution of sample matrices. The bombs were allowed to cool at room temperature, and their contents transfered to a 100 cm^3 polypropylene beaker, to which 25 cm^3 of a saturated boric acid solution was added. Solution were then made up to 50 cm^3 with 1.0 M HNO_3 and transfered to polycarbonate bottles for storage. A second method using a microwave dissolution technique was used. Between 0.5 g and 1.0 g of powdered rock was placed in a 100 cm^3 polypropylene screw top container to which 5 cm^3 38% HF and 5 cm^3 concentrated HNO_3 was added. The lid was screwed on lightly to allow evolution of gasses on heating and placed in an adapted desiccator with a nitrogen feed to pass fumes from the dissolutions through a solution of 10% (w/v) KOH. The desiccator is then placed in a Kenwood microwave oven adapted by Koch and Pougnet [146],

for 15 minutes at power level 3, (500 w for 50% of the time). A further 2 cm^3 of concentrated HNO_3 was added to the solutions after cooling. The samples were then returned to the oven for 5 minutes at power 5 (500 w for 100% of the time). Samples were removed from the oven and allowed to cool. The contents of the polypropylene vessels were transfered to 50 cm^3 volumetric flasks to which 25 cm^3 of saturated boric acid was added, and the solutions were made up to volume with Milli-Q water. The solutions were transfered to polycarbonate bottles for storage purposes.

3.5 METHODS FOR DETERMINATION OF REE IN ROCK SAMPLES

Following dissolution, the rock samples were loaded onto a 15 cm by 20 mm column of Zeocarb 225. The chromatographic procedure was as follows:

1) Load 50 cm^3 digest onto the pre-equilibrated column.

2) Elute with 140 cm^3 of a 1.5 M H^+ solution containing 0.75 M NO_3^- and 0.75 M Cl^-.

3) Elute with 100 cm^3 of 3 M HNO_3, to be used for REE analysis.

The REE fraction was collected and evaporated to dryness, and taken up in 5 cm^3 of 1.5 M HNO_3 and warmed. The solution was then allowed to cool and transfered to a 10 cm^3 volumetric flask, and made up to volume with Milli-Q water. The solution was then analysed for REE content.

4. RESULTS AND DISCUSSION

4. RESULTS AND DISCUSSION

4.1 SPECTROSCOPIC METHOD DEVELOPMENT

The REE have become increasingly important in science and industry. Consequently, analysis of REE using methods with both high powers of detection and rapid simultaneous multi-element capabilities are required. ICP-AES has generally supplied a fairly rapid means of determining REE, due to high sensitivity and sample throughput. However, analysis may be complicated by spectral and matrix interferences, and a lack of sensitivity for some elements with concentrations close to crustal abundance levels [38].

Although a number of papers have been published on usable analytical lines and instrumental parameters, it was decided to carry out our own optimization studies. As design and operation of instruments varies widely, parameters set for one instrument may not necessarily be suitable for another. This is due to differences in power sources and their control, monochromator and polychromator designs yielding different stray light characteristics and the degree of shielding of the plasma, producing differences in background emission [128].

4.1.1 OPTIMIZATION OF ICP PARAMETERS

There are a number of parameters that affect the performance of an ICP. These parameters are not

independent of each other and changing any one of them may affect the optimal value of the other parameters. Such parameters include:

1) Torch power.

2) Nebulizer driving pressure.

3) Plasma gas flow.

4) Sample aspiration rate (pump rate).

5) Torch observation height.

6) Wavelength selection.

7) Pump delay and settling times.

Although the REE have similar chemistry, it was found that they did not necessarily behave in the same manner when analysed in the ICP. All optimization experiments were carried out on single element standard solutions of approximately 10 ppm.

4.1.1.1 TORCH POWER

As the torch power must be held constant throughout the analytical program, a compromise level must be established for both analytes and concomitants of interest. As power was increased, the peak to background intensity ratio was found to decrease, indicating that lower powers would yield better detection limits. However, this effect was minimal for a number of elements chosen for close scrutiny, except between power levels 4 (1.2 kw) and 5 (1.4 kw), where the coolant gas

flow rate is increased from 13 l min^{-1} to 18 l min^{-1} affecting the temperature of the plasma. Generally, the highest emission intensities for the REE were obtained at power 3 (1.2 kw) and this setting was used for all analytical programs, for both REE and concomitants. These trends were found to be consistant with variations of nebulizer pressure. Typical examples are shown Figures 4.1 and 4.2.

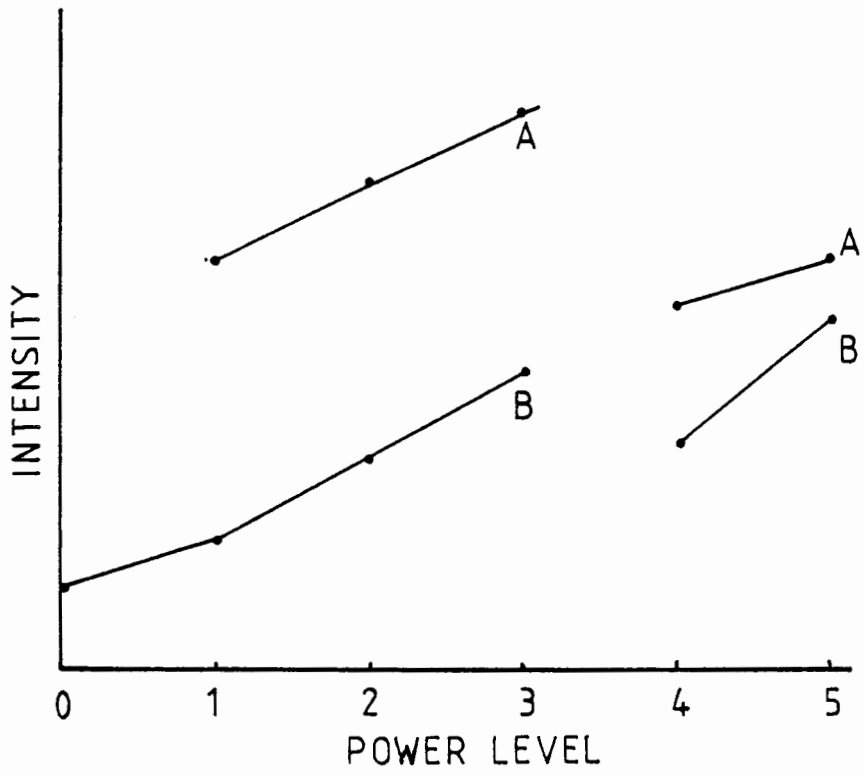

FIGURE 4.1

Effect of power level on emission intensity for Eu 381.97 nm. A = gross intensity (peak and background), B = background intensity (measured at a torch height of 18 mm at a pump rate of 1.0 ml min^{-1} at 30 psi.)

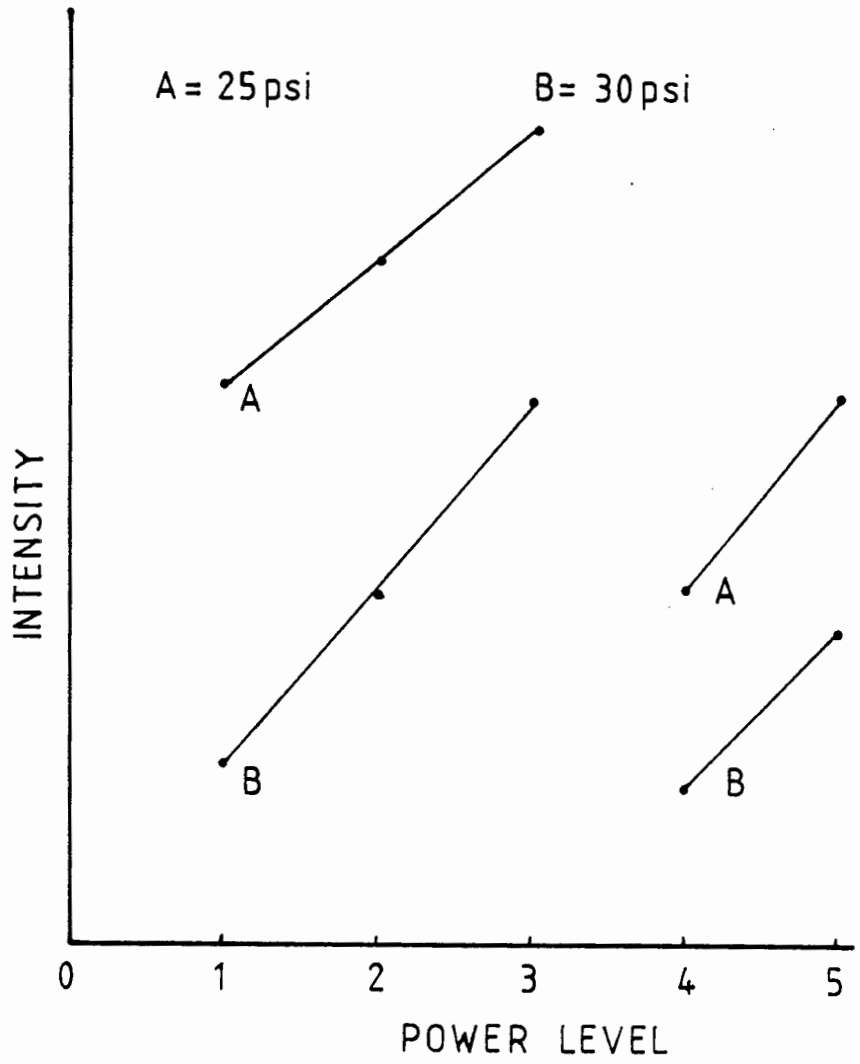

FIGURE 4.2

Effect of power level on emission intensity for Y 371.03 nm. A = nebulizer pressure of 25 psi, B = nebulizer pressure of 30 psi (measured at a torch height of 16 mm with a pump rate of 1.0 ml min^{-1}).

Low torch powers were not used due to the poor stabilities of some line backgrounds and peak intensities, especially in the presence of EIE, as the analytes may not be efficiently excited,

leading to variations in enhancements lower in the plasma due to increases in collisional excitation [72].

4.1.1.2 NEBULIZER DRIVING PRESSURE

This parameter influences the rate of sample transport through the plasma, and consequently the residence time of the analyte in the plasma. This parameter is set manually and must be constant for a particular analytical program. It was found that the optimum nebulizer pressures were between 20 and 30 psi for the REE. At lower nebulizer pressures (15 - 20 psi) net emission intensity may be greater than emission intensity at higher pressures (25 - 35 psi). However, at high nebulizer pressures, background emission and noise in background emission decreases. Residence time of the sample in the plasma is inversely proportional to the nebulizer pressure. The effect of residence time on analyte emission intensity depends upon the line type (atom or ion) used. For ionic emission, emission intensity increases with increased residence time, while with atomic emission, increased residence time provides a longer excitation period for the analyte, promoting ionization, which will lead to depression, or increased excitation which will lead to enhancement.

If the torch observation height is optimized for each nebulizer pressure, the effect of nebulizer pressure on analyte emission appears to be

reduced, due to different residence times. Different optimum viewing heights in the plasma are caused by differences in the optimum excitation height, which is governed by the rate at which the sample passes through the plasma. However, if trends in background emission of the analyte line are investigated, and compared with the background intensity when only one viewing height is used for all nebulizer pressures, (Figure 4.5), the background intensities at lower nebulizer pressures with optimum torch heights are higher than those obtained when using a fixed torch observation height. At higher nebulizer pressures, backgrounds using optimized torch heights are lower than those obtained with a fixed torch height. By varying the torch heights the populations of atomic and ionic species in the plasma region under investigation may vary due to differences in the temperature of the plasma at different heights above the load coil. This causes differences in the rates of collisional excitation and ambipolar diffusion of both analyte atoms and ions, and background matrix component atoms and ions in the plasma. Thus nebulizer pressure effects on both analyte and background emission intensity vary significantly depending upon the characteristics of the analyte and the matrix of the analyte due to differences in ionization potentials and excitation energies.

In some cases loss of sensitivity was traded for an increase in background stability, especially with Ce, Pr and Nd analyte lines. Thus relatively high nebulizer pressures of 30 psi were used

throughout for analysis. Examples are shown in Figures 4.3, 4.4 and 4.5

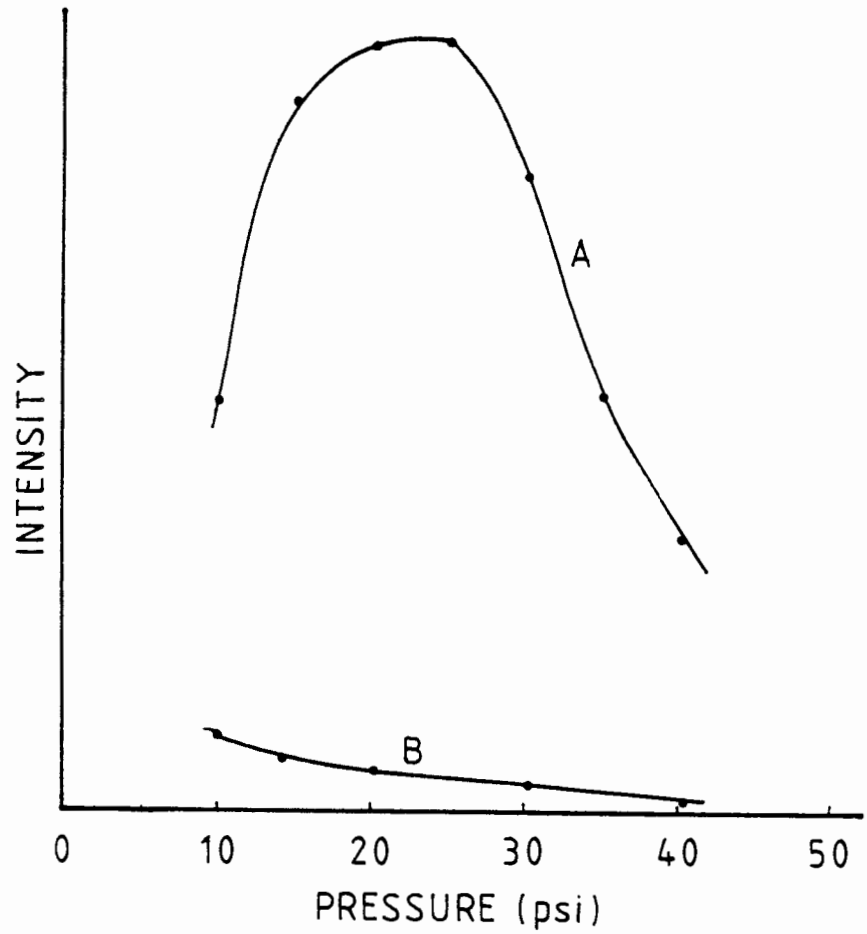

FIGURE 4.3

Effect of nebulizer pressure on emission intensity for Eu 381.97 nm, A = net emission intensity, B = background emission intensity, (measured at power 3 with a torch height of 16 mm and a pump rate of 1.0 ml min^{-1}).

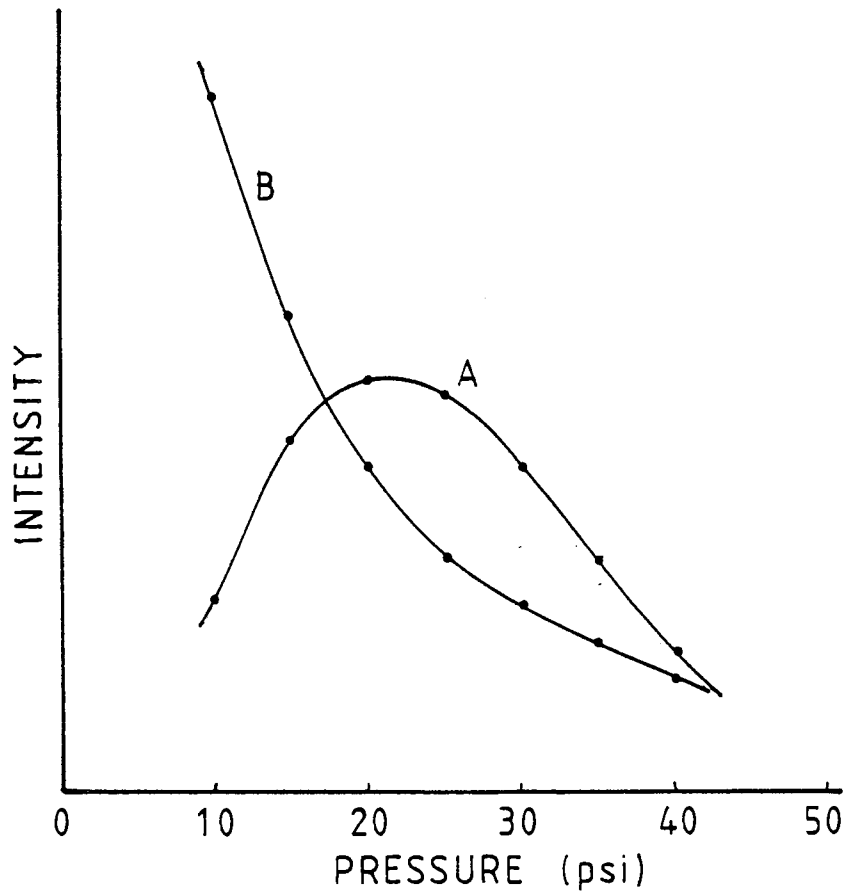

FIGURE 4.4

Effect of nebulizer pressure on emission intensity for Ce 413.77 nm, A = net intensity, B= background intensity, (measured at power 3 with a pump rate of 1.0 ml min^{-1} at a torch height of 18 mm).

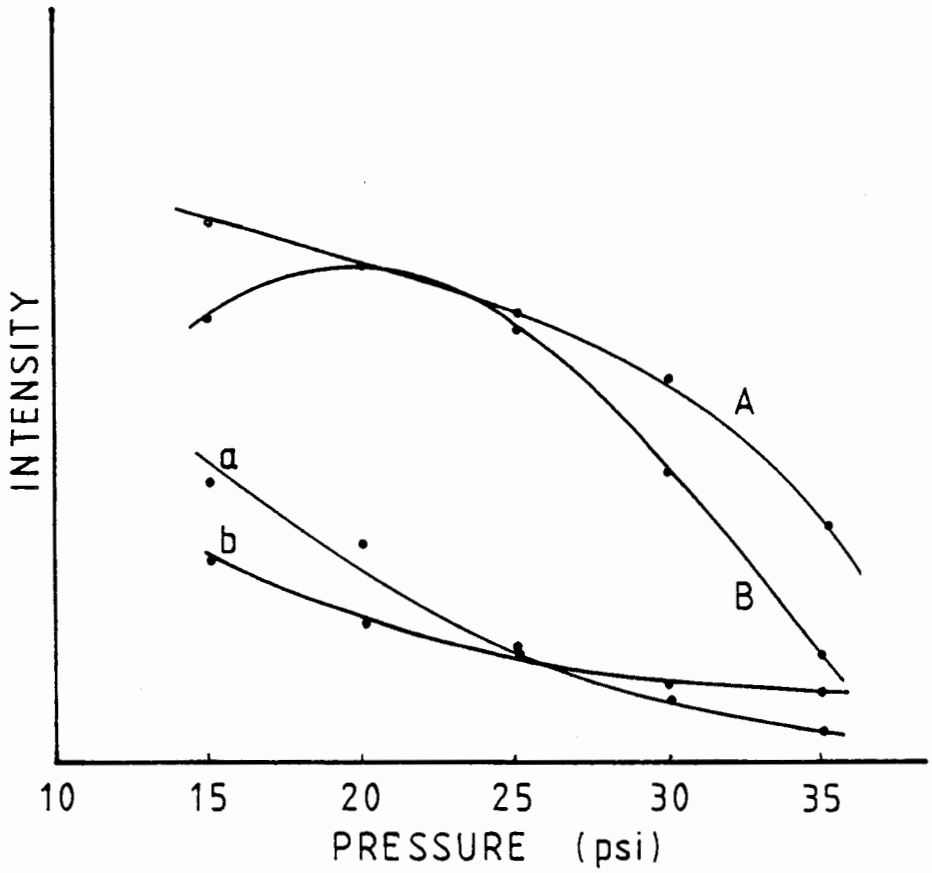

FIGURE 4.5

Effect of pressure on emission intensity for Gd 335.05 nm, A = net emission intensity, (heights at nebulizer pressures were: 15 and 20 psi, 10 mm; 25 psi, 16 mm; 30 psi, 18 mm; 35 psi, 20 mm) B = net emission intensity at 16 mm, a = background emission for A, b = background emission for B (measured at power 3 and at a pump rate of 1.0 ml min^{-1}).

4.1.1.3 PLASMA GAS FLOW RATES

This is divided into a primary and secondary flow by a fixed orifice system. The total flow rate is 13 l min $^{-1}$ for powers 0 to 3, and 18 l min $^{-1}$ for powers 4 and 5. Higher gas flow rates for powers 4 and 5 are necessary to lift the plasma to prevent melting of the sample introduction tube. At higher powers the coolant gas flow is also increased, cooling the plasma, reducing emission. This effect may be seen in Figures 4.1 and 4.2.

4.1.1.4 SAMPLE ASPIRATION RATE (PUMP RATE)

Sample aspiration rate controls the rate of sample introduction into the plasma, consequently, the amount of sample introduced into the plasma. High aspiration rates reduce the temperature of the plasma. Elements with lower ionization energies tend to have improved analytical performance at high sample aspiration rates, while elements with high ionization energies yield improved performance at low aspiration rates. Studies showed that optimum sample introduction rates for the REE are between 1.5 ml min^{-1} and 2.0 ml min^{-1}. However, with sequential multi-element analysis, high sample introduction rates required relatively large volumes of solution. At lower pump rates, 0.5 ml min^{-1} to 0.75 ml min^{-1}, background intensities tended to increase, reducing the signal to background ratios, yielding poorer sensitivity. It was noted that these trends were not affected by either nebulizer pressure or power levels chosen for analysis. It was decided to use

a compromise pump rate of 1.0 ml min^{-1}. This parameter is kept constant during an analytical program. Examples of the effect of pump rate on emission intensity are given in Figures 4.6 and 4.7.

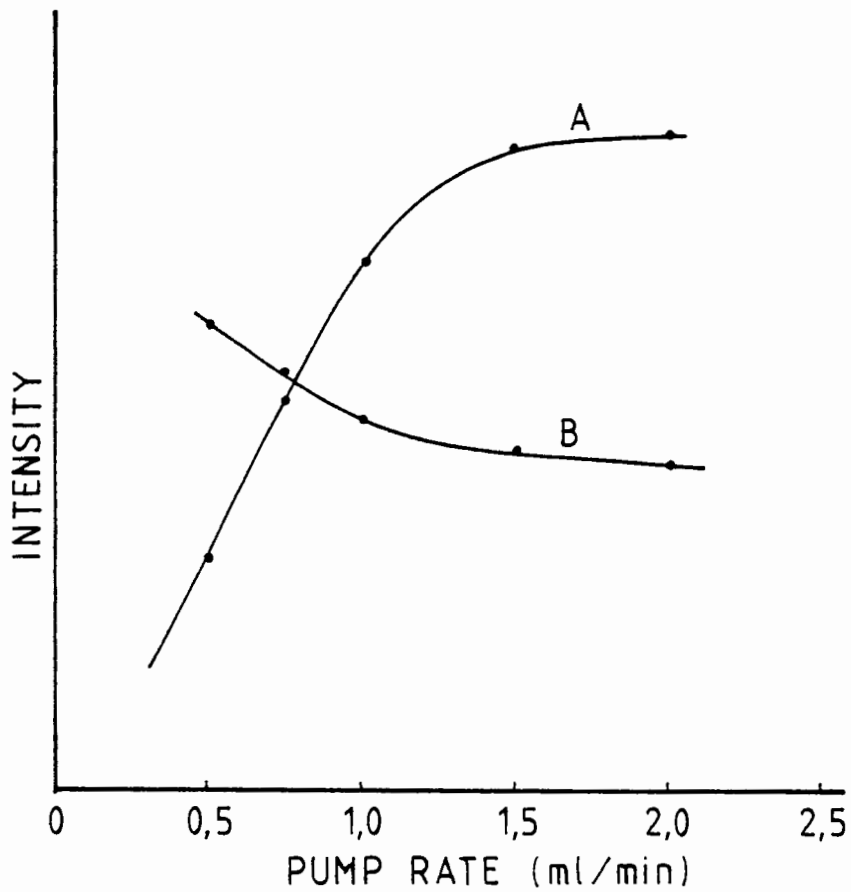

FIGURE 4.6

Effect of pump rate on emission intensity for Ce 413.77 nm. A = net peak intensity, B = background intensity, (measured at power 3, a torch height of 10 mm at a nebulizer pressure of 20 psi).

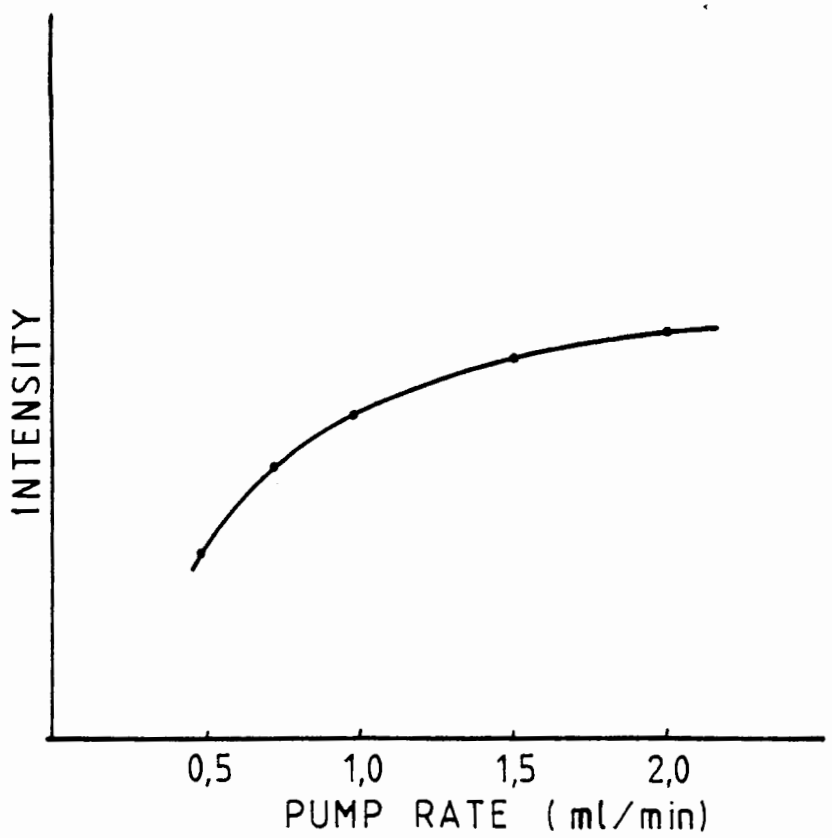

FIGURE 4.7

Effect of pump rate on emission intensity for La 333.75 nm, (measured at power 3, at a torch height of 18 mm with a nebulizer pressure of 30 psi).

4.1.1.5 TORCH OBSERVATION HEIGHT

This may be varied in 2 mm increments between 0 and 48 mm above the load coil for each line within the analytical program. The best analytical torch height varies from element to element, based on the type of emission, (atomic or ionic), of the particular line used for analysis. Another important consideration is the behaviour of background emission in the region of the analyte line, as variations in background emission with varying torch heights were observed. The highest signal to background ratio is not necessarily obtained at the point of maximum analyte emission intensity. This parameter may also vary with the sample matrix to be analysed. A high concentration of EIEs will either cause enhancement or depression of emission intensity depending on the observation height, caused by shifts in the region of maximum emission intensity, although this shift is normally relatively small.

Nebulizer pressure was also found to have a severe effect on the region of maximum emission intensity, as well as the emission intensity. As the nebulizer pressure is increased, the region of maximum emission intensity was found to increase. This is due to a cooling of the plasma due to an increased gas flow as well as a shorter residence time of the analyte atoms and ions in the plasma. Examples of the influence of torch height on emission intensity may be seen in Figures 4.8, 4.9 and 4.10.

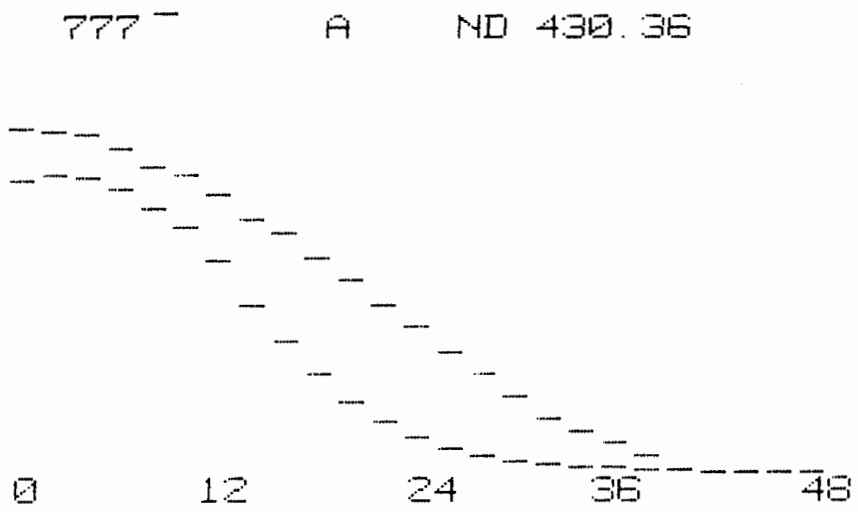

FIGURE 4.8

Plot of intensity with torch heights for analyte and background for Nd 430.36 nm.

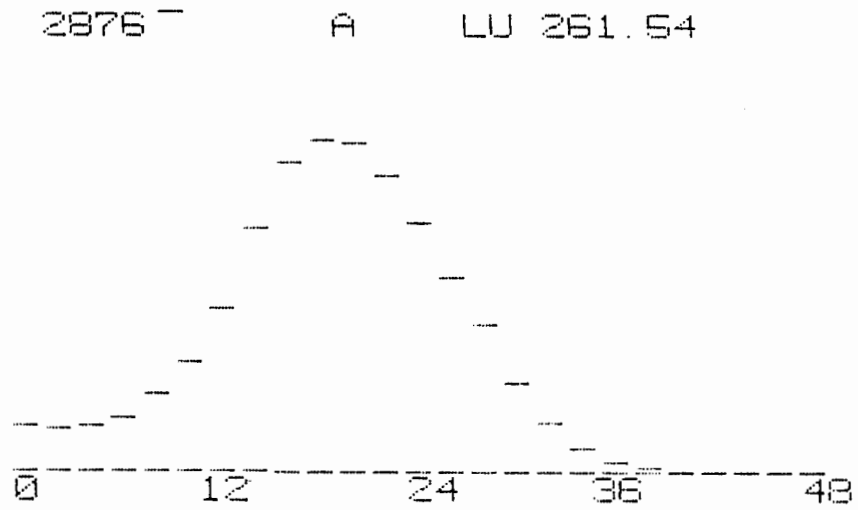

FIGURE 4.9

Plot of intensity with torch height for analyte and background for Lu 261.54 nm.

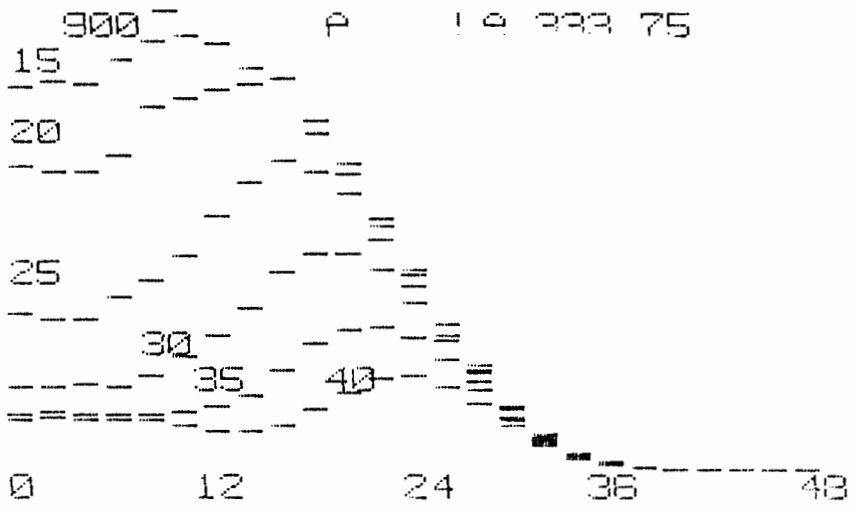

FIGURE 4.10

Plot of intensity with torch height at different nebulizer pressures for La 333.75 nm.

4.1.1.6 PUMP DELAY AND SETTLING TIME

The pump delay is that period of time at the beginning of each analysis during which the peristaltic pump is run at the maximum rate of 2.2 ml min^{-1}, which reduces the time required for the sample to equilibrate with the sample introduction system. For some matrices where analyte concentrations are expected to vary widely, a long period of delay may be required to reduce carry over of the previous sample to a minimum. The default time of 30 seconds was used during analyses.

The settling time is the time between the fastpump cycle (pump rate of 2.2 ml min^{-1}), and the commencement of analysis. This time is used to allow equilibration of the analytical pump rate, and allow time for the monochromater to move to the first line of the analytical program. As the first lines used for analysis were less than 100 nm in wavelength from the rest position of 365 nm, the default setting of 3 seconds was used.

4.1.1.7 LINE SELECTION

The REE all have complex emission spectra, with some 30000 spectral lines being reported in the MIT wavelength tables for these elements [48]. This allows the analyst a choice of a number of spectral lines for each element based on the following criteria:

1) Expected elemental concentrations in the samples to be analysed.

2) Spectral interferences.

3) Detection limits of the spectral lines chosen.

As the IL Plasma 200 has a library of the 3 most sensitive lines for each element, these were chosen for initial studies. Additional lines, selected from line coincidence tables [141] were also examined for spectral interferences.

Systematic characterization of spectral interferences was achieved by aspirating 100 ppm solutions of Na, Ca, K, Si, Al, Fe, Cr, Cu, Ba, Zr, Sr, Ti, Mn, Mg; 50 ppm solutions of Ni, V, W and approximately 10 ppm solutions of REE at the analytical wavelength. Range of scans were either 0.2 or 0.4 nm.

The choice of lines of comparable sensitivity will depend upon the method of sample preparation. If samples are to be analysed directly, lines should be chosen to minimize interferences from major and minor element constituents. If some form of sample pretreatment is envisaged, with removal of most major and minor element constituents by a separation technique, then greater consideration must be given to the number and magnitude of interferences from concomitant REE on the lines of interest. Traces of spectral studies are given in diagrams for Chapter 4, and detection limits for lines chosen are given in Appendix 5.

YTTRIUM

Of the four lines investigated, the 377.43 nm line shows the lowest degree of spectral interference. The 371.03 nm line shows interferences from REE, (with high expected REE concentrations in dissolved rock solutions), iron and zirconium, both of which are difficult to separate from REE by column chromatography. Y 324.23 nm suffers from severe titanium interference and Y 360.07 nm

suffers interferences from a number of REE and Zr. The line of choice is 377.43 nm.

LANTHANUM

La 333.75 nm suffers REE interferences from Ho and Er, both of which are expected to have relatively low concentrations in dissolved rock solutions. The interference from Ti, could be largely eliminated by chromatographic separation of Ti from the REE, while interference from vanadium could be reduced by use of a narrow window setting. The 379.48 nm line shows small interferences from Sm, Ce, Pr, Tm, V and Fe, although in samples with high iron content, chromatographic separation may not remove sufficient iron from the REE fraction, necessitating an alternative choice of analytical line. Strontium was observed to interfere strongly on La 408.67 nm causing an uneven background. This interference could be removed by preliminary chromatographic separation procedures. Interferences from Y, Ce, Pr, Nd, Gd and Zr were also observed. For analysis of the sample without pretreatment, La 379.48 nm would be the best line to use, while after chromatographic separation, La 408.67 nm would be the line of choice.

CERIUM

Of the five lines investigated Ce 395.26 nm shows unacceptable levels of interferences. Ce 446.02 nm shows no interferences from REE but has a

strong interference from V, which is removable by sample pretreatment. Ce 413.38 nm shows interferences from Pr, Nd and V; Ce 418.66 nm from Dy and Tm; Ce 413.77 nm from Gd and W. After sample pretreatment Ce 413.38 nm would be the line of choice, while by direct analysis of sample solution, Ce 413.77 nm would be used. A problem encountered with all of these lines is the sensitivity of the background to acid concentration and matrix type, necessitating the use of background correction.

PRAESODYMIUM

All Praesodymium lines studied showed interferences from matrix elements. Of these Pr 440.88 nm, 390.84 nm, 414.31 nm and 422.54 nm also showed strong interferences from REE. The line of choice is Pr 417.94 nm, but corrections for Nd, Sm and Zr will have to be made after analysis.

NEODYMIUM

Four lines were analysed for spectral interferences. Nd 415.61 nm suffers strong interference from zirconium, while Nd 406.11 nm shows interferences from Tb, Gd, Ce and Zr; Nd 401.23 nm interferences from Eu, Ce, Tb, Pr and Ti; and Nd 430.36 nm interferences from Pr, Ca, Zr and Sr. Of these Nd 430.36 nm shows an interference from only Pr if a narrow window is used. The interference of Ce on Nd 401.23 nm is relatively strong, negating the use of this line

in analysis as expected Ce concentrations are higher than those of Pr in most samples. Nd 406.11 nm will require spectral interference corrections for interferences from Tb, Gd and Zr, thus the choice of analytical line is Nd 430,36 nm.

SAMARIUM

Lines examined include Sm 359.26 nm, Sm 442.43 nm, Sm 360.95 nm and Sm 363.42 nm. Sm 359.26 nm has interferences from Dy, Ho, Nd, Gd, Y, W, V, Cr and Zr and is not suitable for analysis. Sm 363.42 nm has a structured background, but only has interferences from Y and Zr. Sm 442.43 nm also has a structured background, but only suffers small interferences from Ce and Pr, while Sm 360.95 nm has interferences from Tm, Ce and Nd. Of the four lines investigated, the line of choice is Sm 442.43 nm.

EUROPIUM

Three lines were analysed for interferences. Eu 381.97 nm showed interferences from Y, Pr, Ce, Gd, V and Fe. All the REE interferences except that of Gd can be removed by use of a narrow window. The V and Fe interferences can be removed by preliminary chromatographic separation. Eu 412.97 nm has interferences from Pr, Sm, Gd, Tb, Dy, Ca and Ba. Due to the low expected levels of Eu in sample matricies, corrections for all REE would be necessary. Interferences from Ba and Ca could be

removed by preliminary chromatographic separation. Eu 420.51 nm shows interferences from La, Y, Nd, Sm, Gd, V, Ca, Si and Sr. Due to the nature and number of interferences on both Eu 420.51 nm and Eu 412.97 nm, the line of choice is Eu 381.97 nm.

GADOLINIUM

Gd 335.05 nm shows interferences from Er, Ho, Sm and Ti. The Ti interference extends to Gd 335.86 nm, and is due to a complex band spectra with elevated background. Gd 335.86 nm also shows interference from Cr, Zr (also background), Ho and Er, although the REE interferences would be excluded by use of a medium or narrow window. The chromium and titanium interferences on these two lines may be removed by preliminary chromatographic separation. Two other lines, Gd 310.05 nm and Gd 342.25 nm were inspected for interferences. Gd 310.05 nm shows interferences from Fe, Si, V and Ti; and Gd 342.25 nm interferences from Ce and Cr. After chromatographic separation, the lines of choice for analysis are Gd 335.86 nm, Gd 310.05 nm and Gd 342.25 nm which requires correction for the Ce interference.

TERBIUM

Tb 384.87 nm, Tb 387.41 nm and Tb 356. 86 nm all show unacceptable levels of interferences. Tb 356.17 nm suffers interferences from Nd, Sm, Ti and Zr. The REE interferences are very small, and

the Ti interference can be removed by chromatographic separation prior to analysis. Correction would be necessary for the Zr interference. Tb 367.64 nm shows interference from Dy only, while Tb 350.92 nm shows interference from Sm, Ho and Zr. The line of choice is Tb 350.92 nm, due to the greater stability of background emission compared with Tb 367.64 nm, although all three interferences would need to be corrected for.

DYSPROSIUM

Interferences of REE on Dy 364.54 nm occur with Sm, La, Gd and Pr. Dy 394.47 nm has an interference from Al, although this line was not thoroughly checked. Dy 353.60 nm has interferences from Tm, Tb and Sm, with interferences from Ti, Zr, W and Fe being excluded by using a narrow window. Dy 340.78 nm shows interferences from Gd, Ho, Ti and Zr, while Dy 353.17 nm has interferences from Tb, Zr and Mn. Of these latter three lines Dy 353.17 nm is the line chosed for analysis, due to the relatively small interferences from Tb and Zr, the Mn interference being removed by chromatographic separation. The degree of interference of Zr on Dy 340.78 nm requires the choice of an alternative line. Spectral interference corrections for Tb and Tm on Dy 353.60 nm would make this line an alternative choice for analysis.

HOLMIUM

Of the five lines investigated, Ho 389.10 nm, Ho 339.90 nm and Ho 341.65 nm showed unacceptable levels of interferences. The interference of Mn on Ho 347.43 nm may be removed by use of preliminary chromatographic separation, leaving small interferences from Dy and Sm to be corrected for. Interferences from REE on Ho 345.60 nm can be removed by use of a medium window or ignored, as in the case of Eu, due to the low expected concentrations of Eu in the sample matrices. The Ti interference can be removed by chromatographic separation, but correction will have to be made for the Zr interference.

ERBIUM

Er 326.49 nm shows interference from Tb, Sm, Zr, Mn, Si, Ti and V, the last three elements contributing to background emission below the peak. The Zr interference is severe and with the other interferences negates the use of this line for analysis. Er 323.06 nm suffers interferences from Sm, Mn, Zr and Ti. The Mn and Ti interferences may be removed by preliminary chromatographic separation, and the Zr interference minimized by using a narrow window. Er 337.27 nm has interferences from Tb, Zr and Ti, with the severe Ti interference being removed as described above. Er 349.91 nm shows interferences from Dy, Ho and Zr. Although Zr appears to interfere strongly, this background is level, and could be excluded by use of a narrow window and

background correction placed well left of the peak. After application of these corrections, either Er 337.27 nm or Er 349.91 nm would be suitable for analysis, with the appropriate element interference corrections being made.

THULIUM

Of the four lines investigated, Tm 384.80 nm is unsuitable for analytical purposes due to the high degree of REE interferences. Tm 342.51 nm has interferences from Gd, Eu, Dy, Er, Ho and Zr. Of the remaining lines, Tm 313.13 nm shows interferences from Ce, Ho, Eu, Ti, Be, V and Zr, the last two being background interferences. Of the REE interferences, only the Ho interference may be considered important, while the interferences from Be and Ti may be removed using ion-exchange chromatography. Tm 346.22 nm has interferences from Ho, Gd, Ni, Ti and Zr. Due to the degree of interferences of Ho and Zr the line of choice is Tm 313.13 nm.

YTTERBIUM

Yb 222.45 nm suffers from an interference from Tm. From the point of view of interferences, this line would be the line of choice. However, analysis must be carried out using the B channel, (vacuum ultra-violet), where background and peak intensities are very noisy. As Yb is expected to be found in very low concentrations, the detection limit or the lower limit of determination using

this line is not likely to be sufficiently low. Yb 289.14 nm suffers interferences from Ho, Ti, Cr and V and Yb 369.42 nm from Er, Sm, Gd, Tm, Dy and V. With Yb 328.94 nm no interferences from REE were observed, while Zr, V and Ti interfere. The Zr interference can be removed by use of a narrow window, and the Ti and V interferences removed by preliminary ion-exchange chromatography. Thus Yb 328.94 nm is the line of choice.

LUTETIUM

Lu 219.55 nm has interferences from Cu, W and Fe, and would be suitable for analysis but was not selected for the same reasons as Yb 222.45 nm. Lu 291,14 nm suffers from interferences by V, W and Cr, while Lu 261.54 nm suffers from interferences from W and possibly Er, this peak possibly being an impurity in the Er standard solution due to Lu. With preliminary ion-exchange chromatography Lu 261.54 nm is ideal for analysis.

During the course of the project, three different gratings were fitted to the A channel monochromator. These were found to have some effect on the degree of interference of a concomitant on a particular line, and in some cases, the concomitant interferences were completely different. This can be ascribed to the optical characteristics of each grating; differences in orientation of the monochromator lenses, and reflections from the mirrors and lenses in the monochromators [90]. Also it is

possible that variations of observation heights of up to 8 mm occurred, significantly affecting the observed emission, as some element lines show relatively rapid decreases in emission intensity with observation height between 14 and 22 mm above the load coil. These variations, although not programmed, resulted from adjustments made to the mechanism governing torch observation heights between analyses. Differences in emission intensity may also be attributed to the fogging of the grating, due to the formation of ozone in the monochromator, this ozone being produced by the mercury calibration lamp. This would account for a decrease in sensitivity, and consequently a reduction in the intensity and number of lines observed over a period of time. Comparisons of interferences are given in Appendix 6.

Roelandts and Michel [141] have recently completed a study of REE inter-element interferences during analysis. Although it has been stated that comparisons of instrumentation and results from different laboratories will yield discrepencies [78], it is of interest to note differences in reported interferences. A comparison shows that an instrument with a higher resolution monochromator allows a greater choice of analytical lines, due to a reduction in spectral overlap. However, no quantitative comparison is possible due to the differences in operating power, torch observation height, sample flow rate and gas flow rates. Further comparisons of choice of wavelengths of analytical lines used by other authors [43, 45, 47, 48, 54] shows that line

selection is also dependant upon the matrix type to be analysed and resulting expected interferences.

4.1.1.8 MATRIX AND CALIBRATION EFFECTS

During analysis of samples, it was found that the sample matrix played an important role in the accuracy of results obtained. A number of experiments were conducted to determine the influence of matrix components used during the sample dissolution procedures. Since REE are often found in high silica containing rocks, dissolutions involved the use of hydrofluoric acid, nitric acid and boric acid. In order to determine the effects of these acids, solutions containing 19.09 ppm La and 18.13 ppm Eu were prepared with different concentrations of hydrofluoric, boric and nitric acids. Normally, two of the acids were held at the expected concentration of that acid in the dissolution solution, while the concentration of the third was not. Results are shown in Figures 4.11, 4.12, 4.13.

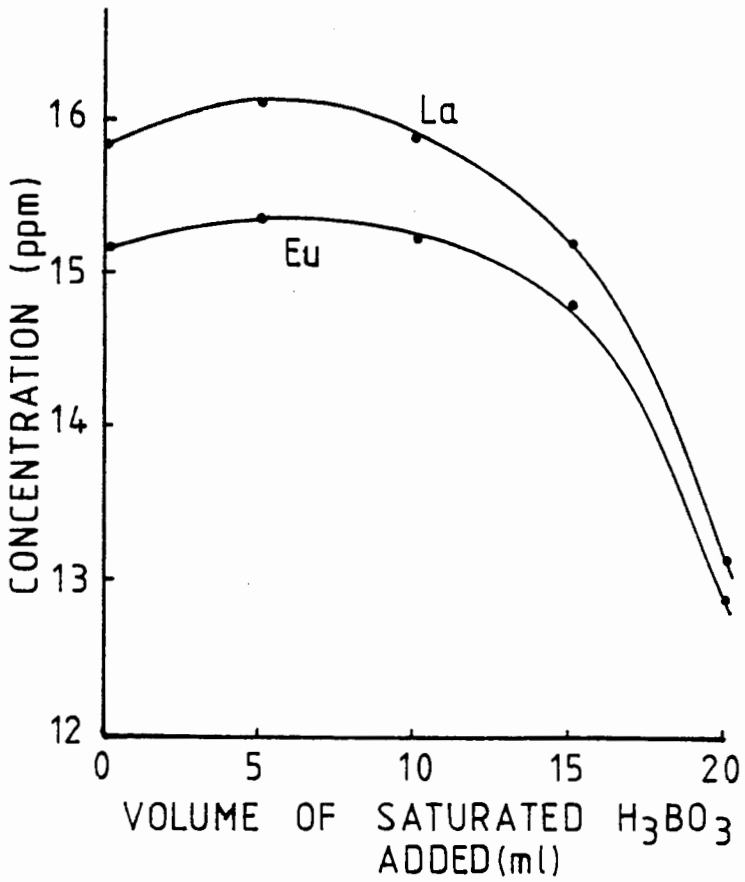

FIGURE 4.11

Effect of boric acid concentration on emission intensity of La and Eu (solutions contain 6 cm^3 HNO_3, 3 cm^3 HF, 3cm^3 1% Triton - X 100, a surfactant and various volumes of saturated H_3BO_3 at 20° C).

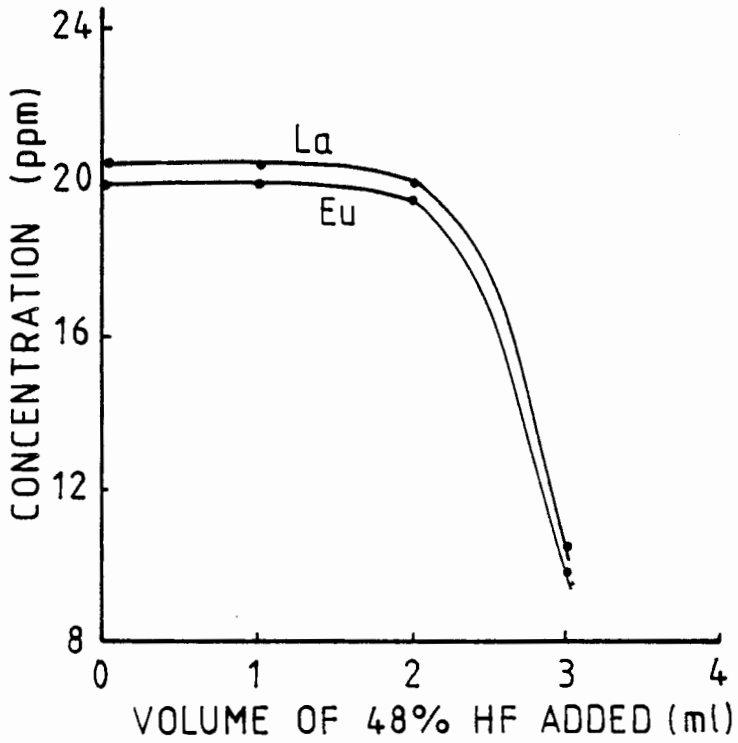

FIGURE 4.12

Effect of hydrofluoric acid concentration on emission intensity of La and Eu (solutions contain 6 cm^3 HNO_3, 25 cm^3 H_3BO_3 (sat), 3 cm^3 1% Triton- X 100 at 20° C).

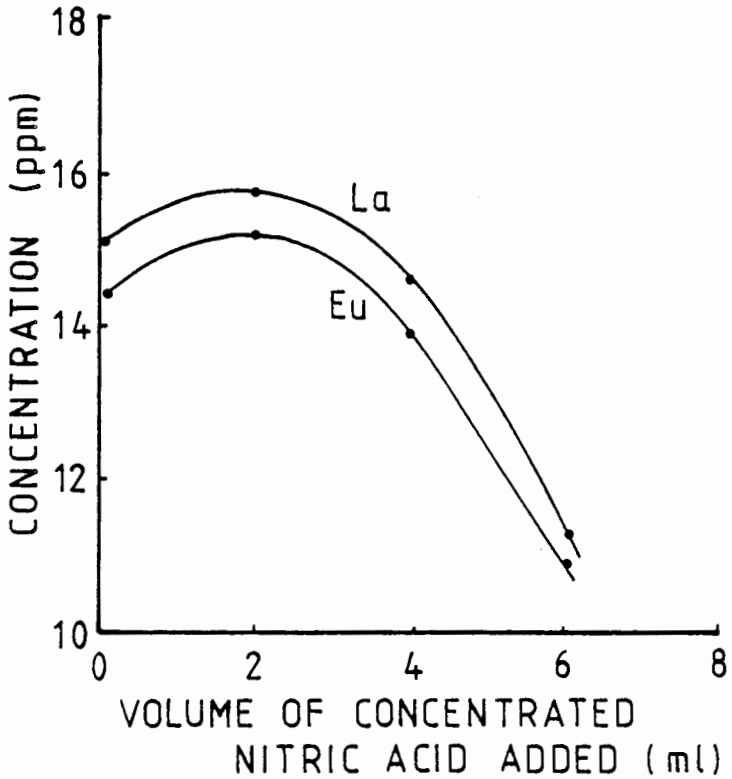

FIGURE 4.13

Effect of nitric acid concentration on emission intensity of La and Eu (solutions contain 3 cm^3 HF, 25 cm^3 H_3BO_3 (sat) 3 cm^3 1% Triton-X 100 at 20° C).

Trends found in these experiments agree with those proposed by Greenfield *et al* [85]. This shows that the viscosity increase of the solution with increase in acid concentration will affect the nebulizer yield, as solutions were aspirated at a constant flow rate of 1 ml min^{-1}. Another factor that will affect the emission intensity is the amount of energy required to break up the acid molecules in the plasma, an increase in acid concentration requiring more energy to dissociate

the acid. The sudden drop in intensity with increase in hydrofluoric acid concentration, with 3 cm^3 of acid added, may be attributed to the insolubility of REE fluorides, which would precipitate in the sample bottle. This would also account for the lower values obtained for the variations of both boric and nitric acid, as 3 cm^3 of hydrofluoric acid was present in each solution in these experiments. This shows that it is both necessary to matrix match standards, and reduce the amount of hydrofluoric acid to a minimum if reasonable analytical results are to be obtained.

A problem encountered during analyses was the instability of the blank value. An experiment was performed over a period of two hours where the same solutions and blanks were continually analysed. Solutions analysed were 10 ppm La, Y and Ce standards. The deviations shown in Figures 4.14, 4.15 and 4.16 are based on the calibrations using these standards. A number of calibrations which were performed during the analysis, represented by new starting points on the sample axis.

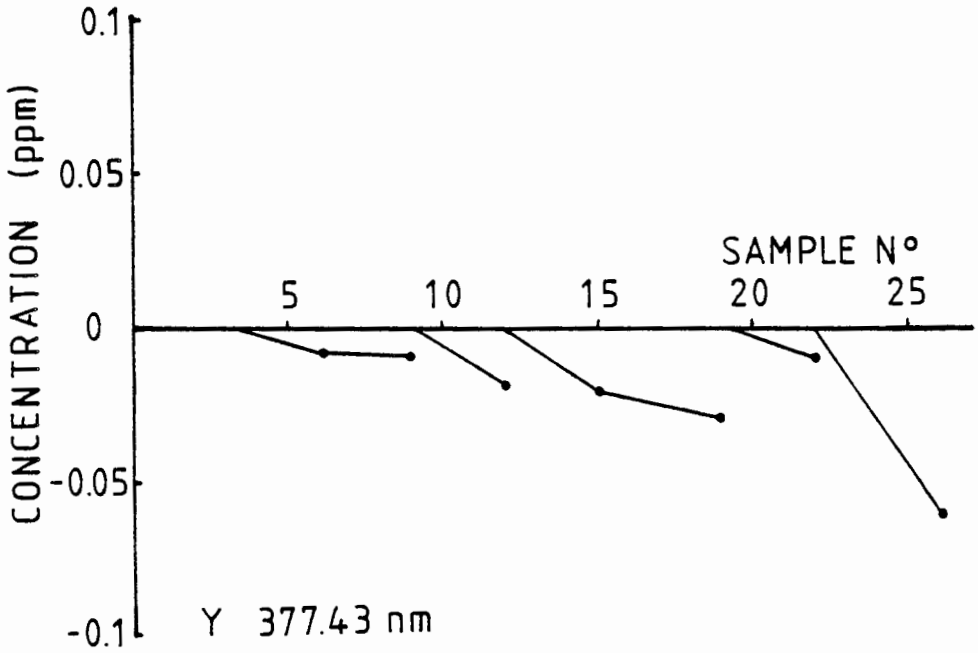

FIGURE 4.14

Drift of blank concentration with samples analysed (each analysis takes approximately four minutes).

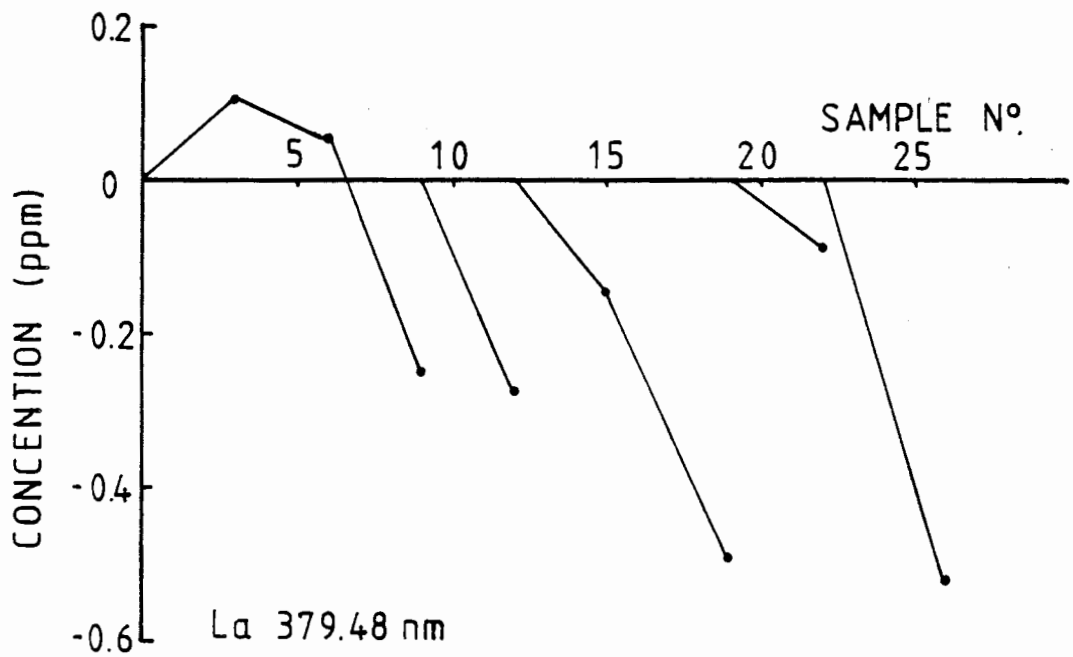

FIGURE 4.15

Drift of background concentration with samples analysed (each analysis takes approximately four minutes).

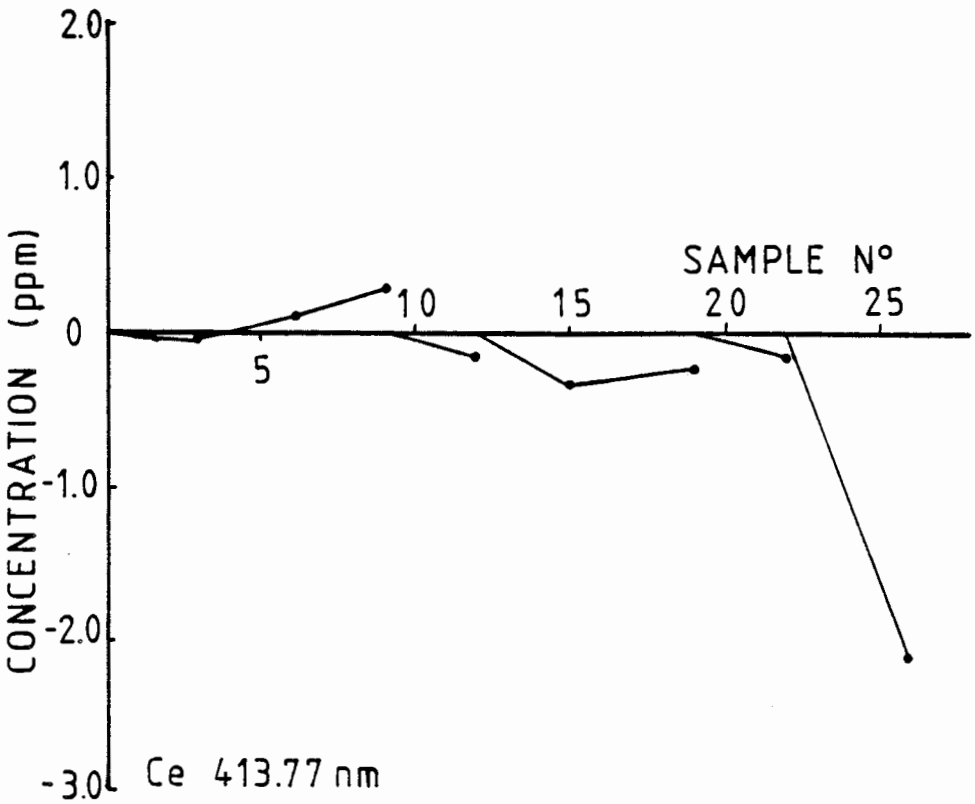

FIGURE 4.16

Drift of background concentration with samples analysed (each analysis takes approximately four minutes).

Variations in background are not consistant over the period of analysis. This can be attributed to instability in the photomultiplier tubes. Normally thermal equilibrium is reached within the first 30 minutes of analysis. If this is not achieved, an apparent drift in analysis is observed, with a 1% loss of intensity for every 1° C rise in temperature for both R 106 UH and R 955 H (red sensitive) photomultiplier tubes [142]. Thus, to prevent unacceptable drift in both blank

and standard, two methods of correction must be employed. Firstly, for analytical lines with high background intensities, a background correction must be used during analysis. Secondly, a blank must be analysed every two or three samples to adjust for drift. This is essential when analysis close to detection limits is required.

4.2 OPTIMIZATION OF GROUP SEPARATION OF THE RARE EARTH ELEMENTS FROM MATRIX ELEMENTS

The requirements of ion-exchange separation for this study were:

1) To recover the REE and Y quantitatively as a group.

2) To reduce the easily ionizable element content of the sample and thus reduce matrix effects in analysis.

3) To reduce to a minimum the number and concentrations of elements such as V, W, Ti, Fe and Zr which produce spectral interferences.

4) To allow the dissolution of a relatively large sample, and concentrate that sample into a relatively small volume.

This method was established on the premise that rock samples would be dissolved using an acid dissolution technique rather than a fusion technique. Although acid dissolutions allow a larger sample to be taken, reducing sampling inhomogeneity, the method does have the

disadvantage of incomplete attack on acid resistant minerals such as zircon, sphene and monazite which contain substantial concentrations of REE.

Cation exchange separations of REE and non-REE were investigated to remove background and spectral line interferences. A number of elements interfered on more than one REE analytical line, the most common interfering elements being Ti, Zr and V. These elements are also likely to be present in rocks in concentrations considerably in excess of expected REE values, introducing errors in analysis.

Solutions prepared for investigation of chromatographic separations contained a number of elements that represented their group behaviour. La and Ce represented the light REE behaviour while Y and Ho represented heavy REE behaviour. Na, Ca, Mg, Ba and Sr represented the behaviour of the electrolytes and EIEs. The transition elements Ti, Zr, Fe, Mn and Al represented elements that were likely to cause interferences with REE analytical lines.

Flow rates of approximately 1 ml min^{-1} were observed throughout for Zeocarb 225 and Dowex 50-W-X8, and approximately 3 ml min^{-1} for Amberlite 1R 120 (H). These were found to decrease slightly with an increase in acid concentration due to the

dehydration of the resin. However, these effects were minimal when compared with the effect of changing acid concentration. All three resins employed in experiments were strong cation exchange resins, with a cross-linked polystyrene base structure, and active sulphonic acid groups ($-SO_2OH$). Thus the analysis of behaviour of the resins was based on the size of the resin bed and the sample flow rate. All eluates were collected in 10 ml aloquots, unless otherwise stated.

4.2.1 CHROMATOGRAPHY 1

A resin bed of Amberlite IR 120 (H) was prepared. A synthetic solution of 50 ml containing 80 ppm Al, Fe, Ti, Mn, Mg, Na, Ca; 40 ppm Sr, Ba, Zr and 10 ppm Y, La, Ce and Ho was loaded onto the column. Gradient elution was carried out as follows:

1) Elute with 100 ml of 1.0 M HNO_3.

2) Elute with 100 ml of 2.0 M HNO_3.

3) Elute with 80 ml of 6.0 M HNO_3.

4) Elute with 60 ml of 8.0 M HNO_3.

Results show that there is little separation of REE from any of the other elements except sodium. This could be due to the length of the column being too short, and the elution flow rate too high, due to the size of the resin beads. The anomolous aluminium behaviour was due to an unclean resin (Figure 4.17).

FIGURE 4.17 CHROMATOGRAPHY 1

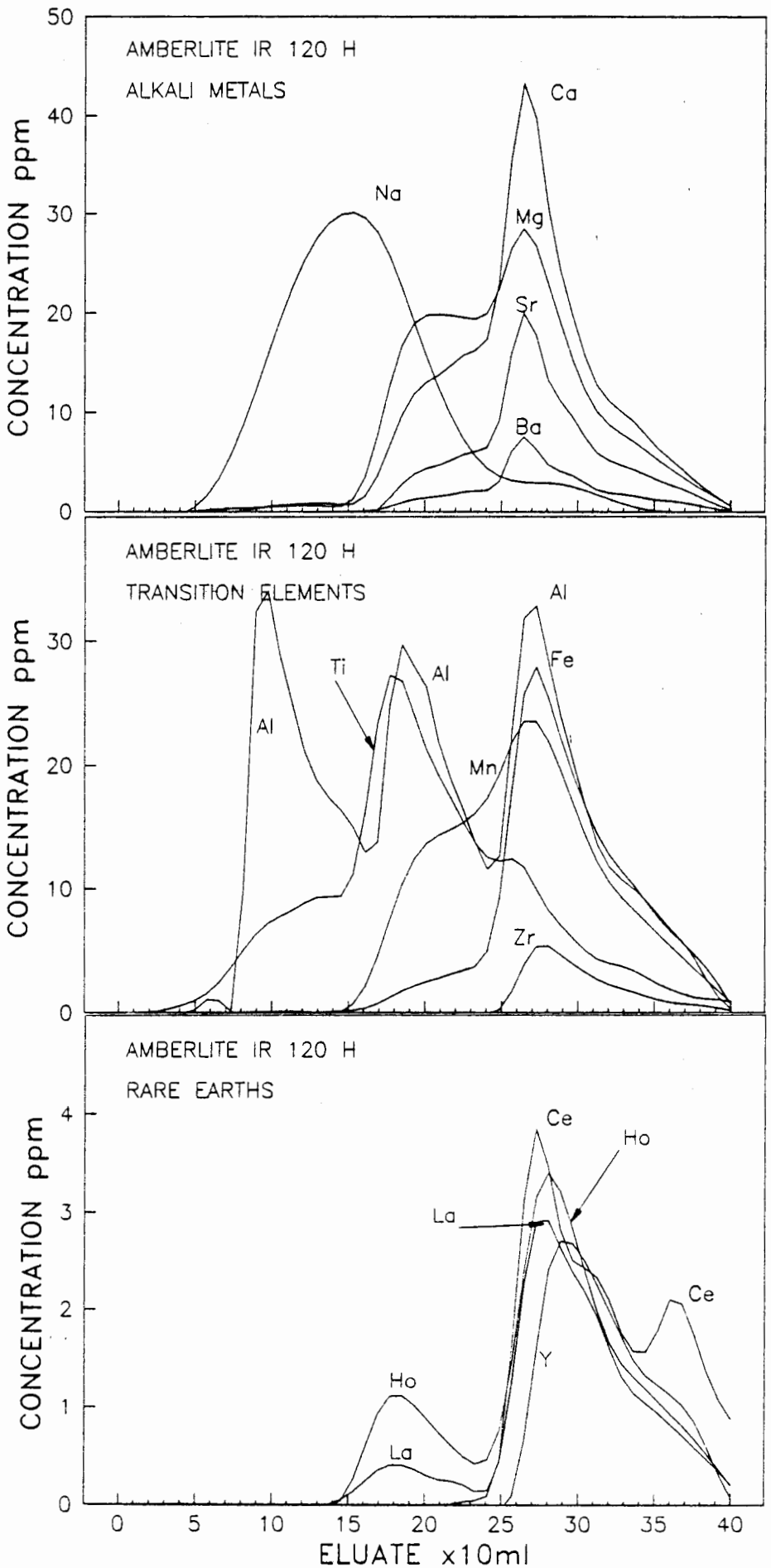

4.2.2 CHROMATOGRAPHY 2

A 10 cm column of Zeocarb 225 of 20 mm diameter was loaded with a 25 ml solution containing 50 ppm of all indicator elements. Elution was carried out as follows:

1) Elute with 100 ml of 2.0 M HNO_3.

2) Elute with 80 ml of 6.0 M HNO_3.

3) Elute with 60 ml of 8.0 M HNO_3.

Chromatogram (Figure 4.18) shows an increased degree of separation of the REE from the other groups. This is facilitated by the lower elution flow rate, and the smaller resin bead size. Since poor separation was observed, all the peaks appearing during the 2.0 M acid elution stage, (except Zr), it was necessary to reduce the acid concentrations of the eluent stages. Results using lower acid concentrations are shown in Chromatography 4 and Figure 4.20.

Recoveries of REE from the resin are as follows: La, 73,6%; Ce, 90,3%; Y, 85,3% and Ho, 104,5%. Of these, only the result for Ho is within experimental error. The results of the other REE are low due to either calibration errors, or incomplete stripping of the elements from the resin.

FIGURE 4.18 CHROMATOGRAPHY 2

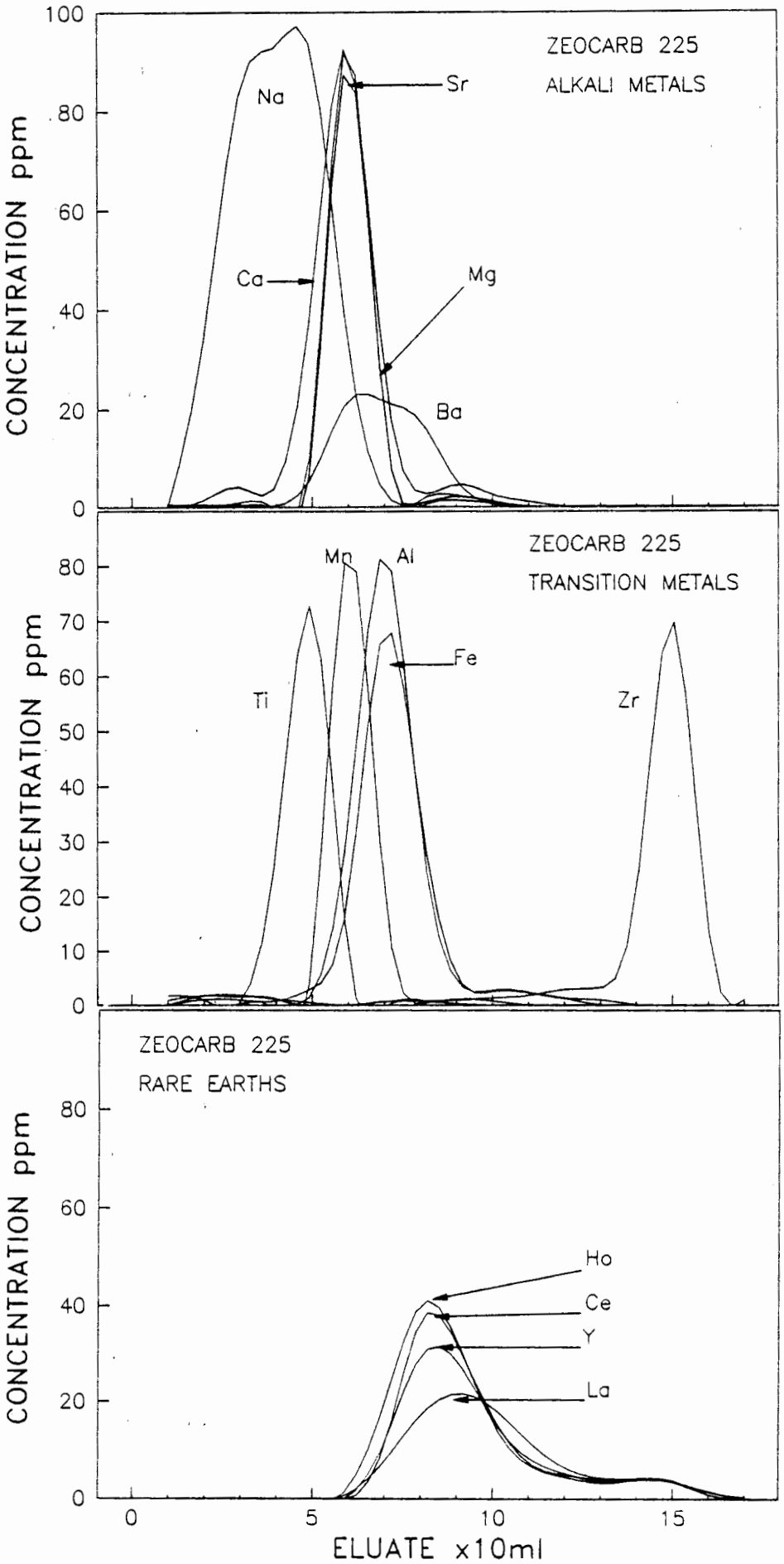

4.2.3 CHROMATOGRAPHY 3

Up to now, only nitric acid elution behaviour has been studied. Hydrochloric acid may be used as an alternative eluting agent, and has the advantage of producing lower matrix effects in the plasma when compared with HNO_3. HNO_3 aspiration introduces both nitrogen and oxygen into the plasma creating the possibility of NO band emission. The identical experiment to Chromatography 2 was performed, except elution was carried out with HCl (Figure 4.19).

A comparison shows that the REE elution behaviour with the two acids is different. With HCl elution there is a distinct separation of the light and heavy REE, while with nitric acid, the REE are eluted as a group. With HCl, barium is eluted with the REE fraction, but the transition metals , Fe, Ti, Mn and Al are all eluted together. With HNO_3 elution, barium is eluted with the alkali and alkali earths while the transition metal group is spread over a wider elution range. The zirconium elution pattern with HCl elution shows a large degree of band spreading while with HNO_3 elution, the zirconium peak is sharply defined. These results compare well with results obtained by Crock *et al* [58]. However, the degree of separation of the groups is poorer due to a shorter resin bed, thus the number of theoretical plates would be reduced, reducing separation efficiencies. Yields are comparable with those obtained for Chromatography 2.

FIGURE 4.19 CHROMATOGRAPHY 3

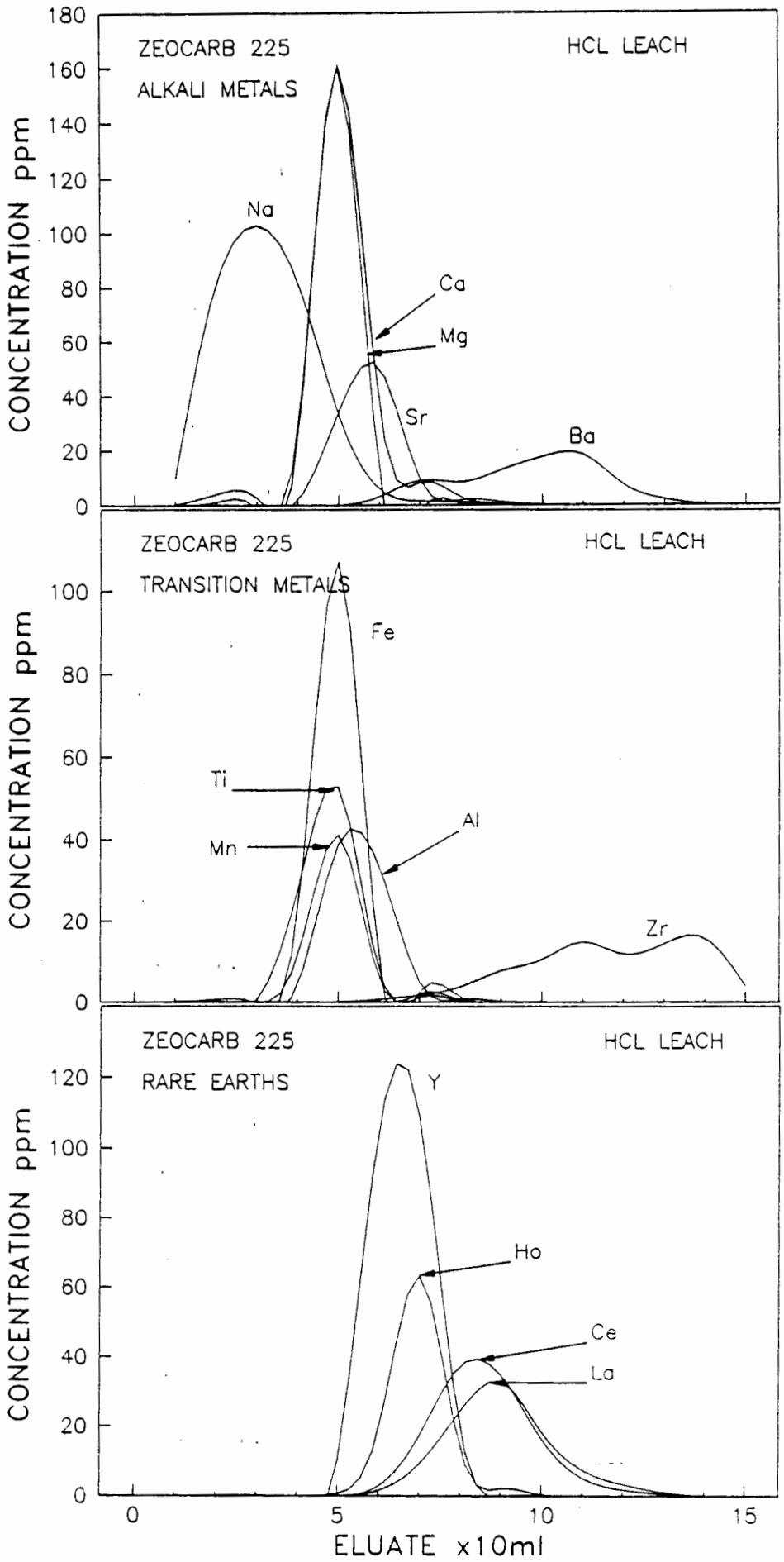

4.2.4 CHROMATOGRAPHY 4

Using a similar column to the previous experiment, with the same load solution, elution was carried out with lower acid concentrations as follows:

1) Elute with 100 ml of 0.5 M HNO_3.

2) Elute with 60 ml of 1.0 M HNO_3.

3) Elute with 80 ml of 2.0 M HNO_3.

The degree of separation of the alkali and alkali earth elements is improved to almost complete separation. Mn and Ti are completely resolved from the REE, but Al and Fe are still eluted with the REE fraction. The amount of zirconium eluted with the REE fraction is relatively small, and results in a significant reduction in total Zr content of the solution to be analysed (Figure 4.20). Also the REE are now completely eluted from the resin using 2.0 M HNO_3. This has the advantage of reducing the matrix interferences in the ICP due to elevated backgrounds caused by the amount of energy required to dissociate the acid, and viscosity effects due to high acid concentrations. However, recoveries are on average 5% lower than for Chromatography 2 and Chromatography 3.

FIGURE 4.20 CHROMATOGRAPHY 4

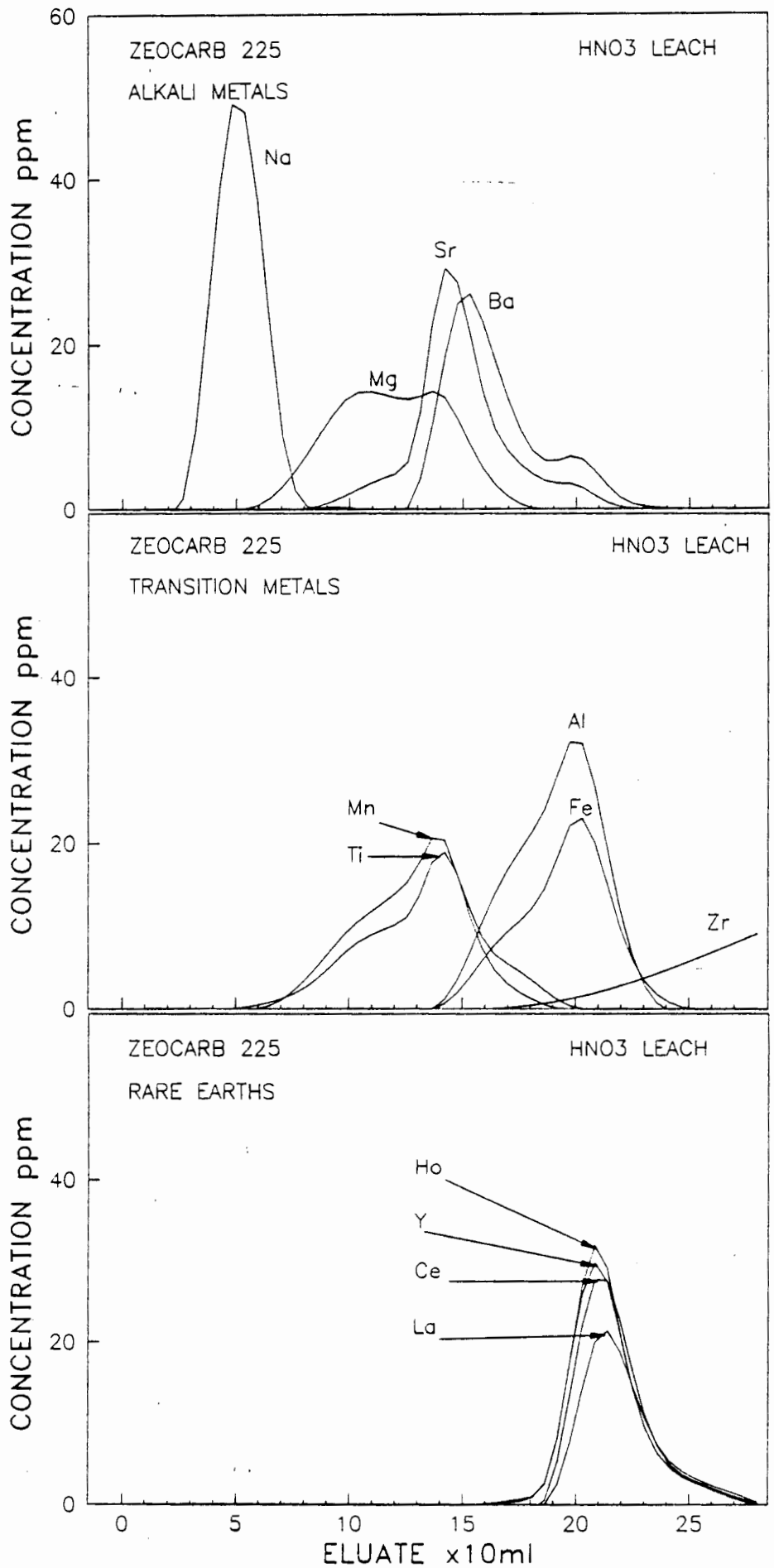

4.2.5 CHROMATOGRAPHY 5

Using the same column, 20 ml of a solution containing 50 ppm of all elements with 10 mls of a pH 5 buffer were loaded onto the column. With the results of the previous experiment it was decided to investigate the effect of increasing the volume of low acid concentration on the elution patterns, with a view to increasing the separation of the alkali and alkali-earth elements from the REE fractions. Elution procedure was as follows:

1) Elute with 250 ml of 0.5 M HNO_3.

2) Elute with 90 ml of 1.5 M HNO_3.

3) Elute with 60 ml of 6.0 M HNO_3.

Since the volume of eluate was expected to be approximately 450 ml, aloquots collected were 20 cm^3.

Results show that the acid concentration of the eluate for the first two stages of the gradient elution was too low. (Figure 4.21). Only sodium was eluted in this region. The remaining elements were all eluted with 6.0 M HNO_3. The anomolous elution patterns of Fe, Ca and Ba can be attributed to an incorrectly prepared resin. Up to this point in the investigation of chromatographic separations, the resin had been prepared for use by washing with 2.0 M nitric acid. This was not sufficient to remove some of the elements likely to be contaminating the resin after manufacture. The high concentrations of sodium eluted are due to the presence of sodium in the buffer solution

FIGURE 4.21 CHROMATOGRAPHY 5

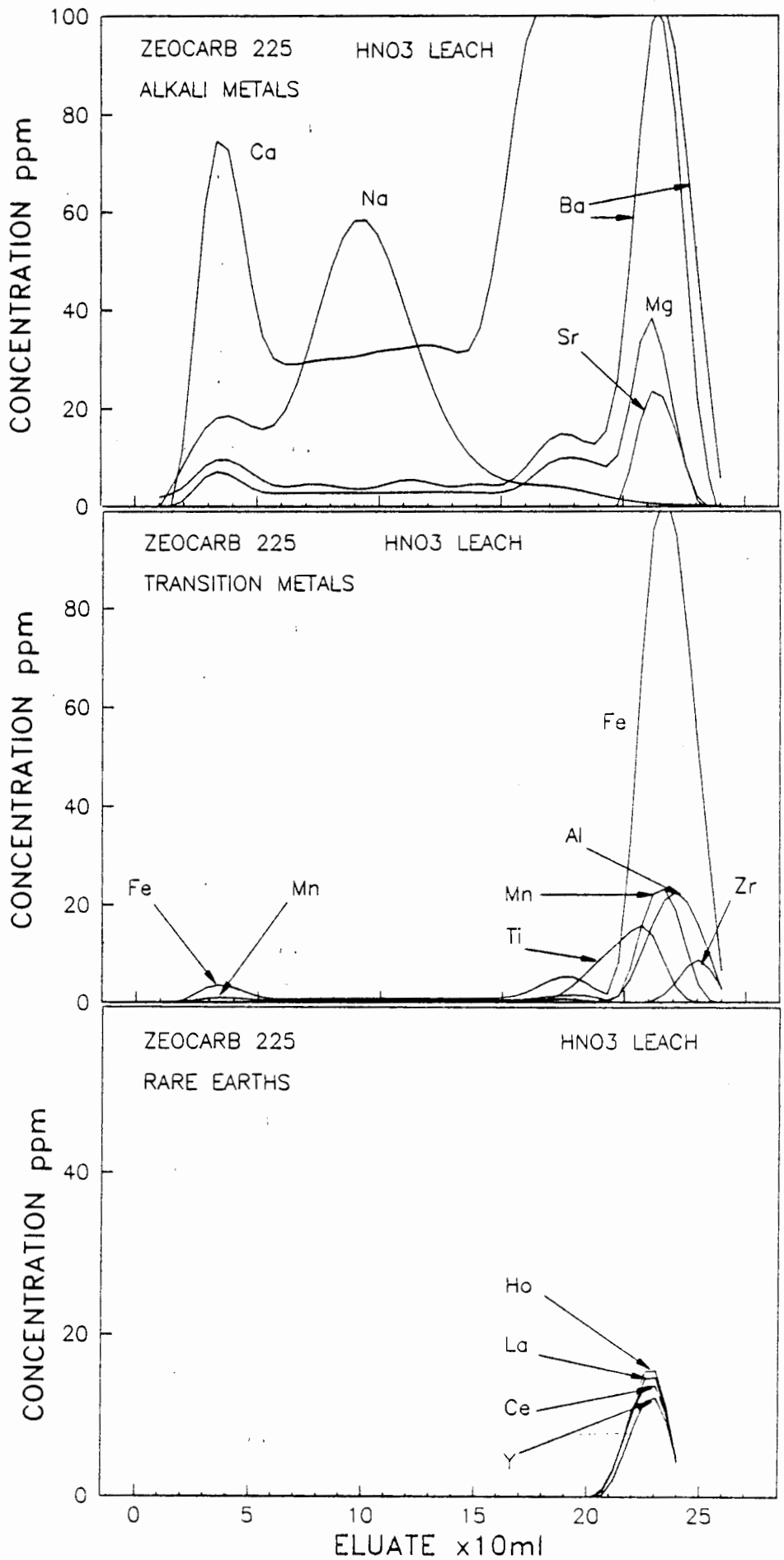

which is added to the load solution, before passing the load solution through the column.

4.2.6 CHROMATOGRAPHY 6

A different resin bed was used during this experiment. A 20 cm column of 30 mm diameter of Zeocarb 225 was prepared in the manner described in Chapter 3. The column was loaded with a 20 ml solution containing 50 ppm of all elements, to which 10 ml of pH 5 buffer had been added. The loaded metals were eluted from the column in the following manner:

1) Elute with 150 ml of 1.0 M HNO_3.

2) Elute with 70 ml of 2.0 M HNO_3 .

3) Elute with 60 ml of 3.0 M HNO_3.

4) Elute with 60 ml of 5.0 M HNO_3.

5) Elute with 50 ml of 10.0 M HNO_3.

Aloquots were collected in 20 ml volumes.

Sodium is eluted with the 1.0 M acid fraction. The alkali earth elements are eluted with the 2.0 M acid fraction. The transition element group is eluted over a wide range of acid concentrations, from 1.0 M to 10.0 M HNO_3. The REE begin to elute with the 2.0 M acid fraction, and are stripped more rapidly in 3.0 M and 5.0 M acid (Figure 4.22). Complete separation of the REE from the alkali and alkali-earths, manganese and titanium

FIGURE 4.22 CHROMATOGRAPHY 6

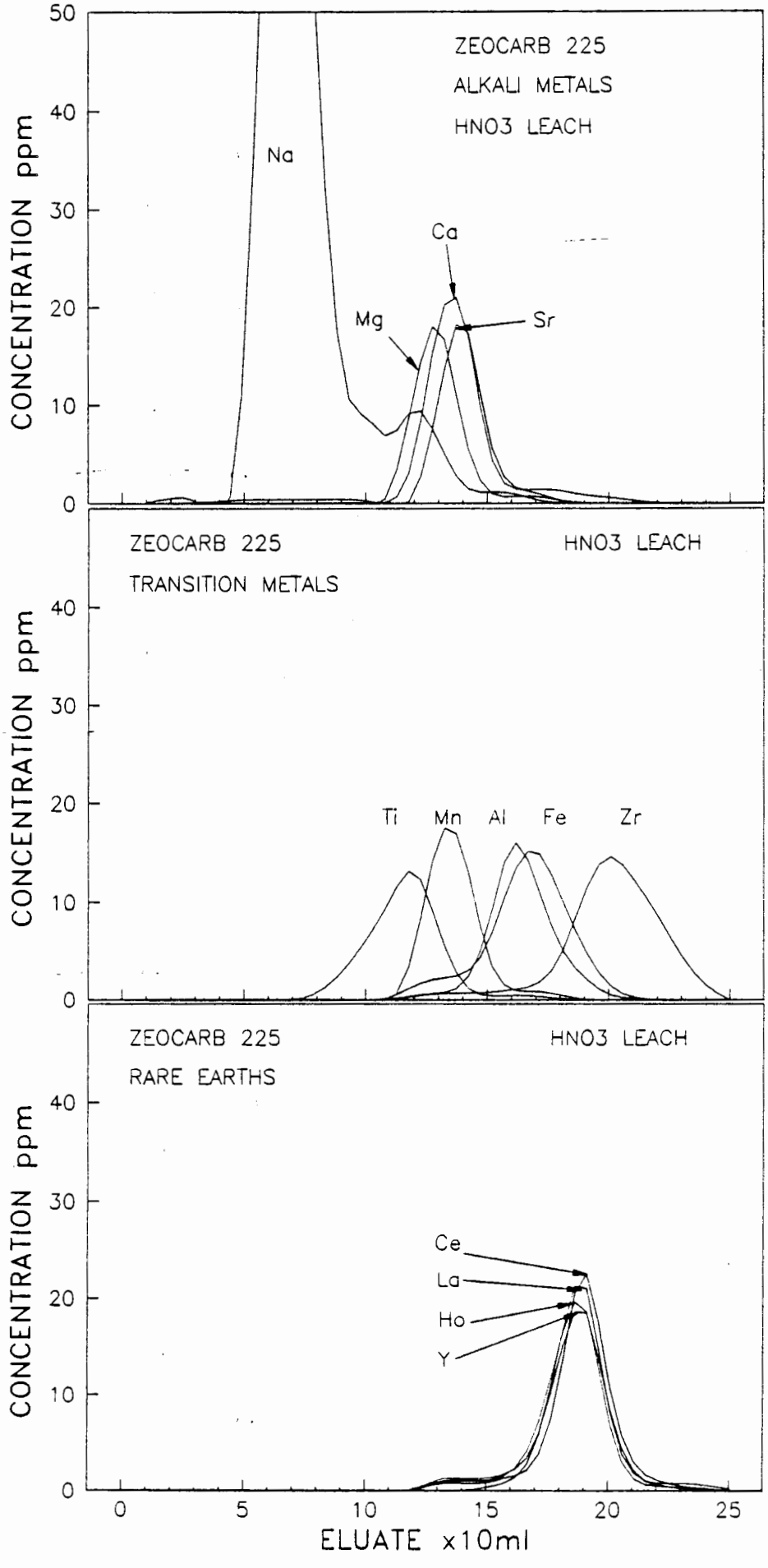

is achieved. This experiment shows that each of the non-REE elements are eluted from the column under slightly different conditions, the affinity of the elements for the active group on the resin being in the order:

$$Na < Ti < Mg < Mn < Ca < Sr < Al < Fe < REE < Zr$$

This is due to the affinity of the elements for the SO_2O^- group when compared with their affinity for the NO_3^- group in solution. All the peaks show a high degree of tailing which is due to deviations in flow of the mobile phase through the stationary phase such as eddy diffusion, mobile phase mass transfer, and stagnant mobile phase mass transfer. This is possibly a function of the length of the columnn, the increase in length leading to increased band spreading. Yields of REE are 110 $\pm$ 3.5% for this experiment.

4.2.7 CHROMATOGRAPHY 7

Chromatography 7.1, (Figure 4.23) and 7.2, (Figure 4.24) shows a comparison of Dowex 50-W-X8 and Zeocarb 225, as the stationary phase for group separation of REE from other matrix elements. Both columns were 10 cm in height and 20 mm in diameter and were loaded with 20 ml of solution containing 50 ppm of all elements buffered with 10 ml of a pH 3 buffer. Elution was as follows:

1) Elute with 100 ml of 1.0 M HNO_3.

2) Elute with 100 ml of 3.0 M HNO_3.

3) Elute with 60 ml of 5.0 M HNO_3.

4) Elute with 50 ml of 8.0 M HNO_3.

A comparison of the elution patterns shows that there is little difference in the overall elution pattern of the elements. However, with Dowex 50-W-X8 the REE are eluted at slightly higher acid concentrations, and show a greater degree of band spreading, the REE being eluted in a 100 ml fraction, compared with 80 ml for Zeocarb 225. Both REE fractions begin eluting with 3.0 M HNO_3, but complete removal of the REE from the Dowex 50-W-X8 required 5.0 M HNO_3. The degree of separation from the alkali and alkali-earths was found to be the same.

A comparison of the recoveries for the REE shows that not all the REE have been stripped from the Dowex 50-W-X8 resin as is seen in Table 4.1.

TABLE 4.1. Percentage Recoveries of the four REE analysed from Zeocarb 225 and Dowex 50-W-X8.

RESIN	% RECOVERY REE			
	La	Ce	Y	Ho
Zeocarb 225	114.1	110.3	110.3	108.3
Dowex 50-W-X8	85.3	90.0	88.7	93.6

FIGURE 4.23 CHROMATOGRAPHY 7.1

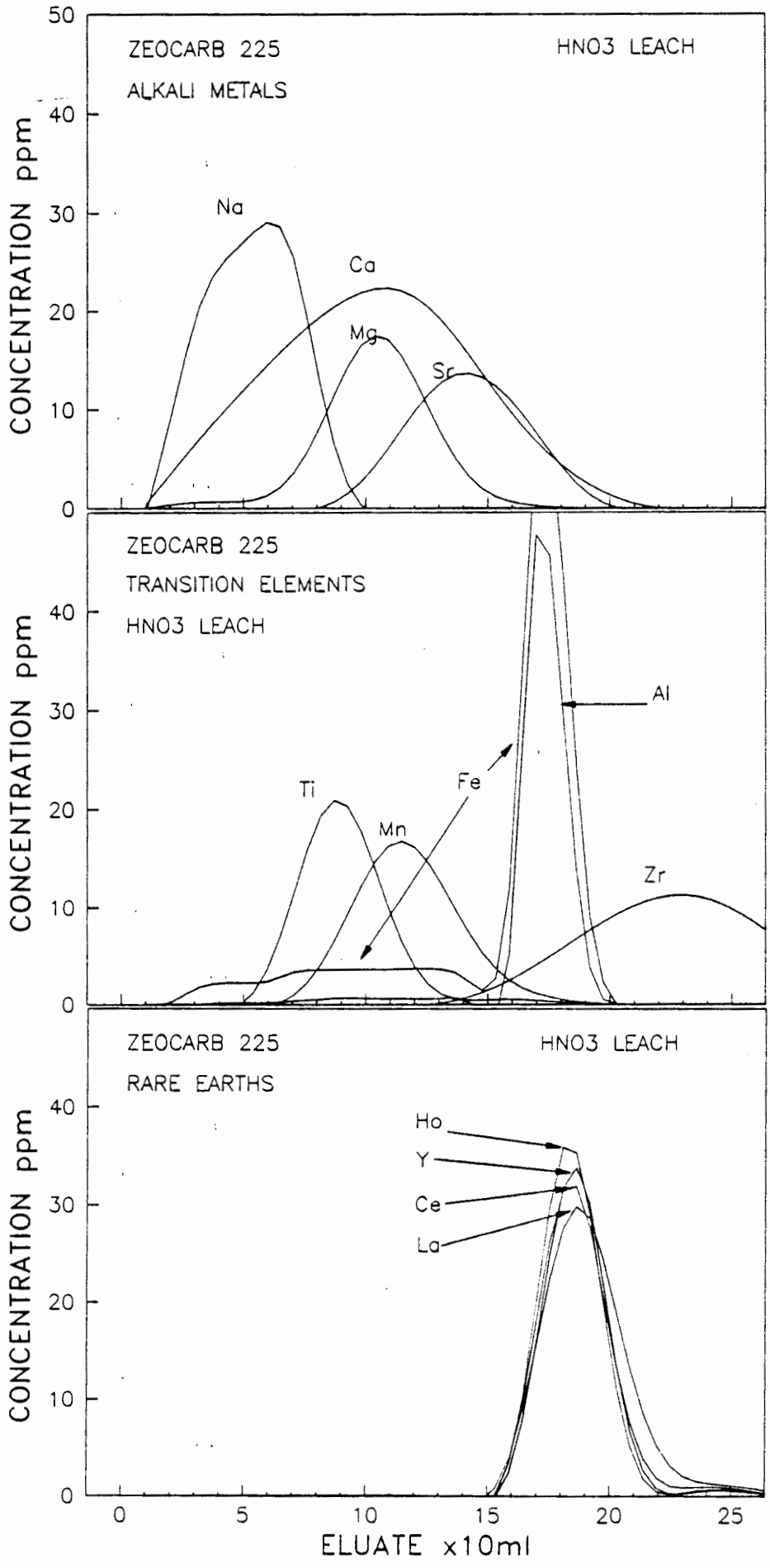

FIGURE 4.24 CHROMATOGRAPHY 7.2

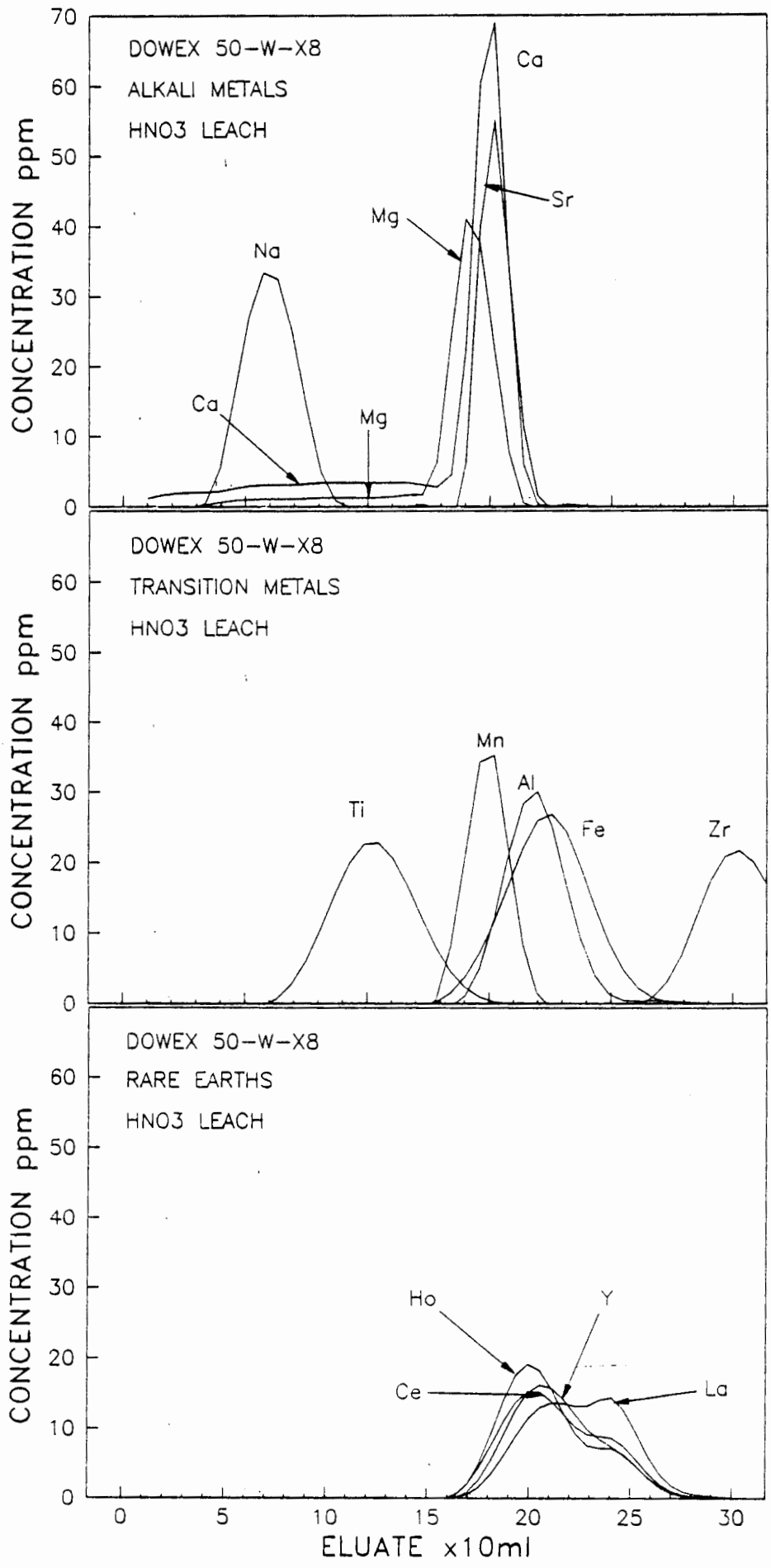

4.2.8 CHROMATOGRAPHY 8.

An experiment was conducted to observe the feasibility of loading the resin with REE and analysing the resin by a slurry injection method directly into the ICP without any elution steps. All three resins, Amberlite IR 120 (H), Zeocarb 225 and Dowex 50-W-X8 were all ground to 250 mesh in an agate ball grinder. Two grams of the dry ground resin were weighted into a 25 ml pill vial. 5 ml of a solution containing 20 ppm of all elements were added to each vial, the solutions being made up to have final log $[H^+]$ values of -5.0, -4.0, -3.0, - 2.0, - 0.19, 0.0, 0.12, 0.30 and 0.78 using the appropriate buffers or nitric acid to give a final volume of 15 ml. All the vials were shaken for 5 minutes and allowed to stand to reach equilibrium. The liquid was then analysed to determine the amount of metal in solution, and consequently the amount still bonded to the resin.

Results for Amberlite IR 120 (H), (Figure 4.25), and Zeocarb 225 (Figure 4.26), show that REE are completely held by the resin until pH 2 and pH 1 respectively. Dowex 50-W-X8, (Figure 4.27), shows that at pH 4 and pH 5 the REE were not completely loaded onto the resin. Generally in ion-exchange chromatography the rule is that, for ions of the same valency, the affinity for the ion increases with molecular weight, and also increases with increase in valency. This would explain why Na is not loaded at low hydrogen ion concentrations, (high pH) and is present in all solutions equilibrated with the resins. The anomolus REE results may be due to the degree of

hydrolysis of the REE, but if this was the case, one would expect this effect to be observed with the other resins.

Zeocarb 225 shows the highest affinity for the metals analysed, requiring stronger acidic conditions to remove the ions from the resin. Results are anomolus as at an acid concentration of 6.0 M HNO_3, all the REE and Zr are completely removed from the resin, while some Ti, Mn, Al, Ca, Mg and Sr are bonded to the resin at this acid concentration. However at an acid concentration of 0.66 M, only small amounts of REE and Zr are present in solution in comparison with the rest of the elements analysed.

These experiments show that the loading and elutions of various resins will vary depending upon the structure of the resin and are not totally predictable when resins of the same type with the same active groups are used. From these results and results of previous experiments most work was carried out using Zeocarb 225.

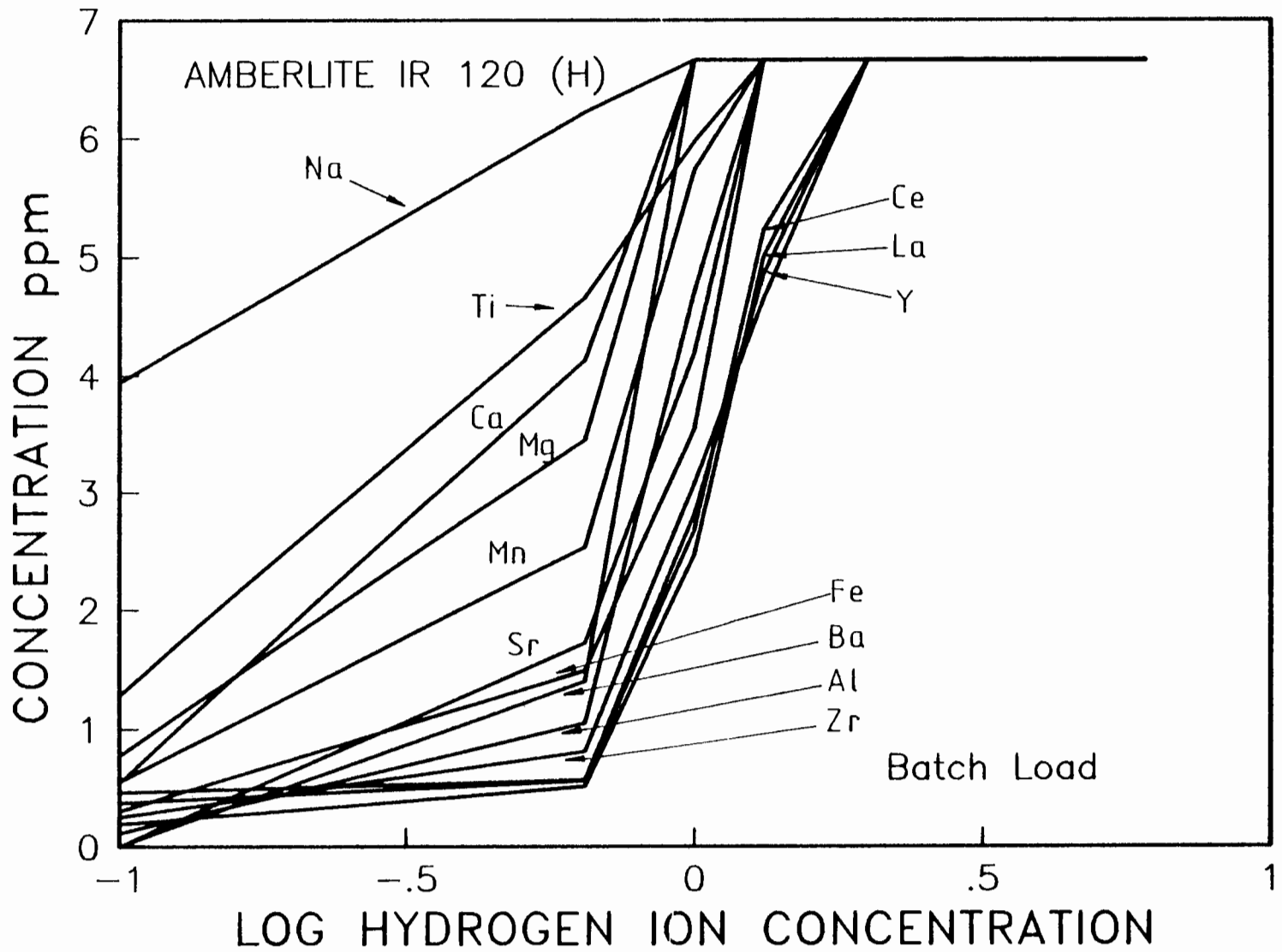
CHROMATOGRAPHY 8A
AMBERLITE IR 120 (H)
Na
Ti
Ca
Mg
Mn
Sr
Fe
Ba
Al
Zr
Ce
La
Y
Batch Load
CONCENTRATION ppm
0
1
2
3
4
5
6
7
−1
−.5
0
.5
1
LOG HYDROGEN ION CONCENTRATION

FIGURE 4.25

CHROMATOGRAPHY 8B

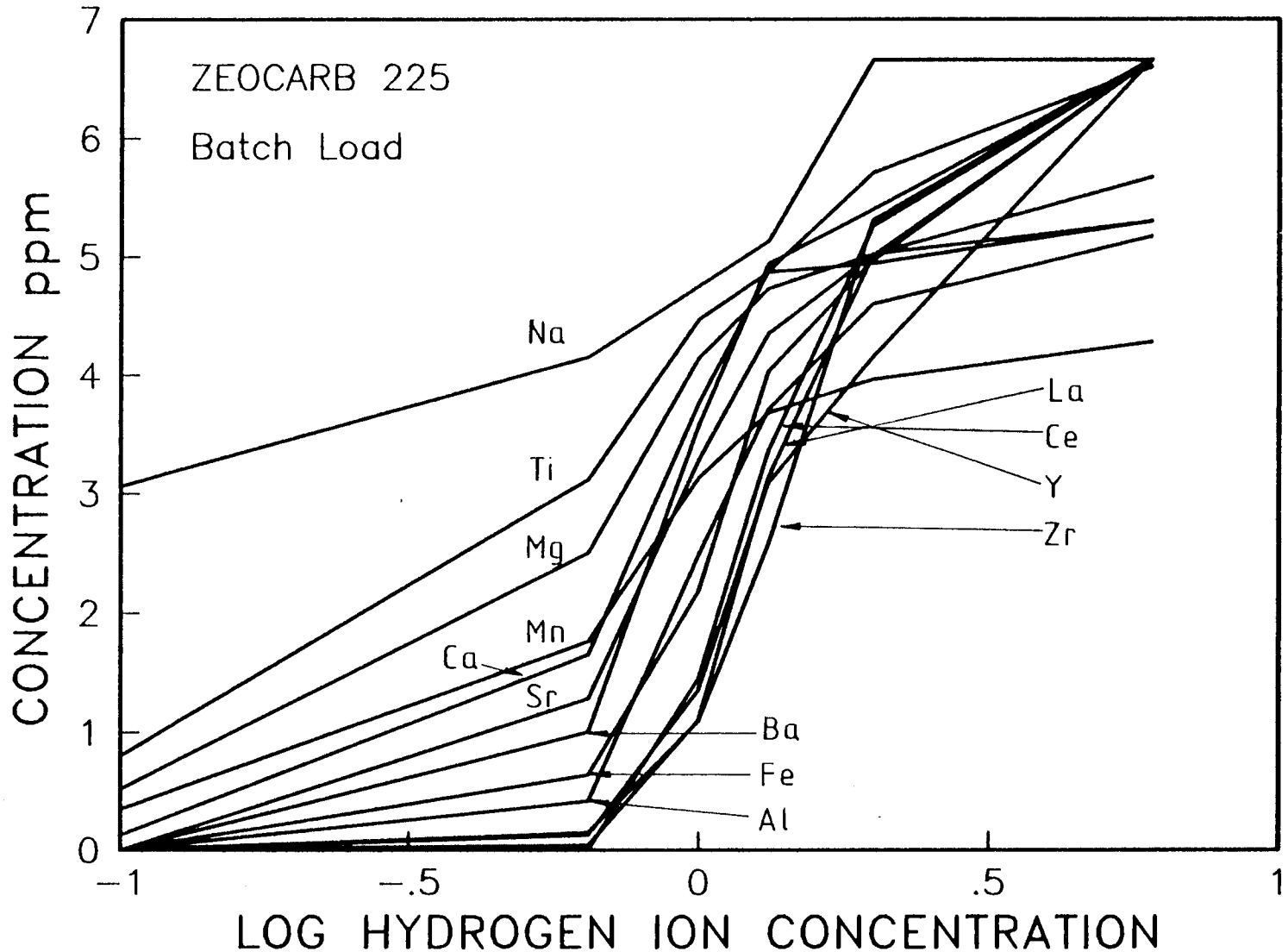

FIGURE 4.26

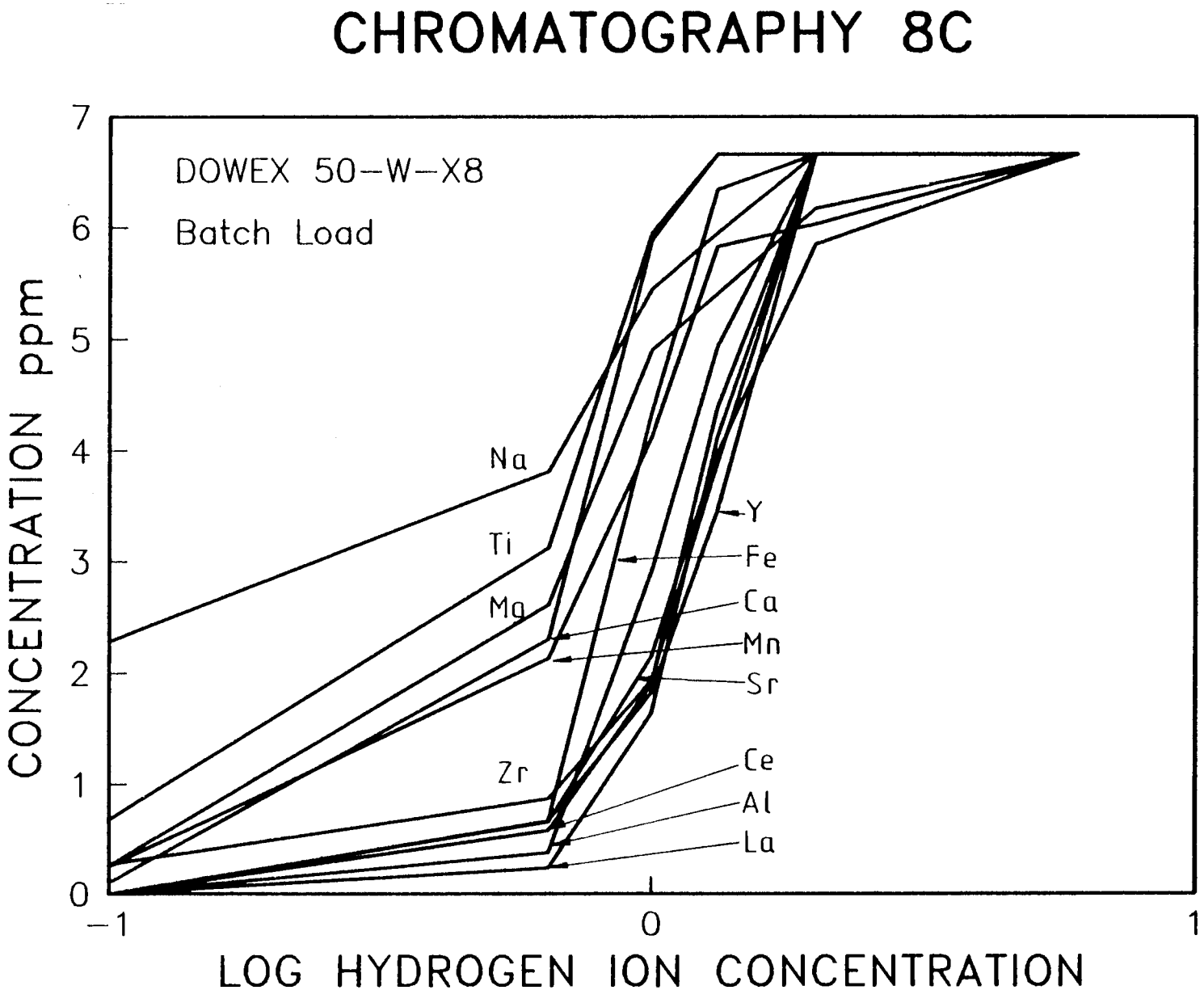
CHROMATOGRAPHY 8C
DOWEX 50-W-X8
Batch Load
CONCENTRATION ppm
LOG HYDROGEN ION CONCENTRATION
0
1
2
3
4
5
6
7
−1
0
1
Na
Ti
Mg
Zr
Y
Fe
Ca
Mn
Sr
Ce
Al
La

FIGURE 4.27

4.2.9 CHROMATOGRAPHY 9

The concentration of acid used to elute metals from the column was reduced for this experiment using results obtained from chromatography 7. In addition, the means of adding the eluting acid to the column was changed. Instead of filling all vacant space above the resin in the column with acid, the acid was allowed to flow down the side of the column at the same rate as acid passed through the resin column. This was done to reduce variations in hydrostatic pressure throughout the experiment, as these variations may affect the flow rate, and consequently the reproducibility of separations carried out on the column. Elution was carried out as follows:

1) Load a Zeocarb 225 15 cm by 20mm diameter column with 25 ml of a solution containing 20 ppm of all metals.

2) Elute with 50 ml of 1.0 M HNO_3.

3) Elute with 50 ml of 1.5 M HNO_3.

4) Elute with 100 ml of 3.0 M HNO_3.

5) Elute with 50 ml of 5.0 M HNO_3.

Results (Figure 4.28), show that a reduction in acid elution concentration increased the degree of band spreading of the non-REE elements, for example, Fe. The reason for this could be attributed to the fact that a 1.5 M HNO_3 elution concentration is close to the critical point where the affinity of Fe for the SO_2O^- group on the

resin is close to the affinity of Fe for the NO_3^- ion in solution. If this acid concentration is plotted on diagram Chromatography 8B, (Figure 4.28), the observed distribution of Fe between the aqueous phase and the resin is: 63.56 µg in solution and 36.44 µg on the resin. Using 1.0 M HNO_3 the distribution is: 32.7 µg in solution and 67.3 µg on the resin. Thus Fe will be eluted slowly while the eluting acid concentration is 1.0 M but will be eluted more rapidly when the acid concentration is 1.5 M due to the position of the equilibrium in the reaction:

$$(R\text{-}SO_3)_3\text{-}Fe^{3+} + 3H^+ \rightleftharpoons 3RSO_3\text{-}H^+ + Fe^{3+}$$

Alternatively, spreading may be attributed to the presence of both Fe^{2+} and Fe^{3+} on the column, different elution patterns being expected due to the different oxidation states.

Separation of the REE from all elements except Fe and Al has been achieved. It was found that the concentration of the acid used in elution was critical when determining the degree of separation obtained. Since Fe interferes with REE during spectrometric analysis, and both Fe and Al represent the expected behaviour of other elements such as V, Zn and Cu [57, 58]. It was decided to optimize the separation of Fe and Al from the REE, without adding any other elements to the synthetic solutions as their behaviour during elution was characterized by the relative elution of positions of Fe and Al.

Anomolous results for Ca, Na, Fe and T, were due to a poorly prepared resin and deviations in calibration of the ICP during analysis of the eluate.

REE recoveries from the resin were as follows: La, 98.93%; Ce, 92.03%; Y, 100. 90%; and HO 101.15%, giving a mean recovery of 95.5% $\pm$ 4.27% which is analytically acceptable.

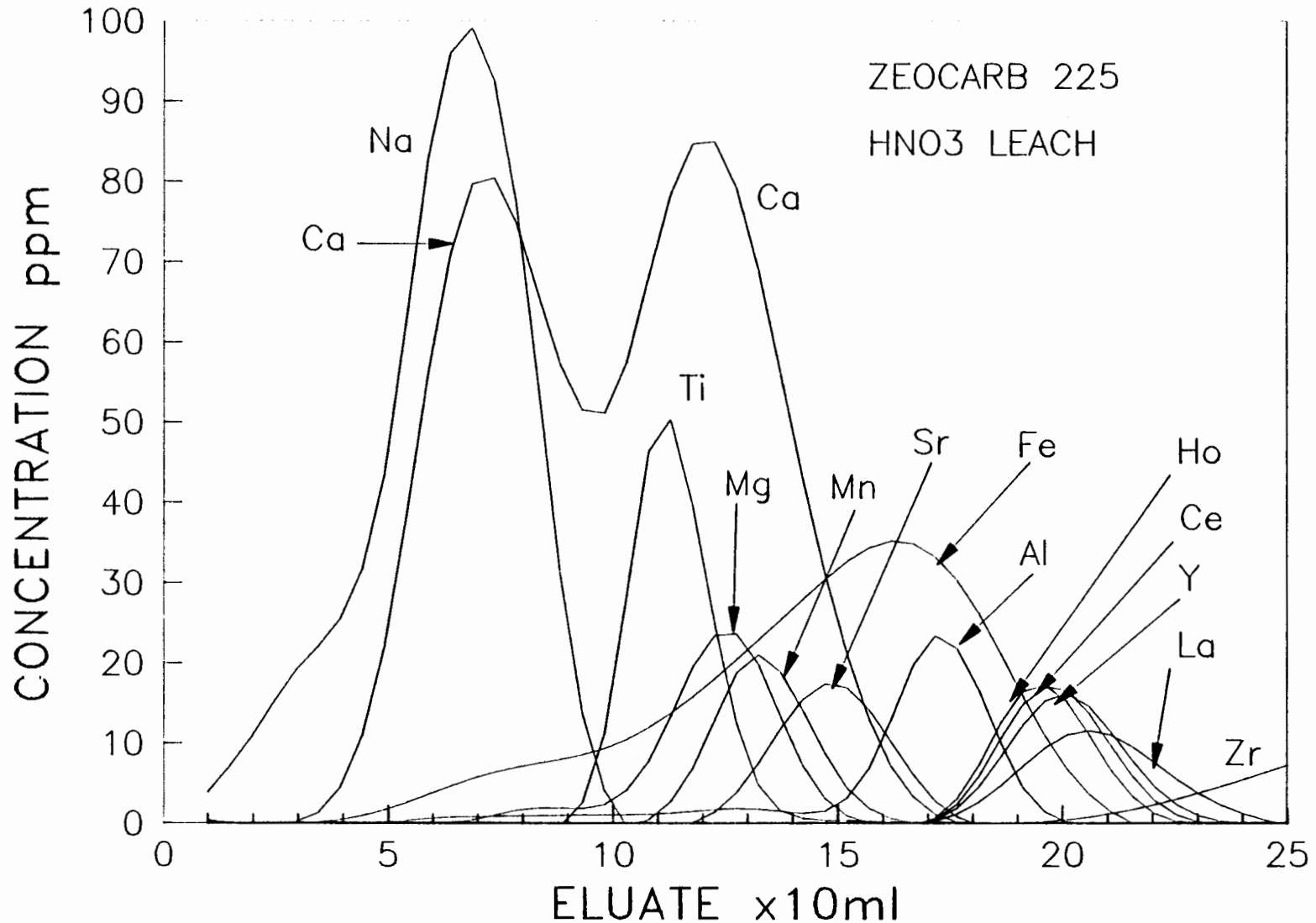
CHROMATOGRAPHY 9
ZEOCARB 225
HNO3 LEACH
CONCENTRATION ppm
ELUATE x10ml
100
90
80
70
60
50
40
30
20
10
0
0
5
10
15
20
25
Na
Ca
Ca
Ti
Mg
Mn
Sr
Fe
Al
Ho
Ce
Y
La
Zr

FIGURE 4.28

4.2.10 CHROMATOGRAPHY 10

Using the results obtained from Chromatography 9, the acid concentration of the eluate was reduced. The elution procedure was as follows:

1) Load a 15 cm by 20 mm diameter column of Zeocarb 225 with 25 ml of a standard solution containing 20 ppm of La, Ce, Y and Ho and 50 ppm of Al, Fe and Zr.

2) Elute with 100 ml of 1.5 M HNO_3.

3) Elute with 50 ml of 2.0 M HNO_3.

4) Elute with 50 ml of 3.0 M HNO_3.

The introduction of the 2.0 M acid elution step between the 1.5 M amd 3.0 M acid elution steps improved the degree of separation of the REE fraction from Fe and Al. From the chromatogram, (Figure 4.29) Fe was removed slowly at an acid concentration of 1.5 M H^+, but was removed more rapidly at 2.0 M H^+. Also it was found that the REE fraction was only eluted with 3.0 M acid as the eluate. At this acid concentration the two groups of REE were observed to separate slightly indicating that they behaved slightly differently in their elution behaviour. Thus an increased volume of 3.0 M acid would be required to entirely remove the REE from the resin, introducing errors in analysis of the resulting solution. Recovery of the REE was 89.46% $\pm$ 8.31%.

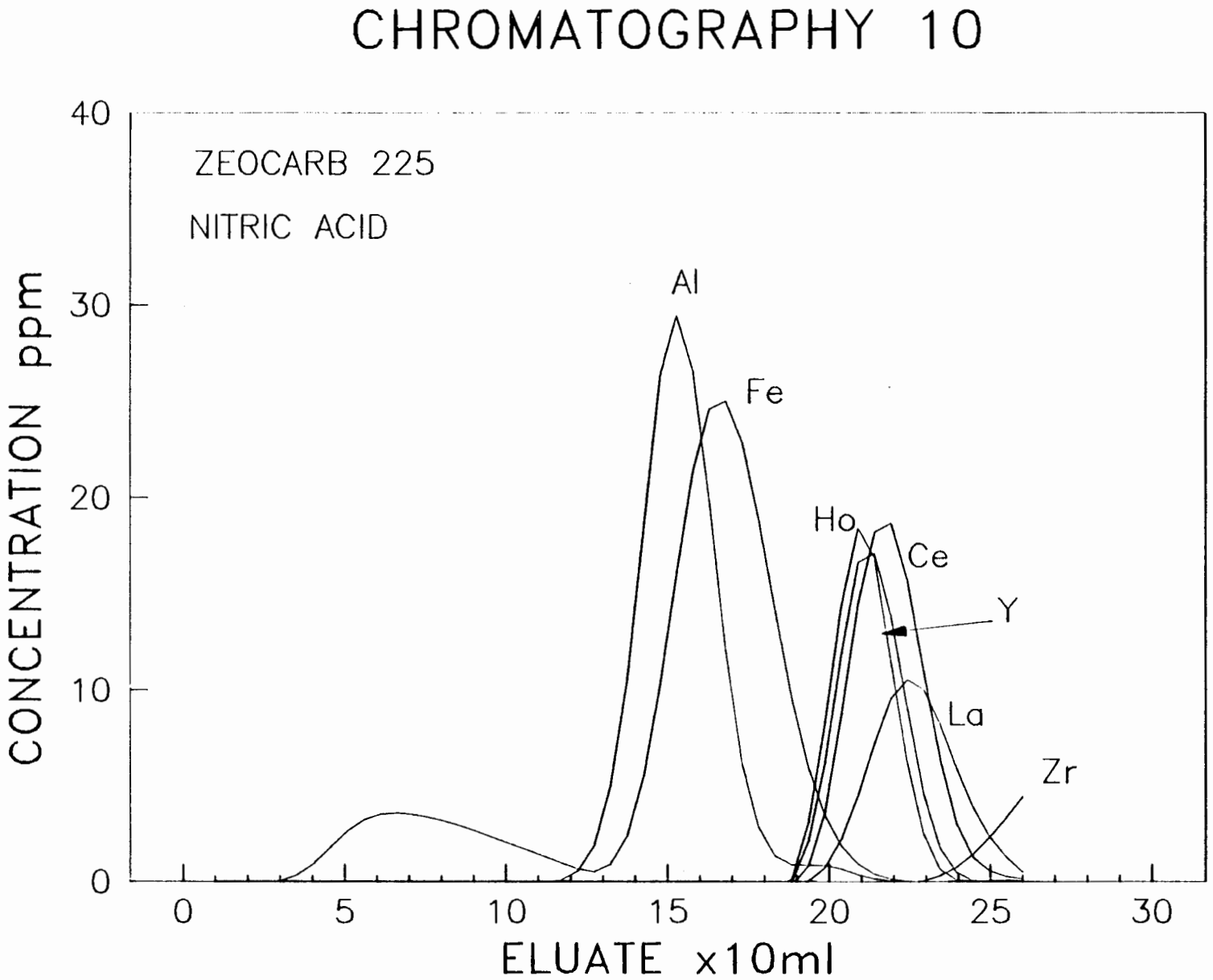
CHROMATOGRAPHY 10
ZEOCARB 225
NITRIC ACID
CONCENTRATION ppm
ELUATE x10ml
Al
Fe
Ho
Ce
Y
La
Zr
0
10
20
30
40
0
5
10
15
20
25
30

FIGURE 4.29

4.2.11 CHROMATOGRAPHY 11

This experiment was performed in an identical manner as Chromatography 10 except that the volume of 2.0 M acid used in elution was increased to 100 ml. The eluate from the column loading solution and the 1.5 M acid fraction was collected as a single aloquot and analysed, before individual 10 ml aloquots were collected and analysed. The column eluate and 1.5 M acid fraction showed no metal content (Figure 4.30). With an increased volume of 2.0 M acid used in elution, the REE indicator elements were observed to elute with this fraction, peaks showing a high degree of band spreading, with the volume of the REE fraction collected being 140 ml. These results, in comparison with both Chromatography 9 and Chromatography 10 may be explained by the equilibrium.

$$(R\text{-}SO_2O^-)_3\ M^{3+} + 3H^+ \rightleftharpoons 3R\text{-}SO_2OH + M^{3+}$$

Considering the concentrations of the M^{3+} ions in solution, an increase in M^{3+} ions will force the equilibrium to the left. Thus, while there are high concentrations of Al^{3+} and Fe^{3+} present in the 2.0 M eluent, the REE are not eluted from the resin. However, as the concentration of Al^{3+} is reduced the equilibrium will shift to the right, and elution of the REE will begin. However, this hypothesis must be viewed in conjunction with the fact that the affinity of a resin for metals will increase with increased ionic radius for the same group [143] . If we consider the ionic radii: Al^{3+}, 0.45 Å; Fe^{3+}, 0.50 Å; Ho^{3+}, 0.89 Å; Y^{3+}, 0.90 Å; Ce^{3+}, 1.02 Å and La^{3+}, 1.04 Å [144], then La should

have the highest affinity with the resin, and Al^{3+} the lowest. This confirms the order of elution of the elements of interest.

In Chromatography 9, not all the Fe^{3+} and Al^{3+} had been removed from the resin by the 1.5 M HNO_3 acid, and the REE are eluted with the increase in $[H^+]$, in this case with 3.0 M HNO_3. With Chromatography 10, the 1.5 M HNO_3 elutes very little Fe^{3+}, the remainder. along with Al^{3+} being eluted with 2.0 M HNO_3. The volume of 2.0 M HNO_3 is just sufficient to elute the Fe^{3+} and Al^{3+},and consequently no REE is eluted. However in Chromatography 11, the volume of 2.0 M HNO_3 is sufficient to elute all the Fe^{3+} and Al^{3+}, as well as a portion of the REE, which are only eluted once the concentrations of Fe^{3+} and Al^{3+} are low. 2.0 M HNO_3 does not remove REE from the resin very rapidly. Thus to obtain separation of REE from Al^{3+} and Fe^{3+}, the acid used to elute must be sufficiently strong to elute Fe^{3+} and Al^{3+} without eluting the REE, and must have a concentration between 1.5 M and 2.0 M .

Recoveries of REE were 99.69 $\pm$ 7,70 %.

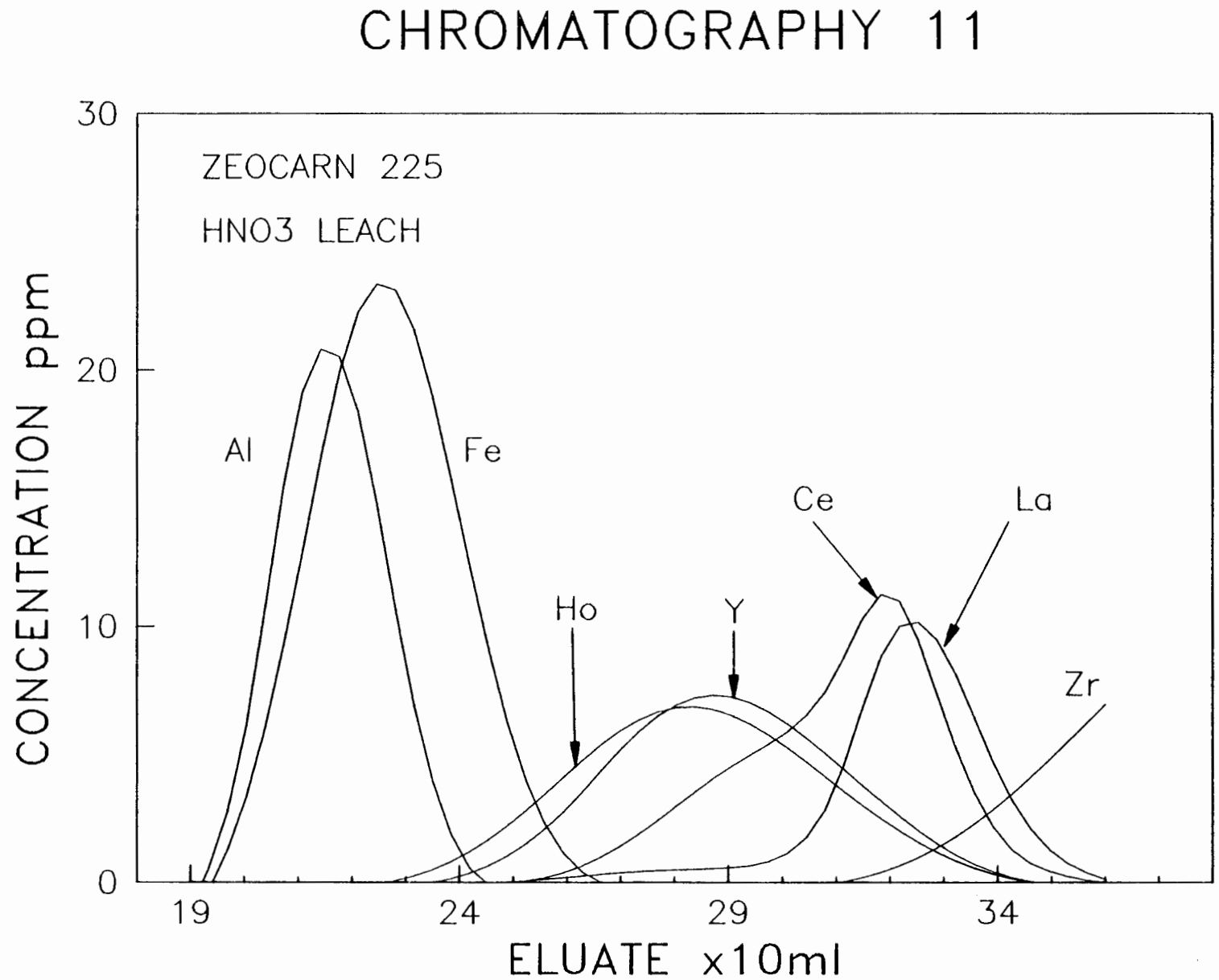
CHROMATOGRAPHY 11
ZEOCARN 225
HNO3 LEACH
CONCENTRATION ppm
30
20
10
0
Al
Fe
Ho
Y
Ce
La
Zr
19
24
29
34
ELUATE x10ml

FIGURE 4.30

4.2.12 CHROMATOGRAPHY 12

Two identical Zeocarb 225 columns were prepared. Each 15 cm by 20 mm diameter column was loaded with a 20 ml solution containing 20 ppm of La, Ce, Y and Ho and 50 ppm Al, Zr and Fe. The columns were eluted as follows:

1) Elute with 100 ml of 1.8 M H^+.

2) Elute with 70 ml of 3.0 M H^+.

A comparison of the two chromatograms showed that the REE were eluted as a group with nitric acid, (Figure 4.31), but showed more distinct band spreading and inter-element separation with HCl, (Figure 4.32). The degree of separation of zirconium from the REE was improved with nitric acid.

The most important difference between the two chromatograms was the elution behaviour of Fe in relation to Al. With HNO_3 elution, Al is eluted first and Fe second. With HCl elution, the reverse occurs. In a hydrochloric acid medium the predominant Fe species present in solution is the hexachloroferrate (III) anionic complex. In nitric acid, Fe is mainly present as the cation, Fe^{3+}. Fe, as the anionic complex is not held by the resin and is eluted more rapidly with HCl, but with HNO_3 as the eluting acid, Fe as the cation will tend to elute with the REE fraction. Since the overlap of Al and Fe on REE must be minimized, an experiment was carried out using a combination

FIGURE 4.31 CHROMATOGRAPHY 12a

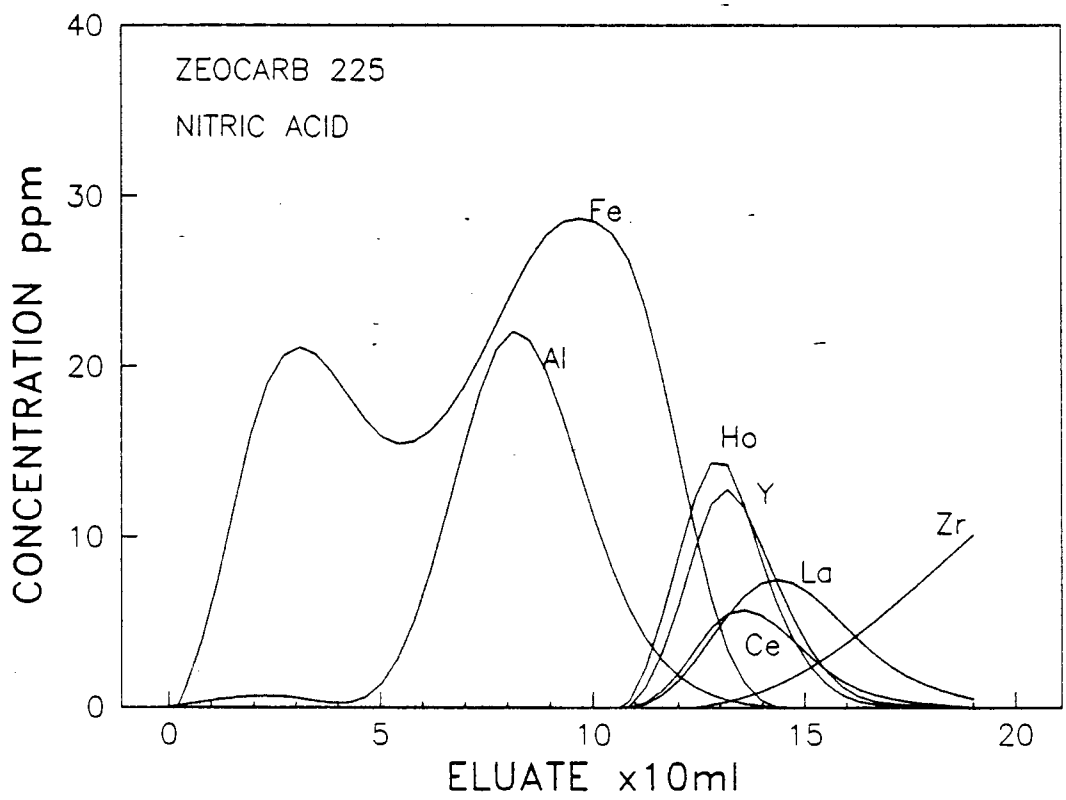

FIGURE 4.32 CHROMATOGRAPHY 12b

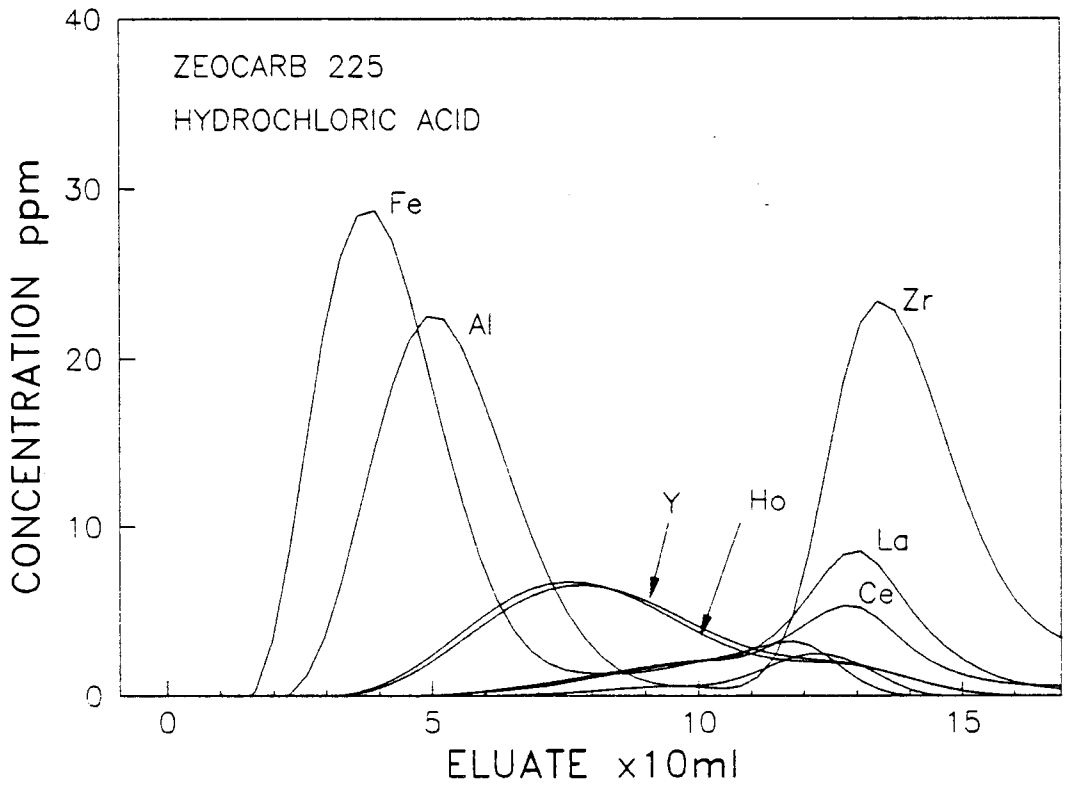

of the two acids, with the aim of obtaining identical elution patterns with Al and Fe.

Due to incomplete elution, no recoveries of REE were calculated.

4.2.13 CHROMATOGRAPHY 13

Two Zeocarb 225 columns were prepared, with each 15cm by 20mm diameter column loaded with a 20 ml solution containing 50 ppm of Al, Fe and Zr, and 20 ppm of La, Ce, Y and Ho. Elution of the columns were as follows:

Column A

1) Elute with 50 ml of a 1.5 M H^+ containing 0.75 M NO_3^- and 0.75 M Cl^-.

2) Elute with 100 ml of 1.8 M H^+ solution containing 0.9 M NO_3^- and 0.9 M Cl^-.

3) Elute with 80 ml of 3.0 M HNO_3.

Column B

1) Elute with 50 ml of 1.5 M HNO_3.

2) Elute with 100 ml of 1.8 M HNO_3.

3) Elute with 80 ml of 3.0 M HNO_3.

A comparison of Figure 4.33 and 4.34 shows that the elution patterns were different. The order of elution of Al and Fe was reversed when the HNO_3: HCl 1:1 (V/V) mixture was used. However, the volume required to elute Al and Fe with the acid mixture was reduced. The heavy REE indicator elements, Y and Ho showed considerably less band

spreading with the nitric acid elution, while both elution patterns showed a distinct separation of the REE into two groups. With the mixed acid elution, the separation of Fe from REE was achieved, although some Al was eluted with the REE fraction. Using only nitric acid as eluent, Al was separated from the REE fraction but some Fe was observed to elute with the REE fraction. Since Fe is more likely to cause interferences during analysis of the REE in the ICP, the mixed acid elution technique showed some advantages with separation of Fe from the REE.

Recoveries of REE from the two columns can only be compared for the heavy REE as incomplete elution was achieved for the light REE. The results show that using the mixed acid elution method, recoveries of REE were approximately 10% better. These are shown in Table 4.2 .

TABLE 4.2 Percentage Recovery of heavy REE indicators from Zeocarb 225 using two different elution procedures.

ELEMENT	HNO_3/HCl (1:1)	HNO_3
Y	92.77%	83.59%
Ho	98.77%	88.67%

FIGURE 4.33 CHROMATOGRAPHY 13a

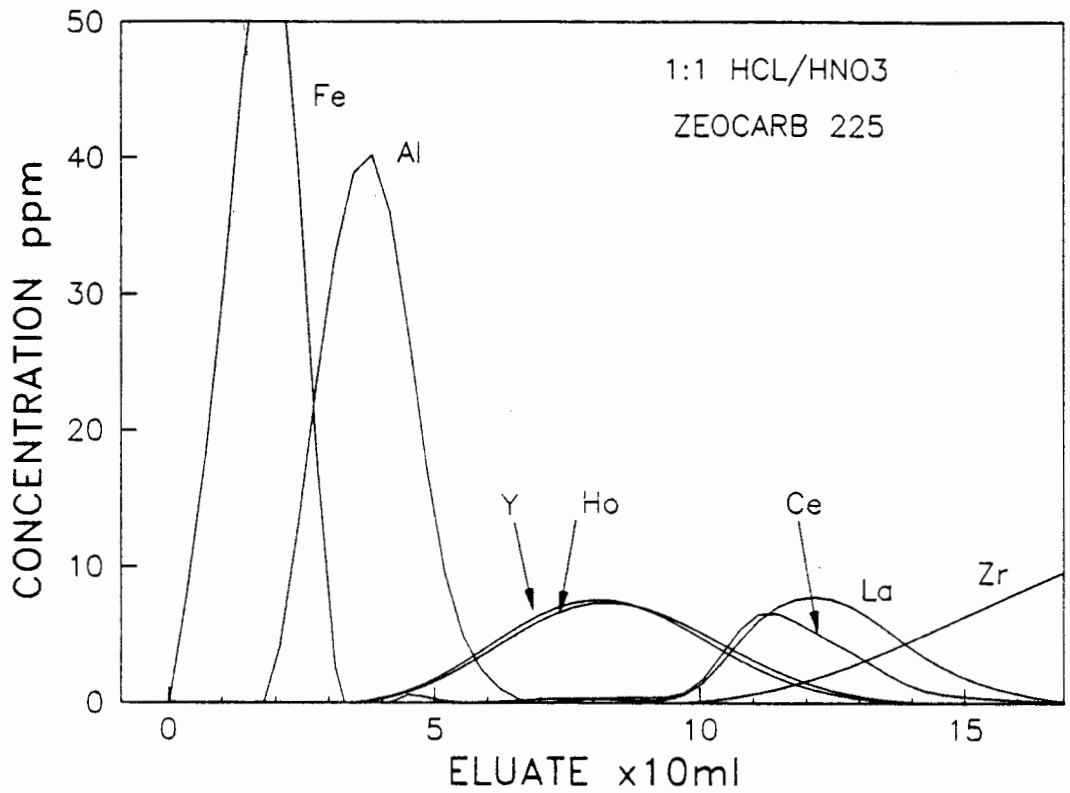

FIGURE 4.34 CHROMATOGRAPHY 13b

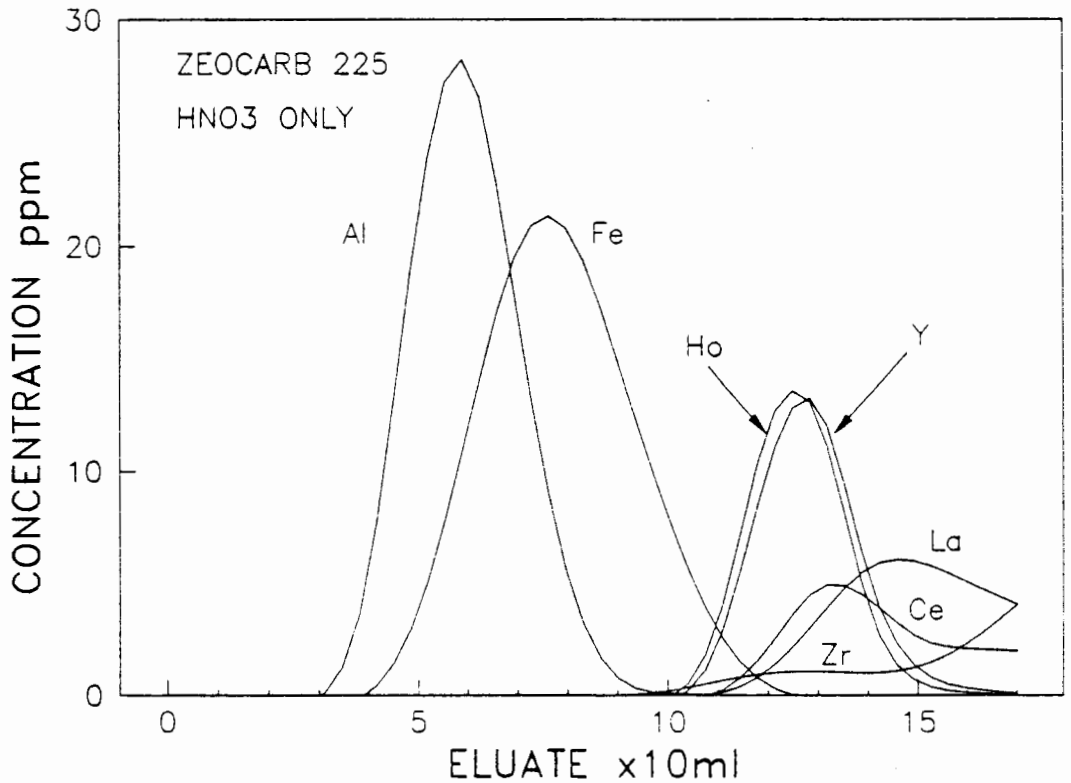

4.2.14 CHROMATOGRAPHY 14

Using the results above, the experiment was repeated using only mixed acid elution. Conditions for the experiment were identical except the initial elution step was carried out using a 1.44 M H^+ solution containing 0.72 M NO_3^- and 0.72 M Cl^-. The chromatogram shown in Figure 4.35 showed that complete separation of Fe and Al from the REE was achieved. Although La was not tested, Ce showed a high degree of band spreading using these elution conditions, which suggests that once the Fe and Al have been eluted from the column, a higher acid concentration would be used to elute the REE fraction. Also, since it was reported above, that the elution caused the REE to separate into two groups, only nitric acid should be used for elution after the Fe and Al have been eluted.

The elution behaviour of Fe and Al were similar using a 1.44 M H^+ or a 1.5 M H^+ mixed acid elution. However, although a greater degree of separation of the REE from Fe was achieved using a 1.44 M H^+ acid elution, the elution of Fe and Al required 100 ml of 1.44 M acid, but only 70 ml of 1.5 M acid. As increases in elution volume increased the time required to complete the analysis, the higher mixed acid concentration was used in the first elution step during experiments carried out with rock solutions.

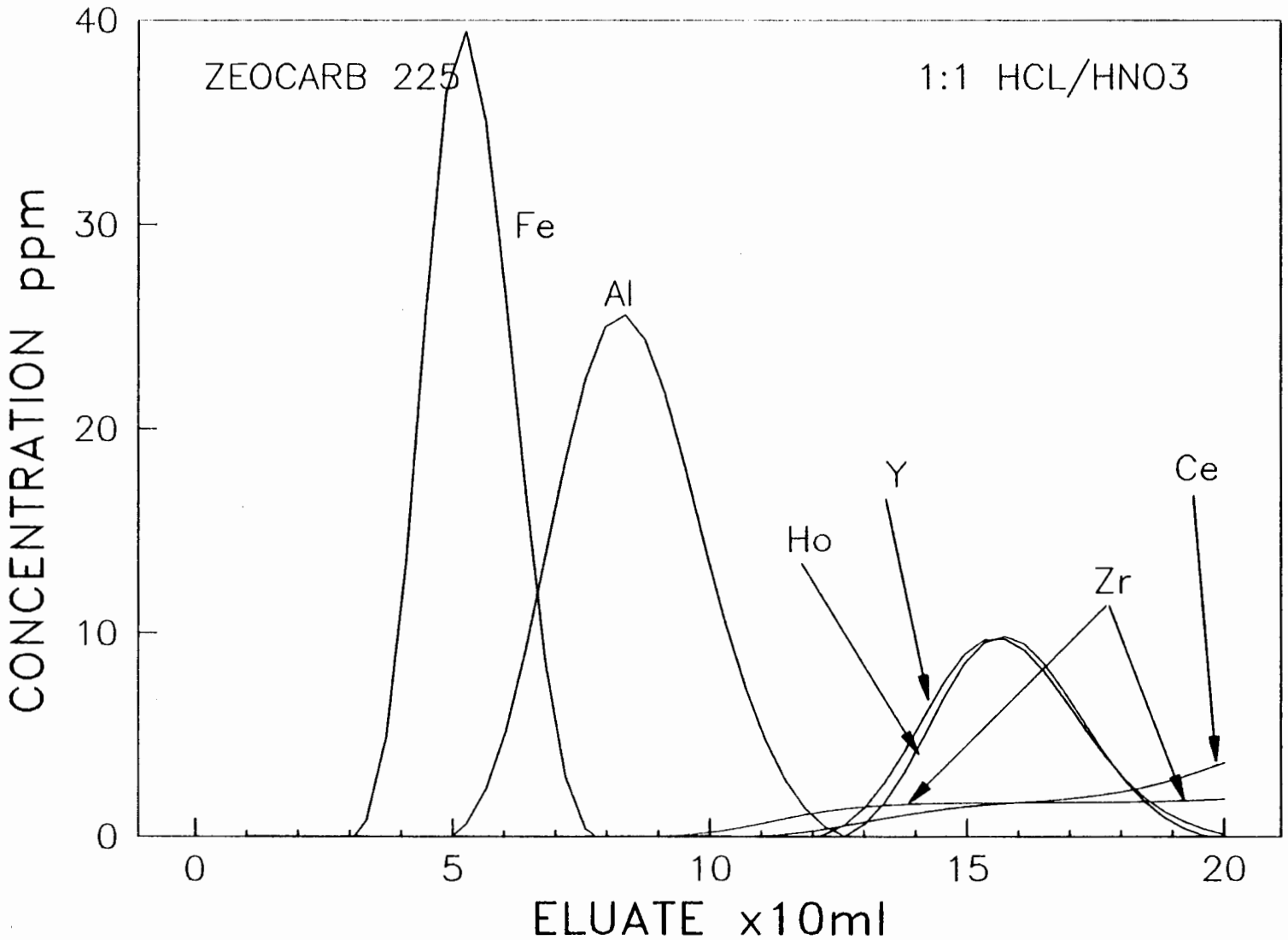
CHROMATOGRAPHY 14
ZEOCARB 225
1:1 HCL/HNO3
Fe
Al
Ho
Y
Zr
Ce
CONCENTRATION ppm
ELUATE x10ml
0
10
20
30
40
0
5
10
15
20

FIGURE 4.35

A comparison of this method with methods discussed in the literature [21,54,56-8,60] shows some advantages. Crock and co-workers [54,57,58] used 50 ml of 6.0 M H^+ to elute the REE from Bio-Rad AG 50-X8. This solution was evaporated to dryness before uptake into an appropriate solution. The use of strong acid elution means the resin could only be regenerated twenty times before resin breakdown was observed. With lower acid concentrations, the resin may be used for a longer period before resin breakdown was observed. Eby, [21] used 280 ml of 6.6 M HCl to elute the REE, while Walsh *et al* [60] used 500 ml of 4 M HCl and Brenner *et al*, [56] 400 ml of 4 M HCl. Volumes used to elute the REE fractions in these experiments were typically 100 ml. The reduced volume of acid passed through the column, normally 300 ml, allows a relatively rapid sample throughput, with a complete elution taking approximately four hours. There are, however, disadvantages, with using ion-exchange columns. Resin particle size is relatively large, to permit eluent flow at reasonable rates, which can result in significant element band spreading, creating potential overlap of REE and matrix element appearances. Also, recoveries of REE may be reduced. It is difficult to judge the point in fraction collection where the REE begin to elute, especially as this may vary from column to column. Large volumes of eluates obtained, which are often greater than the initial sample volumes, require post column treatment before analysis may be carried out. This process will introduce errors in analysis.

The most important aspect of this procedure was to obtain 100% recovery of the REE, with a minimal amount of carry over of matrix or non-REE elements. As 30-40 elution fractions needed to be collected to construct an elution pattern, the measurement of REE recovery was prone to a large degree of error. The quantitative recovery of REE was checked by the analysis of a standard reference material, NIM-G (SARM-1) and a high REE containing rock, SS-18, for which concentrations of Y, La, Ce and Nd were known

4.3 DETERMINATION OF REE IN NIM-G AND SS-18

A preliminary experiment was carried out to determine the volumes of acid required to elute both the matrix elements and the REE from the resin. The procedure used was as follows.

1) Load 20 ml of the SS-18 rock solutions onto a 15 cm by 20 mm Zeocarb 225 column.

2) Elute with a solution of 1.5 M H^+ solution containing 0.75 M Cl^- and 0.75 M NO_3^- until all the Al has been eluted from the column.

3) Elute with 3 M HNO_3 until all the La and Ce has been eluted from the column.

The eluate was collected in 10 ml fractions.

The elution patterns, Figure 4.36, shows that 140 ml of the mixed acid was required to remove all the matrix elements and 100 ml of 3.0 M HNO_3 was sufficient to remove the REE from the column. With the mixed acid solution, complete separation of the REE from the matrix elements was achieved.

FIGURE 4.36 REE SEPARATION OF SS18

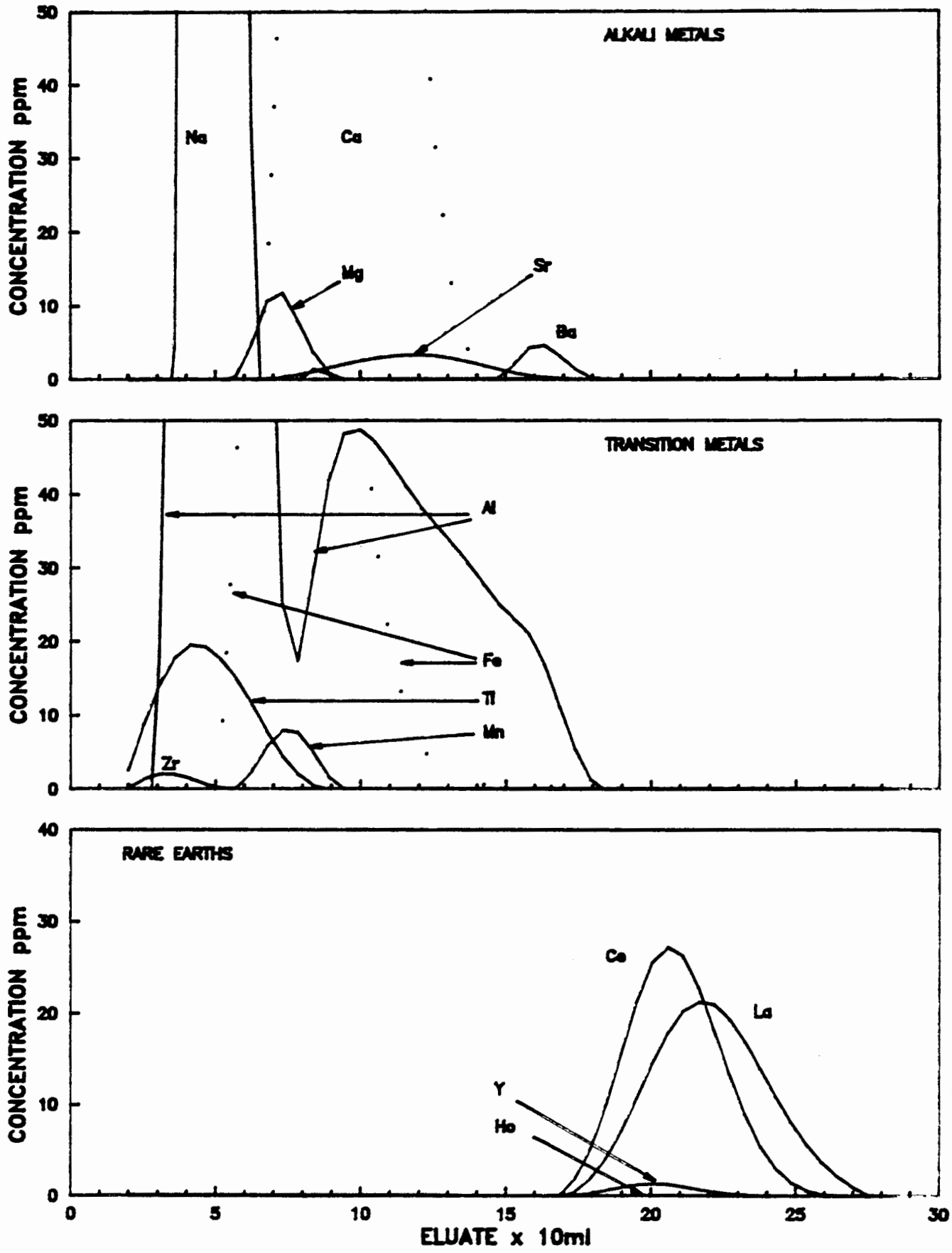

It is of interest to note the position of the Zr elution peak. In all previous cases Zr was eluted with Ti and Na as was found by Crock *et al* [58]. This may be due to differences in the oxidation states of Zr in the rock dissolution and 'spectrosol' standards, the lower oxidation state being found in the rock dissolution. Alternatively the zirconium species may be different in the different matrices.

Determinations were carried out as described in section 3.5, or the solutions were aspirated directly into the ICP without any column pre-treatment. Results obtained using correction factors given in Appendix 6 are shown in Table 4.3.

TABLE 4.3 Determination of SS-18 for REE content by sample pretreatment and direct aspiration into the ICP.

ELEMENT	COLUMN	DIRECT	REFERENCE*
	(ppm)	(ppm)	(ppm)
Y	265.0 ± 2.6	238	299
La	4698 ± 14.2	5238	4328
Ce	8008 ± 88.0	7938	7447
Pr	546 ± 12.0		
Nd	1934 ± 6.6		1871
Sm	292 ± 4.3		
Eu			
Gd	35 ± 3.3		
Tb	9 ± 1.0		
Dy	31 ± 1.0		
Ho	14 ± 1.0	15.3	
Er	43		
Tm	7		
Yb	37		
Lu	3.5		

* Results obtained by XRF, supplied by J M Moore, Department of Geology UCT.

The results obtained by ICP for La, and Ce were higher than those obtained by XRF, as was expected, due to the uncertainty of the results obtained by XRF. A second determination was carried out using NIM-G. The results are shown in Table 4.4.

TABLE 4.4 Comparative concentrations of REE (in ug g^{-1} or ppm) in NIM-G (SARM-1)

ELEMENT	COLUMN (ppm)	DIRECT (ppm)	REFERENCE[a] (ppm)
Y	128.4 ± 1.2	114.8 ± 1.2	143
La	108.6 ± 0.5	96.7 ± 1.2	109
Ce	187.7 ± 0.5	155.9 ± 4.4	195
Pr	17.0 ± 1.2	21.7 ± 1.2	(20)*
Nd	69.0 ± 1.2	54.8 ± 2.1	72
Sm	16.6 ± 4.4	24.6 ± 4.4	15.8
Eu			0.35
Gd	12.3 ± 1.2	21.3 ± 1.6	(14)*
Tb	5.4 ± 7.0	3.5 ± 1.2	3.0
Dy	18.1 ± 0.5	17.1 ± 1.2	(17)*
Ho	6.2 ± 0.5	5.0 ± 1.2	5.0
Er	21.0 ± 0.5	15.0 ± 2.1	13.5
Tm	2.5 ± 1.2		2.0
Yb	18.1 ± 0.8	14.5 ± 1.2	14.2
Lu	2.5 ± 0.5		2.0

* Proposed Values.

a Results supplied by T W Steele, Mintek, Randburg.

Results show that there is 95.0 ± 7.1% recovery of the light REE from the column. High values of the heavy REE may be due to incorrect interference coefficients or deviations in the calibration of

the instrument. Direct analysis of a NIM-G solution showed poor analytical results. This is due to the use of non matrix matched standards. Thus the high expected concentrations of Na and Ca would cause ionization interferences in the plasma. The increased total salt content of the solution will increase solution viscosity and reduce nebulizer yield, reducing the amount of solution reaching the plasma. Values of Eu, Tm and Lu are not quoted as their solution concentrations would be close to the detection limit and values obtained would be subject to large errors. The method described in sections 3.5 and 4.2 has been shown to successfully reduce the total salt content of the REE fractions used for analysis, separating the REE from matrix elements that are likely to cause interferences, and allowing a five times concentration of the REE elements before analysis.

The main disadvantage of this method is the length of time required to dissolve the rock sample. Microwave heating has the advantage of reducing the time required to dissolve the rock matrix in preparation for analysis. An experiment was carried out to determine the viability of using a microwave heated dissolution procedure, compared with a method using pressure digestion vessels heated in a laboratory oven. The conditions of this experiment are described in section 3.4. Results of direct analysis of SS-18 rock solutions are given in Table 4.5 below.

TABLE 4.5 Results of direct analysis of SS-18 rock solutions obtained by microwave heated acid attack. (Results are in ug g^{-1} unless stated).

ELEMENT	REFERENCE*	A[1]	B[2]	C[3]	D[4]
Na	3.56%	5.88%	5.71%	6.40%	6.01%
Ca	5.43%	5.67%	5.96%	5.74%	5.81%
Mg	0.29%	0.13%	0.13%	0.14%	0.15%
Sr	557	929	912	1001	891
Al	9.20%	9.20%	9.30%	9.40%	9.50%
Mn	0.10%	0.09%	0.09%	0.09%	0.09%
Fe	4.40%	4.30%	4.50%	4.40%	4.60%
Zr	346	137	138	137	318
Ti	0.39%	0.43%	0.43%	0.43%	0.43%
La	4328	5180	5239	5184	5238
Ce	7447	7956	7925	8012	7938
Y	299	236	234	261	238

* Results obtained by XRF, supplied by J M Moore, Department of Geology, UCT.

1 A = 0.7393 g dissolved and made up to 50 ml using microwave heating.

2 B = 0.9867 g dissolved and made up to 50 ml using microwave heating.

3 C = 1.0187 g dissolved and made up to 100 ml using microwave heating.

4 D = 0.4226 g dissolved using a teflon lined digestion bomb, and made up to 50 ml.

A comparison of the results shown in columns A-C with column D shows that generally there is good agreement between results obtained with the two methods. However, results for zirconium are low using microwave heating, which indicates that some of the resistant minerals in the rock matrix were not completely attacked using this dissolution technique. A more complete attack could be

achieved by using teflon pressure vessels, or by increasing the heating time at full power, or increasing the power of the microwave oven used. A disadvantage of the system used in these experiments is the location of "hot spots" in the oven which produced uneven heating of the samples, as the turn-table could not be used in the modified oven. This could be avoided by using a commercially supplied laboratory microwave oven system.

The results given in Table 4.5 are subject to error when compared with the results obtained by XRF. This is due to the use of non matrix matched standards, as no interference corrections were made for non-REE elements, as these were not elements of interest in this study.

4.4 LIQUID-LIQUID EXTRACTION OF REE

Experiments were carried out to investigate the possibility of using liquid-liquid extraction as an alternative method of separation, and preconcentration of the REE before determination. As solvent extraction studies of the REE [14,27,29,64,65,68-71] used a synergistic extraction system of a β-diketone and another group, it was decided to carry out experiments using similar systems.

4.4.1 EXTRACTION WITH AcAc AND MIBK

Investigation of REE extraction behaviour was carried out using a series of solutions prepared in following manner:

5 ml of a solution containing 50 ppm of Na, Ca, Mg, Ba, Sr, Al, Mn, Fe, Zr, Ti; 20 ppm La, Ho, Eu; 10 ppm Yb were pipetted into a separation funnel. To this solution 5 ml of a pH 1, 2, 3 or 4 buffer was added and the solutions mixed. (Buffers were prepared using methods described in [147]). The organic extracting solutions were prepared by dissolving 25 ml AcAc and 30 ml MIBK in CCl_4, and making up to 250 cm^3 with CCl_4. 10 mls of this solution was added to each separating funnel and the solutions were mixed for two hours using a wrist action shaker. After separation of the two phases, the organic phase was shaken for 1 hour with a solution of 2.5 M HCl. The aqueous phases were retained for determination of their metal content.

Standards used in the analysis were shaken with 20 ml of the organic phase in an attempt to reduce the effects of dissolved AcAc and MIBK in the aqueous phase, which would significantly alter the viscosity of the solution and the amount of energy required to atomize the sample matrix. Results are shown in Table 4.6.

The dissolution ratio measured is determined as:

$$D = \frac{\text{Total conc. of metal in org. phase}}{\text{Total conc. of metal in aq. phase}}$$

TABLE 4.6 Distribution ratios obtained for the liquid-liquid extraction of REE and matrix elements using AcAc and MIBK dissolved in CCL_4

ELEMENT	pH 1	pH 2	pH 3	pH 4
Na	0.03	0.00	0.00	0.02
Ca	0.04	0.01	0.00	0.01
Mg	0.01	0.01	0.00	0.01
Ba	3.12	2.10	1.11	0.77
Sr	0.01	0.01	0.00	0.00
Al	0.01	0.01	0.00	0.00
Mn	0.00	0.00	0.00	0.00
Fe	0.04	0.08	0.10	0.15
Zr	0.01	0.01	0.01	0.01
Ti	0.01	0.01	0.01	0.01
La	0.00	0.01	0.00	0.00
Ho	0.00	0.02	0.00	0.00
Eu	0.00	0.01	0.01	0.00
Yb	0.00	0.01	0.01	0.00

Results show that no extraction of REE occurred using this extraction system. Stary and Liljenzin [148] reported that the distribution constants for rare earth acetylacetonates, (MA_3), increase with increasing atomic number from Nd between pure acetylacetone and water with low ionic strength, the log $K_{D(MA_3)}$ for Nd being -0.39. However acetylacetonates lighter than Sm have very little solubility in acetylacetone. This factor, combined with the solubility of acetylacetone in water, 1.72 mol dm^{-3} at 20° C, means that all the acetylacetone used in this experiment could be solubilized in the aqueous phase of the experiment. Also the solvent used to dilute the extracting species plays an important part in the effectiveness of the extractant, where a lowering of K_D by as much as 1000 may occur with a change in diluent [149]. As the solubility of acetylacetone is reduced in the organic diluent

with increased ionic strength of the aqueous phase, the addition of large quantities of buffer solutions will minimize the concentration of acetylacetone in the organic diluent, CCl_4, [148]. Considering the behaviour of both acetylacetone and the REE acetylacetonates, little or no extraction of REE from the aqueous phase could be expected.

It has been reported that varying the concentration of methyl isobutyl ketone (MIBK) produces both synergistic and antisynergistic extraction of species being studied, [116]. Consequently, if the concentration of MIBK is too high, the amount of metal ion extracted is reduced. This may further contribute to the poor extraction of REE using this system.

4.4.2 EXTRACTION OF REE USING HHFA AND HTPB WITH QUINOLINE IN CCl_4

The use of fluorinated B-diketones to extract the REE from an aqueous solution has been reported when synergistic extraction was carried out with neutral donor ligands, [27,29,69], as the neutral donor ligands replace water in the hydration sphere, and increase the solubility of the complex in the organic phase. Using this principle, an experiment was performed using an extraction medium of HHFA and quinoline or HTPB and quinoline. Two 25 ml aqueous solutions buffered to pH 4.5 with hexamine containing 50 ppm Na, Ca, Mg, Ba, Sr, Al, Mn, Fe, Zr, Ti, Y, La, Ce and Ho were prepared. These solutions were shaken for three hours on a wrist action shaker with a CCl_4

solution containing 0.05 M HHFA and 0.07 M quinoline or 0.05 M HTPB and 0.07 M quinoline. After shaking, the organic phase was removed and shaken in separate separation funnels with 25 ml of 2.0 M HCl. The two aqueous phases were then analysed for their metal content, and distribution ratios determined. Results are shown in Table 4.7.

TABLE 4.7 Distribution ratios for metals between a pH 4.5 aqueous solution and an organic solution containing HHFA and Quinoline or HTPB and Quinoline.

ELEMENT	HHFA	HTPB
Na	0.04	0.63
Ca	0.04	0.41
Mg	0.03	0.04
Ba	120.63	35.00
Sr	0.04	0.04
Al	0.01	0.22
Mn	0.02	0.02
Fe	1.78	26.15
Zr	1.41	25.17
Ti	5.08	20.37
La	0.04	0.02
Ce	0.05	0.01
Y	0.06	0.14
Ho	0.08	0.28

A comparison of the results of HHFA extraction with those obtained by Mitchell and Banks [27] show that results are very low for the REE studied. These authors used Tri-n-butyl phosphate (TBP) as the neutral donor ligand, and Sekine and Dyrssen, [69] stated that TBP had a greater synergistic extraction effect than quinoline, when extracting EuIII-TTA complexes in $CHCl_3$ or CCl_4.

HHFA and quinoline reacts to form a salt; quinoline-H^+ HFA^-, in CCl_4, and to a lesser extent in $CHCl_3$. The formation of this salt, and the reduced synergistic extraction properties of the HHFA-quinoline extraction species would account for a reduction in complex formation when compared with the HHFA-TBP species, and consequently, a poorer extraction of metals from the aqueous phase. Results show that, generally, better REE extraction was achieved with HTPB than with HHFA. This may be due to the reduced acidity of the HTPB α-hydrogen which would reduce the formation of a salt, allowing greater complexation and extraction of metals from the aqueous phase. The increase in extraction with increase in atomic weight of the REE can be ascribed to the decrease in ionic radius (Y≈Ho) and consequently a stronger attraction for the anionic extracting species.

4.4.3 EXTRACTION OF REE WITH HHFA AND QUINOLINE IN $CHCl_3$

Similar experimental conditions to those described in section 4.4.2 were used for this experiment. However, the organic diluent used was $CHCl_3$ and experiments were carried out at pH 0.5, 2.0, 3.0, and 4.5, the pH of each solution being adjusted by adding 1.0 M NH_4OH or HCl. Results of REE extraction are shown in Table 4.8.

TABLE 4.8 Distribution ratios for the extraction of REE into HHFA-Quinoline-$CHCl_3$ mixture from aqueous solutions of various pH.

ELEMENT	pH							
	0.5	2.0	2.0	3.0	3.0	3.0	4.5	4.5
VOLUME	10*/10	10*/10	10*/20	10*/10	10*/20	20*/10	10*/10	20*/10
Y	0.00	0.30	1.70	0.39	1.69	0.00	15.6	3.15
La	0.00	0.26	0.42	0.35	0.44	0.00	262	0.25
Ce	0.00	0.29	1.49	0.41	1.39	0.00	249	2.40
Ho	0.00	0.33	2.20	0.43	2.20	0.00	12.4	3.24

* Volume of aqueous phase/volume of organic phase.

Various volumes of organic and aqueous phases were investigated for metal extraction behaviour at the various pHs chosen. Trends in the 1:1 aqueous:organic volume ratio (10 ml organic phase and 10 ml aqueous phase) for the extraction of REE show that as the pH of the aqueous phase was increased, the degree of extraction of the REE increased. At pH 4.5 96.4 $\pm$ 3.7% of the REE was extracted from the aqueous phase. By varying the volumes of the two phases, the degree of extraction was varied, with increased REE extraction being observed with higher volumes of organic phase used. This was due to an increase in the ratio of HHFA and quinoline to metal ions, increasing the excess of complexing species in the system. Since other ions were also present in the aqueous solution, competition for complexation between these ions and REE was observed. With any

small excesses of complexing species, no REE was extracted, due to possible preferential complexation with other ions.

It has been reported that the ionic strength of the aqueous phase will affect the stability constants of REE acetylacetonate [148], which effects the separation of the REE in AcAc. It was assumed that variations in the ionic strength of the aqueous phase would also effect REE extraction characteristics with HHFA and quinoline in $CHCl_3$. Thus if this method of preconcentration was used on rock solutions, differences in concentrations of electrolytes such as Na, Ca, Mg, and K would alter the degree of REE extraction for different samples. Also it would be preferential to set up a method for direct analysis of REE in the $CHCl_3$, HHFA and quinoline mixture, using the ICP, rather than rely on back extraction of the REE into an aqueous acidic medium before analysis, as this would reduce errors in analysis. However, analysis of REE in a complex organic matrix would require a re-evaluation of matrix and spectral interferences, and the preparation of matrix matched standards which would be difficult to obtain. Consequently, no further work was carried out using liquid-liquid extraction techniques, and analysis of REE contents of rocks was carried out using chromatographic separation and preconcentration.

4.5 CRYSTAL STRUCTURES OF 3.5 -DIACETYL- 1.4-DIHYDRO-2.6 -DIMETHYL PYRIDINE

During an unsuccessful experiment to investigate the extraction of the REE from an aqueous solution, yellow crystals were observed to form, as described in section 3.2. Microanalysis of the recrystallized compounds are shown in Table 4.9

TABLE 4.9 Empirical formulas of the two crystals of 3.5-Diacetyl-1.4-Dihydro-2.6-Dimethyl Pyridine obtained by recrystallization from acetone, or by sublimation.

SUBLIMATION (HEXSUB)			ACETONE (HEXAC)		
ELEMENT	%	n	ELEMENT	%	n
C	67.55	11	C	62.70	11
H	7.50	14	H	7.75	16
N	7.25	1	N	6.60	1
O	17.70	2	O	22.95	3

The empirical formulas of the two compounds were $(C_{11}\ H_{14}\ NO_2)_n$, and $(C_{11}\ H_{16}\ NO_3)_n$, a difference of H_2O. Mass spectrometry indicated a molecular mass of 192 a.m.u, showing that the empirical formula was also the molecular formula. Interpretations of the proton and carbon-13 nuclear magnetic resonance spectra were ambiguous, and no structure could be determined using these techniques.

It was decided to try and grow reasonable single crystals for X-ray crystallographic analysis. This proved to be difficult for a number of reasons:

1) Solvents were insoluble in a number of solvents including H_2O, CCl_4, $CHCl_3$, ether and petroleum ether.

2) Crystals obtained from methanol, ethanol, dimethyl sulphoxide, dimethyl formamide and acetonitrile were too small to be used for crystallographic analysis.

3) Crystals obtained from acetone, while being larger, tended to form aggregates with very few single crystals.

4) Any single crystals obtained were often hollow, a phenomenon that was very difficult to observe, even using a polarized light source microscope.

Single crystals, suitable for X-ray diffraction techniques, were eventually obtained. Preliminary cell parameters and space group were obtained from oscillation and Weissenberg photographs. Accurate lattice constants were determined by least squares analysis of 24 reflections measured in the range: 1) $10^\circ < \theta < 11^\circ$, and 2) $16^\circ < \theta < 17^\circ$ for Hexac and Hexsub respectively on a Nonius CAD 4 diffractometer with graphite monochromated Mo K_α radiation (λ = 0.7107 Å). The small size, and poor and diffracting power of the crystal of Hexac resulted in reflections of suitable strength only being located in the lower θ range. Intensity data was collected at 298 K, during which 3 reference

reflections were periodically monitored to check crystal stability, and recentering was carried out every 100 measured reflections. Crystal data and experimental details are shown in Table 4.10. All intensities were corrected for Lorentz polarization and empirical absorption corrections were carried out on both crystals.

TABLE 4.10 Crystal data, experimental and refinement parameters for Hexac and Hexsub.

COMPOUND		
	HEXAC	HEXSUB
Molecular Formula	$C_{11}H_{14}NO_2.H_2O$	$C_{11}H_{14}NO_2$
Space Group	P $2_1/C$	P $2_1/C$
a / Å	10.544(3)	4.273(1)
b / Å	14.927(6)	12.034(2)
c / Å	7.176(4)	10.024(1)
B / Deg	104.24(3)	98.54(1)
Volume / $Å^3$	1094.7	509.7
Z	4	2
D_m / g cm^{-3}	1.28	
D_c / g cm^{-3}	1.275	1.357
μ (Mo K_α / cm^{-1})	0.862	0.500
F (000)	444	206

DATA COLLECTION		
Crystal Dimensions /mm	0.3x0.6x0.12	0.56x0.50x31
Scan Mode	W-2θ	W-2θ
Scan Width /ΔW/°	0.84 + 0.35 tanθ	1.14 + 0.35 tanθ
Vertical Apperture		
Length / mm	4	6
Apperture		
Width / mm	1.11 + 1.05 tanθ	1.66 + 1.05 tanθ
Final Acceptance		
limit	20σ at 20° min^{-1}	20σ at 20° min^{-1}
Max Recording time /s	40	40
Total N° Unique Refln's	792	784
Crystal Stability / %	0.4	0.2
2θ Range / °	2-40	2-50
FINAL REFINEMENT		
N° Variables	57	98
Total N° Observed Refln's	669	730
$(I_{rel} > 2\sigma\ I_{rel})$		
$R = (\Sigma \ \lvert\lvert F_o\rvert - \lvert F_c\rvert\rvert \ / \ \Sigma \ \lvert F_o\rvert)$	0.122	0.096
$R_w = (\Sigma w^{1/2} \lvert\lvert F_o\rvert - \lvert F_c\rvert\rvert \ / \ \Sigma w^{1/2} \lvert F_o\rvert)$	0.083	0.086
Weighting Scheme	$(\sigma^2 F)^{-1}$	$(\sigma^2 F)^{-1}$
Average Transmition / %	97.2	96.3

The structures were solved by direct methods using the SHELXS-86 program [150], and refined using the SHELX-76 [151] program system. For Hexac, the solution of the majority of the structure proved to be routine, but difficulties were experienced with the positioning of the water of crystallisation. A difference electron density map was calculated and contoured. This revealed the position of the oxygen, and ridges of electron density running between the oxygen atom and the two carbonyl oxygens and a nitrogen atom of three adjacent molecules, indicating that the molecule may exist in a partial enol form with some three fold static disorder. Structures are shown in Figures 4.37-4.40.

The second crystal analysed showed a different structure, with the water of crystallisation removed from the unit cell. Initial results obtained by direct methods gave a "chicken wire" picture which could not be ascribed to any reasonable molecule structure. However, by plotting out an entire unit cell using the symmetry of the known space group, it became apparent that the molecular arrangement in the cell was disordered, with the molecule lying about a center of symmetry at a Wyckoff position d. Care was taken to ensure that each atom was assigned its correct site occupancy factor as several atoms are common to both forms of the disordered compound, (Figure 4.41), with a perspective view of the molecule in the unit cell shown in Figures 4.42-4.44. Fractional atomic co-ordinates are

shown in Tables 4.11 and 4.12; bond lengths and angles in Tables 4.13 and 4.14.

It was of interest to note the reduction in unit cell volume on removal of the water of crystallisation. The water of crystallisation is responsible for the stabilization of the Hexac structure through hydrogen bonding. The second structure analysed, Hexsub, was found to be very hydrophilic, with any water present causing the crystal to break up. This shows that the Hexsub crystal structure is not particularly stable due to the disorder of the structure, and the proximity of adjacent molecules, which would cause electrostatic repulsions.

Analysis of the reaction conditions showed the following:

1) The reaction was found to occur with or without an organic diluent.

2) Without quinoline or pyridine, no reaction was observed.

3) No AcAc, no reaction.

4) No hexamine, no reaction.

5) No acid in the aqueous phase, no reaction.

6) No reaction was observed when AcAc was substituted by another β-diketone.

This showed that the acidity of the α-hydrogen of the β-diketone was an important factor in the reaction, as well as the presence of acid in the aqueous phase, and base in the organic phase. A

proposed reaction scheme is shown in Figure 4.45. The occurrance of this reaction precludes the use of AcAc as an extracting species when hexamine is used to buffer the aqueous phase.

FIGURE 4.37 Structure of Hexac, (3.5-diacetyl-1.4-dihydro-2.6-dimethyl pyridine).

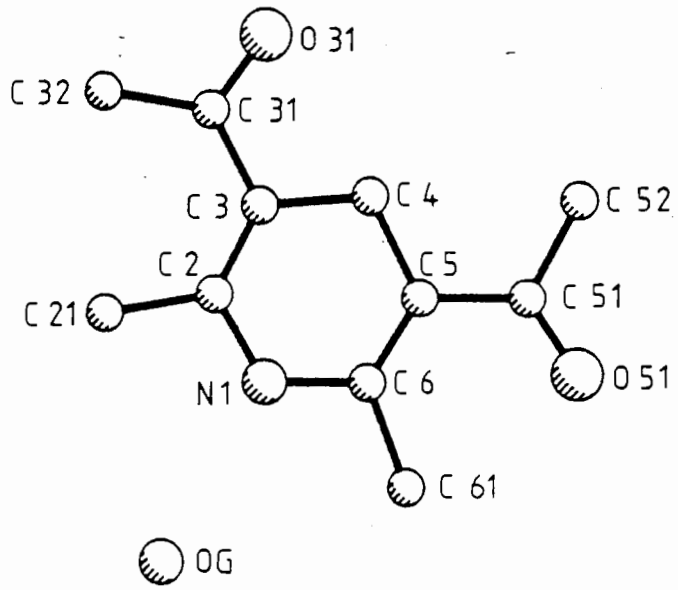

FIGURE 4.38 Hexac: View down 1 0 0.

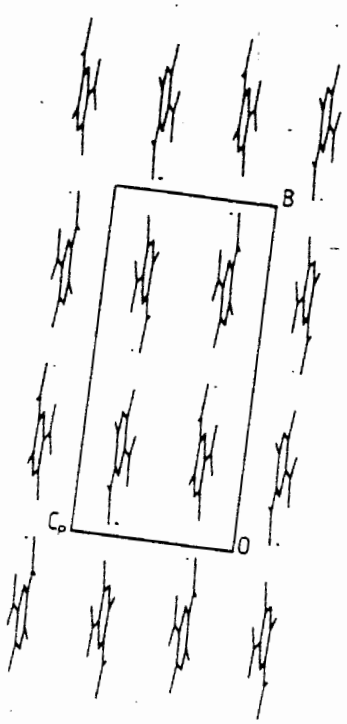

FIGURE 4.39 Hexac: View line down 0 1 0.

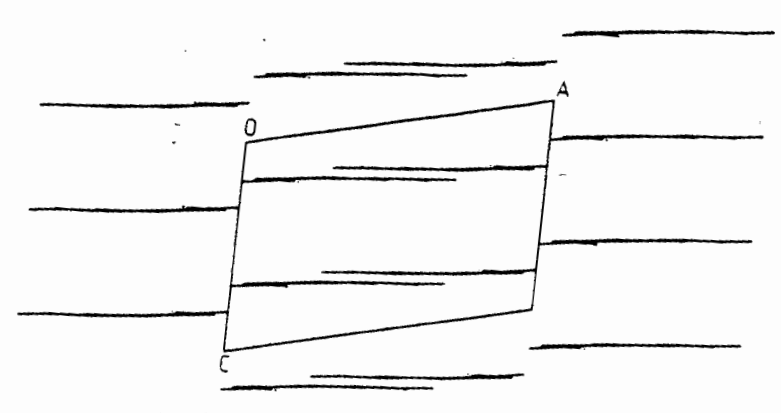

FIGURE 4.40 Hexac: view line down 0 0 1.

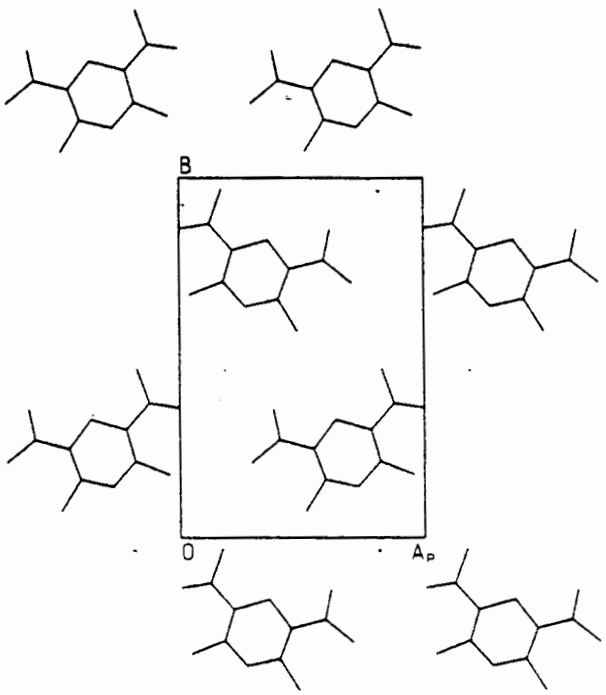

FIGURE 4.41 Structure of Hexsub showing disorder of the molecule at the Wyckoff position d.

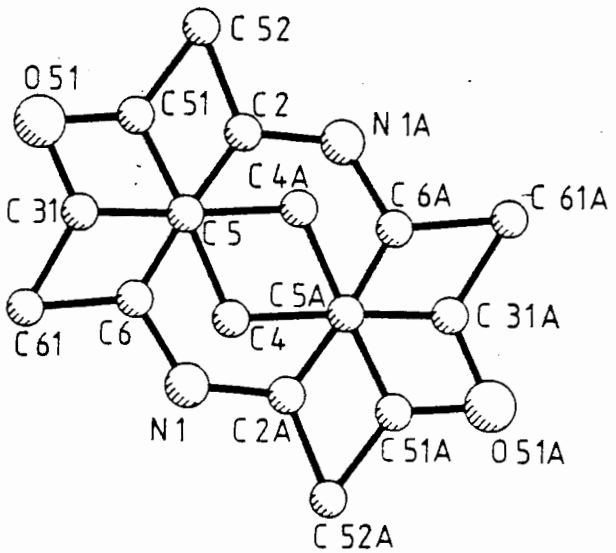

FIGURE 4.42 Hexsub: View line down 1 0 0.

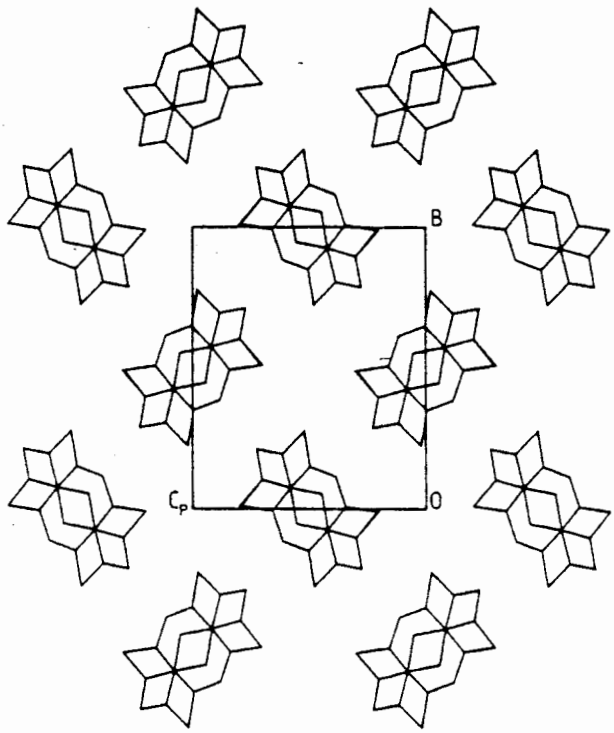

FIGURE 4.43 Hexsub: View line down 0 1 0.

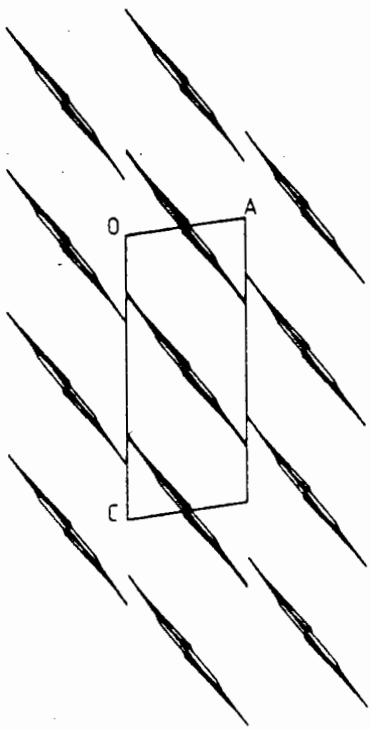

FIGURE 4.44 Hexsub: View line down 0 0 1.

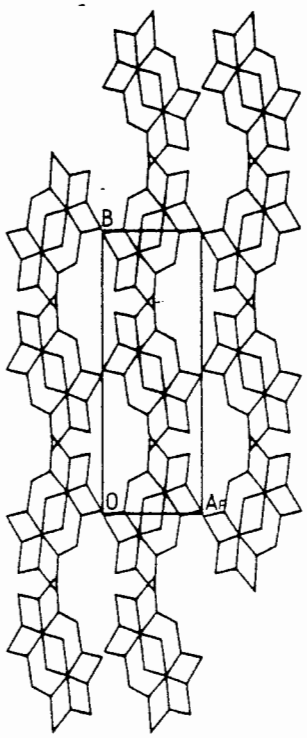

FIGURE 4.45 Proposed reaction mechanism for Hexac or Hexsub.

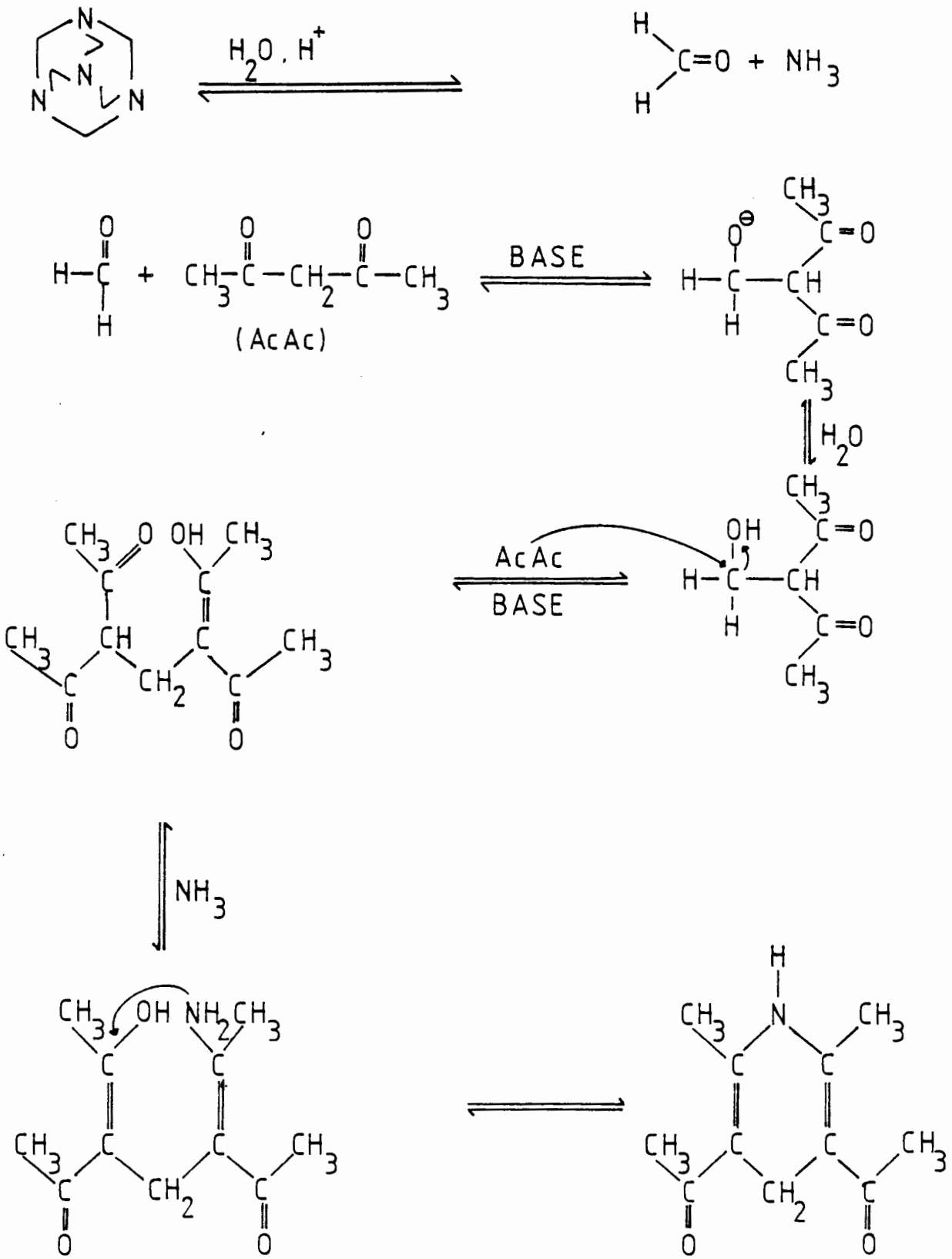

TABLE 4.11 Fractional atomic coordinates (x 10**4) and thermal parameters (a**2 x 10**3) with e.s.d.s in parentheses for Hexac.

Atom	x/a	y/b	z/c	Uiso/Uequiv(*)
N(1)	2619(16)	3854(6)	8835(7)	59(3) *
C(2)	5420(20)	6501(7)	10028(9)	55(3) *
C(31)	1622(21)	6040(8)	7977(9)	64(3) *
C(4)	4101(22)	4451(8)	9439(9)	63(4) *
C(5)	3740(9)	5744(3)	9187(4)	49(1) *
C(51)	3308(21)	6950(7)	8805(9)	64(3) *
O(51)	1259(9)	7128(3)	7732(4)	107(2) *
C(52)	5200(13)	7752(4)	9776(5)	80(2) *
C(6)	2181(20)	4930(7)	8416(8)	55(4) *
C(61)	115(13)	5103(4)	7091(5)	77(2) *

Anisotropic atoms have thermal parameters (a**2 x 10**3) of the form:

$$\exp(-2\ \pi^2\ (U_{11}h^2a^{*2} + U_{22}k^2b^{*2} + U_{33}l^2c^{*2} + 2U_{23}klb^*c^* + 2U_{13}hla^*c^* + 2U_{12}hka^*b^*)) \times 10^3$$

Atom	U11	U22	U33	U23	U13	U12
N(1)	71(5)	37(4)	59(5)	0(4)	-20(4)	-9(4)
C(2)	64(6)	45(5)	56(5)	-3(5)	14(4)	-6(4)
C(31)	69(6)	61(6)	60(6)	0(5)	2(5)	11(5)
C(4)	70(7)	53(6)	62(6)	3(5)	-6(5)	-5(5)
C(5)	53(3)	45(2)	48(2)	3(2)	4(2)	4(2)
C(51)	72(6)	51(5)	64(6)	1(5)	-2(5)	7(5)
O(51)	139(4)	82(3)	89(3)	13(2)	-22(3)	37(2)
C(52)	106(4)	41(3)	86(4)	-2(3)	-10(3)	-6(3)
C(6)	59(6)	55(6)	48(5)	-2(4)	0(4)	-1(4)
C(61)	88(4)	69(3)	62(3)	-11(3)	-28(3)	2(3)

TABLE 4.12 Fractional atomic coordinates (x 10**4) and thermal parameters (a**2 x 10**3) with e.s.d.s in parentheses for Hexsub.

Atom	x/a	y/b	z/c	Uiso/Uequiv(*)
N(1)	2619(16)	3854(6)	8835(7)	59(3) *
C(2)	5420(20)	6501(7)	10028(9)	55(3) *
C(31)	1622(21)	6040(8)	7977(9)	64(3) *
C(4)	4101(22)	4451(8)	9439(9)	63(4) *
C(5)	3740(9)	5744(3)	9187(4)	49(1) *
C(51)	3308(21)	6950(7)	8805(9)	64(3) *
O(51)	1259(9)	7128(3)	7732(4)	107(2) *
C(52)	5200(13)	7752(4)	9776(5)	80(2) *
C(6)	2181(20)	4930(7)	8416(8)	55(4) *
C(61)	115(13)	5103(4)	7091(5)	77(2) *

Anisotropic atoms have thermal parameters (a**2 x 10**3) of the form:

$$\exp(-2\pi^2 (U_{11}h^2a^{*2} + U_{22}k^2b^{*2} + U_{33}l^2c^{*2} + 2U_{23}klb^*c^* + 2U_{13}hla^*c^* + 2U_{12}hka^*b^*)) \times 10^3$$

Atom	U11	U22	U33	U23	U13	U12
N(1)	71(5)	37(4)	59(5)	0(4)	-20(4)	-9(4)
C(2)	64(6)	45(5)	56(5)	-3(5)	14(4)	-6(4)
C(31)	69(6)	61(6)	60(6)	0(5)	2(5)	11(5)
C(4)	70(7)	53(6)	62(6)	3(5)	-6(5)	-5(5)
C(5)	53(3)	45(2)	48(2)	3(2)	4(2)	4(2)
C(51)	72(6)	51(5)	64(6)	1(5)	-2(5)	7(5)
O(51)	139(4)	82(3)	89(3)	13(2)	-22(3)	37(2)
C(52)	106(4)	41(3)	86(4)	-2(3)	-10(3)	-6(3)
C(6)	59(6)	55(6)	48(5)	-2(4)	0(4)	-1(4)
C(61)	88(4)	69(3)	62(3)	-11(3)	-28(3)	2(3)

TABLE 4.13A Bond lengths (angstrom) with e.s.d.s in parenthesis for Hexac.

N(1)	- C(4)	1.082(11)
N(1)	- C(6)	1.365(11)
C(2)	- C(5)	1.370(9)
C(2)	- C(51)	1.510(12)
C(2)	- C(52)	1.527(10)
C(31)	- C(5)	1.445(9)
C(31)	- C(51)	1.493(12)
C(31)	- O(51)	1.337(10)
C(31)	- C(6)	1.415(13)
C(31)	- C(61)	1.519(10)
C(4)	- C(5)	1.579(10)
C(4)	- C(6)	1.344(12)
C(5)	- C(51)	1.505(9)
C(5)	- C(6)	1.359(9)
C(51)	- O(51)	1.299(9)
C(51)	- C(52)	1.516(10)
C(6)	- C(61)	1.496(9)

TABLE 4.14A Bond lengths (angstrom) with e.s.d.s in parenthesis for Hexsub.

N(1)	- C(4)	1.082(11)
N(1)	- C(6)	1.365(11)
C(2)	- C(5)	1.370(9)
C(2)	- C(51)	1.510(12)
C(2)	- C(52)	1.527(10)
C(31)	- C(5)	1.445(9)
C(31)	- C(51)	1.493(12)
C(31)	- O(51)	1.337(10)
C(31)	- C(6)	1.415(13)
C(31)	- C(61)	1.519(10)
C(4)	- C(5)	1.579(10)
C(4)	- C(6)	1.344(12)
C(5)	- C(51)	1.505(9)
C(5)	- C(6)	1.359(9)
C(51)	- O(51)	1.299(9)
C(51)	- C(52)	1.516(10)
C(6)	- C(61)	1.496(9)

TABLE 4.13B Bond angles (degrees) with e.s.d.s in parenthesis for Hexac.

C(4)	- N(1)	- C(6)	65.5(7)
C(51)	- C(2)	- C(52)	59.9(5)
C(5)	- C(2)	- C(52)	122.7(7)
C(5)	- C(2)	- C(51)	62.8(5)
C(6)	- C(31)	- C(61)	61.2(5)
O(51)	- C(31)	- C(61)	126.3(7)
O(51)	- C(31)	- C(6)	172.3(8)
C(51)	- C(31)	- C(61)	176.0(8)
C(51)	- C(31)	- C(6)	118.4(8)
C(51)	- C(31)	- O(51)	54.3(5)
C(5)	- C(31)	- C(61)	117.8(7)
C(5)	- C(31)	- C(6)	56.7(5)
C(5)	- C(31)	- O(51)	115.9(7)
C(5)	- C(31)	- C(51)	61.6(5)
N(1)	- C(4)	- C(6)	67.5(7)
N(1)	- C(4)	- C(5)	121.9(8)
C(5)	- C(4)	- C(6)	54.7(5)
C(31)	- C(5)	- C(4)	114.3(6)
C(2)	- C(5)	- C(4)	121.8(6)
C(2)	- C(5)	- C(31)	123.9(6)
C(4)	- C(5)	- C(6)	53.8(5)
C(4)	- C(5)	- C(51)	174.5(5)
C(31)	- C(5)	- C(6)	60.5(5)
C(31)	- C(5)	- C(51)	60.7(5)
C(2)	- C(5)	- C(6)	175.6(6)
C(2)	- C(5)	- C(51)	63.2(5)
C(51)	- C(5)	- C(6)	121.3(5)
C(31)	- C(51)	- C(5)	57.6(5)
C(2)	- C(51)	- C(5)	54.0(5)
C(2)	- C(51)	- C(31)	111.7(7)
C(5)	- C(51)	- C(52)	114.6(6)
C(5)	- C(51)	- O(51)	114.3(6)
C(31)	- C(51)	- C(52)	172.3(8)
C(31)	- C(51)	- O(51)	56.7(5)
C(2)	- C(51)	- C(52)	60.6(5)
C(2)	- C(51)	- O(51)	168.1(8)
O(51)	- C(51)	- C(52)	131.0(7)
C(31)	- O(51)	- C(51)	68.9(6)
C(2)	- C(52)	- C(51)	59.5(5)
C(4)	- C(6)	- C(5)	71.5(6)
C(31)	- C(6)	- C(5)	62.7(5)
C(31)	- C(6)	- C(4)	134.1(8)
N(1)	- C(6)	- C(5)	118.3(7)
N(1)	- C(6)	- C(4)	47.1(6)
N(1)	- C(6)	- C(31)	178.2(9)
C(5)	- C(6)	- C(61)	125.4(6)
C(4)	- C(6)	- C(61)	161.8(8)
C(31)	- C(6)	- C(61)	62.8(5)
N(1)	- C(6)	- C(61)	116.2(7)
C(31)	- C(61)	- C(6)	56.0(5)

TABLE 4.14B Bond angles (degrees) with e.s.d.s in parenthesis for Hexsub.

C(4)	- N(1)	- C(6)	65.5(7)
C(51)	- C(2)	- C(52)	59.9(5)
C(5)	- C(2)	- C(52)	122.7(7)
C(5)	- C(2)	- C(51)	62.8(5)
C(6)	- C(31)	- C(61)	61.2(5)
O(51)	- C(31)	- C(61)	126.3(7)
O(51)	- C(31)	- C(6)	172.3(8)
C(51)	- C(31)	- C(61)	176.0(8)
C(51)	- C(31)	- C(6)	118.4(8)
C(51)	- C(31)	- O(51)	54.3(5)
C(5)	- C(31)	- C(61)	117.8(7)
C(5)	- C(31)	- C(6)	56.7(5)
C(5)	- C(31)	- O(51)	115.9(7)
C(5)	- C(31)	- C(51)	61.6(5)
N(1)	- C(4)	- C(6)	67.5(7)
N(1)	- C(4)	- C(5)	121.9(8)
C(5)	- C(4)	- C(6)	54.7(5)
C(31)	- C(5)	- C(4)	114.3(6)
C(2)	- C(5)	- C(4)	121.8(6)
C(2)	- C(5)	- C(31)	123.9(6)
C(4)	- C(5)	- C(6)	53.8(5)
C(4)	- C(5)	- C(51)	174.5(5)
C(31)	- C(5)	- C(6)	60.5(5)
C(31)	- C(5)	- C(51)	60.7(5)
C(2)	- C(5)	- C(6)	175.6(6)
C(2)	- C(5)	- C(51)	63.2(5)
C(51)	- C(5)	- C(6)	121.3(5)
C(31)	- C(51)	- C(5)	57.6(5)
C(2)	- C(51)	- C(5)	54.0(5)
C(2)	- C(51)	- C(31)	111.7(7)
C(5)	- C(51)	- C(52)	114.6(6)
C(5)	- C(51)	- O(51)	114.3(6)
C(31)	- C(51)	- C(52)	172.3(8)
C(31)	- C(51)	- O(51)	56.7(5)
C(2)	- C(51)	- C(52)	60.6(5)
C(2)	- C(51)	- O(51)	168.1(8)
O(51)	- C(51)	- C(52)	131.0(7)
C(31)	- O(51)	- C(51)	68.9(6)
C(2)	- C(52)	- C(51)	59.5(5)
C(4)	- C(6)	- C(5)	71.5(6)
C(31)	- C(6)	- C(5)	62.7(5)
C(31)	- C(6)	- C(4)	134.1(8)
N(1)	- C(6)	- C(5)	118.3(7)
N(1)	- C(6)	- C(4)	47.1(6)
N(1)	- C(6)	- C(31)	178.2(9)
C(5)	- C(6)	- C(61)	125.4(6)
C(4)	- C(6)	- C(61)	161.8(8)
C(31)	- C(6)	- C(61)	62.8(5)
N(1)	- C(6)	- C(61)	116.2(7)
C(31)	- C(61)	- C(6)	56.0(5)

TABLE 4.13C Torsion angles (degrees) with e.s.d.s in parenthesis for Hexac.

(RIGHT-HAND RULE,KLYNE & PRELOG.(1960).EXPERIENTIA,16,521)
(E.S.D.'S, FOLLOWING STANFORD & WASER,ACTA CRYST.(1972).A28,213)

C(4)	- N(1)	- C(6)	- C(61)	171.3(9)
C(4)	- N(1)	- C(6)	- C(5)	-5.8(8)
C(6)	- N(1)	- C(4)	- C(5)	5.2(8)
C(5)	- C(2)	- C(52)	- C(51)	-.5(7)
C(5)	- C(2)	- C(51)	- O(51)	11.8(39)
C(5)	- C(2)	- C(51)	- C(52)	179.5(6)
C(52)	- C(2)	- C(51)	- C(31)	-179.5(8)
C(5)	- C(2)	- C(51)	- C(31)	.0(6)
C(52)	- C(2)	- C(51)	- C(5)	-179.5(6)
C(52)	- C(2)	- C(5)	- C(31)	.6(11)
C(51)	- C(2)	- C(5)	- C(31)	.0(8)
C(52)	- C(2)	- C(5)	- C(4)	177.7(6)
C(51)	- C(2)	- C(5)	- C(4)	177.2(6)
C(52)	- C(2)	- C(5)	- C(51)	.5(6)
C(52)	- C(2)	- C(51)	- O(51)	-167.7(40)
C(5)	- C(31)	- C(51)	- C(2)	.0(6)
C(51)	- C(31)	- C(5)	- C(2)	.0(8)
O(51)	- C(31)	- C(5)	- C(2)	-2.7(10)
C(6)	- C(31)	- C(5)	- C(2)	179.9(7)
C(61)	- C(31)	- C(5)	- C(2)	175.5(6)
O(51)	- C(31)	- C(51)	- C(2)	177.1(9)
C(6)	- C(31)	- C(51)	- C(2)	.0(11)
O(51)	- C(31)	- C(61)	- C(6)	-177.9(11)
C(5)	- C(31)	- C(61)	- C(6)	4.2(6)
C(51)	- C(31)	- C(6)	- C(61)	-175.5(9)
C(5)	- C(31)	- C(6)	- C(61)	-175.5(6)
C(61)	- C(31)	- C(6)	- C(4)	171.8(12)
C(51)	- C(31)	- C(6)	- C(4)	-3.7(15)
C(5)	- C(31)	- C(6)	- C(4)	-3.7(10)
C(61)	- C(31)	- C(6)	- C(5)	175.5(6)
C(51)	- C(31)	- C(6)	- C(5)	.1(7)
C(61)	- C(31)	- O(51)	- C(51)	-175.1(10)
C(5)	- C(31)	- O(51)	- C(51)	2.9(7)
C(5)	- C(31)	- C(51)	- O(51)	-177.1(7)
C(6)	- C(31)	- C(51)	- C(5)	-.1(7)
O(51)	- C(31)	- C(51)	- C(5)	177.1(7)
C(61)	- C(31)	- C(5)	- C(4)	-1.9(9)
C(6)	- C(31)	- C(5)	- C(4)	2.5(7)
O(51)	- C(31)	- C(5)	- C(4)	179.9(6)
C(51)	- C(31)	- C(5)	- C(4)	-177.4(6)
C(51)	- C(31)	- C(5)	- C(6)	-179.9(7)
O(51)	- C(31)	- C(5)	- C(6)	177.4(9)
O(51)	- C(31)	- C(5)	- C(51)	-2.7(6)
C(6)	- C(31)	- C(5)	- C(51)	179.9(7)
C(61)	- C(31)	- C(5)	- C(6)	-4.4(6)
C(61)	- C(31)	- C(5)	- C(51)	175.5(9)
C(6)	- C(31)	- C(51)	- O(51)	-177.1(10)
N(1)	- C(4)	- C(5)	- C(31)	-8.6(12)
N(1)	- C(4)	- C(5)	- C(2)	174.0(9)
N(1)	- C(4)	- C(6)	- C(31)	178.1(12)
C(5)	- C(4)	- C(6)	- N(1)	-174.6(8)
C(5)	- C(4)	- C(6)	- C(31)	3.5(9)

N(1)	- C(4)	- C(6)	- C(61)	-25.8(26)
N(1)	- C(4)	- C(6)	- C(5)	174.6(8)
N(1)	- C(4)	- C(5)	- C(6)	-5.9(9)
C(6)	- C(4)	- C(5)	- C(31)	-2.7(7)
C(6)	- C(4)	- C(5)	- C(2)	179.9(7)
C(5)	- C(4)	- C(6)	- C(61)	159.5(27)
C(2)	- C(5)	- C(51)	- C(31)	180.0(7)
C(31)	- C(5)	- C(51)	- C(2)	-180.0(7)
C(31)	- C(5)	- C(6)	- C(4)	177.2(8)
C(31)	- C(5)	- C(6)	- N(1)	-178.4(10)
C(4)	- C(5)	- C(6)	- C(31)	-177.2(8)
C(4)	- C(5)	- C(6)	- N(1)	4.5(6)
C(51)	- C(5)	- C(6)	- N(1)	-178.5(7)
C(51)	- C(5)	- C(6)	- C(31)	-.1(7)
C(51)	- C(5)	- C(6)	- C(4)	177.1(7)
C(4)	- C(5)	- C(6)	- C(61)	-172.3(10)
C(31)	- C(5)	- C(6)	- C(61)	4.9(7)
C(31)	- C(5)	- C(51)	- O(51)	2.7(6)
C(2)	- C(5)	- C(51)	- O(51)	-177.4(9)
C(31)	- C(5)	- C(51)	- C(52)	179.5(9)
C(2)	- C(5)	- C(51)	- C(52)	-.5(6)
C(6)	- C(5)	- C(51)	- C(31)	.1(7)
C(6)	- C(5)	- C(51)	- C(2)	-179.9(7)
C(51)	- C(5)	- C(6)	- C(61)	4.8(10)
C(6)	- C(5)	- C(51)	- C(52)	179.6(6)
C(6)	- C(5)	- C(51)	- O(51)	2.8(10)
C(2)	- C(51)	- O(51)	- C(31)	-13.2(38)
C(5)	- C(51)	- O(51)	- C(31)	-2.7(6)
C(5)	- C(51)	- C(52)	- C(2)	.4(6)
O(51)	- C(51)	- C(52)	- C(2)	176.7(11)
C(52)	- C(51)	- O(51)	- C(31)	-178.9(10)
N(1)	- C(6)	- C(61)	- C(31)	178.3(9)
C(4)	- C(6)	- C(61)	- C(31)	-160.9(27)
C(5)	- C(6)	- C(61)	- C(31)	-4.9(7)

Parent atom	H	x/a	y/b	z/c
N(1)	H(11)	1945(16)	2994(6)	8673(7)
C(4)	H(41)	3682(22)	4607(8)	10460(9)
	H(42)	6617(22)	4442(8)	9409(9)
C(52)	H(521)	4521(13)	8373(4)	9011(5)
	H(522)	7744(13)	7744(4)	10039(5)
	H(523)	4136(13)	7943(4)	10661(5)
C(61)	H(611)	772(13)	4303(4)	6731(5)
	H(612)	-40(13)	5701(4)	6281(5)
	H(613)	-2152(13)	5037(4)	7439(5)

TABLE 4.14C Torsion angles (degrees) with e.s.d.s in parenthesis for Hexsub.

(RIGHT-HAND RULE,KLYNE & PRELOG.(1960).EXPERIENTIA,16,521)
(E.S.D.'S, FOLLOWING STANFORD & WASER,ACTA CRYST.(1972).A28,213)

C(4)	- N(1)	- C(6)	- C(61)	171.3(9)
C(4)	- N(1)	- C(6)	- C(5)	-5.8(8)
C(6)	- N(1)	- C(4)	- C(5)	5.2(8)
C(5)	- C(2)	- C(52)	- C(51)	-.5(7)
C(5)	- C(2)	- C(51)	- O(51)	11.8(39)
C(5)	- C(2)	- C(51)	- C(52)	179.5(6)
C(52)	- C(2)	- C(51)	- C(31)	-179.5(8)
C(5)	- C(2)	- C(51)	- C(31)	.0(6)
C(52)	- C(2)	- C(51)	- C(5)	-179.5(6)
C(52)	- C(2)	- C(5)	- C(31)	.6(11)
C(51)	- C(2)	- C(5)	- C(31)	.0(8)
C(52)	- C(2)	- C(5)	- C(4)	177.7(6)
C(51)	- C(2)	- C(5)	- C(4)	177.2(6)
C(52)	- C(2)	- C(5)	- C(51)	.5(6)
C(52)	- C(2)	- C(51)	- O(51)	-167.7(40)
C(5)	- C(31)	- C(51)	- C(2)	.0(6)
C(51)	- C(31)	- C(5)	- C(2)	.0(8)
O(51)	- C(31)	- C(5)	- C(2)	-2.7(10)
C(6)	- C(31)	- C(5)	- C(2)	179.9(7)
C(61)	- C(31)	- C(5)	- C(2)	175.5(6)
O(51)	- C(31)	- C(51)	- C(2)	177.1(9)
C(6)	- C(31)	- C(51)	- C(2)	.0(11)
O(51)	- C(31)	- C(61)	- C(6)	-177.9(11)
C(5)	- C(31)	- C(61)	- C(6)	4.2(6)
C(51)	- C(31)	- C(6)	- C(61)	-175.5(9)
C(5)	- C(31)	- C(6)	- C(61)	-175.5(6)
C(61)	- C(31)	- C(6)	- C(4)	171.8(12)
C(51)	- C(31)	- C(6)	- C(4)	-3.7(15)
C(5)	- C(31)	- C(6)	- C(4)	-3.7(10)
C(61)	- C(31)	- C(6)	- C(5)	175.5(6)
C(51)	- C(31)	- C(6)	- C(5)	.1(7)
C(61)	- C(31)	- O(51)	- C(51)	-175.1(10)
C(5)	- C(31)	- O(51)	- C(51)	2.9(7)
C(5)	- C(31)	- C(51)	- O(51)	-177.1(7)
C(6)	- C(31)	- C(51)	- C(5)	-.1(7)
O(51)	- C(31)	- C(51)	- C(5)	177.1(7)
C(61)	- C(31)	- C(5)	- C(4)	-1.9(9)
C(6)	- C(31)	- C(5)	- C(4)	2.5(7)
O(51)	- C(31)	- C(5)	- C(4)	179.9(6)
C(51)	- C(31)	- C(5)	- C(4)	-177.4(6)
C(51)	- C(31)	- C(5)	- C(6)	-179.9(7)
O(51)	- C(31)	- C(5)	- C(6)	177.4(9)
O(51)	- C(31)	- C(5)	- C(51)	-2.7(6)
C(6)	- C(31)	- C(5)	- C(51)	179.9(7)
C(61)	- C(31)	- C(5)	- C(6)	-4.4(6)
C(61)	- C(31)	- C(5)	- C(51)	175.5(9)
C(6)	- C(31)	- C(51)	- O(51)	-177.1(10)
N(1)	- C(4)	- C(5)	- C(31)	-8.6(12)
N(1)	- C(4)	- C(5)	- C(2)	174.0(9)
N(1)	- C(4)	- C(6)	- C(31)	178.1(12)
C(5)	- C(4)	- C(6)	- N(1)	-174.6(8)
C(5)	- C(4)	- C(6)	- C(31)	3.5(9)

N(1)	- C(4)	- C(6)	- C(61)	-25.8(26)
N(1)	- C(4)	- C(6)	- C(5)	174.6(8)
N(1)	- C(4)	- C(5)	- C(6)	-5.9(9)
C(6)	- C(4)	- C(5)	- C(31)	-2.7(7)
C(6)	- C(4)	- C(5)	- C(2)	179.9(7)
C(5)	- C(4)	- C(6)	- C(61)	159.5(27)
C(2)	- C(5)	- C(51)	- C(31)	180.0(7)
C(31)	- C(5)	- C(51)	- C(2)	-180.0(7)
C(31)	- C(5)	- C(6)	- C(4)	177.2(8)
C(31)	- C(5)	- C(6)	- N(1)	-178.4(10)
C(4)	- C(5)	- C(6)	- C(31)	-177.2(8)
C(4)	- C(5)	- C(6)	- N(1)	4.5(6)
C(51)	- C(5)	- C(6)	- N(1)	-178.5(7)
C(51)	- C(5)	- C(6)	- C(31)	-.1(7)
C(51)	- C(5)	- C(6)	- C(4)	177.1(7)
C(4)	- C(5)	- C(6)	- C(61)	-172.3(10)
C(31)	- C(5)	- C(6)	- C(61)	4.9(7)
C(31)	- C(5)	- C(51)	- O(51)	2.7(6)
C(2)	- C(5)	- C(51)	- O(51)	-177.4(9)
C(31)	- C(5)	- C(51)	- C(52)	179.5(9)
C(2)	- C(5)	- C(51)	- C(52)	-.5(6)
C(6)	- C(5)	- C(51)	- C(31)	.1(7)
C(6)	- C(5)	- C(51)	- C(2)	-179.9(7)
C(51)	- C(5)	- C(6)	- C(61)	4.8(10)
C(6)	- C(5)	- C(51)	- C(52)	179.6(6)
C(6)	- C(5)	- C(51)	- O(51)	2.8(10)
C(2)	- C(51)	- O(51)	- C(31)	-13.2(38)
C(5)	- C(51)	- O(51)	- C(31)	-2.7(6)
C(5)	- C(51)	- C(52)	- C(2)	.4(6)
O(51)	- C(51)	- C(52)	- C(2)	176.7(11)
C(52)	- C(51)	- O(51)	- C(31)	-178.9(10)
N(1)	- C(6)	- C(61)	- C(31)	178.3(9)
C(4)	- C(6)	- C(61)	- C(31)	-160.9(27)
C(5)	- C(6)	- C(61)	- C(31)	-4.9(7)

Parent atom	H	x/a	y/b	z/c
N(1)	H(11)	1945(16)	2994(6)	8673(7)
C(4)	H(41)	3682(22)	4607(8)	10460(9)
	H(42)	6617(22)	4442(8)	9409(9)
C(52)	H(521)	4521(13)	8373(4)	9011(5)
	H(522)	7744(13)	7744(4)	10039(5)
	H(523)	4136(13)	7943(4)	10661(5)
C(61)	H(611)	772(13)	4303(4)	6731(5)
	H(612)	-40(13)	5701(4)	6281(5)
	H(613)	-2152(13)	5037(4)	7439(5)

5. CONCLUSIONS

CHAPTER 5

5 CONCLUSIONS

The objectives of this work have essentially been met. A working analytical program was established for the analysis of REE using the IL 200 ICP. The instrumental parameters chosen were found to be dependant on both the behaviour of the individual REE in the plasma, and the physical characteristics of the instrument. It was found that the optical detection system was prone to drift, and that the degree of spectral interferences observed in the presence of concomitants with the analyte were dependant upon the grating used in the instrument. The choice of analytical wavelength was also dependant upon the matrix of the analyte, different analytical lines being chosen with different matrices.

Cation exchange procedures were developed for the separation of the REE from concomitant matrix elements. This was achieved using Zeocarb 225 SRC 16 (200 mesh) ion-exchange resin. The matrix elements were eluted from the resin using 140 ml of a mixed 1.5 M acid, containing equal concentrations of HNO_3 and HCl. The REE were eluted using 100 ml of 3.0 M HNO_3. Since Al was not totally separated from the REE, it was proposed that the elution REE from the resin depended upon the concentration of other M^{3+} ions present in the solution, forcing the REE to be retained by the resin until the M^{3+} concentration was sufficiently low. The type of acid used during chromatographic experiments was found to influence elution behaviour of a number of elements

including Fe and the REE. The REE content of SS-18 and NIM-G, (SARM 1), was determined using this method.

It was found that the REE could be extracted from a buffered aqueous solution using a synergistic extraction method, where the organic phase contained 0.05 M hexafluoroacetylacetone and 0.07 M quinoline dissolved in chloroform. It was found that hexamethylene tetramine was not a suitable buffer for the aqueous phase when extraction was carried out using acetylacetone, due to formation of a yellow crystalline product, which was identified using X-ray crystallographic techniques.

Samples were prepared for analysis by two different decomposition techniques. Results obtained using a microwave heated dissolution technique were comparable with those obtained using a more conventional pressure bomb digestion method, except for Zr, which showed that resistant minerals were not completely degraded using the microwave technique.

APPENDICES

APPENDIX 1: PREPARATION OF STANDARD REE SOLUTIONS

Standard solutions were prepared by dissolving the appropriate weight of the oxide or nitrate in 5 ml of concentrated HNO_3 or HCl, the solution being warmed where necessary. Solutions were made up to 100 ml with 1 M HCl. Weights, concentrations and dissolution conditions are given below:

ELEMENT	WEIGHT (g)	ACID	CONCENTRATION (ppm)
Y*	0.1270	HCl	976.1
La*	0.1173	HCl	1050.0
Ce*£	0.3099	HCl	992.2
Pr	0.1170	HCl	922.4
Nd	0.1166	HCl	916.9
Sm	0.1160	HCl	880.8
Eu	0.1159	HCl	977.8
Gd	0.1153	HCl	994.4
Tb	0.1176	HNO_3	997.0
Dy	0.1148	HCl	1024.3
Ho*	0.1145	HCl	1018.1
Er	0.1143	HCl	1041.1
Tm	0.1142	HCl	1053.9
Yb	0.1139	HCl	1030.8
Lu	0.1137	HCl	1041.7

* Additional solutions of Y, La, Ce and Ho were required. The concentrations of these solutions were 961.3, 863.2, 1054.9 and 905.6 ppm respectively.

£ Nitrate was used to prepare the standard solution.

APPENDIX 2: CONCENTRATION OF STANDARD TEST SOLUTIONS

ELEMENT	CONCENTRATION (ppm) 999	15	16
K	80.0		
Na	80.0		
Ca	80.0		
Mg	80.0		
Mn	80.0		
Fe	80.0		
Ti	80.0		
Al	80.0		
Cr	8.0		
Co	8.0		
Cu	4.0		
As	0.8		
Se	4.0		
Sr	40.0		
Sb	0.8		
Ba	4.0		
W	0.8		
Zr	20.0		
Zn	16.0		
Ni	4.0		
V	16.0		
Mo	4.0		
Bi	4.0		
Pb	8.0		
Y	1.95	29.28	4.39
La	3.15	31.50	4.72
Ce	5.93	59.52	8.93
Pr	0.46	22.90	0.69
Nd	2.29	22.90	3.48
Sm	0.44	4.40	0.66
Eu	0.98	0.98	0.15
Gd	0.50	4.97	0.75
Tb	0.10	0.99	0.15
Dy	0.41	4.10	0.60
Ho	0.10	1.02	0.16
Er	0.40		
Tm	0.10	0.53	0.07
Yb	0.21	2.06	0.14
Lu	0.10	0.52	0.07

APPENDIX 3: PROGRAMS USED TO INVESTIGATE CHROMATOGRAPHIC SEPARATION OF THE REE FROM MATRIX ELEMENTS.

P#	WP	PWR	NAMED
4	0	3	COLUMN LEACH

ML/M	PDLY	HG	*ANAL	*RDG
1.0	30	1	0	3

#	EL	NM	ORD	CH	MM	BC	SEC
1	NA	589.59	1	A	2	N	2.0
2	CA	317.93	2	A	12	N	2.0
3	MG	285.21	2	A	14	N	0.2
4	BA	233.53	2	A	16	N	2.0
5	SR	216.60	2	A	14	N	0.2
6	AL	309.27	2	A	14	N	2.0
7	MN	257.61	2	A	14	N	2.0
8	FE	259.94	2	A	14	N	2.0
9	ZR	339.20	2	A	14	N	2.0
10	TI	334.94	2	A	14	N	2.0
11	LA	333.75	2	A	14	N	2.0
12	CE	413.77	1	A	14	B	4.0
13	Y	377.43	1	A	14	N	2.0
14	HO	345.60	2	A	14	N	2.0

P#	WP	PWR	NAMED
5	0	3	AL/FE/ZR/REE

ML/M	PDLY	HG	*ANAL	*RDG
1.0	40	1	0	3

#	EL	NM	ORD	CH	MM	BC	SEC
1	AL	309.27	2	A	14	N	2.0
2	ZR	339.20	2	A	18	N	2.0
3	FE	259.94	2	A	18	N	2.0
4	HO	345.60	2	A	20	N	1.0
5	Y	377.43	1	A	20	N	1.0
6	LA	333.75	2	A	18	N	1.0
7	CE	413.77	1	A	20	N	4.0

APPENDIX 4: PROGRAMS USED FOR INVESTIGATION OF INTERFERENCES ON REE FROM CONCOMITANT ELEMENTS.

P#	WP	PWR	NAMED
2	0	3	INTS Y LA CE

ML/M	PDLY	HG	*ANAL	*RDG
1.0	30	1	0	3

#	EL	NM	ORD	CH	MM	BC	SEC
1	Y	371.03	1	A	22	N	2.0
2	Y	324.23	2	A	22	N	2.0
3	Y	377.43	1	A	22	N	2.0
4	LA	379.48	1	A	18	N	2.0
5	LA	333.75	2	A	18	N	2.0
6	LA	408.67	1	A	18	N	2.0
7	CE	418.66	1	A	20	N	3.0
8	CE	413.77	1	A	20	N	3.0
9	CE	446.02	1	A	20	N	3.0
10	CE	395.26	1	A	20	N	3.0

P#	WP	PWR	NAMED
3	0	3	INTS PR ND SM

ML/M	PDLY	HG	*ANAL	*RDG
1.0	30	0	0	3

#	EL	NM	ORD	CH	MM	BC	SEC
1	PR	390.84	1	A	20	N	3.0
2	PR	414.31	1	A	20	N	3.0
3	PR	422.54	1	A	22	N	3.0
4	PR	417.94	1	A	22	N	3.0
5	PR	440.88	1	A	20	N	3.0
6	ND	401.23	1	A	20	N	2.0
7	ND	430.36	1	A	22	N	3.0
8	ND	406.11	1	A	20	N	3.0
9	SM	359.26	2	A	16	N	2.0
10	SM	442.43	1	A	22	N	2.0
11	SM	360.95	2	A	10	N	2.0

P#	WP	PWR	NAMED
6	0	3	EU GD TB

ML/M	PDLY	HG	*ANAL	*RDG
1.0	30	1	0	3

#	EL	NM	ORD	CH	MM	BC	SEC
1	EU	381.97	1	A	18	N	2.0
2	EU	412.97	1	A	18	N	2.0
3	EU	420.51	1	A	18	N	2.0
4	GD	342.25	2	A	18	N	2.0
5	GD	336.22	2	A	18	N	2.0
6	GD	335.05	2	A	16	N	2.0
7	GD	335.86	2	A	16	N	2.0
8	TB	350.92	2	A	16	N	2.0
9	TB	384.87	1	A	20	N	2.0
10	TB	367.64	1	A	18	N	2.0
11	TB	332.44	2	A	16	N	2.0

P#	WP	PWR	NAMED
7	0	3	DY,HO,ER,TM,YB,LU

ML/M	PDLY	HG	*ANAL	*RDG
1.0	30	1	0	3

#	EL	NM	ORD	CH	MM	BC	SEC
1	DY	353.17	2	A	18	N	2.0
2	DY	364.54	2	A	16	N	2.0
3	DY	340.78	1	A	14	N	2.0
4	HO	345.60	2	A	18	N	2.0
5	HO	339.90	2	A	18	N	2.0
6	ER	337.27	2	A	18	N	2.0
7	ER	349.91	2	A	18	N	2.0
8	ER	323.06	2	A	18	N	2.0
9	ER	326.49	2	A	18	N	2.0
10	TM	313.13	2	A	18	N	2.0
11	TM	346.22	2	A	18	N	2.0
12	YB	328.94	2	A	18	N	2.0
13	YB	369.42	1	A	18	N	2.0
14	YB	289.14	2	A	18	N	2.0
15	LU	261.54	2	A	18	N	2.0
16	LU	291.14	2	A	18	N	2.0

APPENDIX 5: CRITERIA FOR LINE SELECTION

The choice of spectral line was based on information obtained from literature, [43,48,142], and line coincidence tables [140]. Spectral interferences were checked by aspirating pure standards of the analyte and concomitants at various wavelengths. Usually background and concomitant interferences were easily seen, although some peaks may have been obscured by fluctuations in background emission intensity, for example, Pr 417.94 nm.

Other parameters were also used in the choice of analytical line and are as follows:

1 DETECTION LIMIT (C_L)

This is defined as the concentration of analyte equal to three times the standard deviation of the background signal (σ_B) :

$$C_L = \frac{3\sigma_B}{S_{ICP}}$$

where S_{ICP} is the slope of the linear calibration curve and

$$S_{ICP} = \frac{I_A - I_B}{C_A}$$

I_A = Intensity of highest standard.

I_B = Intensity of blank or background.

C_A = Concentration of the highest standard.

However, Winge *et al* [145] state that since the standard deviation of the background is in the

region of 1.0% the detection limits may be based on the following equation:

$$C_L = \frac{0.03 \times C_A}{\frac{I_A - I_B}{I_A}}$$

where $I_A - I_B = I_N$, the net signal intensity. Thus the equation becomes:

$$C_L = \frac{0.03 \times C_A \times I_B}{I_N}$$

This was used to determine detection limits for the REE in solution (Table A 5.1).

2 BACKGROUND EQUIVALENT CONCENTRATION (BEC)

Alternatively BEC may be used to determine detection limits or obtain an indication of the sensitivity of the analyte. BEC may be calculated as follows:

$$BEC = \frac{I_B}{I_A} \times C_A$$

3 INTERFERENCE EQUIVALENT CONCENTRATION (IEC)

This is defined as the apparent analyte concentration that is observed for a defined concentration of an interfering concomitant at the analyte wavelength.

$$IEC = \frac{I_I}{I_A} \times C_A$$

where I_I = Intensity of interferent.

Table showing interferent equivalent concentrations are give in Appendix 6

TABLE A 5.1 Detection limits and background equivalent concentrations for REE at the chosen wavelengths.

LINE	C_A (ppm)	I_A	I_B	C_L (ppm)	BEC (ppm)
Y 377.43	9.61	296541	7371	0.007	0.239
La 408.67	8.62	112497	8367	0.021	0.641
Ce 413.77	10.54	81499	16610	0.081	2.148
Pr 417.94	9.22	117656	26210	0.079	2.053
Nd 430.36	9.16	139974	27087	0.065	1.773
Sm 442.43	8.80	43272	7625	0.056	1.550
Eu 381.97	9.77	466390	7135	0.005	0.149
Gd 310.05	9.94	28148	2249	0.026	0.794
Tb 350.92	9.97	66325	4739	0.023	0.712
Dy 353.17	10.24	92117	2298	0.008	0.255
Ho 345.60	9.05	102786	2291	0.006	0.202
Er 337.27	10.41	191640	4983	0.008	0.271
Tm 313.13	10.54	111651	2610	0.008	0.246
Yb 328.94	10.30	603697	2364	0.001	0.040
Lu 261.54	10.42	168589	765	0.001	0.047

APPENDIX 6: INTERFERENCE CORRECTION COEFFICIENTS

During the project, three different monochromator gratings were installed into the IL 200 ICP. Interferences were found to differ to some extent. Tables of comparative interferences are given, with Table A 6.2 being used for analytical purposes.

TABLE A 6.1 Interferences from two monochromators in the IL 200 ICP

		Y1*	Y2*	La1	La2	Ce1	Ce2
Ce	418.66		0.10		0.252		
	413.38						
	446.02	0.11	0.03	0.21			
	395.26						
	413.77						
Pr	390.84					1.18	2.48
	414.31		1.33				0.53
	422.54						
	417.94						0.04
	440.88						1.42
Nd	401.23						4.25
	430.36						
	406.11		0.01				1.09

		Pr1	Pr2	Nd1	Nd2	Sm1	Sm2
Ce	418.66				0.37		
	413.38		0.35		0.87		
	446.02				0.06		0.10
	395.26				2.54		
	413.77						
Pr	390.84				1.12		
	414.31						0.62
	422.54						2.64
	417.94				0.47		
	440.88				0.10		0.98
Nd	401.23		0.10				0.14
	430.36		0.20				0.53
	406.11		0.38			0.04	

		Eu1	Eu2	Gd1	Gd2	Tb1	Tb2
Ce	418.66		0.23				
	413.38						
	446.02		0.08	0.09			
	395.26						
	413.77			1.10	1.30		

Pr	390.84			0.11			
	414.31		0.09				0.18
	422.54						
	417.94						
	440.88				0.94		0.16
Nd	401.23		0.16				1.17
	430.36						
	406.11				0.38	0.29	0.83

		Dy1	Dy2	Ho1	Ho2	Er1	Er2
Ce	418.66						
	413.38						
	446.02	0.10		0.09			
	395.26						
	413.77						
Pr	390.84			0.14			
	414.31		2.05		0.08		1.38
	422.54						
	417.94						
	440.88		0.05				
Nd	401.23						
	430.36						
	406.11	0.06	0.10				

		Tm1	Tm2	Yb1	Yb2	Lu1	Lu2
Ce	418.66						
	413.38						
	446.02	0.13		0.14		0.10	
	395.26						
	413.77						
Pr	390.84	0.08					
	414.31		0.08		0.06		0.07
	422.54						
	417.94						
	440.88						
Nd	401.23						
	430.36						
	406.11	0.04		0.07			

		Si1	Si2	Ca1	Ca2	Fe1	Fe2
Ce	418.66		0.79				0.35
	413.38						
	446.02	0.09	0.35			0.17	
	395.26			17.95	33.73		
	413.77	0.74		0.36		0.31	
Pr	390.84			0.15	5.66		
	414.31		0.29				
	422.54			5.33	0.16		
	417.94	0.18		0.60		0.92	
	440.88		0.33				
Nd	401.23						
	430.36	2.46		1.36		0.92	
	406.11						

		Al1	Al2	Zr1	Zr2	Mn1	Mn2
Ce	418.66		0.25		5.95		
	413.38						
	446.02	0.22					
	395.26	0.30		0.13			
	413.77	0.31		0.41			
Pr	390.84						
	414.31		0.30		0.17		
	422.54						
	417.94	0.64		1.79	5.92		
	440.88		0.40		0.06		
Nd	401.23						
	430.36	0.89		0.71	0.03		
	406.11			0.68	0.18		

		Na1	Na2	Zn1	Zn2	Ba1	Ba2
Ce	418.66		0.38				
	413.38						
	446.02						
	395.26					0.37	
	413.77					0.13	
Pr	390.84						
	414.31		0.20		0.01		
	422.54						
	417.94			0.11			
	440.88		0.21				
Nd	401.23						
	430.36						
	406.11		0.03				

		Cr1	Cr2	V1	V2	W1	W2
Ce	418.66			0.23		0.25	
	413.38						
	446.02						
	395.26			9.99	5.08		
	413.77	0.16				0.10	
Pr	390.84		0.13				
	414.31				0.12		0.31
	422.54						
	417.94	0.91		0.74			
	440.88				9.11		0.72
Nd	401.23	0.16					
	430.36	0.68		1.02			
	406.11						0.06

		Cu1	Cu2	Ti1	Ti2	K1	K2
Ce	418.66				0.51		
	413.38						
	446.02						
	395.26	0.06					
	413.77	0.17				0.08	
Pr	390.84	1.60					
	414.31				0.01		0.13
	422.54						
	417.94	1.84				0.45	
	440.88						0.10
Nd	401.23			0.10	2.61		
	430.36	0.23				0.39	
	406.11	0.04					

		Ni1	Ni2	Mg1	Mg2	Sr1	Sr2
Ce	418.66						1.42
	413.38						0.02
	446.02		0.11		0.24		0.30
	395.26						
	413.77						
Pr	390.84						0.02
	414.31		0.43		0.52		0.68
	422.54						5.96
	417.94						
	440.88		0.72		0.88		1.22
Nd	401.23		0.05		0.01		0.14
	430.36						0.08
	406.11		0.16		0.28		6.81

* Numbering 1 and 2 refers to the two different monochromators used to investigate interferences of REE and matrix elements on the REE lines given.

TABLE A 6.2 Interferences corrections used in the determination of REE in SS-18 and NIM-G.

	377.43 Y	408.67 La	413.77 Ce	417.94 Pr	430.36 Nd
Y				0.10	
La	0.43				
Ce		0.46		0.21	
Pr			0.22		0.69
Nd	0.07	0.05	0.08	1.09	
Sm				0.11	0.17
Eu				0.11	0.08
Gd			1.56		0.08
Tb				0.22	
Dy		0.07	0.06		
Ho					
Er					0.12
Tm			0.09		
Yb					
Lu					

	377.43 Y	408.67 La	413.77 Ce	417.94 Pr	430.36 Nd
Si				0.48	0.39
Ca				0.28	0.34
Al				0.29	0.22
Fe				0.19	0.16
Zr				5.26	0.43
Mn				0.25	0.23
Na				0.20	
Zn					0.10
Ba					
Cu					
Ti			0.31		0.11
Cr					
V				0.26	
W			0.75		

	442.43 Sm	381.97 Eu	310.05 Gd	350.92 Tb	353.17 Dy
Y					
La				0.13	
Ce	0.09			0.35	
Pr	0.37				
Nd	0.11				
Sm				0.18	
Eu	0.17			0.11	
Gd	0.09	0.55			
Tb		0.08	0.11		
Dy				0.22	
Ho				0.41	
Er					
Tm					
Yb					
Lu					
Si	0.40			0.09	
Ca	0.25				
Al	0.25		0.31	0.11	
Fe	0.16				
Zr	0.41			2.05	0.11
Mn	0.22				0.29
Na	0.12				
Zn	0.07				
Ba					
Cu					
Ti			0.39	0.18	
Cr					0.11
V			0.20	0.20	0.10
W			0.16		

	345.60 Ho	337.27 Er	313.13 Tm	328.94 Yb	261.54 Lu
Y					
La					
Ce					
Pr					
Nd					
Sm					
Eu					
Gd					
Tb		0.20			
Dy					
Ho			0.47		
Er	0.12		0.12		0.09
Tm		0.14			
Yb			0.19		
Lu				0.10	
Si		0.10			
Ca					
Al					0.07
Fe					
Zr	0.22	0.20	0.28		
Mn					0.19
Na					
Zn					
Ba					
Cu					
Ti		134.4			
Cr		0.19	0.14		
V			0.25	0.22	
W					

REFERENCES

REFERENCES

1) **J Kaczmarek** Rare Earths: Discovery and Commercial Separations: Text of an Address to the American Chemical Society. August 1980.

2) **I Jarvis** and **K E Jarvis** *Chem. Geol.* 53 335 (1986).

3) **E D Goldberg, M Koide, R A Schmidt** and **R H Smith** *J. Geophys. Res.* 68 4209 (1963).

4) **M A Haskin** and **L A Haskin** *Science* 154 507 (1966).

5) **L A Haskin, M A Haskin, F A Frey** and **T R Wildeman** Relative and Absolute Terrestrial Abundances of Rare Earths in: Ed. **L H Ahrens**," Origin and Distribution of the Elements". p 899, Pergamon Press, Oxford, (1968).

6) **T R Wildeman** and **L A Haskin** *Geochim. Cosmochim. Acta* 37 419 (1973).

7) **S M McLennan, B J Fryer** and **G M Young** *Geochim. Cosmochim. Acta* 43 375 (1979).

8) **S M McLennan, W B Nance** and **S R Taylor** *Goechim. Cosmochim. Acta* 44 1833 (1980).

9) **V A Fassel** *Anal. Chem.* 32 19A (1980).

10) **A G I Dalvi, C S Deodhar** and **B D Joshi** *Talanta* 24 143 (1977).

11) **I Olmez** and **G E Gordon** *Science* 229 966 (1985).

12) **A Hirose, K Kobori** and **D Ishii** *Anal. Chim. Acta* 32 91 (1965).

13) **I Roelandts** *Radio Chim. Acta* 24 139 (1977).

14) **J Alstad, J H Auguston** and **L Farbu** *J. Inorg. Nucl. Chem.* 36 899 (1974).

15) **J Tang** and **C M Wai** *Anal. Chem.* 58 3233 (1986).

16) **B Bernas** *Anal. Chem.* 40 1682 (1968).

17) **J C Sen Gupta** *Talanta* 28 31 (1980).

18) **V A Fassel, H D Cook, L C Krotz** and **P W Kehres** *Spectrochim. Acta* 5 201 (1952).

19) **F B Huke, R H Heider** and **V A Fassel** *J. Opt. Soc. Am.* 43 400 (1952).

20) **I Roelandts** *Anal. Chem.* 53 676 (1981).

21) **N Eby** *Anal. Chem.* 44 2173 (1972).

22) **J-O Burman** and **K Bostrom** *Anal. Chem.* 51 516 (1979).

23) **M D Feigenson** and **M J Carr** *Chem. Geol.* 51 19 (1985).

24) **F Flavelle** and **A D Westland** *Talanta* 33 445 (1986).

25) **T Moeller** and **D E Jackson** *Anal. Chem.* 22 1393 (1950).

26) **V K Manchanda** and **C A Chang** *Anal. Chem.* 59 813 (1987).

27) **J W Mitchell** and **C V Banks** *Talanta* 19 1157 (1972).

28) **A A Ramirez, C J Linares, F A Barrero** and **M R Ceba** *Talanta* 33 1021 (1986).

29) **C Woo, W F Wagner** and **D E Sands** *J. Inorg. Nucl. Chem.* 34 307 (1972).

30) **R Du Preez** and **J S Preston** *S. Afr. J. Chem.* 39 137 (1986).

31) **H Zhang-Fa, J Xi-Pin** and **H Chao-Sheng** *Talanta* 33 455 (1986).

32) **J Wang** and **J M Zadeii** *Talanta* 33 321 (1986).

33) **A R Date** and **A L Gray** *Spectrochim. Acta* 40B 115 (1985).

34) **H P Longerich, B J Fryer, D F Strong** and **C J Kantipuly** *Spectrochim. Acta* 42B 75 (1987).

35) **A R Date, Y Y Cheung** and **M E Stuart** *Spectrochim. Acta* 42B 3 (1987).

36) **J Luck** *ICP Info. Newslett.* 12 800 (1987).

37) **F E Lichte, A L Meier** and **J G Crock** *Anal. Chem.* 59 1150 (1987).

38) **S J Buchanan** and **L S Dale** *Spectrochim. Acta* 41B 237 (1986).

39) **R Aulis, A Bolton, W Doherty, A van der Voet** and **P Wong** *Spectrochim. Acta* 40B 377 (1985).

40) **I B Brenner, A E Watson, T W Steele, E A Jones** and **M Goncalves** *Spectrochim. Acta* 36B 785 (1981).

41) **J A C Broekaert, F Leis** and **K Laqua** *Spectrochim. Acta* 34B 73 (1979).

42) **C C Butler, R N Knisley** and **V A Fassel** *Anal. Chem.* 47 825 (1975).

43) **T Fries P J Lamothe** and **J J Pesek** *Anal. Chim. Acta* 159 329 (1984).

44) **M A Floyd, V A Fassel** and **A P D'Silva** *Anal. Chem.* 52 2168 (1980).

45) **K Iwasaki, K Fuwa** and **H Haraguchi** *Anal. Chim. Acta* 183 239 (1986).

46) **R J Lukasiewicz, F G Dewalt** and **B D Webb** *ICP Info. Newslett.* 11 858 (1986).

47) **R Ni-Chung, C Wu-Min, J Zu-Cheng** and **Z Yun-E** *Spectrochim. Acta* 32B 175 (1982).

48) **S Sato** *ICP Info. Newslett.* 8 143 (1982).

49) **J N Walsh** *Spectrochim. Acta* 35B (1980).

50) **R M Barnes** *Anal. Chem.* 50 100R (1978).

51) **A Petrakiev, L Alexieva** and **L Lasarova** *ICP Info. Newslett.* 12 837 (1987).

52) **P Neras** and **G Wansen** *ICP Info. Newslett.* 12 813 (1987).

53) **C C Schnetzler, H H Thomas** and **J A Philpotts** *Anal. Chem.* 39 1888 (1967).

54) **J G Crock** and **F E Lichte** *Anal. Chem.* 54 1329 (1982).

55) **A Bolton, J Hwang** and **A van der Voet** *Spectrochim. Acta* 38B 165 (1983).

56) **I B Brenner, E A Jones, A E Watson** and **T W Steele** *Chem. Geol.* 45 135 (1984).

57) **J G Crock, F E Lichte, G O Riddle** and **C L Beech** *Talanta* 33 601 (1986).

58) **J G Crock, F E Lichte** and **T R Wildeman** *Chem. Geol.* 45 149 (1984).

59) **A Miyazaki** and **R M Barnes** *Anal. Chem.* 53 299 (1981).

60) **J N Walsh, F Buckley** and **J Barker** *Chem. Geol.* 33 141 (1981).

61) **J S Fritz** and **R G Greene** *Anal. Chem.* 36 1095 (1964).

62) **B L Jangida, N Krishnamachari, M S Varde** and **V Venkatasubramanian** *Anal. Chim. Acta* 32 91 (1965).

63) **D F Wood** and **M Turner** *Analyst* 84 725 (1959).

64) **T V Healy** and **J R Ferraro** *J. Inorg. Nucl. Chem.* 24 1499 (1962).

65) **T V Healy** and **J R Ferraro** *J. Inorg. Nucl. Chem.* 24 1463 (1962).

66) **E A Huff** and **E P Horwitz** *Spectrochim. Acta* 40B 279 (1985).

67) **P K Khopkar** and **J N Mathur** *J. Inorg. Nucl. Chem.* 39 2063 (1977).

68) **T Sekine** and **D Dyrssen** *J. Inorg. Nucl. Chem.* 39 1457 (1967).

69) **T Sekine** and **D Dyrssen** *J. Inorg. Nucl. Chem.* 39 1475 (1967).

70) **T Sekine** and **D Dyrssen** *J. Inorg. Nucl. Chem.* 39 1481 (1967).

71) **T Sekine** and **D Dyrssen** *J. Inorg. Nucl. Chem.* 39 1489 (1967).

72) **M W Blades** and **G Horlick** *Spectrochim. Acta* 36B 881 (1981).

73) **R Herman** and **C T J Alkemade** "Chemical Analysis by Flame Photometry", Wiley Interscience, New York, (1963).

74) **T Maruta, T Takouchi** and **M Suzuki** *Anal. Chim. Acta* 58 452 (1972).

75) **P W J M Boumans** "Theory of Spectrochemical Excitation", Plenum Press, New York or Hilger, London, (1966).

76) **P W J M Boumans** and **F J De Boer** *Spectrochim. Acta* 30B 309 (1975).

77) **G F Larson, V A Fassel, R M Scott** and **R N Knisley** *Anal.Chem.* 47 238 (1975).

78) **G R Kornblum** and **L De Galan** *Spectrochim. Acta* 32B 445 (1977).

79) **P W J M Boumans** and **F J De Boer** *Spectrochim. Acta* 31B 35 (1976).

80) **P W J M Boumans** *Proc. 20th Coll. Spectr. Int.* and *7th Int. Conf. Atomic Spectr.* Prague, (1977), Invited Lectures, 1 7. Statini Pedagogicke Nakladatelstvi Prague, (1977): *ICP Info. Newslett.* 3 142, 173 (1977).

81) **M W Blades** and **G Horlick** *Spectrochim. Acta* 36B 861 (1981).

82) **L J Prell, C Monnig, R E Harris** and **S R Koirtyohann** *Spectrochim. Acta* 40B 1401 (1985).

83) **J P Matousek B J Orr** and **M Selby** *Spectrochim. Acta* 41B 415 (1986).

84) **R K Skogerboe** and **G B Butcher** *Spectrochim. Acta* 40B 1631 (1985).

85) **S Greenfield, H McD McGeachin** and **P B Smith** *Anal. Chim. Acta* 84 67 (1976).

86) **F J M Maessen, J Balke** and **J L M De Boer** *Spectrochim. Acta* 37B 517 (1982).

87) **R I Botto** *Spectrochim. Acta* 40B 397 (1985).

88) **J A C Broekaert, F Leis** and **K Laqua** *Spectrochim. Acta* 34B 167 (1979).

89) **G F Larson** and **V A Fassel** *Appl. Spectrosc.* 33 592 (1976).

90) **G F Larson, V A Fassel, R K Winge** and **R N Knisley** *Appl. Spectrosc.* 30 384 (1976).

91) **P W J M Boumans** and **J J A M Vrakking** *Spectrochim. Acta* 39B 1261 (1984).

92) **R I Botto** *Spectrochim. Acta* 38B 129 (1983).

93) **A R Forster, T A Anderson** and **M L Parsons** *Appl. Spectrosc.* 36 499 (1982).

94) **T A Anderson, A R Forster** and **M L Parsons** *Appl. Spectrosc.* 36 504 (1982).

95) **S O Farwell** and **C T Kagel** *Appl. Spectrosc.* 40 944 (1986).

96) **L L Burton** and **M W Blades** *Spectrochim. Acta* 41B 1063 (1986).

97) **P W J M Boumans** and **J J A M Vrakking** *Spectrochim. Acta* 40B 1085 (1985).

98) **P W J M Boumans** and **J J A M Vrakking** *Spectrochim. Acta* 40B 1107 (1985).

99) **P W J M Boumans** and **J J A M Vrakking** *Spectrochim. Acta* 40B 1423 (1985).

100) **R J Krupa, G L Long** and **J D Winefordner** *Spectrochim. Acta* 40B 1485 (1985).

101) **E H Choot** and **G Horlick** *Spectrochim. Acta* 41B 889 (1986).

102) **E H Choot** and **G Horlick** *Spectrochim. Acta* 41B 907 (1986).

103) **E H Choot** and **G Horlick** *Spectrochim. Acta* 41B 925 (1986).

104) **E H Choot** and **G Horlick** *Spectrochim. Acta* 41B 935 (1986).

105) **R M Belchamber, D Betteridge, A P Wade, A J Cruickshank** and **P Davison** *Spectrochim. Acta* 41B 503 (1986).

106) **G L Moore, P J Humphries-Cuff** and **A E Watson** *Spectrochim. Acta* 39B 915 (1984).

107) **S B Smith (jr), M A Sainz** and **R G Schleicher** *Spectrochim. Acta* 42B 323 (1987).

108) **P Werner** and **H Friege** *Appl. Spectrosc.* 41 39 (1987).

109) **J Korkish, I Hazan** and **G Arrhenius** *Talanta* 10 865 (1963).

110) **Zs Horvath** and **R M Barnes** *Anal. Chem.*58 1353 (1986).

111) **E A Huff** *Spectrochim. Acta* 42B 275 (1987).

112) **P Fuxing, Y Suling, H Qinghua, W Xiaoping, M Heying, H Yanmin, X Yuxin, X Yi** and **W Tingfang** *Spectrochim. Acta* 41B 1211 (1986).

113) **E Merciny, J F Desreux** and **J Fuger** *Anal. Chim. Acta* 189 301 (1986).

114) **D L Massart** and **W Bossaert** *J. Chromatog.* 32 195 (1968).

115) **J E Powell** and **H R Burkholder** *J. Chromatog.* 36 99 (1968).

116) **T V Healy, D F Peppard** and **G W Mason** *J. Inorg. Nucl. Chem.* 24 1429 (1962).

117) **T B Pierce** and **P F Peck** *Analyst* 88 217 (1963).

118) **J S Preston** *Hydrometall* 14 171 (1985).

119) **A W Boorn, M S Cresser** and **R F Browner** *Spectrochim. Acta* 35B 823 (1980).

120) **R I Botto** *Spectrochim. Acta* 42B 181 (1987).

121) **M S Cresser** *Prog. Analyt. Atom. Spectrosc.* 5 35 (1982).

122) **A W Boorn** and **R F Browner** *Anal. Chem.* 54 1402 (1982).

123) **J A C Broekaert, F Leis** and **K Laqua** *Talanta* 28 745 (1981).

124) **R C Ng, H Kaiser** and **B Meddings** *Spectrochim. Acta* 40B 63 (1985).

125) **D D Nygaard, R G Schleicher** and **J J Sotera** *Appl. Spectrosc.* 40 1074 (1986).

126) **N H Suhr** and **C O Ingamells** *Anal. Chem.* 38 730 (1966).

127) **J P Riley** *Anal. Chim. Acta* 19 413 (1958).

128) **B Casetta, A Giaretta** and **G Rampazzo** *Atom. Spectrosc.* 4 152 (1983).

129) **A M Hartstein, R W Freedman** and **D W Platter** *Anal. Chim. Acta* 45 611 (1973).

130) **F J Langmyhr** and **S Sveen** *Anal. Chim. Acta* 32 1 (1965).

131) **F J Langmyhr** and **K Kringstad** *Anal. Chim. Acta* 35 131 (1966).

132) **F J Langmyhr** and **P E Paus** *Anal. Chim. Acta* 43 397 (1968).

133) **L B Jassie** and **H M Kingston** *Shortcut to Elemental Trace Analysis*. Industrial Chemical News. February (1984).

134) **P J Lamothe, T L Fries** and **J J Consul** *Anal. Chem.* 58 1881 (1986).

135) **R A Nadkarni** *Anal. Chem.* 56 2233 (1984).

136) **L B Fischer** *Anal. Chem.* 58 261 (1986).

137) **R A Edge** *Chem. Anal.* 47 72 (1958), in Ion-Exchange Resins 4 th Ed. The British Drug Houses Ltd, BDH Laboratory Chemicals Division, Poole, England.

138) **T Moeller** "The Lanthanides, in Comprehensive Inorganic Chemistry". Ed. **J C Bailar (jr), H J Emeleus, Sir R Nyholm** and **A F Trotman-Dickenson** vol 4 Pergamon Press, New York, (1975).

139) **S J Lyle** and **Mo M Rahman** *Talanta* 10 1177 (1963).

140) **P W J M Boumans**, Line Coincidence Tables for Inductively Coupled Plasma Atomic Emission Spectrometry, vol 1 and 2 Pergamon Press, New York, (1980).

141) **I Roelandts** and **G Michel** *Geostandards Newslett.* 10 135 (1986).

142) **D Nygaard** "Methods Manual of Inductively Coupled Plasma IL 200". Applied Analytical Systems, USA, January (1984).

143) **F C Saville** "Comprehensive Analytical Chemistry". Ed. **C L Wilson, D W Wilson** and **C R N Strouts** vol IIB 223. Physical Separation Methods. Elsevier, Amsterdam, (1968).

144) **F A Cotton** and **G Wilkinson** "Advanced Inorganic Chemistry, A Comprehensive Text". 4 th ed. John Wiley and Sons, USA, (1980).

145) **R K Winge, V J Petersen** and **V A Fassel** *Appl. Spectrosc.* 33 206 (1979).

146) **K R Koch** and **M A B Pougnet** Private Communication.

147) CRC Handbook of Chemistry and Physics; A Ready-Reference Book of Chemical and Physical Data. Ed. **R C Weast, M J Astle** and **W H Beyer**. 64th ed. Chemical Rubber Publishing Company, USA, (1984).

148) **J Stary** and **J O Liljenzin** *Pure Appl. Chem.* 54 2557 (1982).

149) **E K Hulet** and **D D Bode** Separation Chemistry of the Lanthanides and Transplutonium Actinides,p 10 in "MTP International Review of Science, Lanthanides and Actinides", Inorganic Chemistry Series One, vol 7 Ed. **K W Bagnall** and **H J Emeleus**. Butterworths, London, (1972).

150) **G M Sheldrick**, in Crystallographic Computing 3 Ed. **G M Sheldrick, C Kruger** and **R Goddard**, 175-189, Oxford University Press, (1985).

151) **G M Sheldrick**, The SHELX Program System, Univ. Chem. Lab., Cambridge, England, (1976).

SEPARATION, PRECONCENTRATION AND DETERMINATION OF RARE EARTH ELEMENTS BY INDUCTIVELY COUPLED PLASMA EMISSION SPECTROSCOPY

DIAGRAMS FOR CHAPTER FOUR : TRACES OF SPECTRAL INTERFERENCES

DIAGRAMS FOR CHAPTER FOUR

These diagrams are divided into two categories based on the elements chosen to investigate spectral interferences at the various analytical wavelengths for the REE. Diagrams were prepared in the following manner:

1) Investigation of REE interferences.
2) Investigation of non-REE interferences.

REE interferences were determined by aspirating approximately 10 ppm solutions of the individual rare earth solutions at the analytical wavelength of interest. Each trace was recorded over the spectral wavelength, the number of traces that could be superimposed being large. Interferences from non-REE were determined in a similar manner except 100 ppm solutions were aspirated at the analytical wavelength. Traces labeled "Interferences from Non-REE" include interferences from the group of elements including: Na, Ca, Ba, Mg, Sr, K, Al, Mn, Fe, Zr, Ti, Cu, Si, V, W, Cr and Zn, while traces labled "Interferences from REE" include interferences from the REE and Y. Interferences will be shown in the sequence described in Chapter 4.

YTTRIUM 377.43 nm

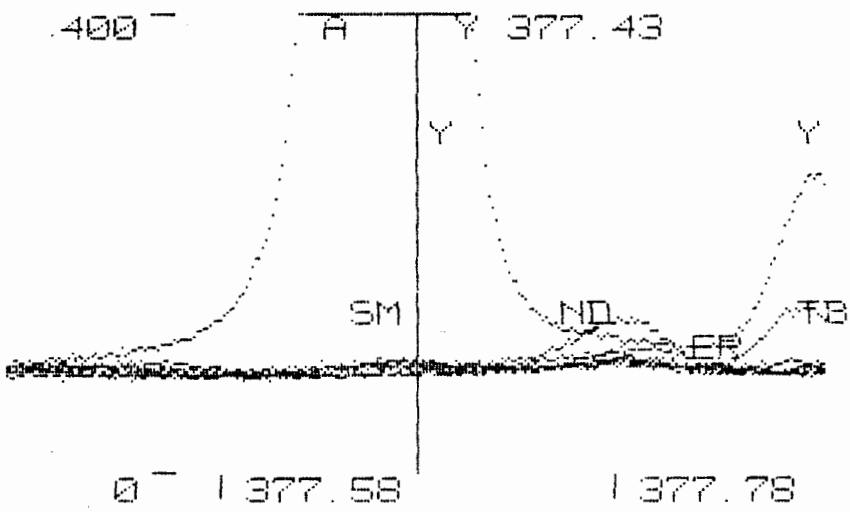

INTERFERENCES FROM REE ON Y.

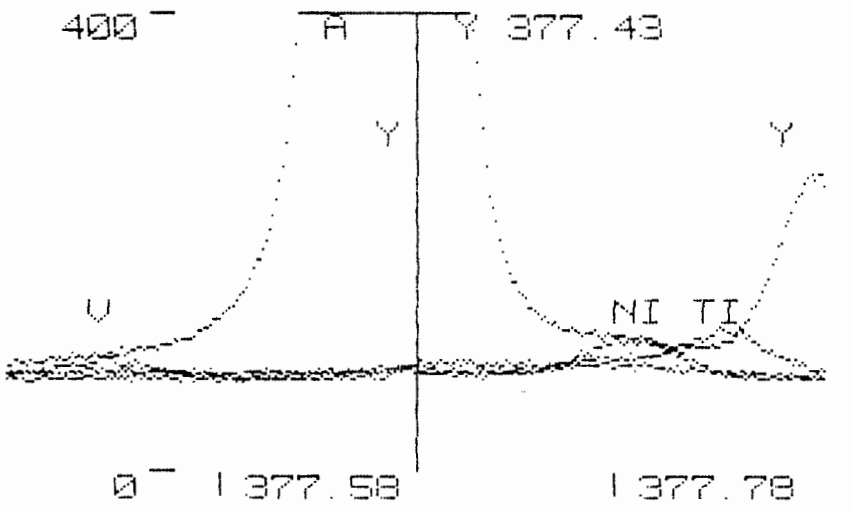

INTERFERENCES FROM NON-REE ON Y.

YTTRIUM 371.03 nm

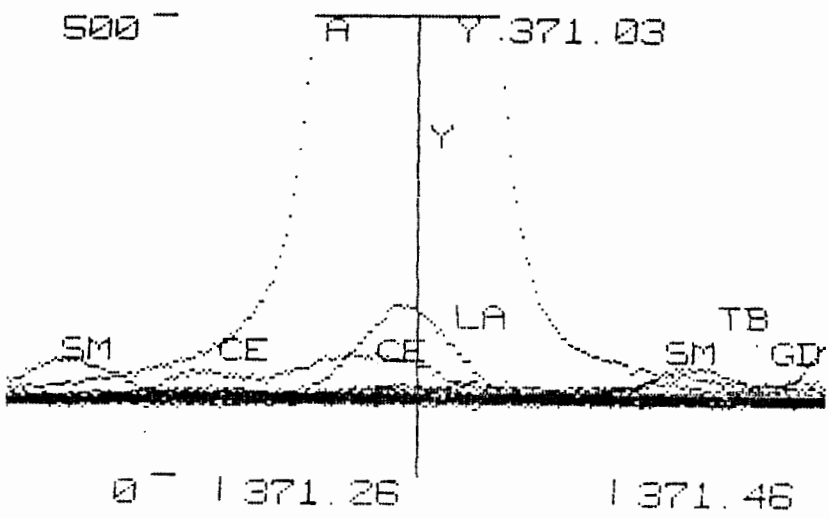

INTERFERENCES OF REE ON Y.

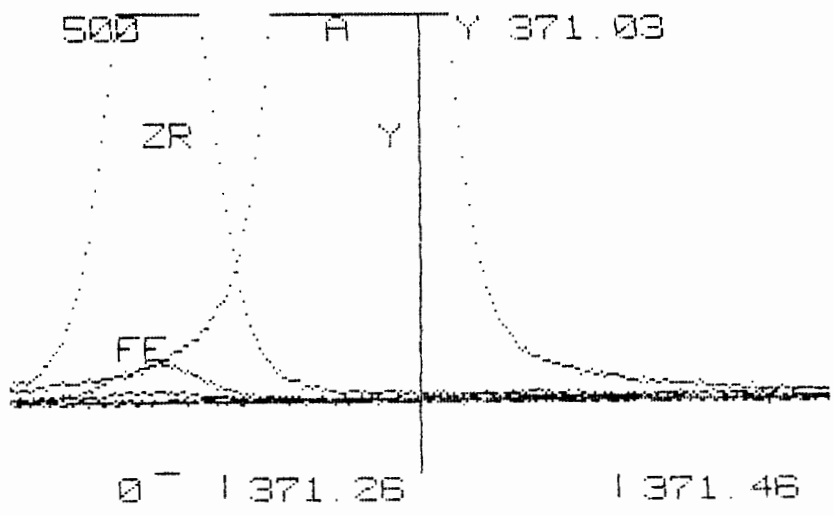

INTERFERENCES FROM NON-REE ON Y.

YTTRIUM 360.07 nm

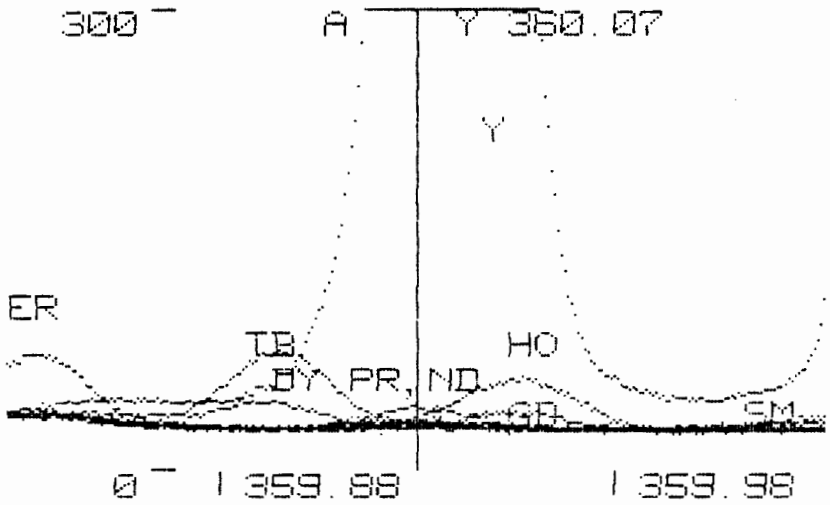

INTERFERENCES FROM REE ON Y.

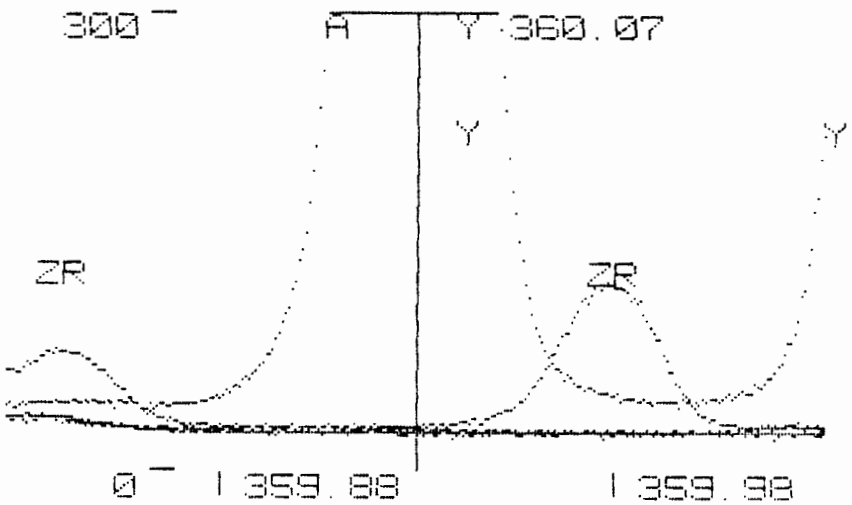

INTERFERENCES FROM NON-REE ON Y.

YTTRIUM 324.23 nm

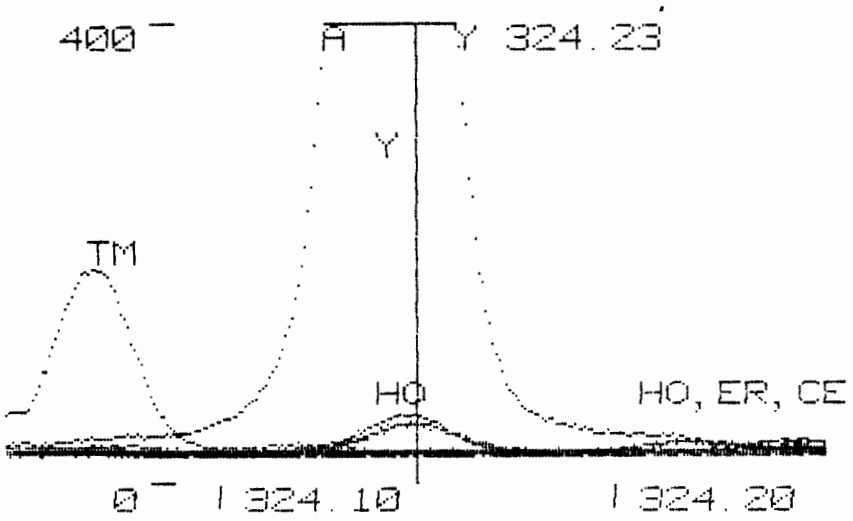

INTERFERENCES FROM REE ON Y.

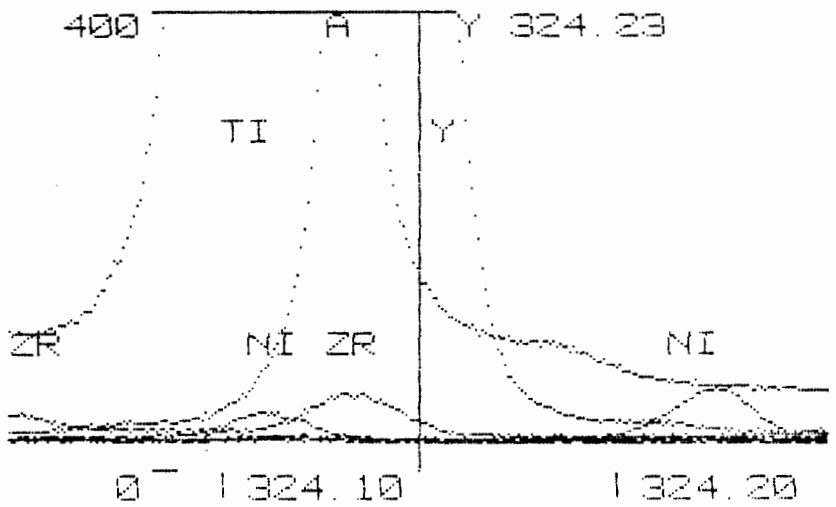

INTERFERENCES FROM NON-REE ON Y.

LANTHANUM 333.75 nm

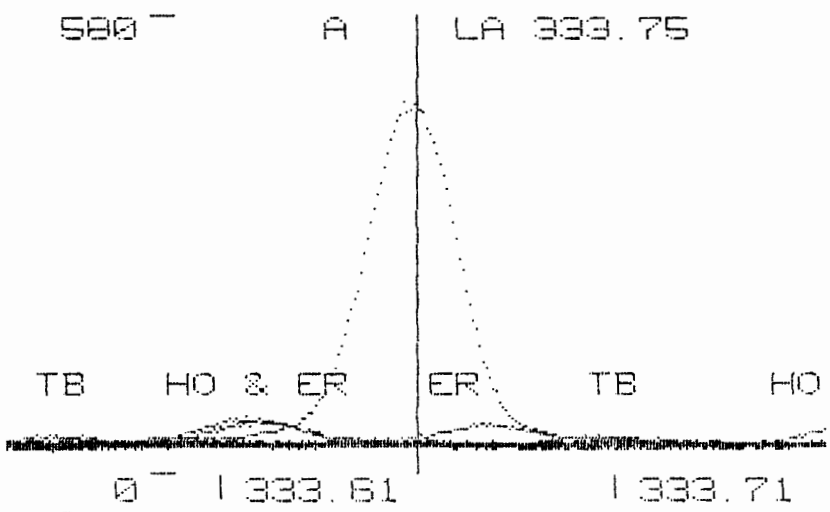

INTERFERENCES FROM REE ON LA.

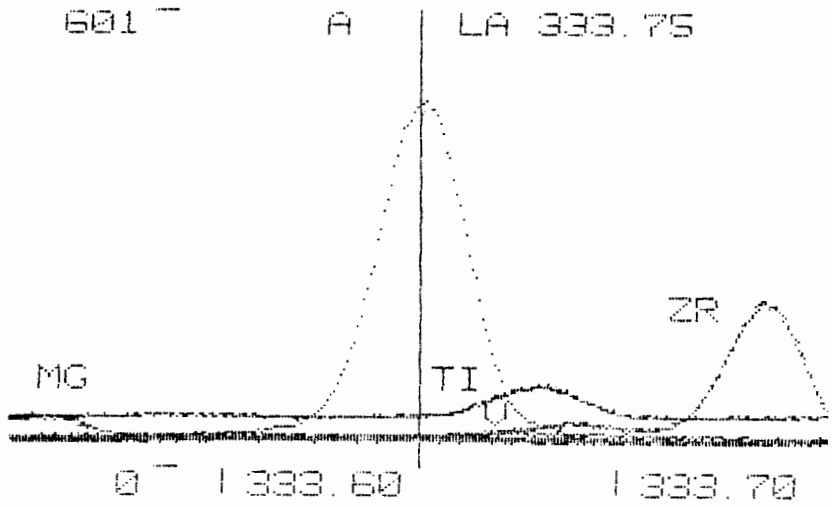

INTERFERENCES FROM NON-REE ON LA.

LANTHANUM 379.48 nm

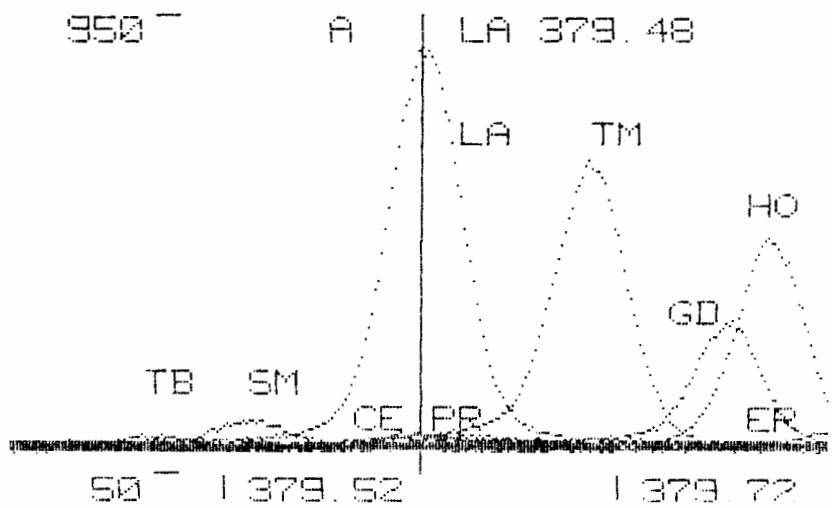

INTERFERENCES FROM REE ON LA.

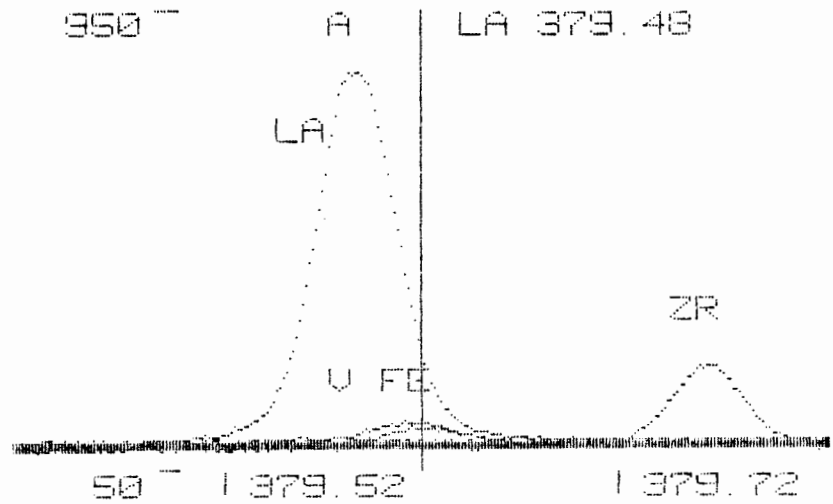

INTERFERENCES FROM NON-REE ON LA.

LANTHANUM 408.67 nm

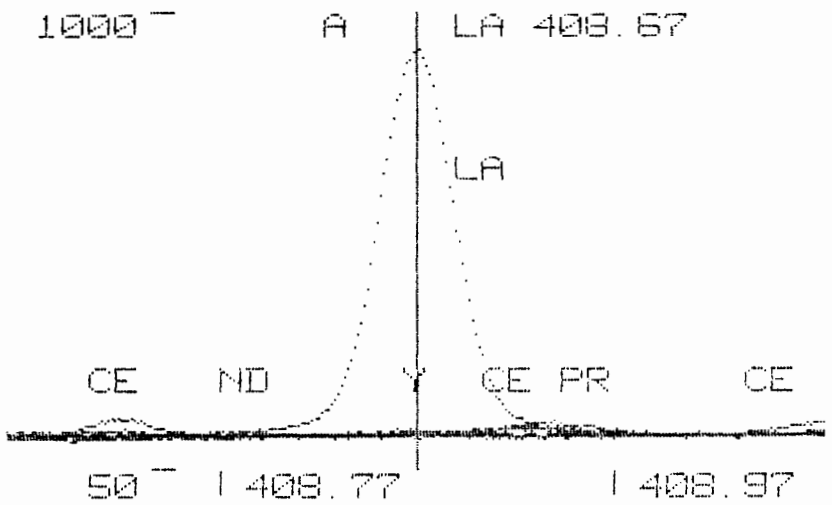

INTERFERENCES FROM REE, Y, CE, PR AND ND ON LA.

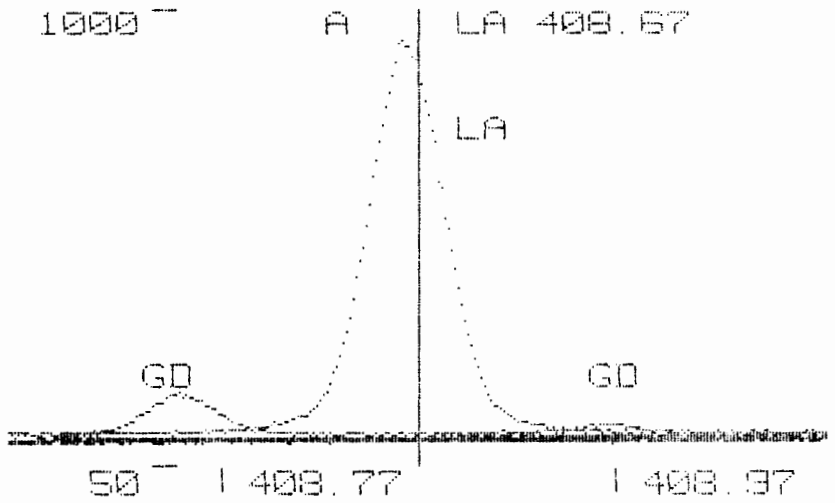

INTERFERENCES FROM SM-LU ON LA.

LANTHANUM 408.67 nm (cont)

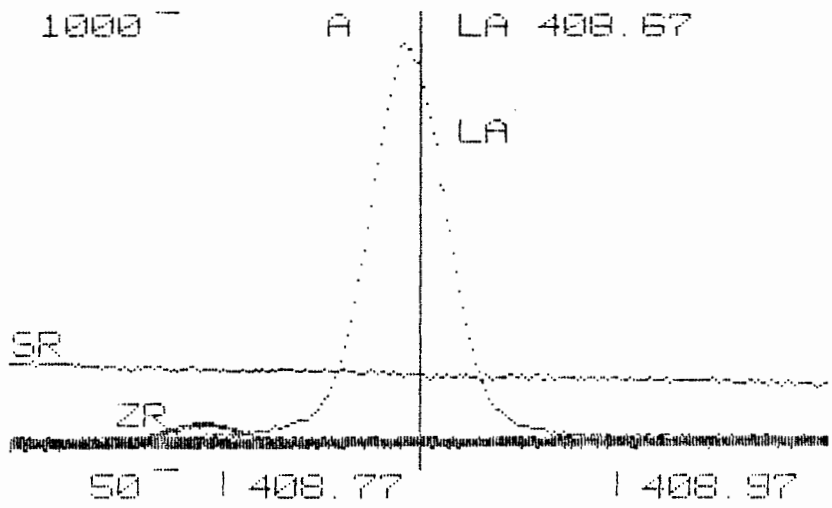

INTERFERENCES FROM NON-REE ON LA.

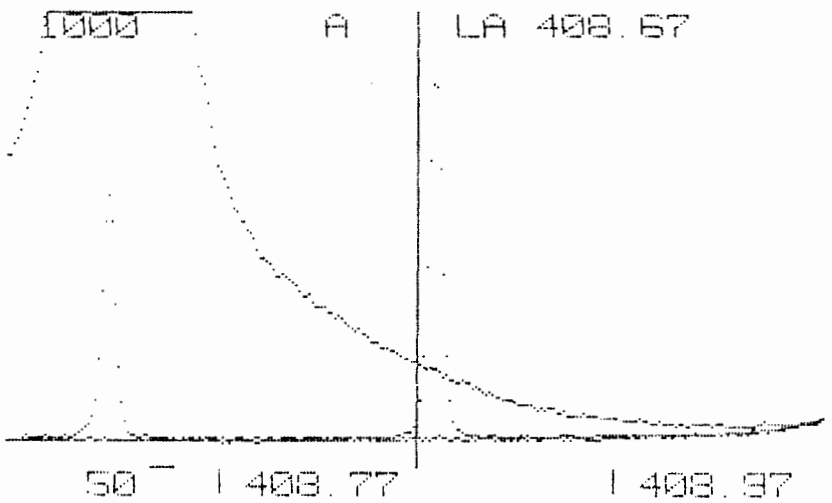

INTERFERENCES FROM SR ON LA.

CERIUM 413.38 nm

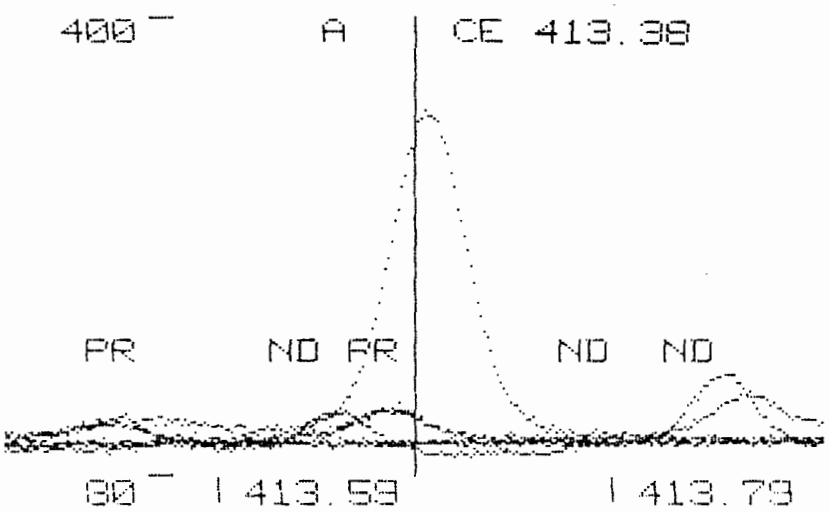

INTERFERENCES FROM REE, Y-ND, ON CE.

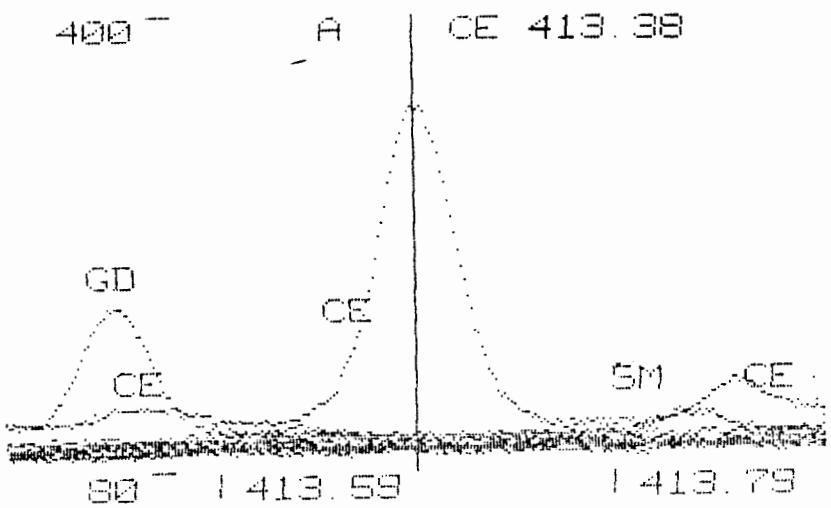

INTERFERENCES FROM REE, SM-LU, ON CE.

CERIUM 413.38 nm (cont)

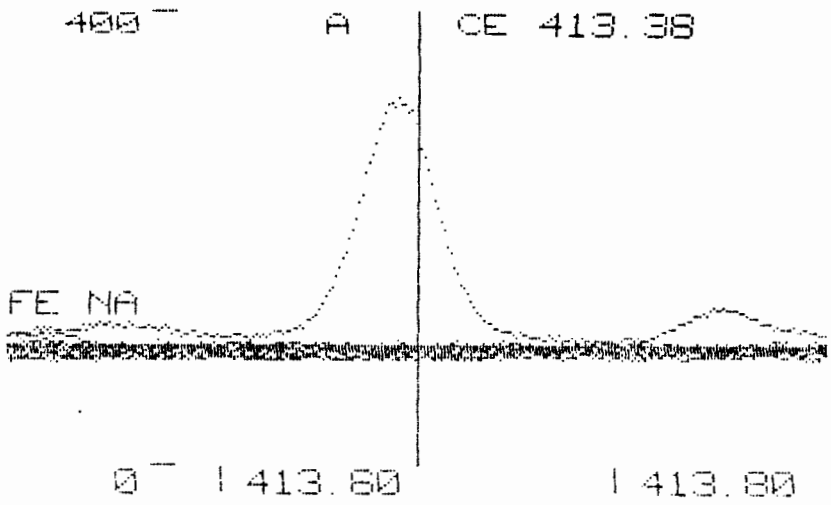

INTERFERENCES FROM NON-REE, SI, AL, FE, ZR, CA, NA AND ZN ON CE.

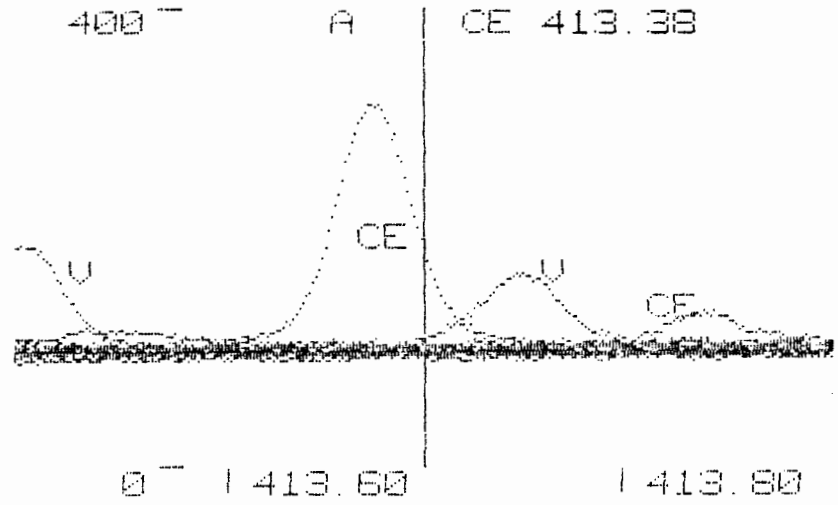

INTERFERENCES FROM NON-REE, BA-SR, ON CE.

CERIUM 413.77 nm

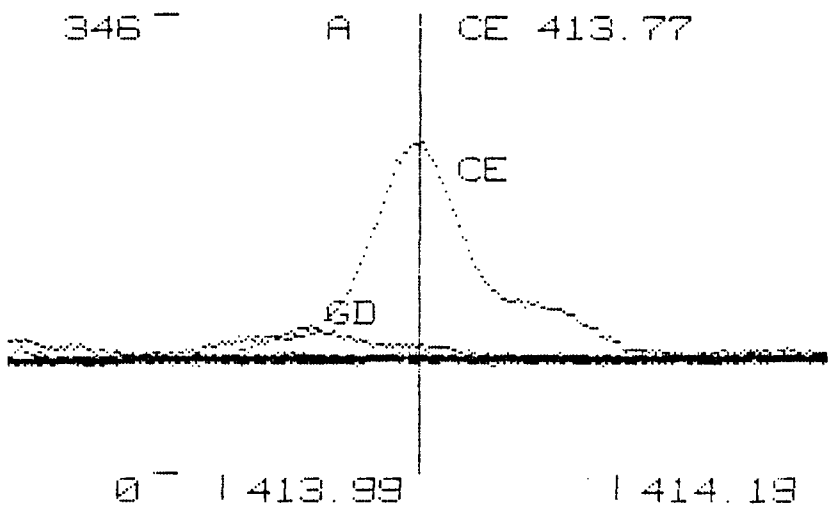

INTERFERENCES FROM REE ON CE.

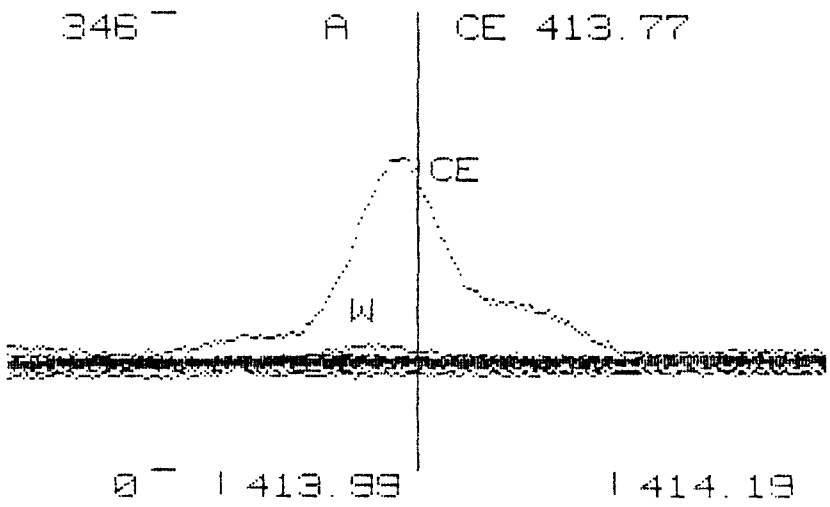

INTERFERENCES FROM NON-REE ON CE.

CERIUM 446.02 nm

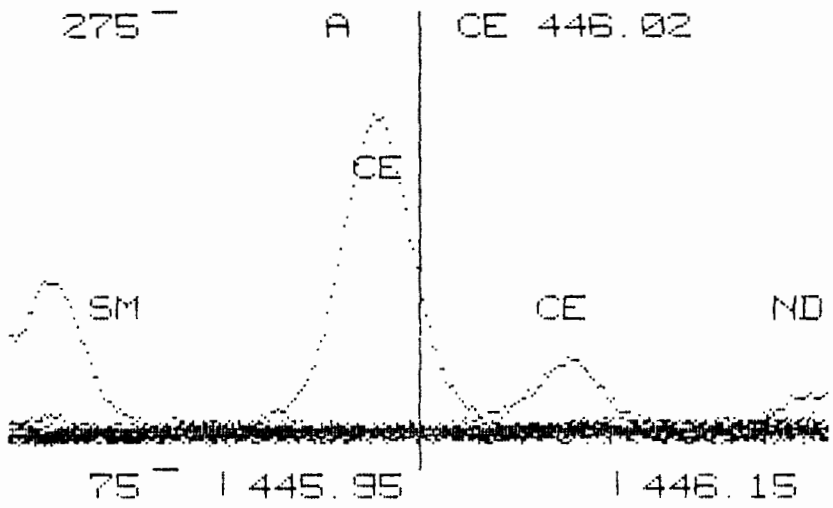

INTERFERENCES FROM REE ON CE.

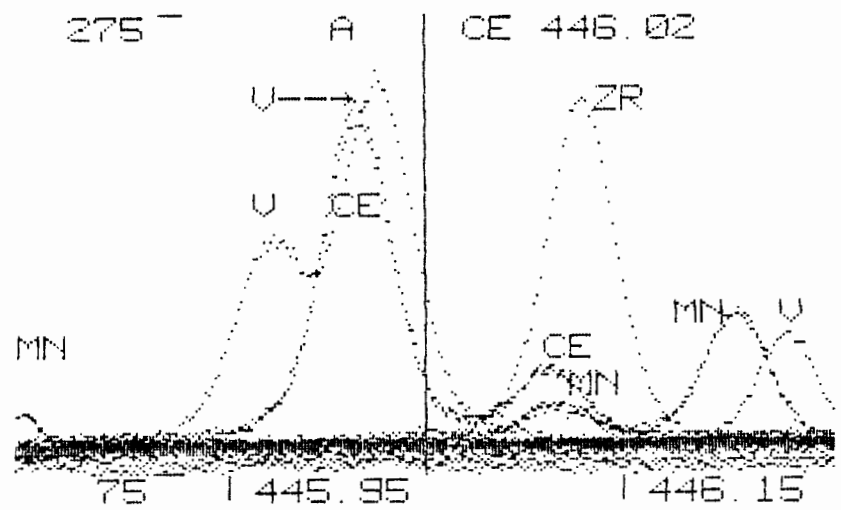

INTERFERENCES FROM NON-REE ON CE.

CERIUM 395.26 nm

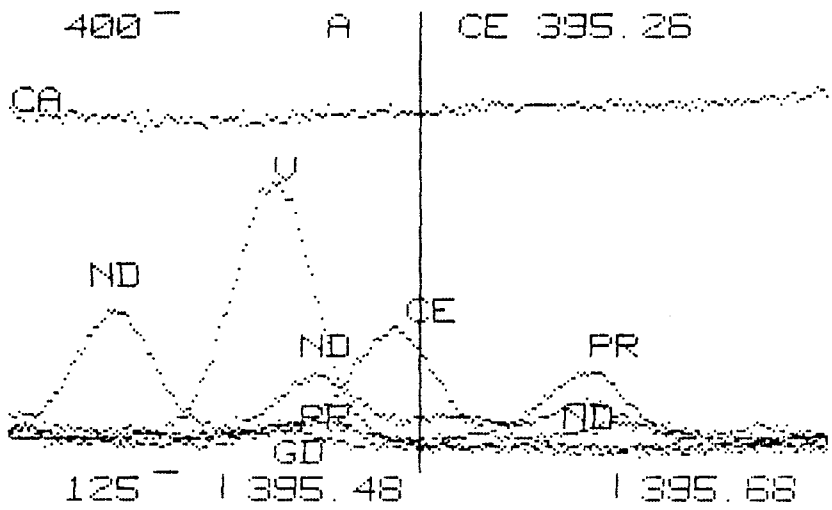

INTERFERENCES FROM ND, PR, CA AND V ON CE.

CERIUM 418.66 nm

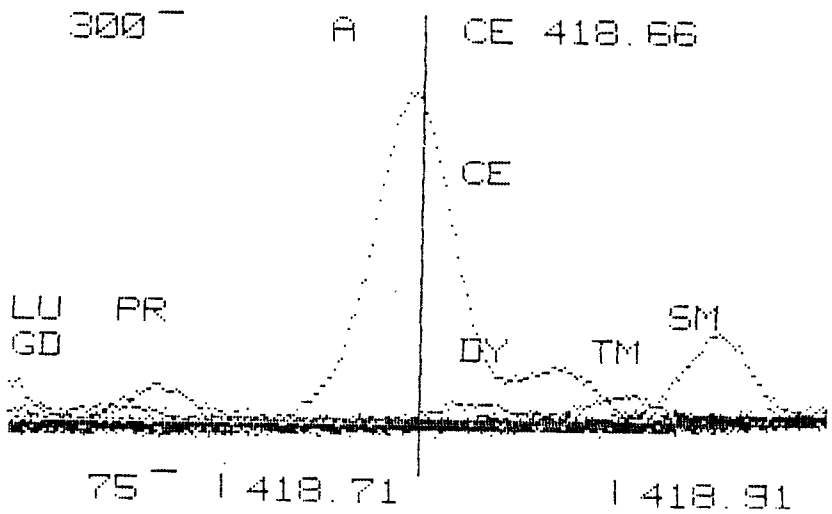

INTERFERENCES FROM REE ON CE

PRAESODYMIUM 422.54 nm

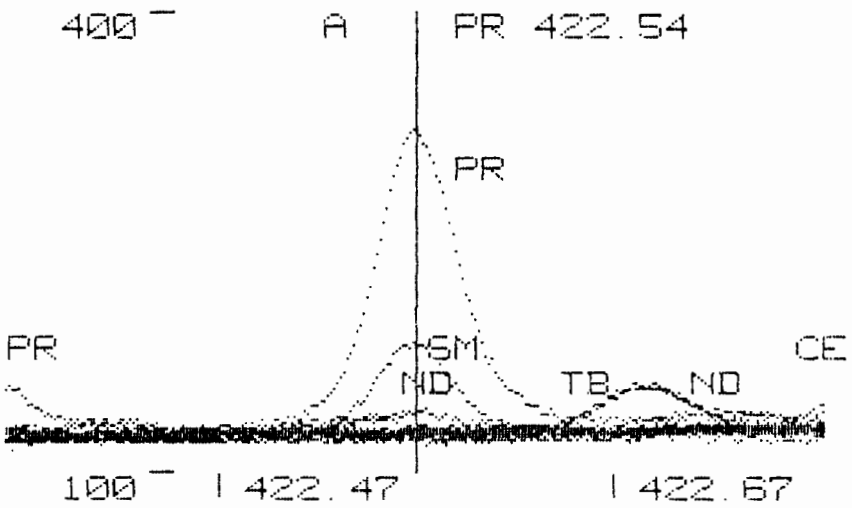

INTERFERENCES FROM REE ON PR.

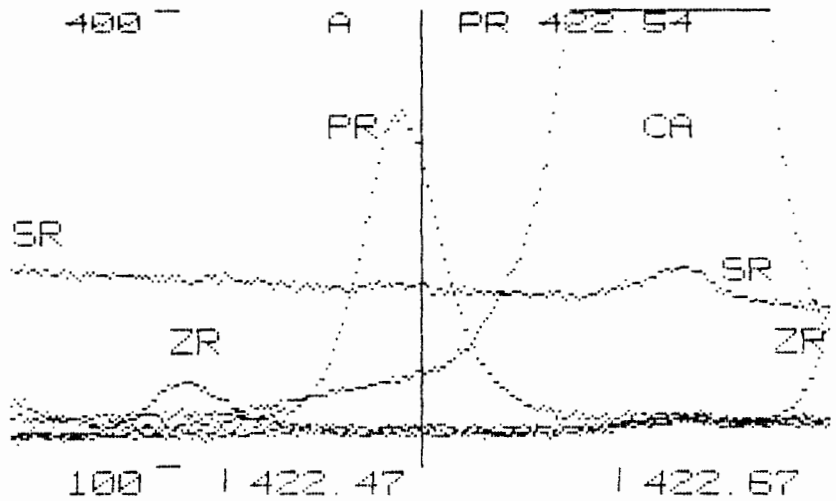

INTERFERENCES FROM NON-REE ON PR

PRAESODYMIUM 414.31 nm

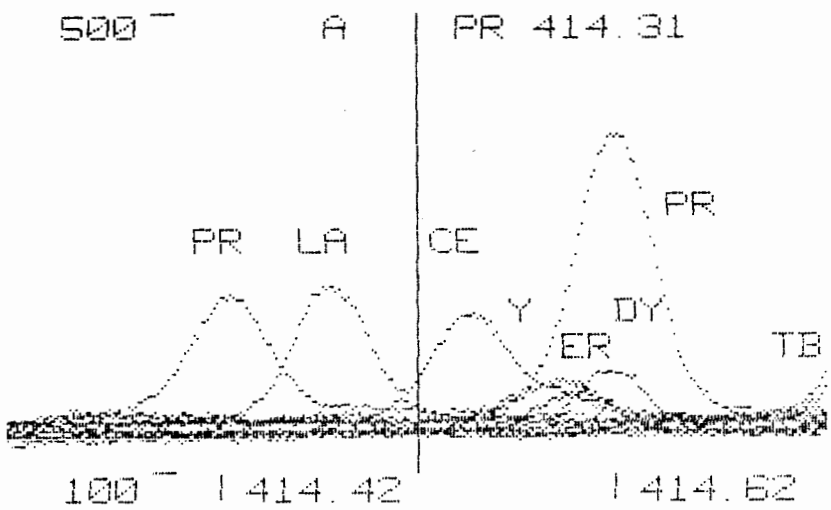

INTERFERENCES FROM REE ON PR.

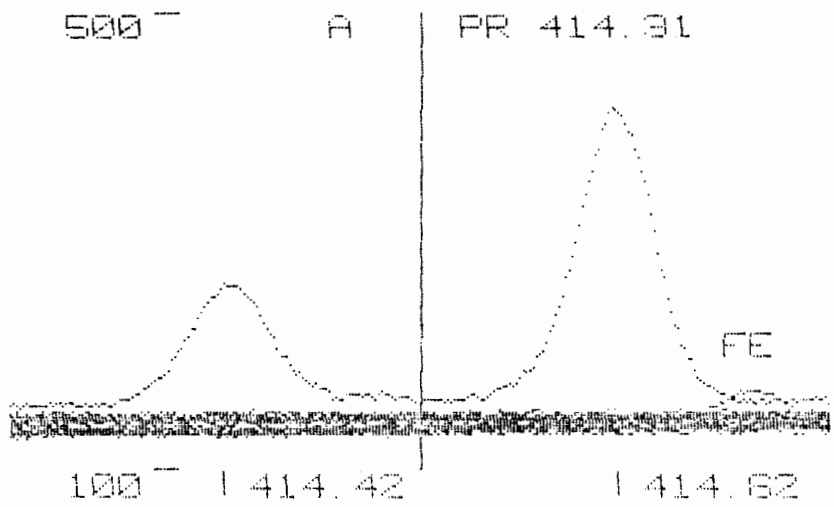

INTERFERENCES FROM NON-REE ON PR

PRAESODYMIUM 390.84 nm

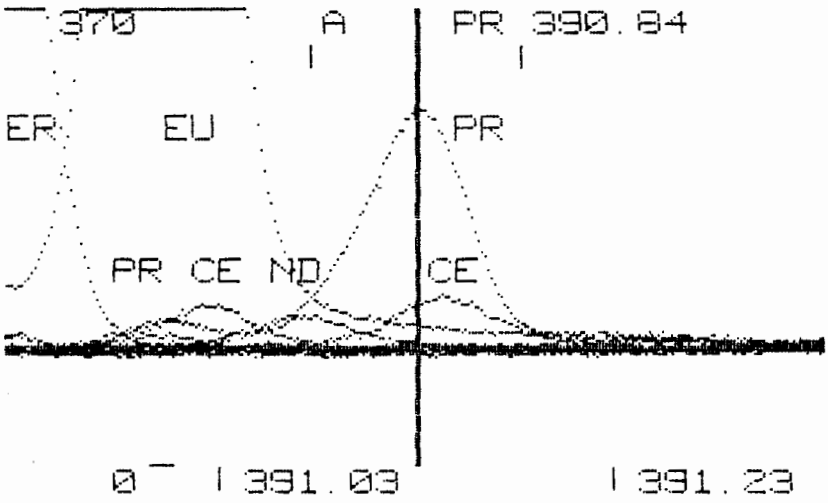

INTERFERENCES FROM REE ON PR.

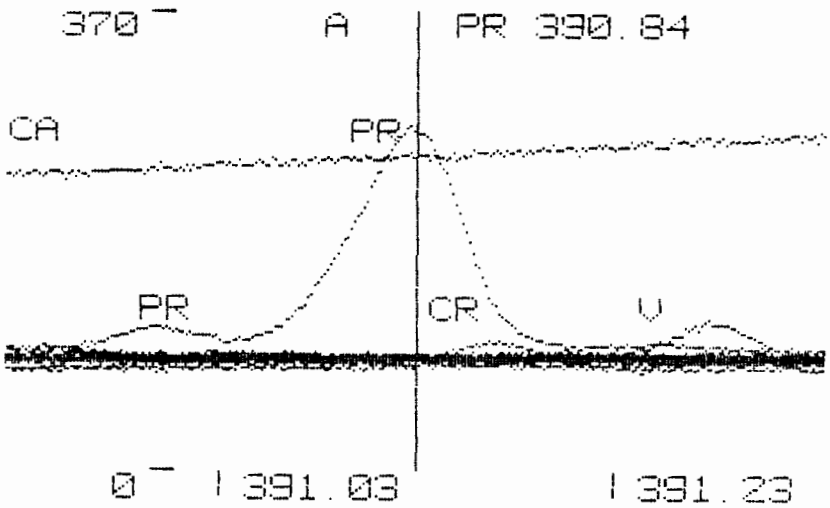

INTERFERENCES FROM NON-REE ON PR.

PRAESODYMIUM 417.94 nm

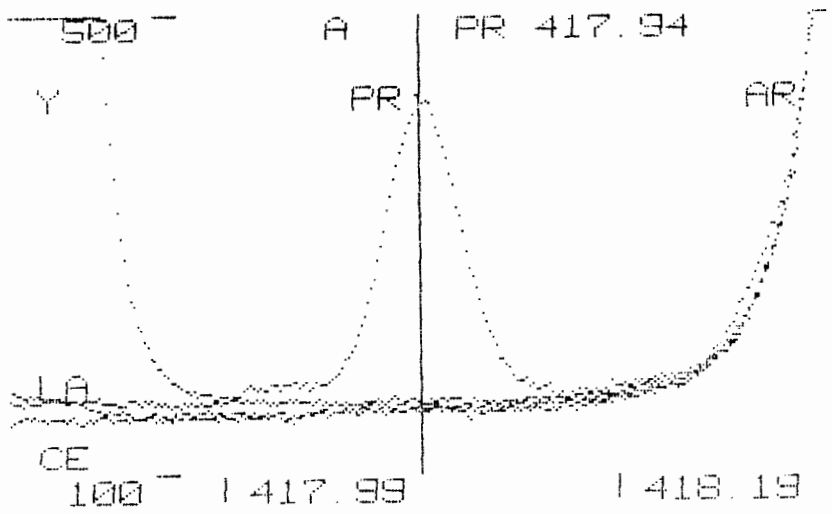

INTERFERENCES FROM Y, LA AND CE ON PR.

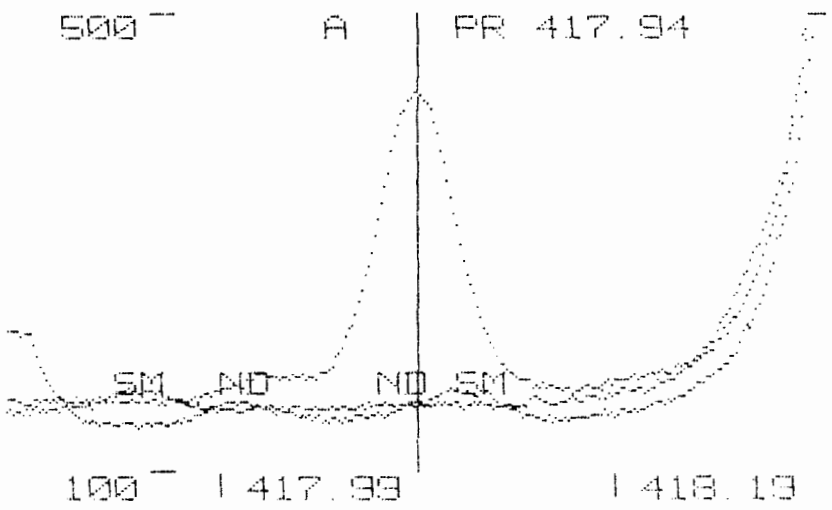

INTERFERENCES FROM SM AND ND ON PR.

PRAESODYMIUM 417.94 nm (cont)

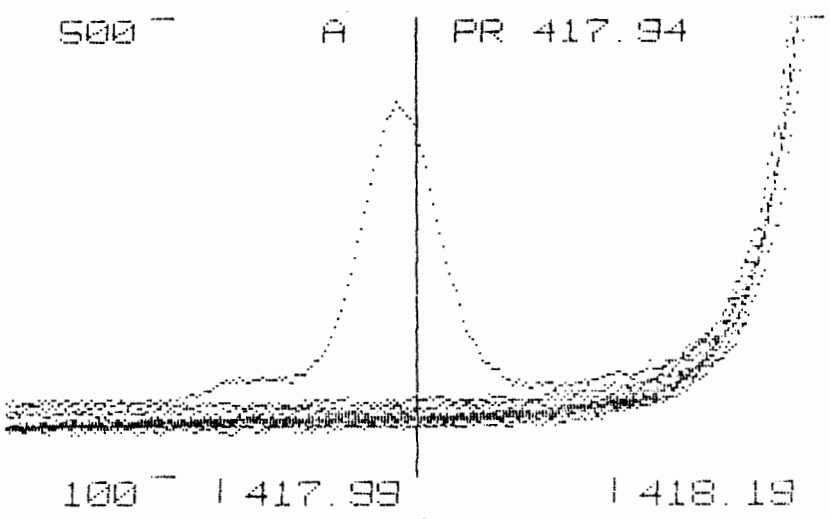

BACKGROUND CHANGES FROM EU TO LU (AT PR 417.94 nm)

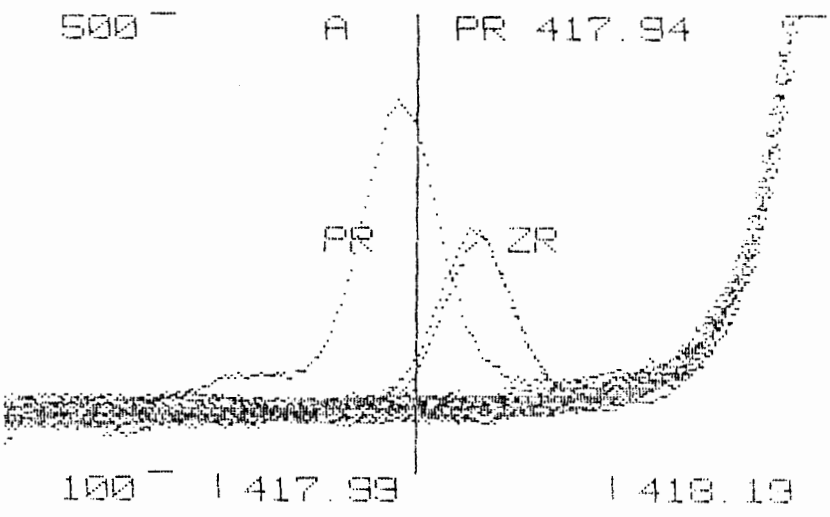

INTERFERENCES FROM NON-REE ON PR.

PRAESODYMIUM 440.88 nm

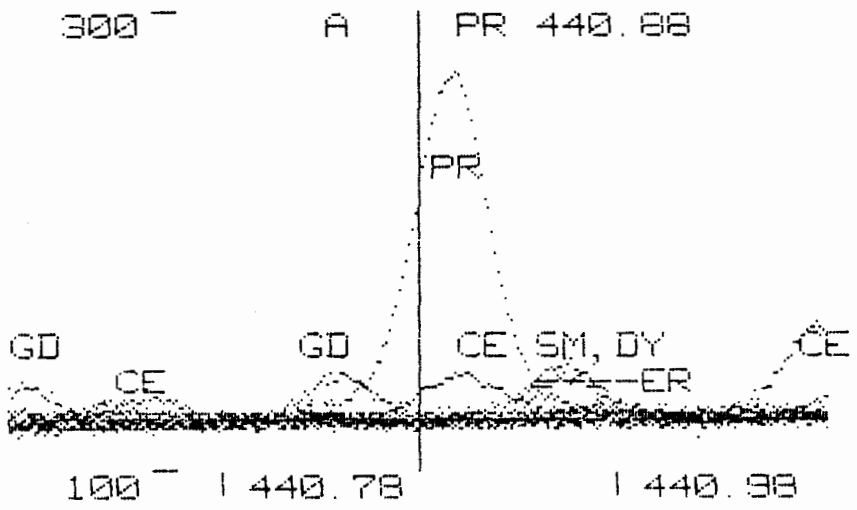

INTERFERENCES FROM REE ON PR.

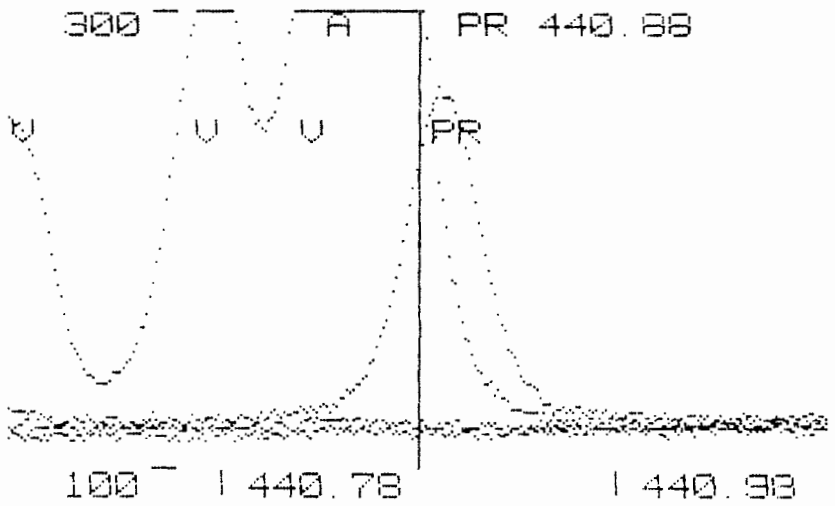

INTERFERENCES FROM NON-REE ON PR.

NEODYMIUM 430.36nm

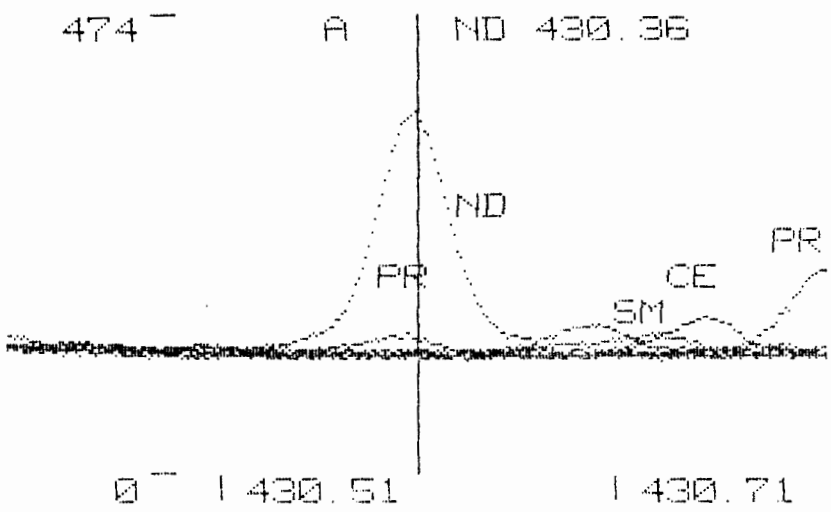

INTERFERENCES ON ND FROM PR, CE AND SM.

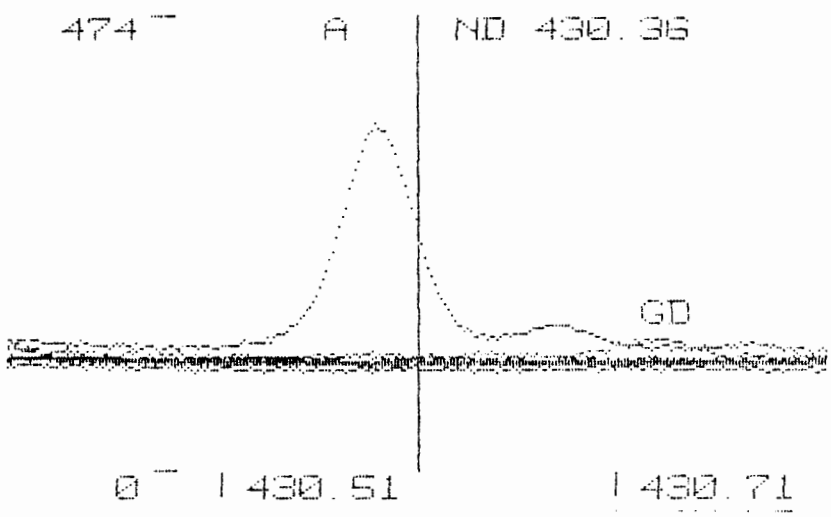

INTERFERENCES FROM EU-LU ON ND.

NEODYMIUM 430.36 nm (cont)

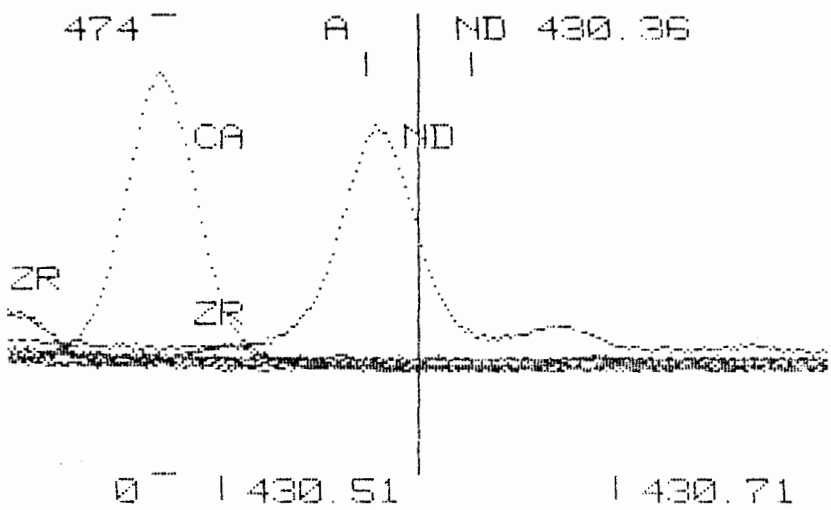

INTERFERENCES FROM CA AND ZR ON ND.

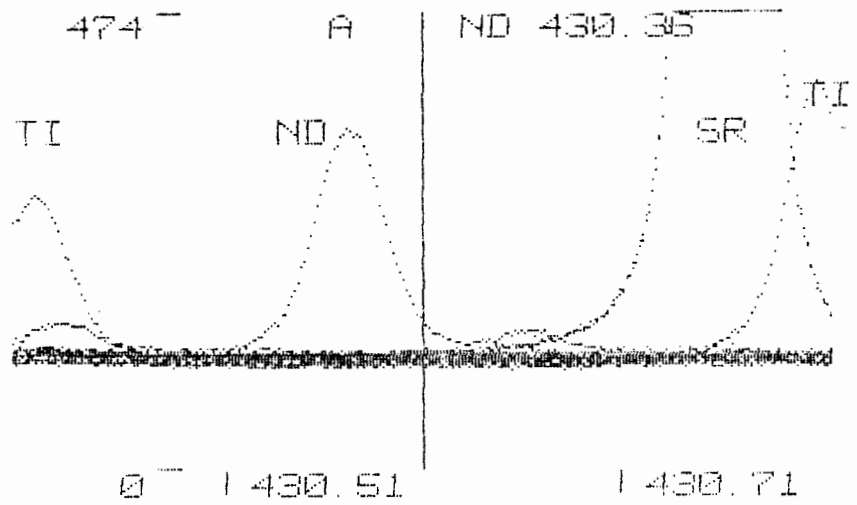

INTERFERENCES FROM TI AND SR ON ND.

NEODYMIUM 401.23 nm

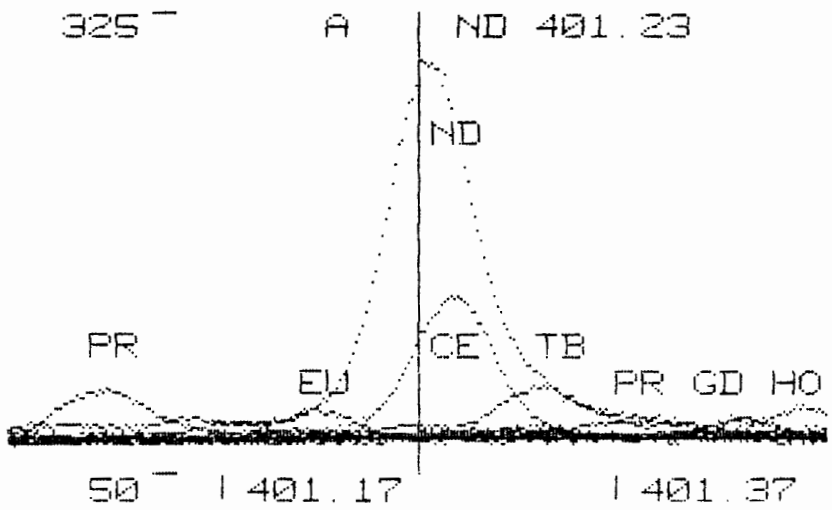

INTERFERENCES FROM REE ON ND.

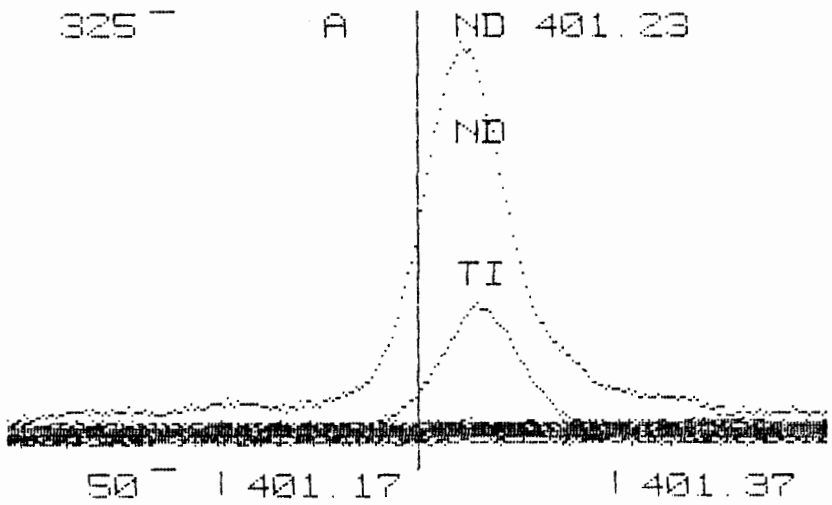

INTERFERENCES FROM NON-REE ON ND.

NEODYMIUM 406.11 nm

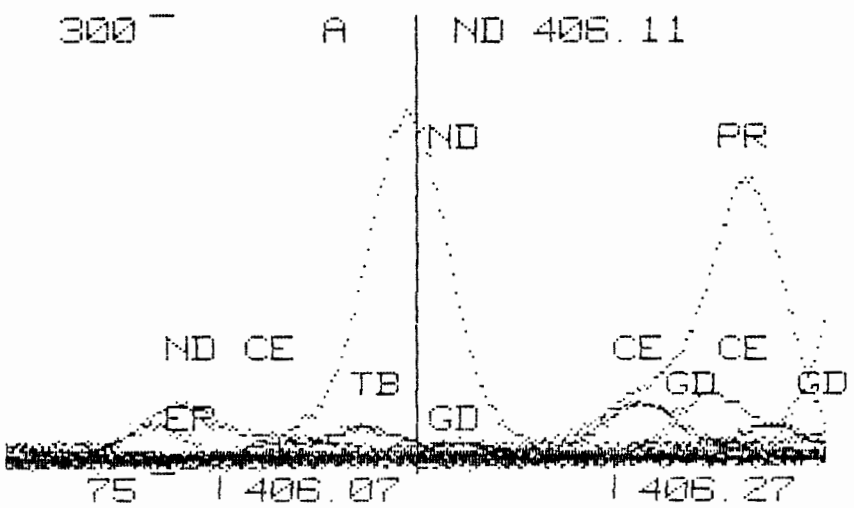

INTERFERENCES FROM REE ON ND.

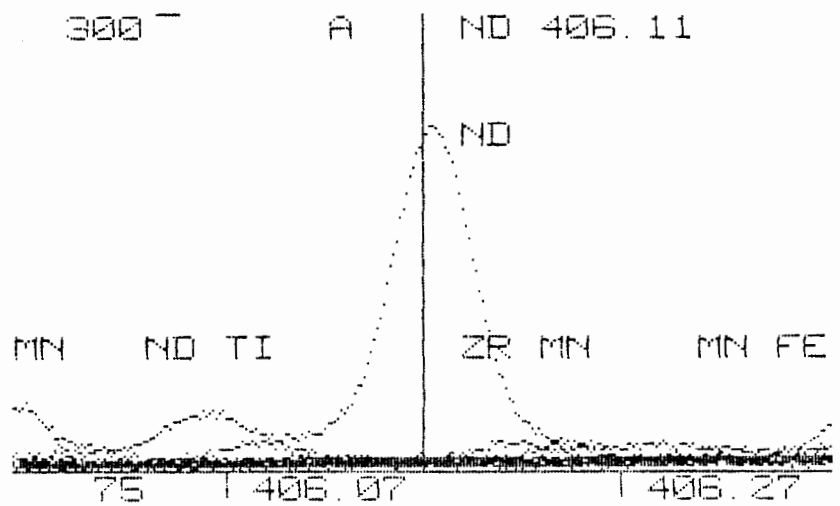

INTERFERENCES FROM NON-REE ON ND.

NEODYMIUM 415.61 nm

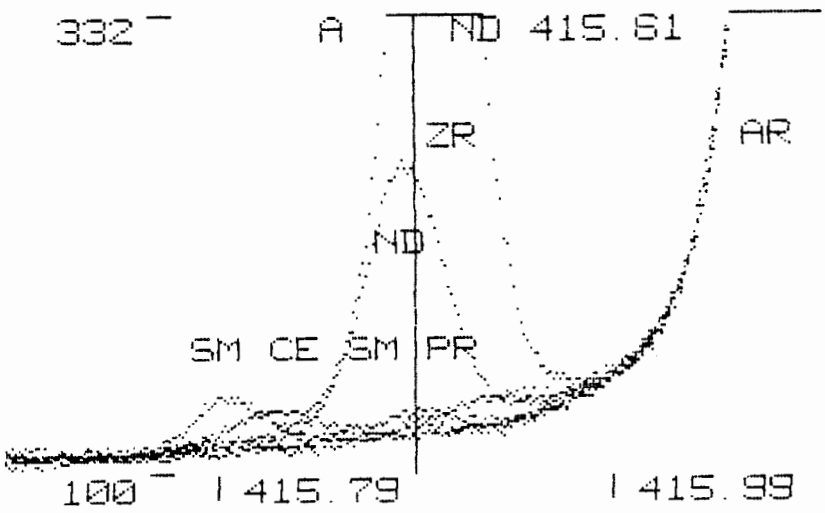

INTERFERENCES FROM REE AND ZR ON ND.

SAMARIUM 359.26 nm

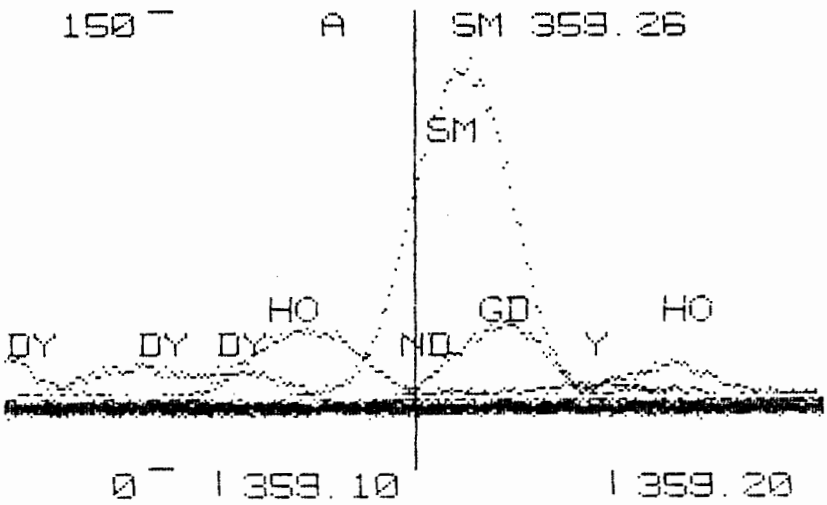

INTERFERENCES FROM REE ON SM.

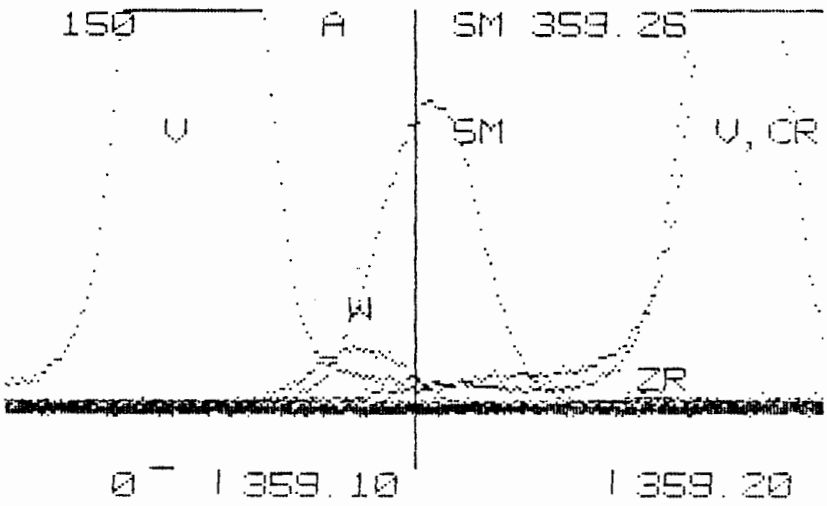

INTERFERENCES FROM NON-REE ON SM.

SAMARIUM 442.43 nm

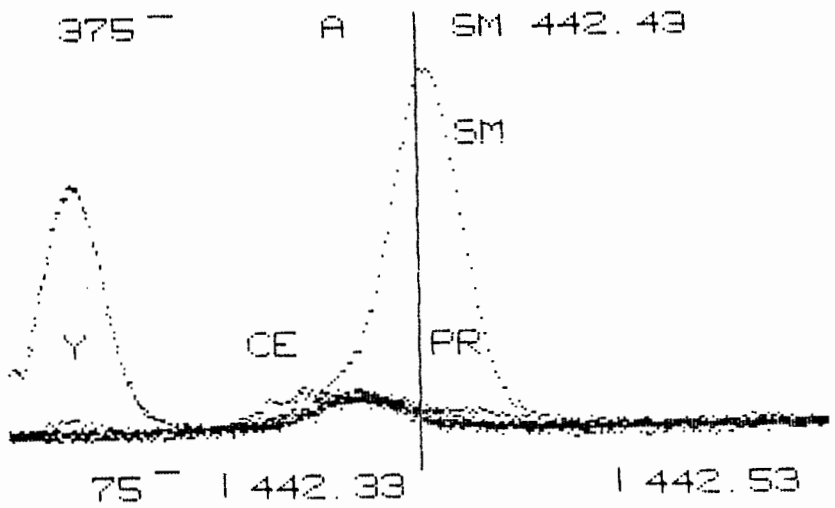

INTERFERENCES FROM REE ON SM.

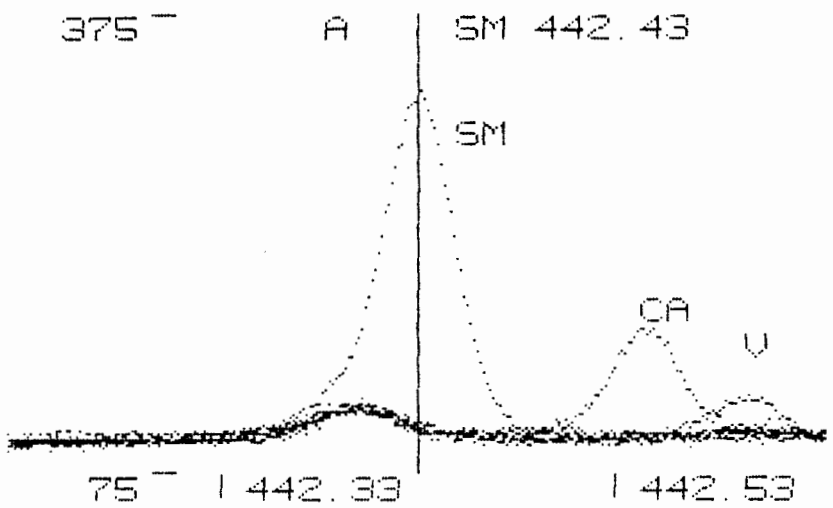

INTERFERENCES FRON NON-REE ON SM.

SAMARIUM 360.95 nm

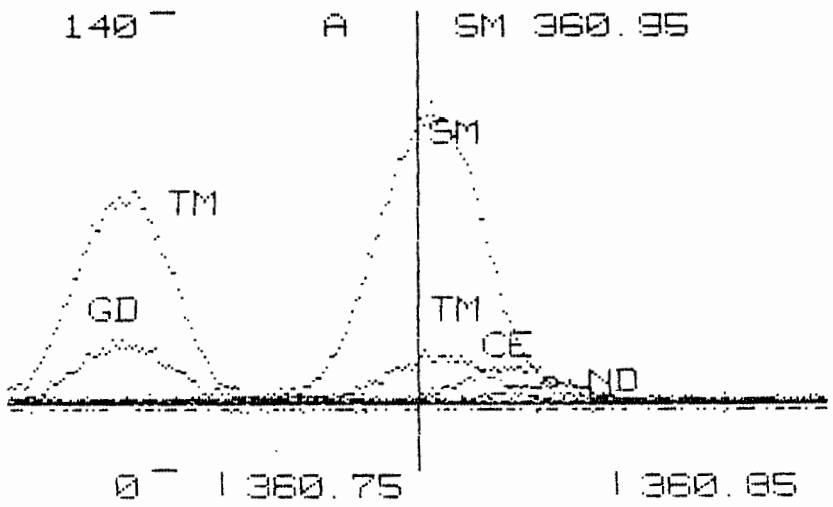

INTERFERENCES FROM REE ON SM.

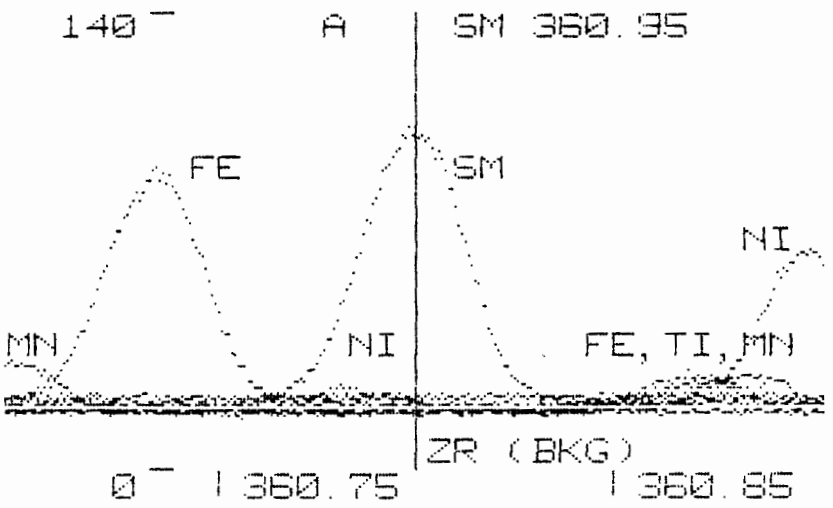

INTERFERENCES FROM NON-REE ON SM.

SAMARIUM 363.42 nm

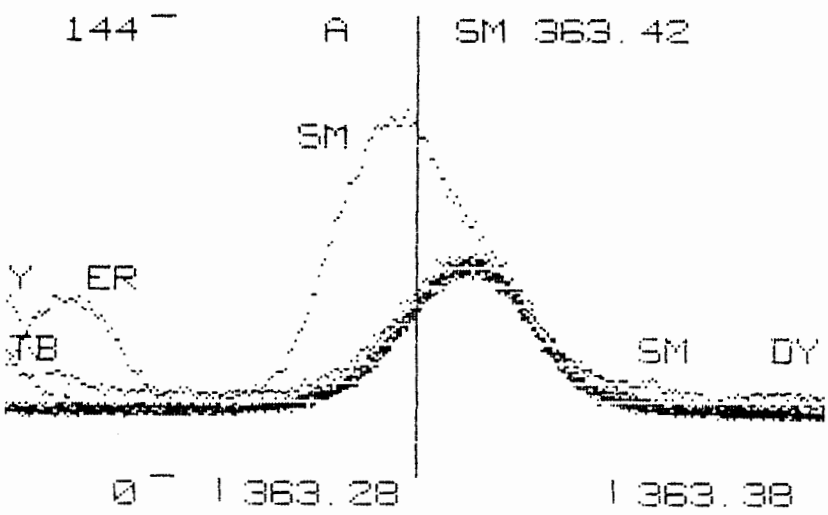

INTERFERENCES FROM REE ON SM.

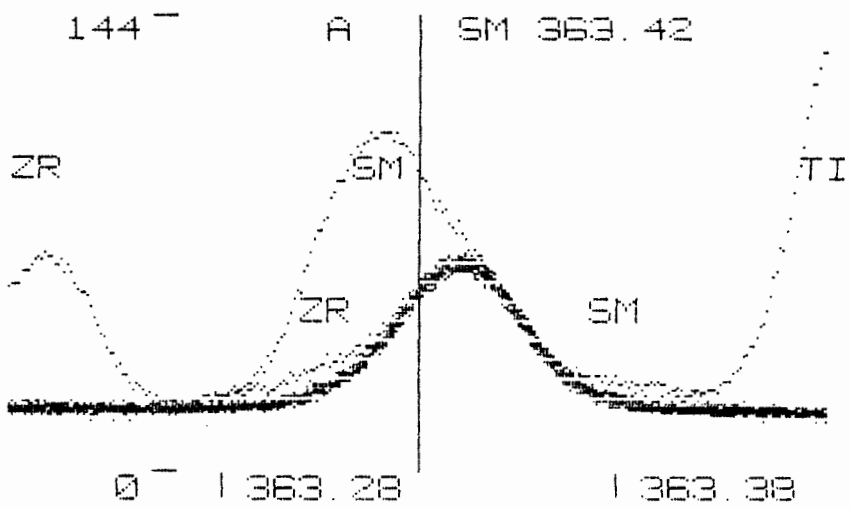

INTERFERENCES FROM NON-REE ON SM.

EUROPIUM 381.97 nm

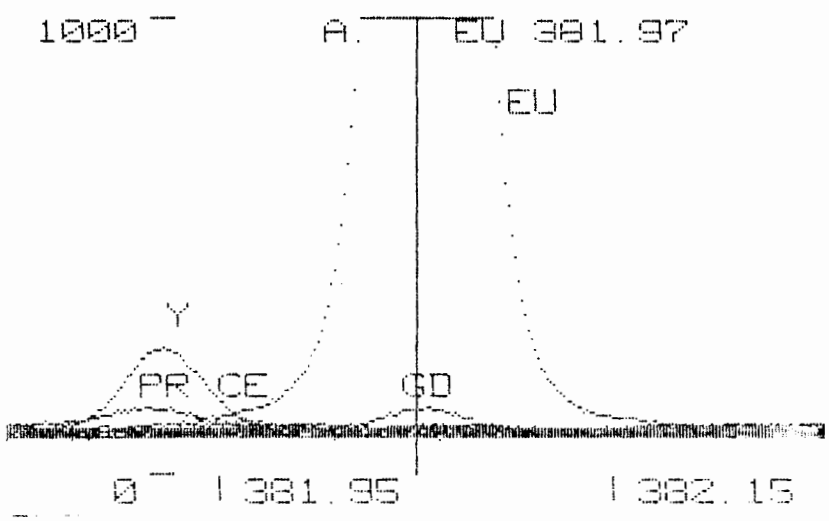

INTERFERENCES FROM REE ON EU.

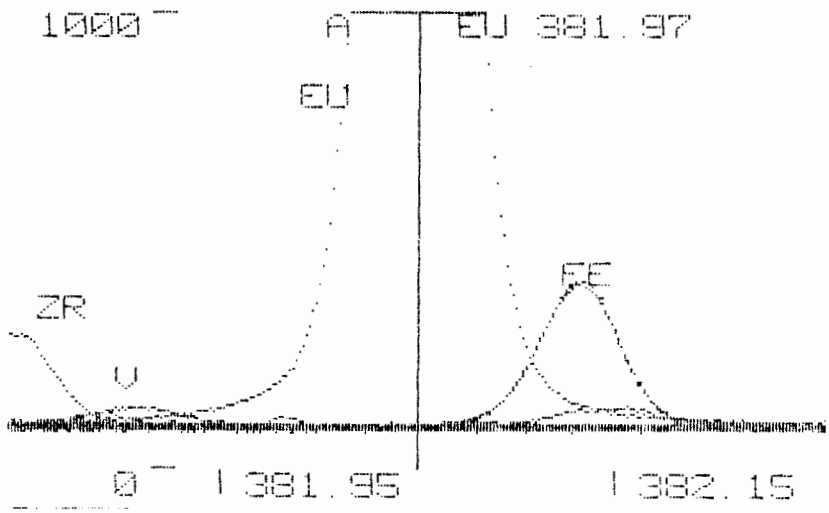

INTERFERENCES FROM NON-REE ON EU.

EUROPIUM 412.97 nm

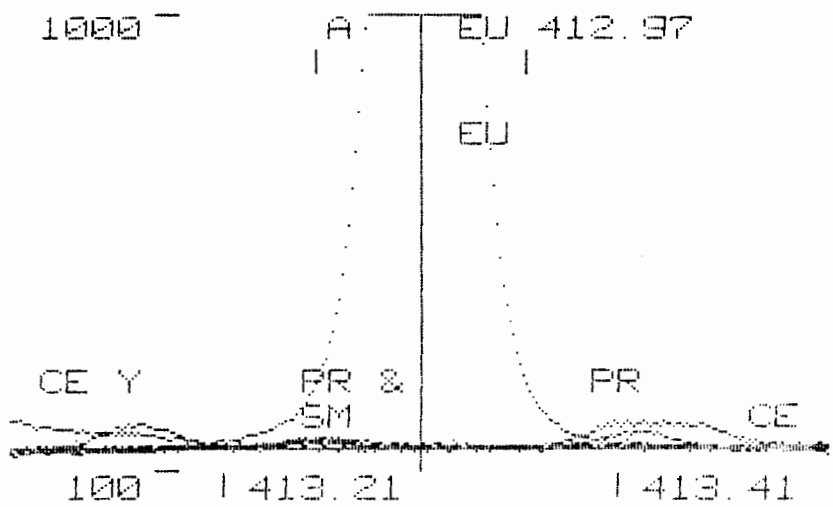

INTERFERENCES FROM Y-SM ON EU.

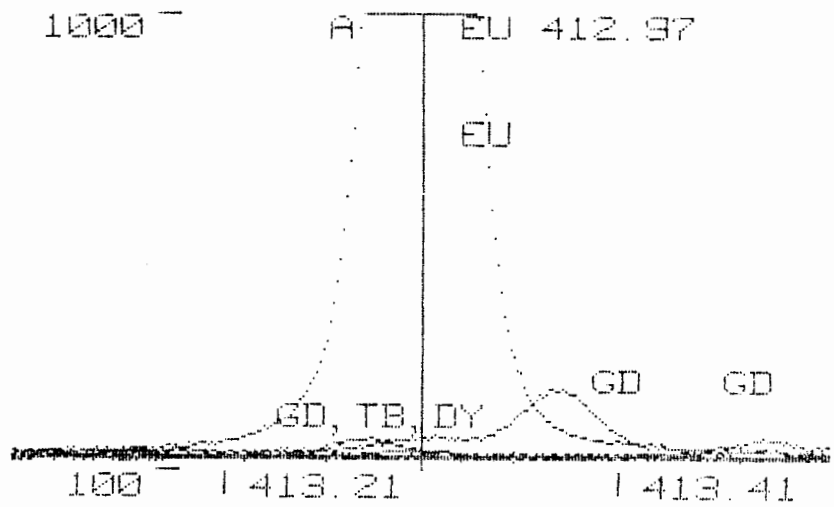

INTERFERENCES FROM GD-LU ON EU.

EUROPIUM 412.97 nm (cont)

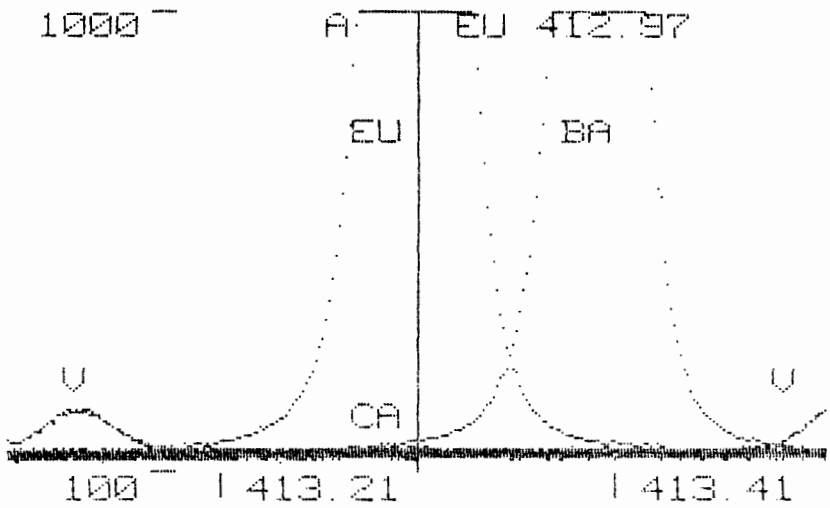

INTERFERENCES FROM NON-REE ON EU.

EUROPIUM 420.51 nm

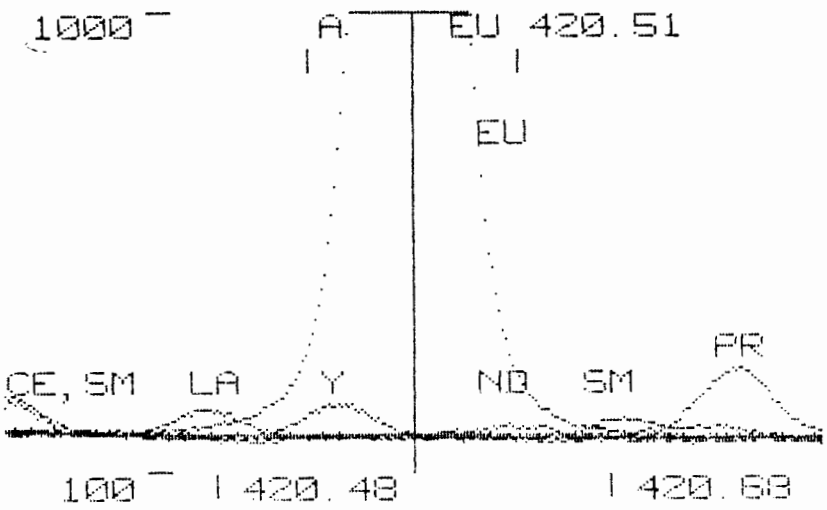

INTERFERENCES FROM Y-SM ON EU.

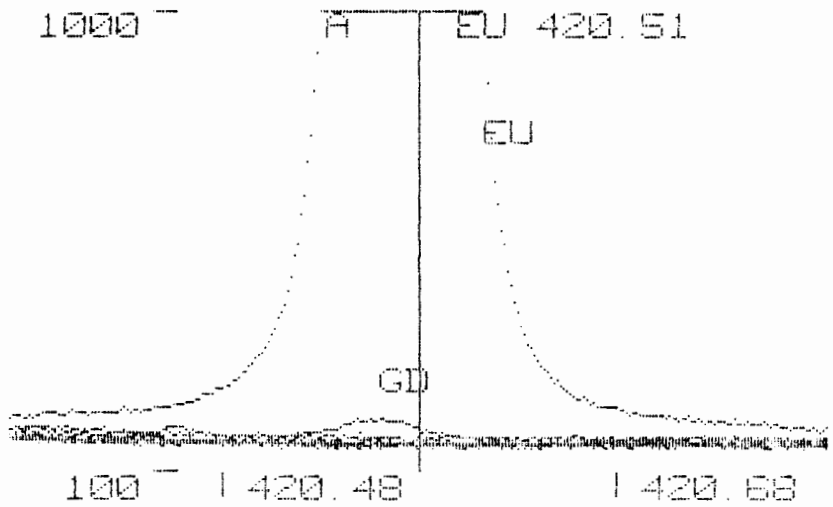

INTERFERENCES FROM GD-LU ON EU.

EUROPIUM 420.51 nm (cont)

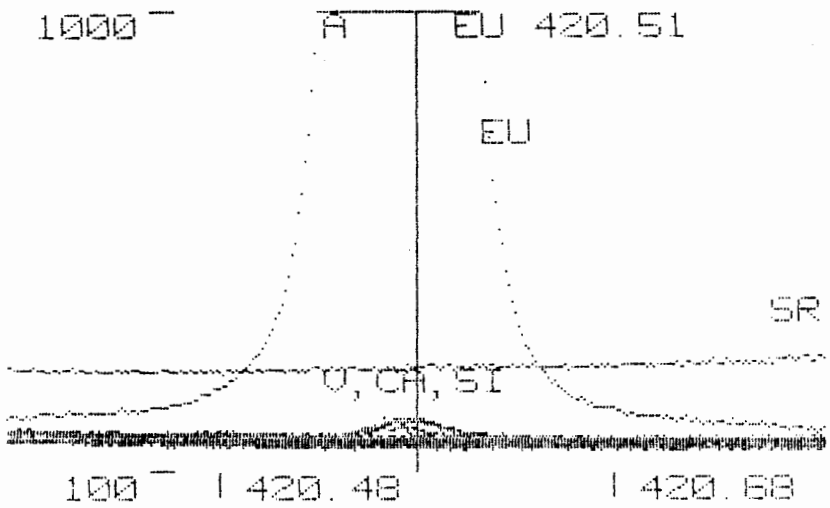

INTERFERENCES FROM NON-REE ON EU

GADOLINIUM 342.25 nm

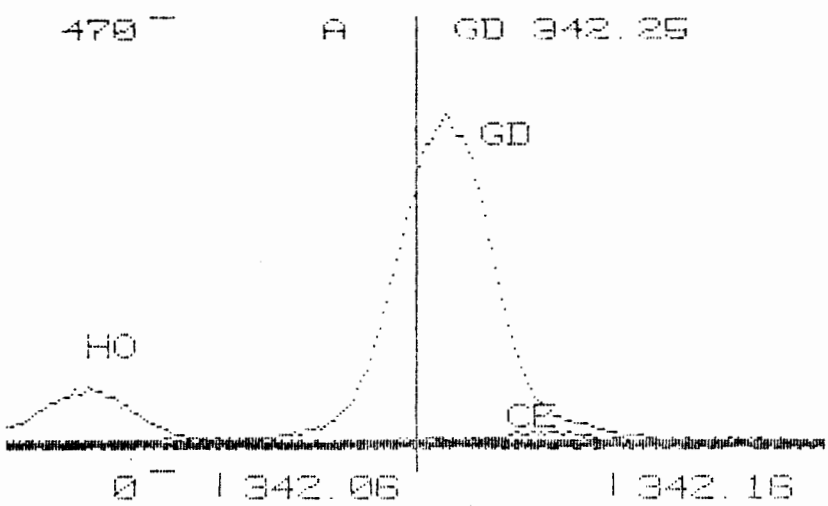

INTERFERENCES FROM REE ON GD.

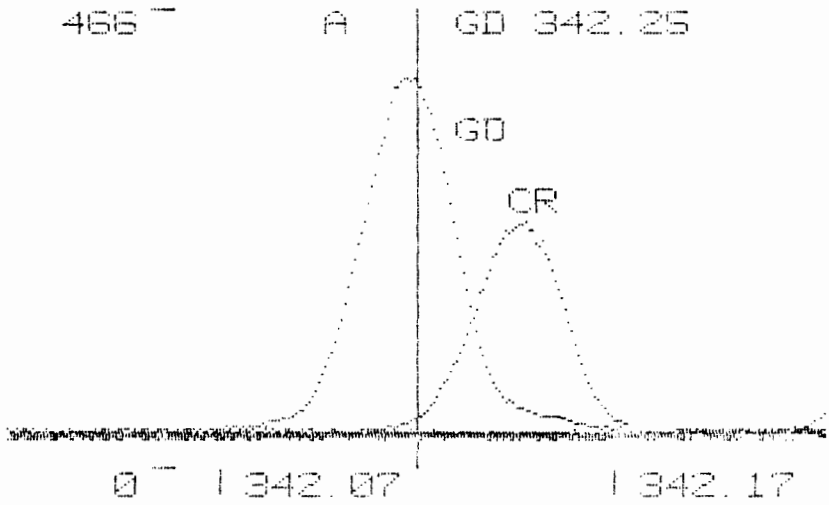

INTERFERENCES FROM NON-REE ON GD.

GADOLINIUM 310.05 nm

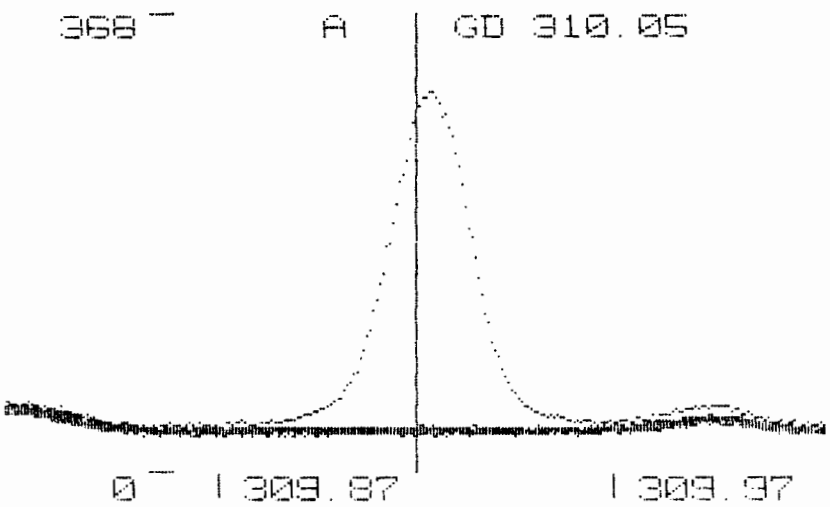

INTERFERENCES FROM REE ON GD.

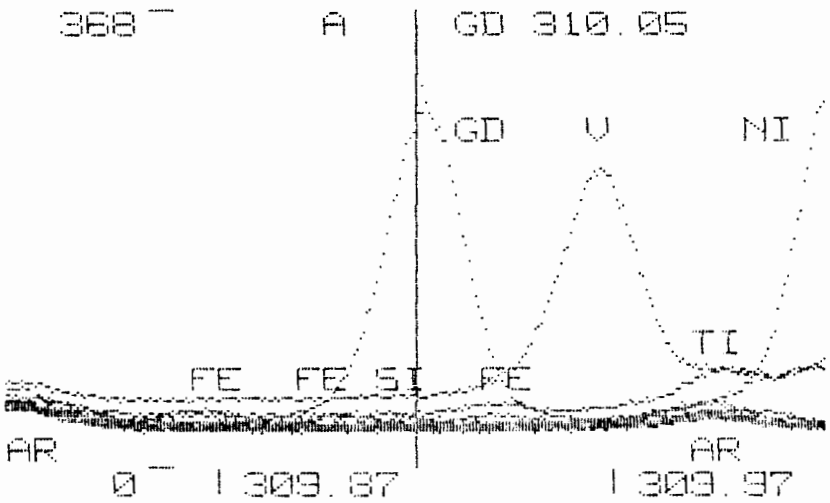

INTERFERENCES FROM NON-REE ON GD.

GADOLINIUM 335.86 nm

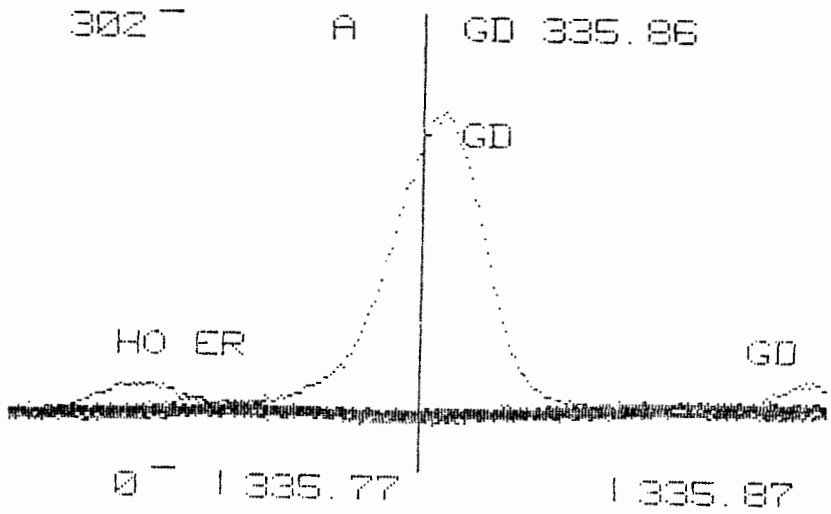

INTERFERENCES FROM REE ON GD.

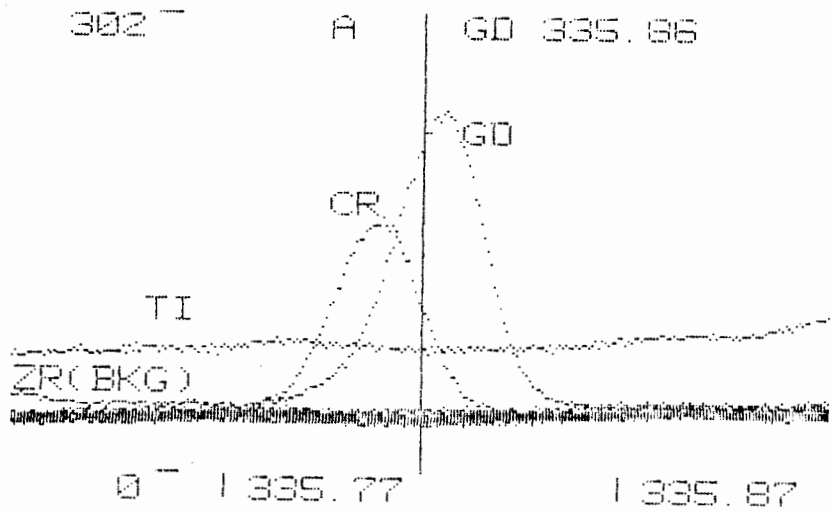

INTERFERENCES FROM NON-REE ON GD.

GADOLINIUM 335.86 nm (cont)

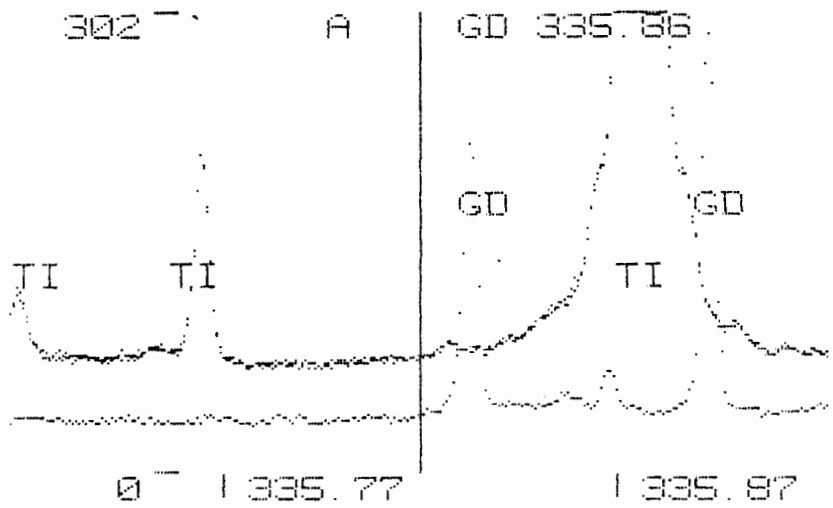

INTERFERENCE FROM TI CONTINUUM AT GD 335.86 nm AND GD 336.22 nm.

GADOLINIUM 335.05 nm

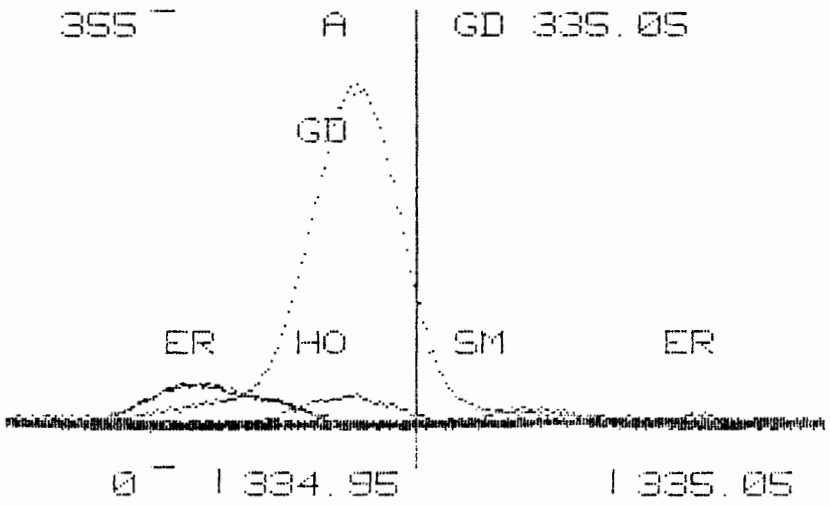

INTERFERENCES FROM REE ON GD.

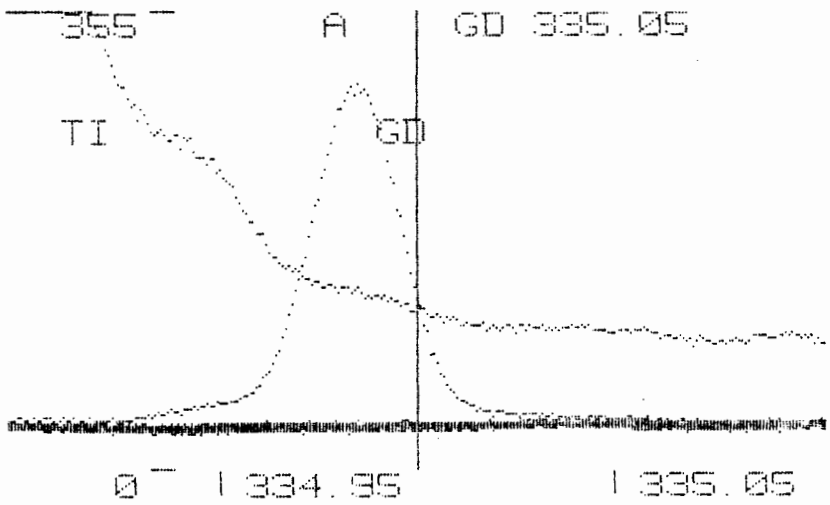

INTERFERENCE FROM NON-REE ON GD WITH TI CONTINUUM.

TERBIUM 356.86 nm

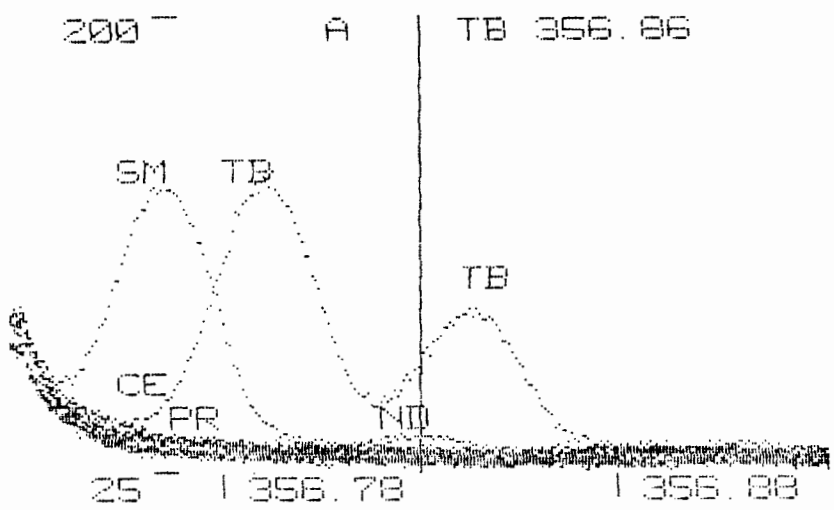

INTERFERENCES FROM REE ON TB.

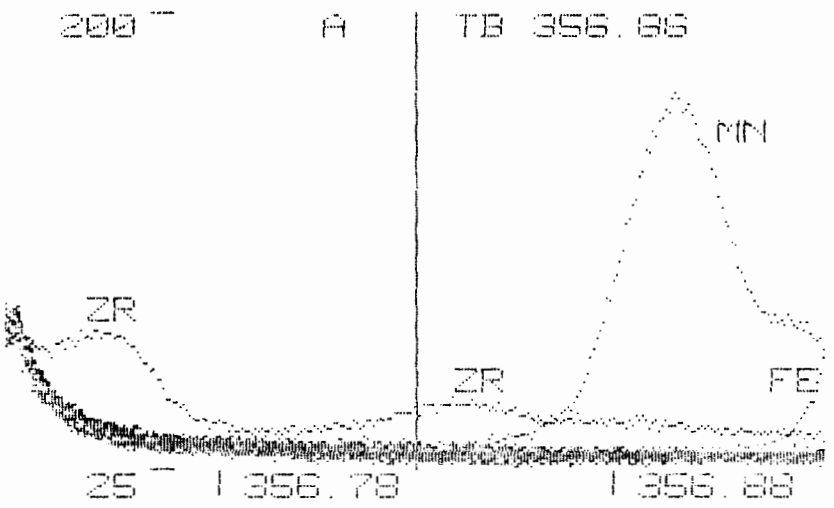

INTERFERENCES FROM NON-REE ON TB.

TERBIUM 356.17 nm

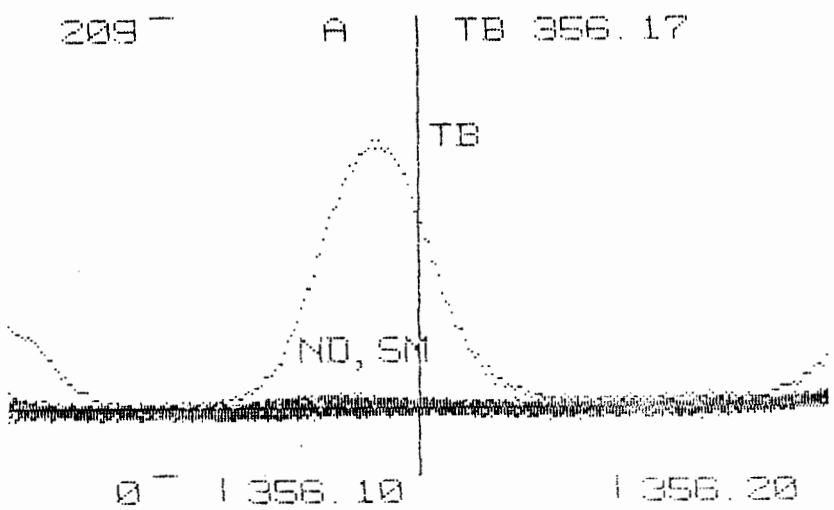

INTERFERENCES FROM REE ON TB.

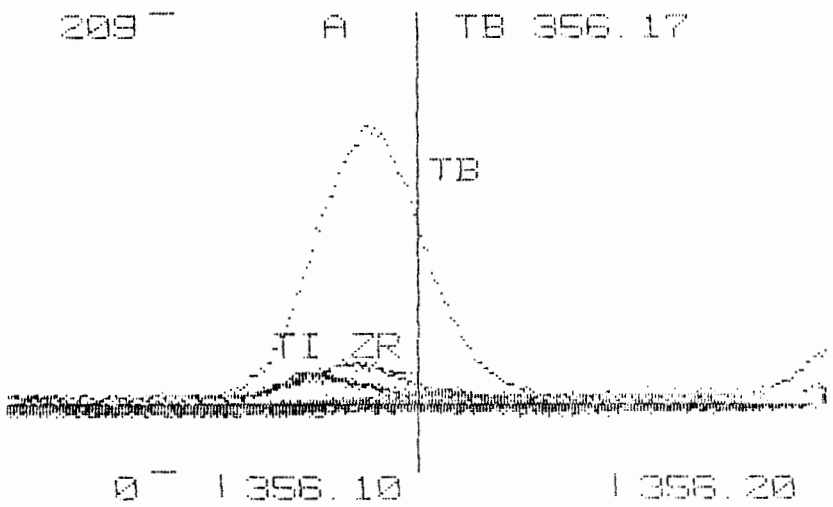

INTERFERENCES FROM NON-REE ON TB.

TERBIUM 367.64 nm

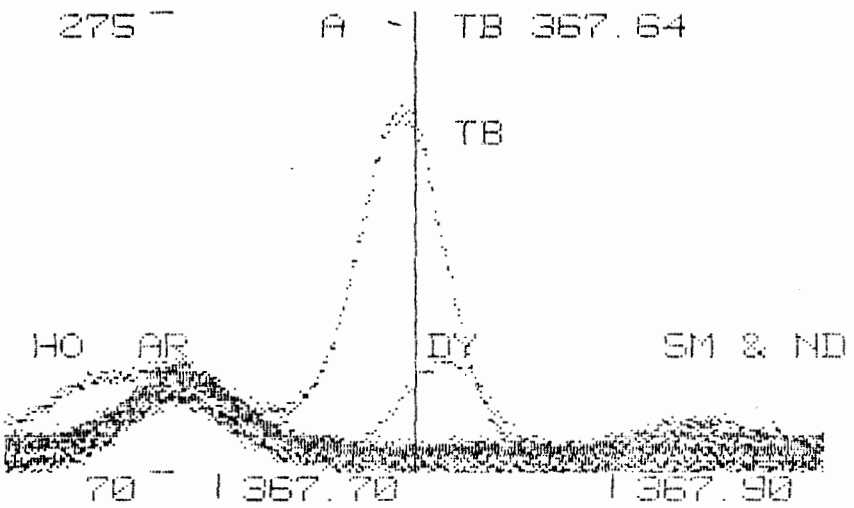

INTERFERENCES FROM REE ON TB.

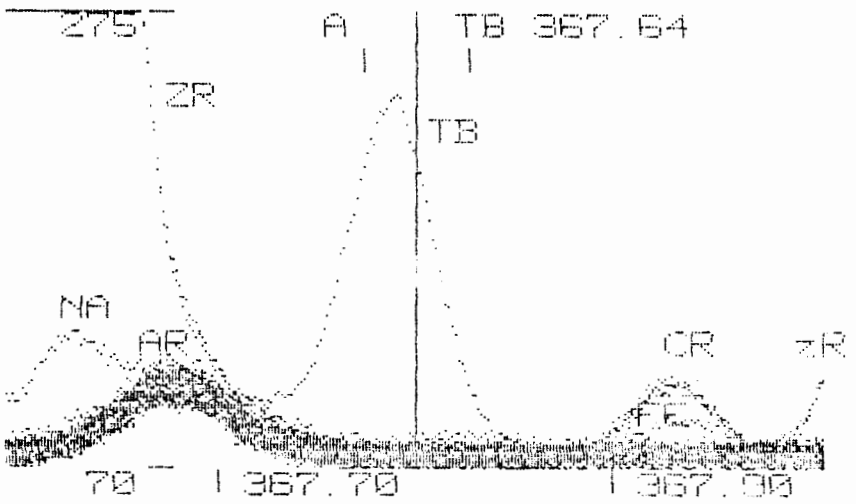

INTERFERENCES FROM NON-REE ON TB.

TERBIUM 350.92 nm

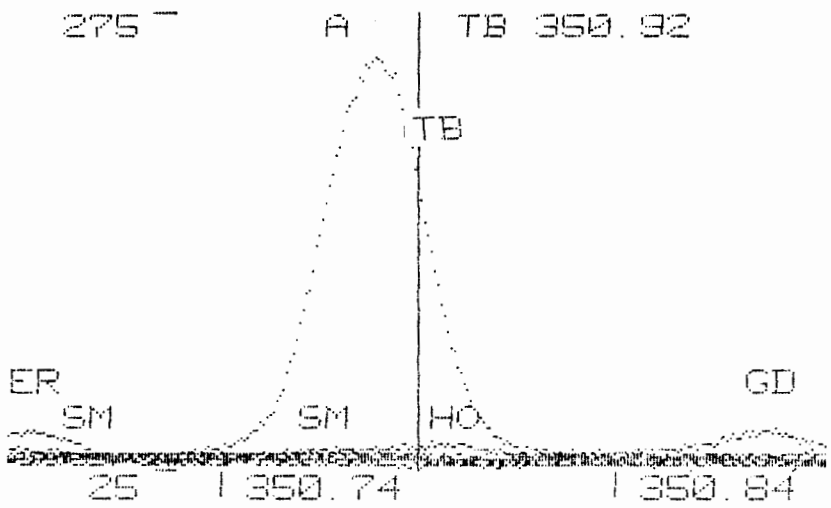

INTERFERENCES FROM REE ON TB.

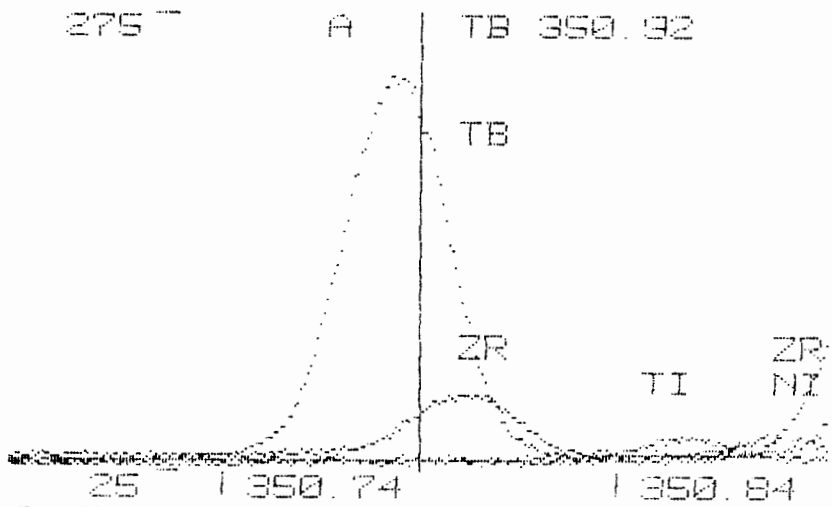

INTERFERENCES FROM NON-REE ON TB.

TERBIUM 387.41 nm

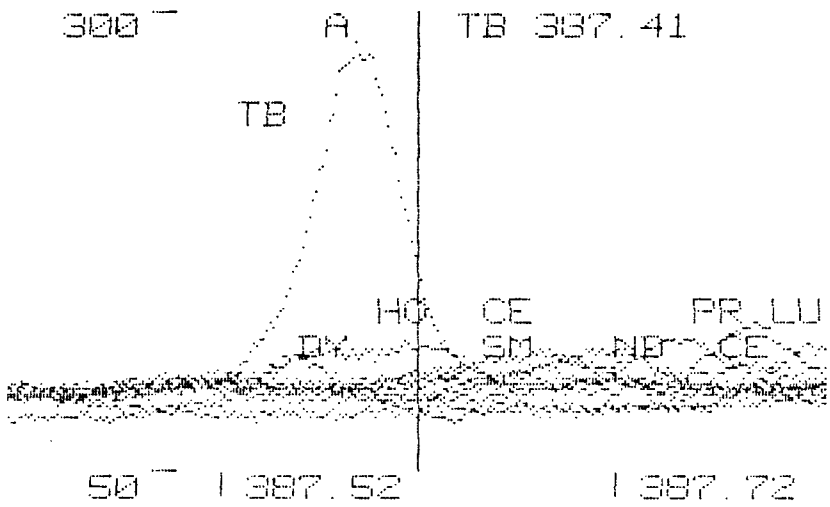

INTERFERENCES FROM REE ON TB.

TERBIUM 384.87 nm

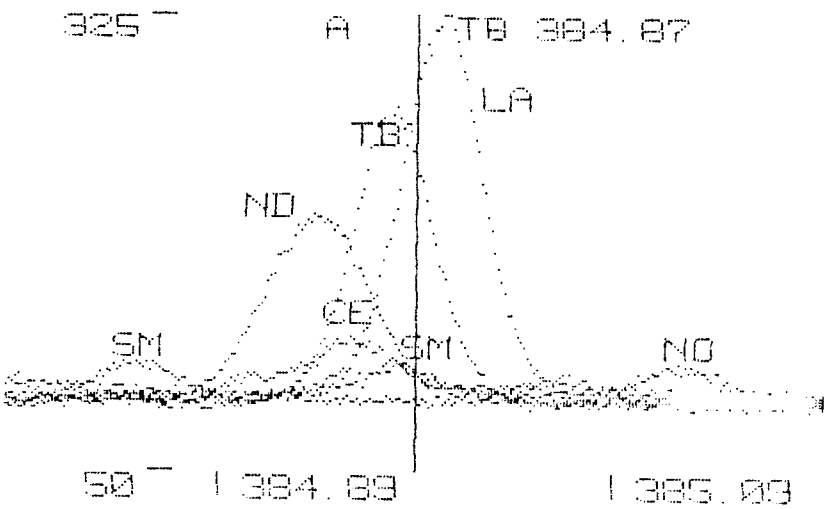

INTERFERENCES FROM REE ON TB.

DYSPROSIUM 353.17 nm

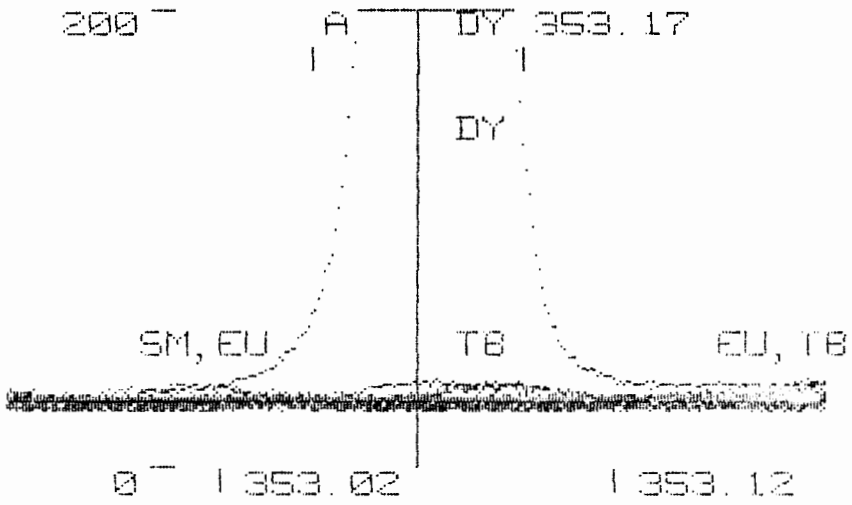

INTERFERENCES FROM REE ON DY.

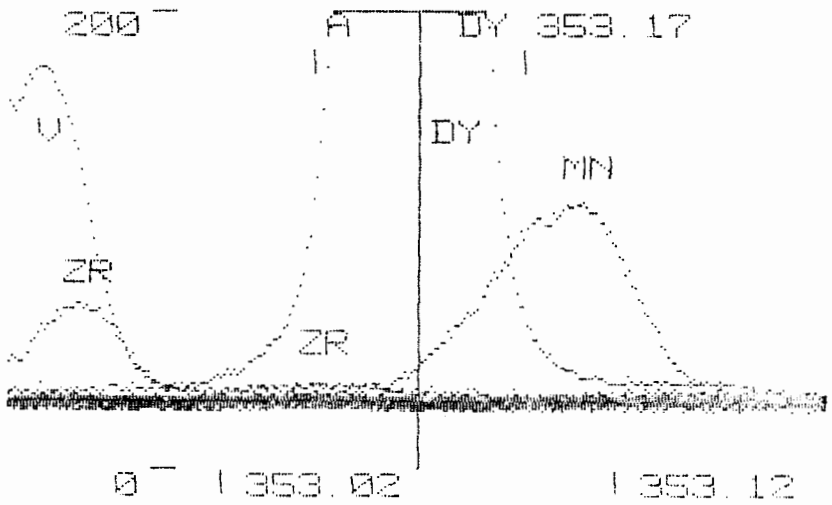

INTERFERENCES FROM NON-REE ON DY.

DYSPROSIUM 340.78 nm

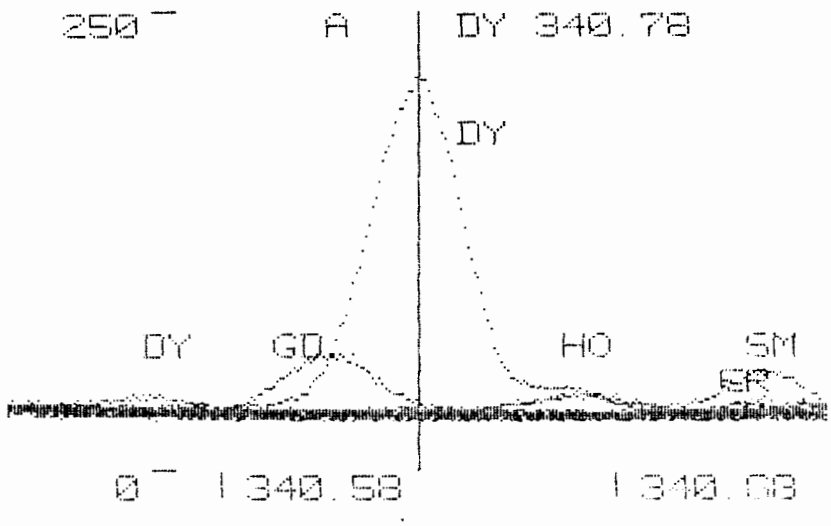

INTERFERENCES FROM REE ON DY.

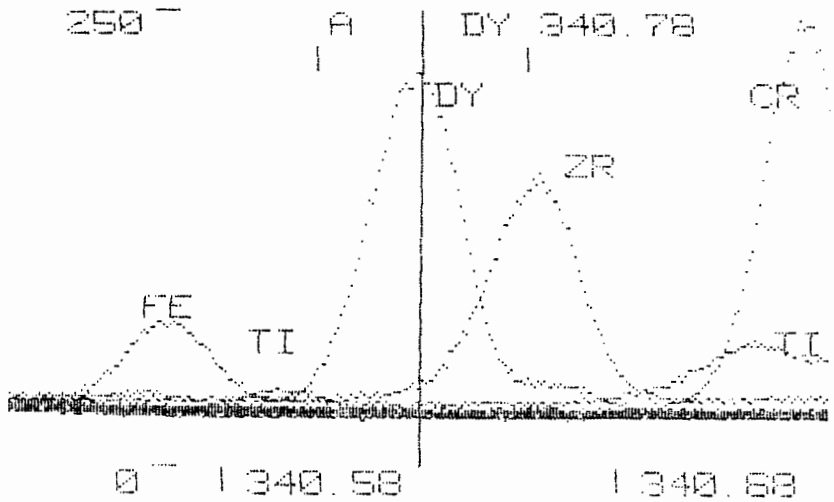

INTERFERENCES FROM NON-REE ON DY.

DYSPROSIUM 353.60 nm

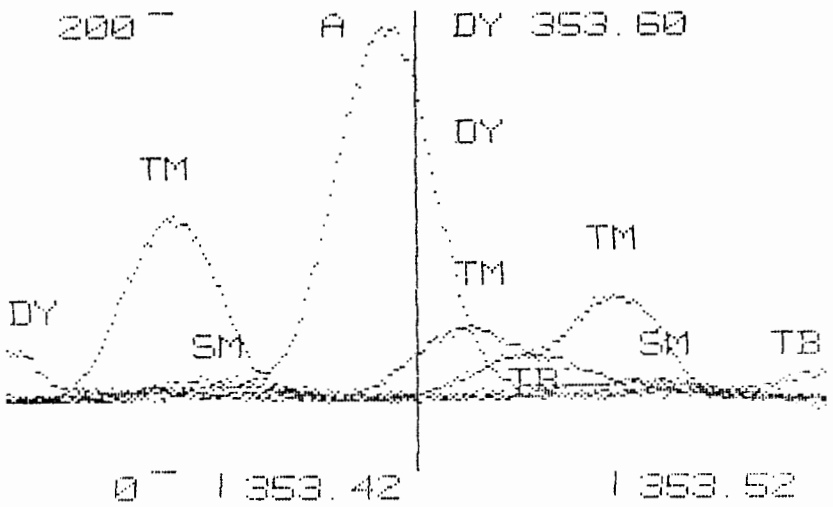

INTERFERENCES FROM REE ON DY.

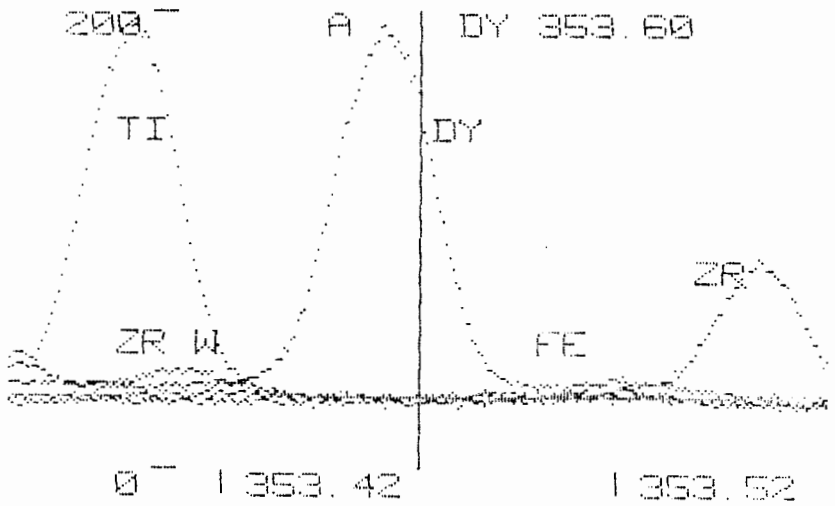

INTERFERENCES FROM NON-REE ON DY.

DYSPROSIUM 364.54 nm

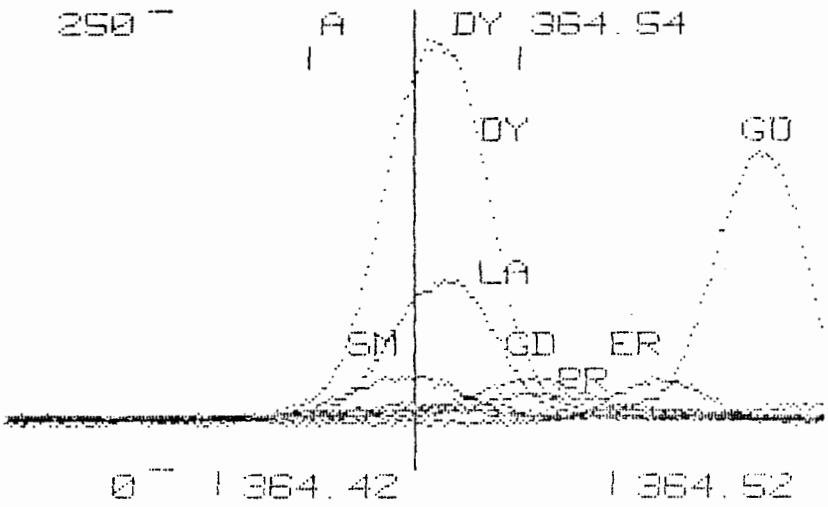

INTERFERENCES FROM REE ON DY.

DYSPROSIUM 394.97 nm

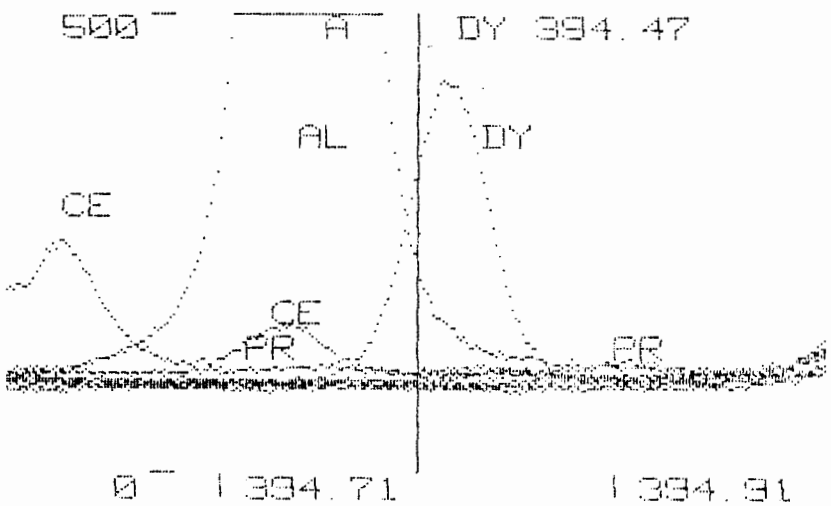

INTERFERENCES FROM AL, CE AND PR ON DY.

HOLMIUM 345.60 nm

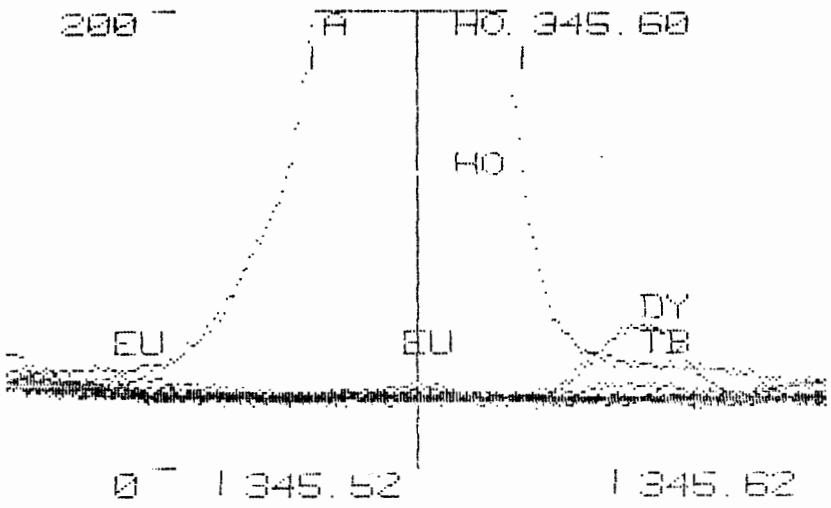

INTERFERENCES FROM REE ON HO.

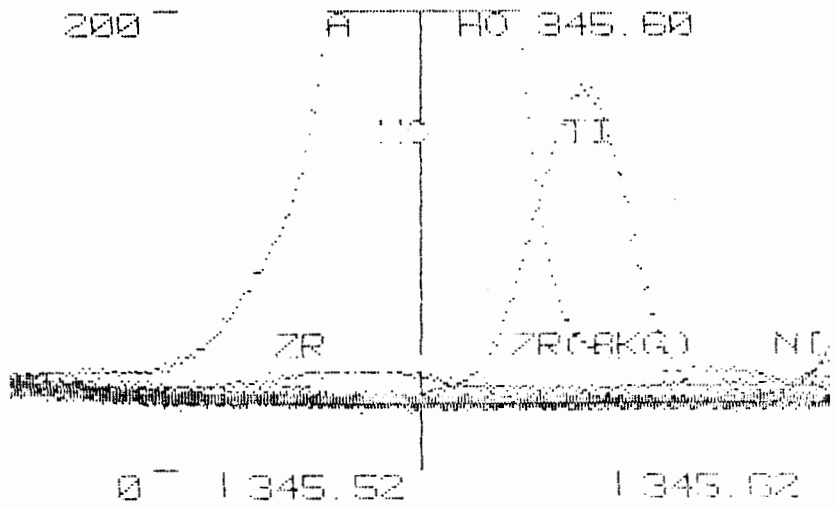

INTERFERENCES FROM NON-REE ON HO.

HOLMIUM 339.90 nm

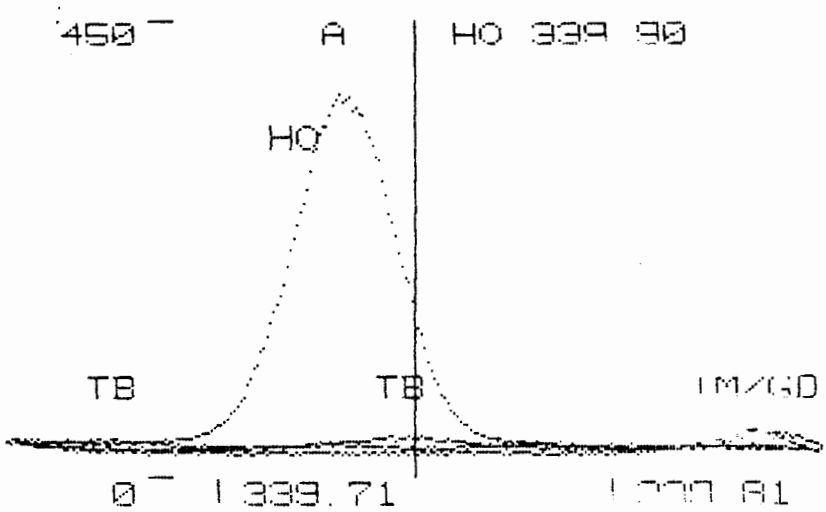

INTERFERENCES FROM REE ON HO.

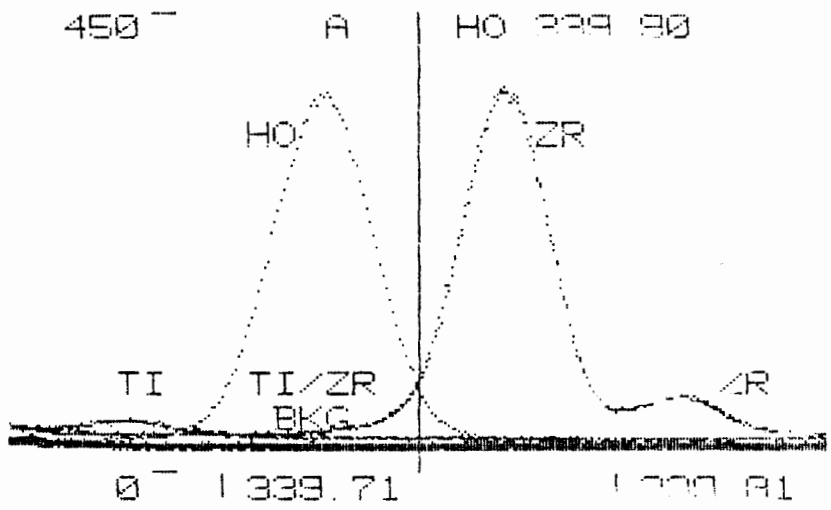

INTERFERENCES FROM NON-REE ON HO.

HOLMIUM 389.10 nm

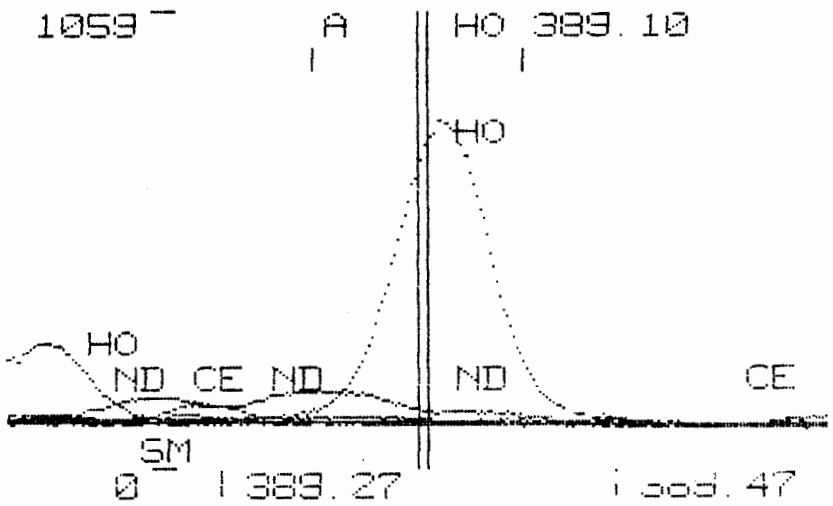

INTERFERENCES FROM Y-EU ON HO.

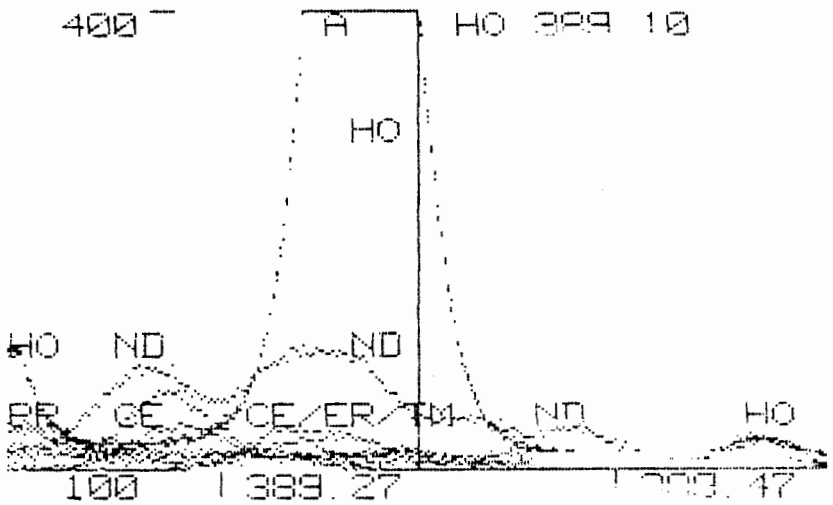

INTERFERENCES FROM REE ON HO.

HOLMIUM 347.43 nm

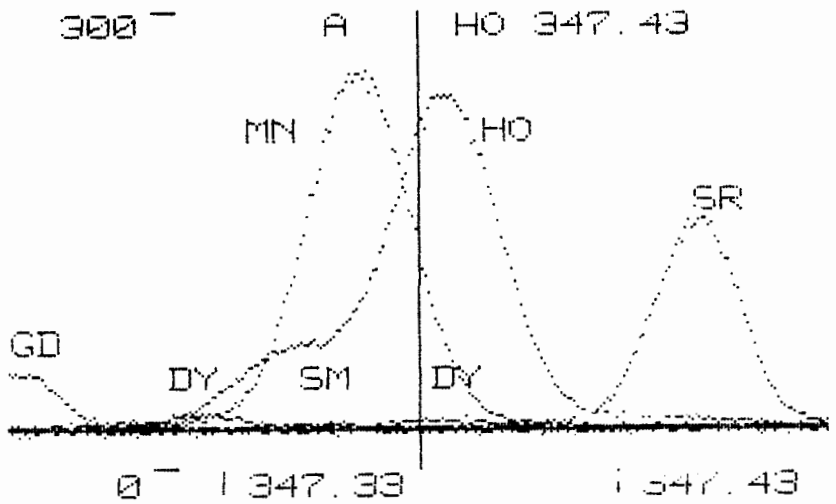

INTERFERENCES FROM GD, DY, SM, MN AND SR ON HO.

HOLMIUM 341.65 nm

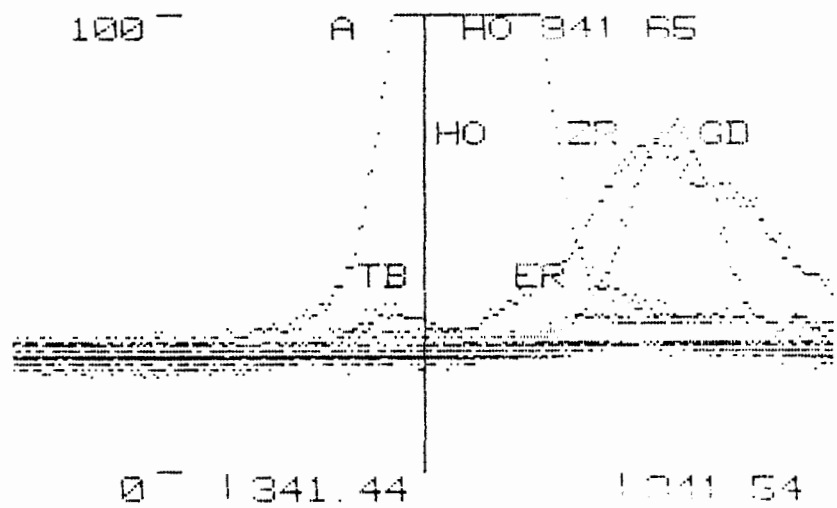

INTERFERENCES FROM TB, ER, ZR AND GD ON HO.

ERBIUM 349.91 nm

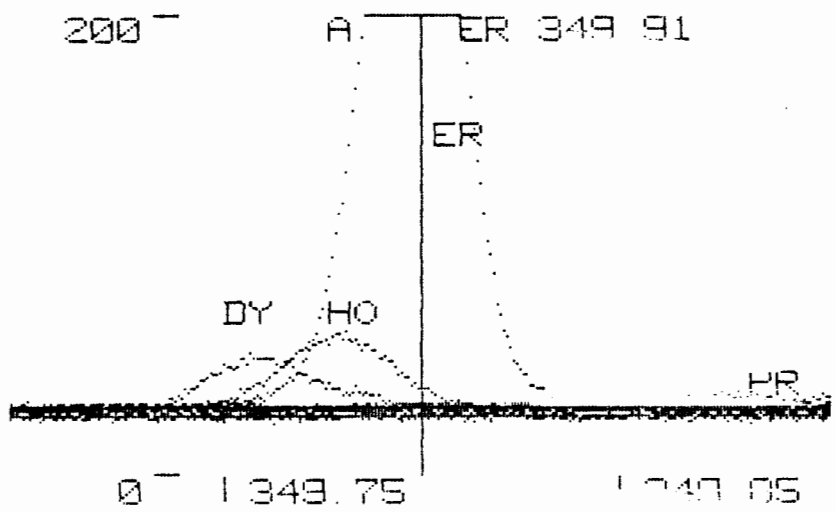

INTERFERENCES FROM REE ON ER.

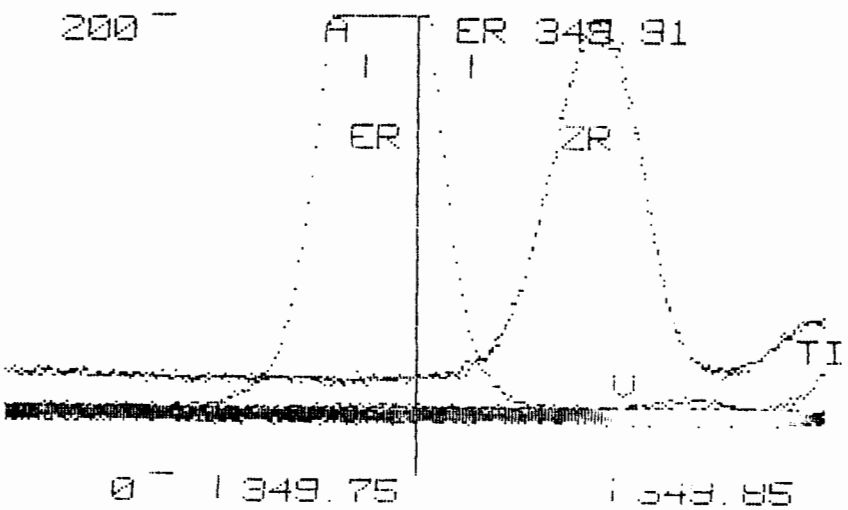

INTERFERENCES FROM NON-REE ON ER.

ERBIUM 323.06 nm

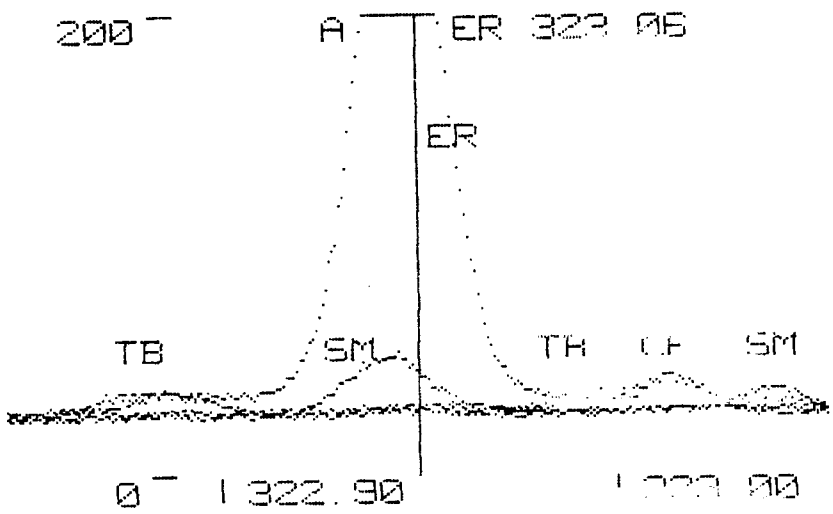

INTERFERENCES FROM REE ON ER.

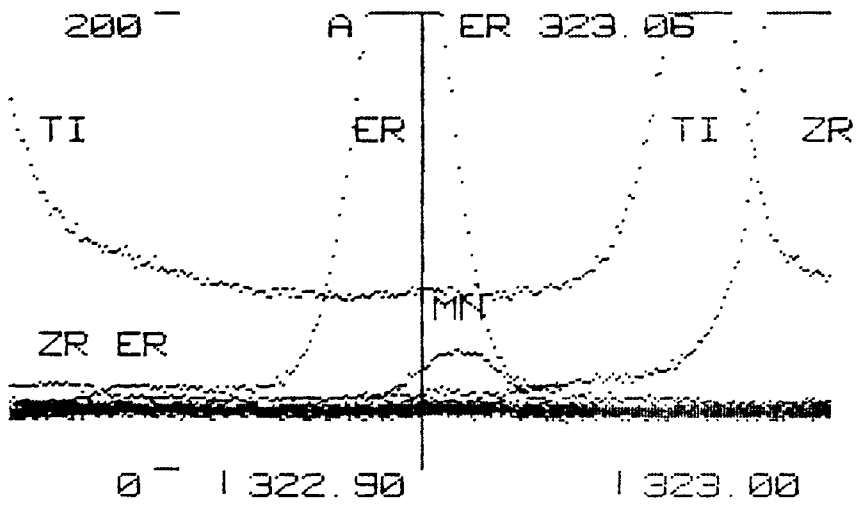

INTERFERENCES FROM NON-REE ON ER.

ERBIUM 326.49 nm

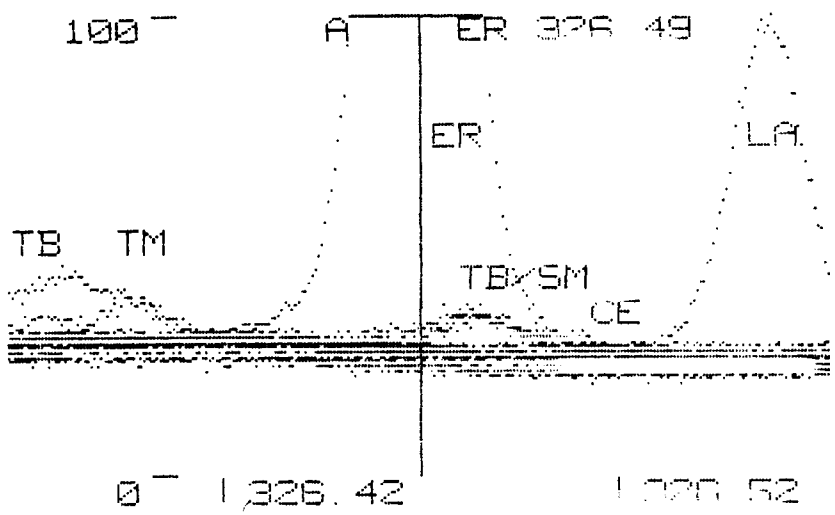

INTERFERENCES FROM REE ON ER.

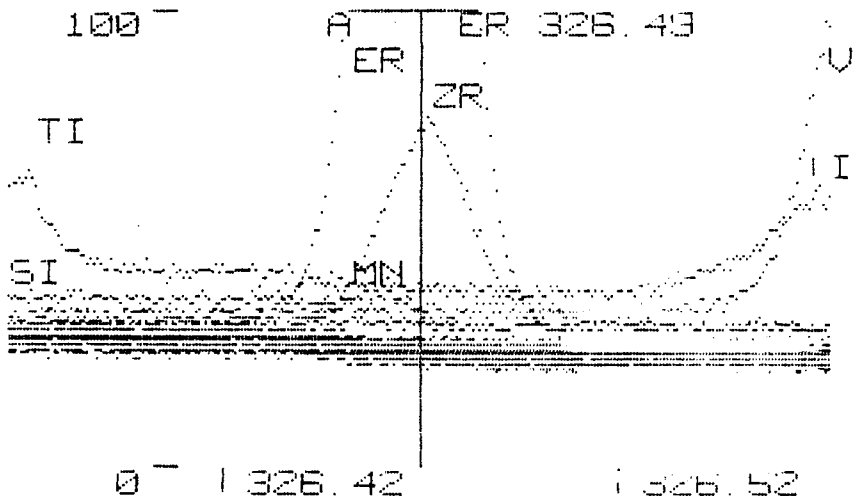

INTERFERENCES FROM V, TI, SI AND ZR CONTINUUM AND MN ON ER.

ERBIUM 337.27 nm

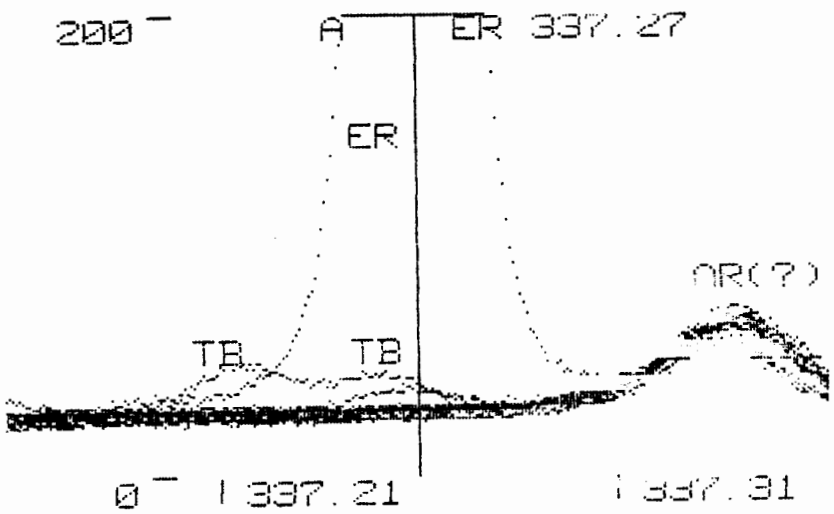

INTERFERENCES FROM REE ON ER.

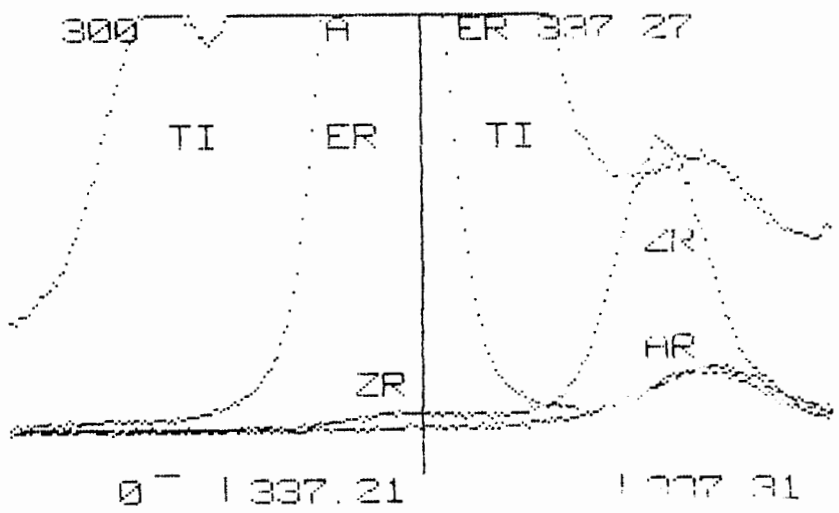

INTERFERENCES FROM TI AND ZR ON ER.

THULIUM 346.22 nm

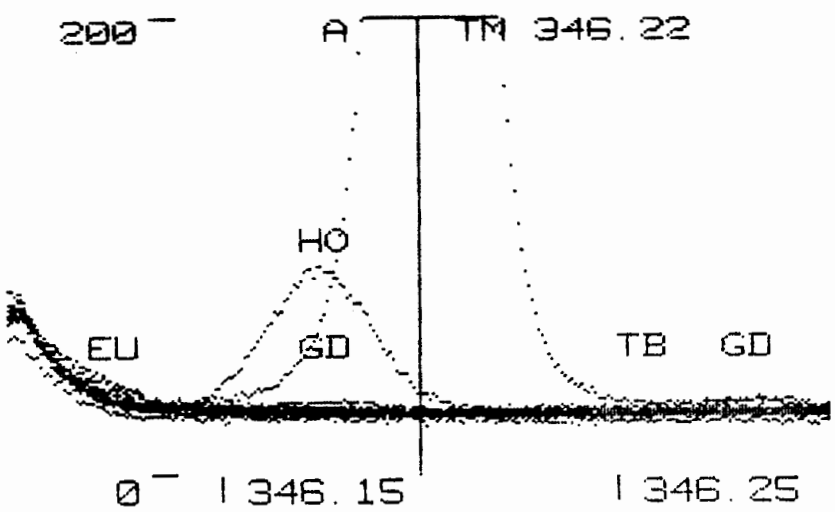

INTERFERENCES FROM REE ON TM.

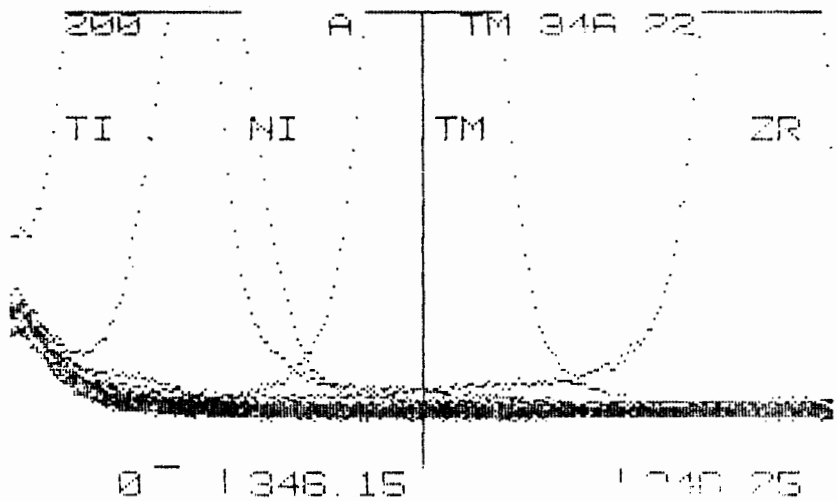

INTERFERENCES FROM NON-REE ON TM.

THULIUM 313.13 nm

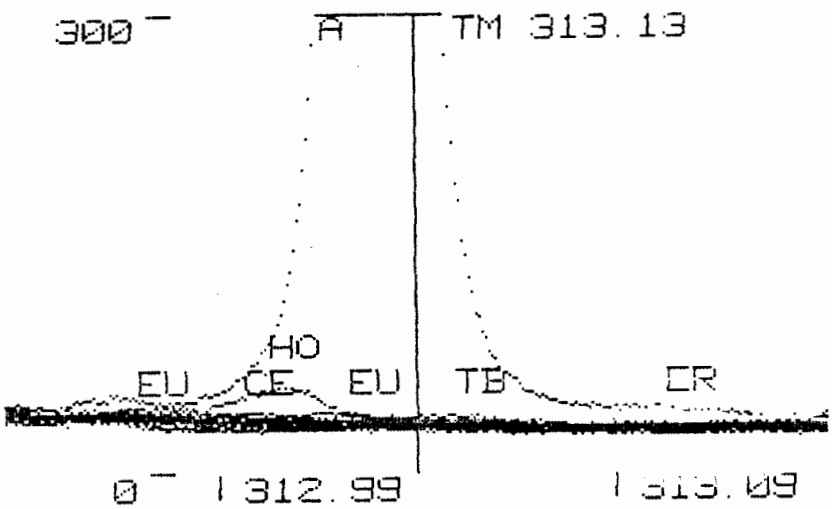

INTERFERENCES FROM REE ON TM.

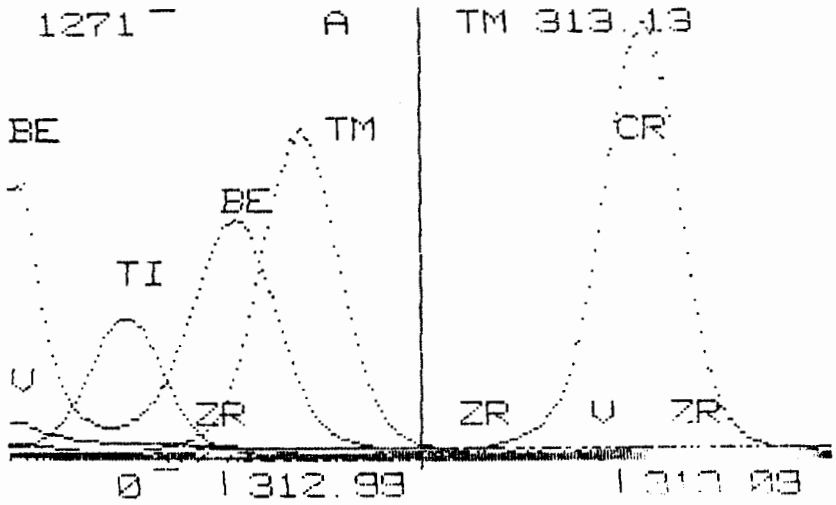

INTERFERENCES FROM NON-REE ON TM, (CONCENTRATION OF BE = 0.5 PPM).

THULIUM 342.15 nm

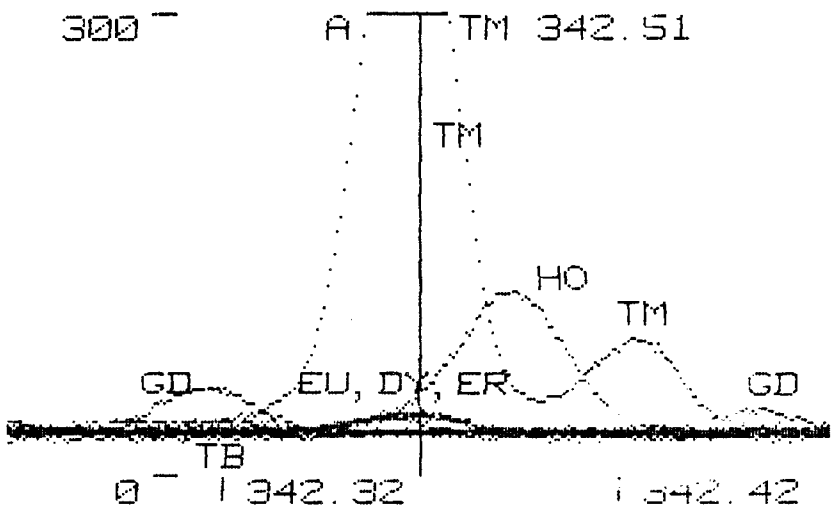

INTERFERENCES FRON REE ON TM.

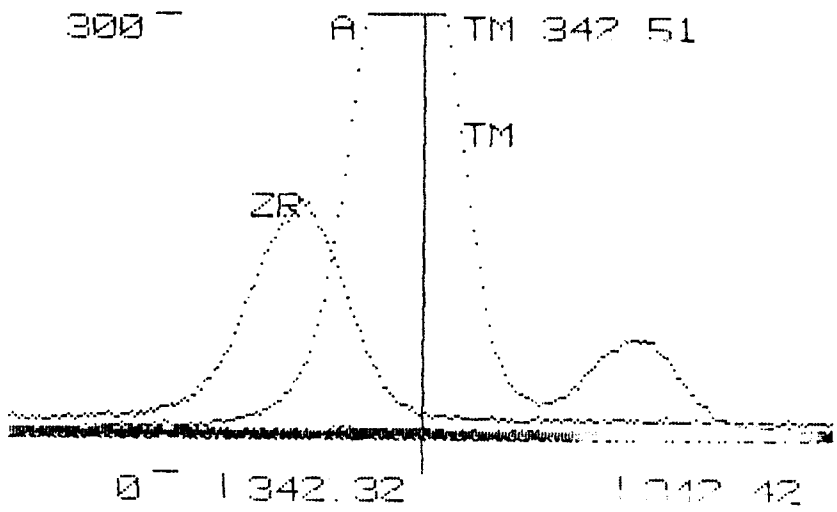

INTERFERENCES FROM NON-REE ON TM.

THULIUM 384.80 nm

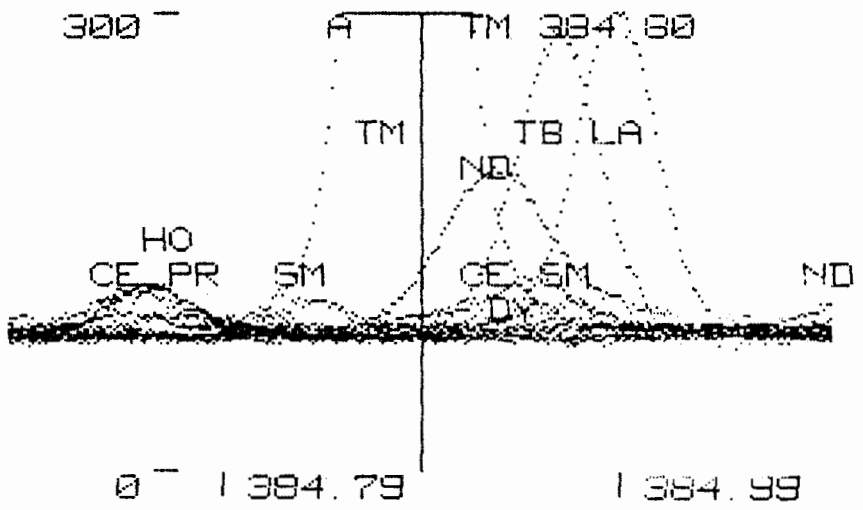

INTERFERENCES FROM REE ON TM.

YTTERBIUM 369.42 nm

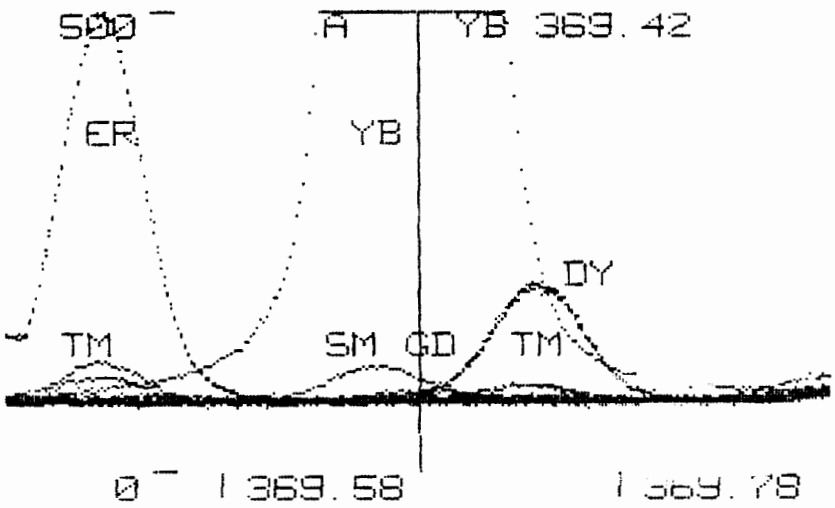

INTERFERENCES FROM REE ON YB.

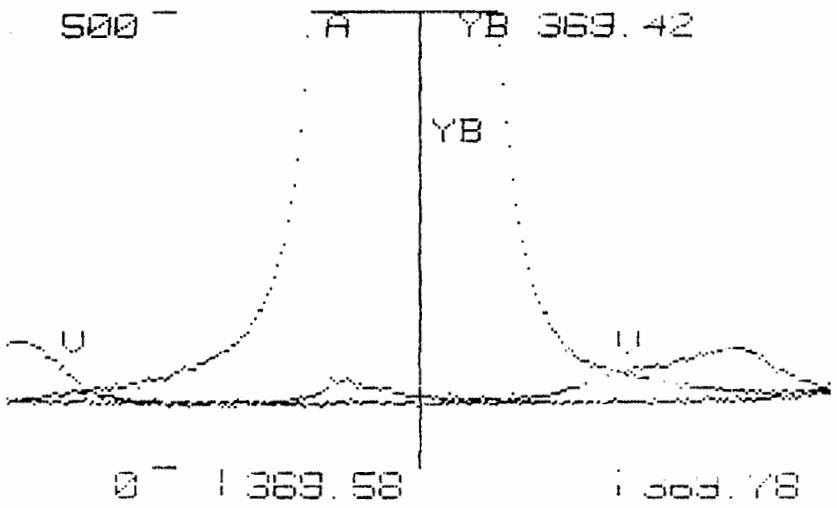

INTERFERENCES FROM NON-REE ON YB.

YTTERBIUM 328.94 nm

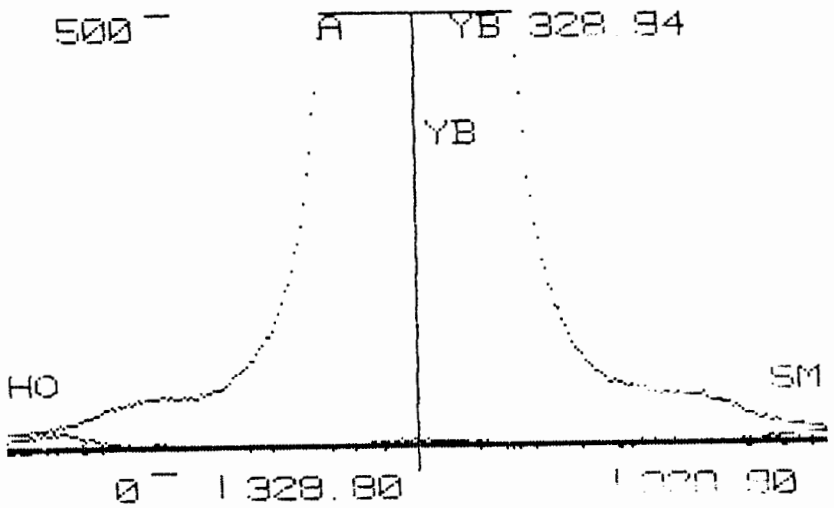

INTERFERENCES FROM REE ON YB.

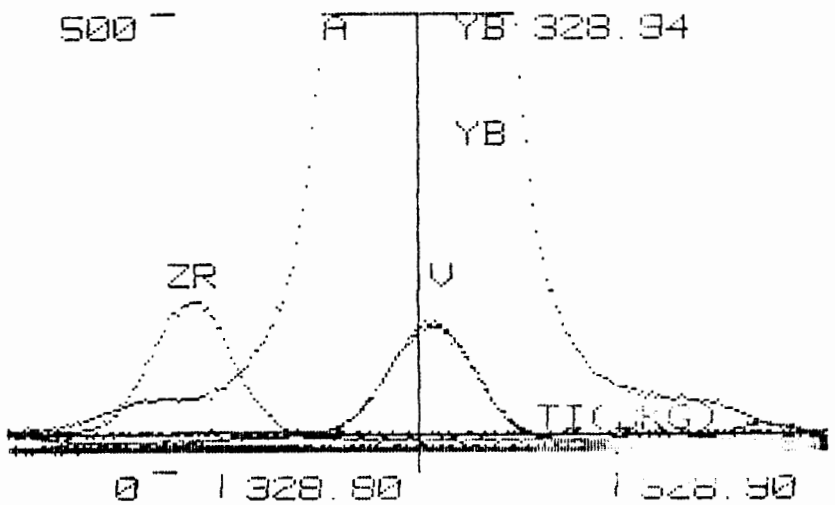

INTERFERENCES FROM NON-REE ON YB.

YTTERBIUM 222.45 nm

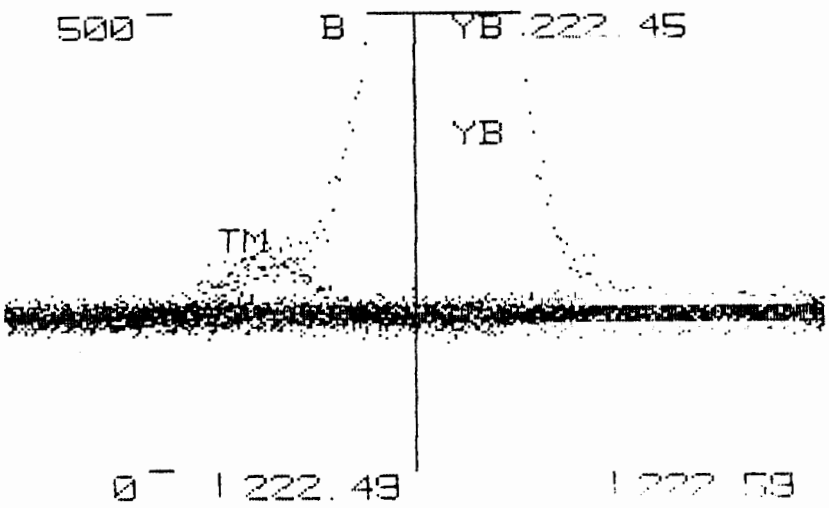

INTERFERENCES FROM REE ON YB.

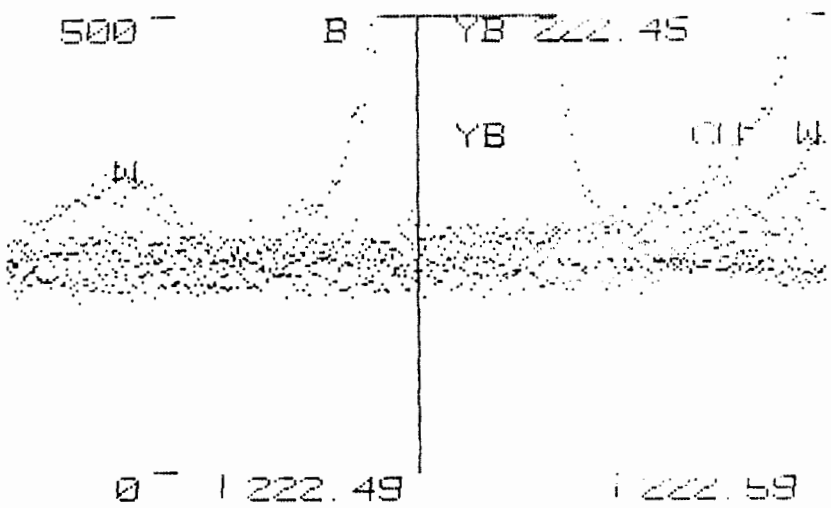

INTERFERENCES FROM NON-REE ON YB.

YTTERBIUM 289.14 nm

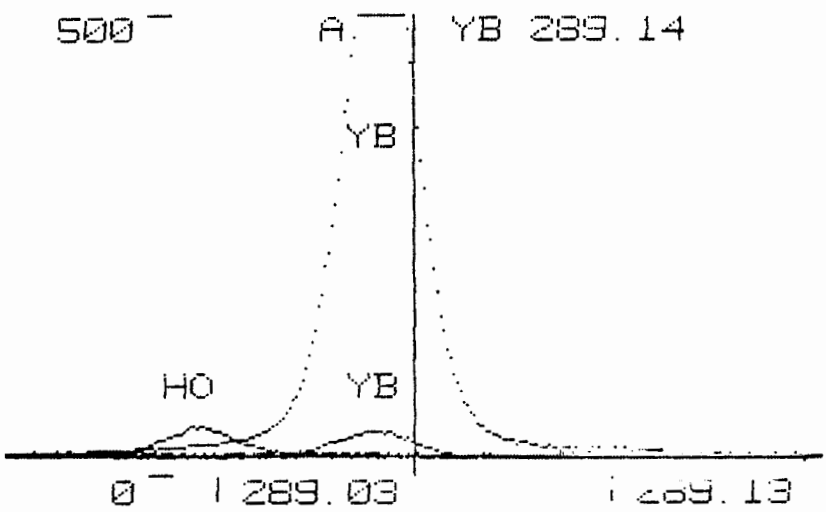

INTERFERENCES FROM REE ON YB.

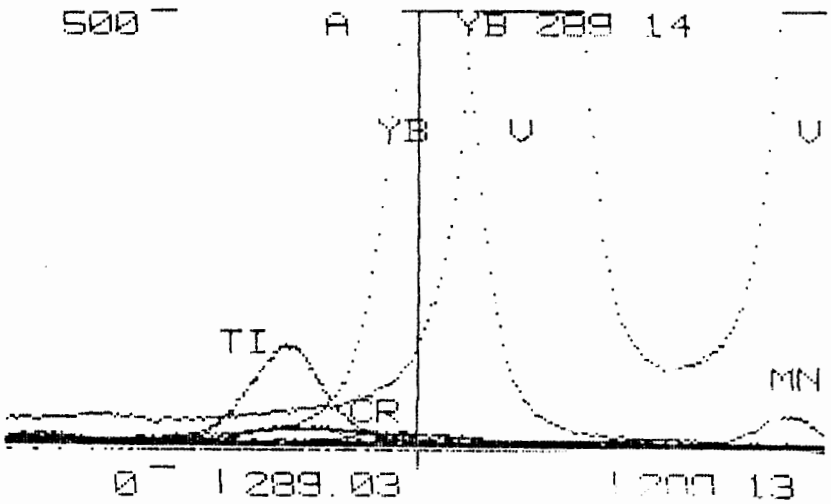

INTERFERENCES FROM NON-REE ON YB.

LUTETIUM 261.54 nm

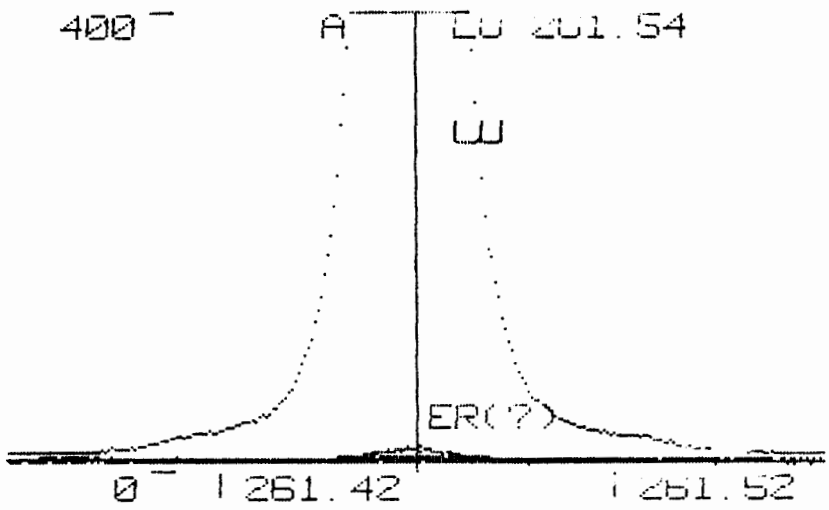

INTERFERENCES FROM REE ON LU.

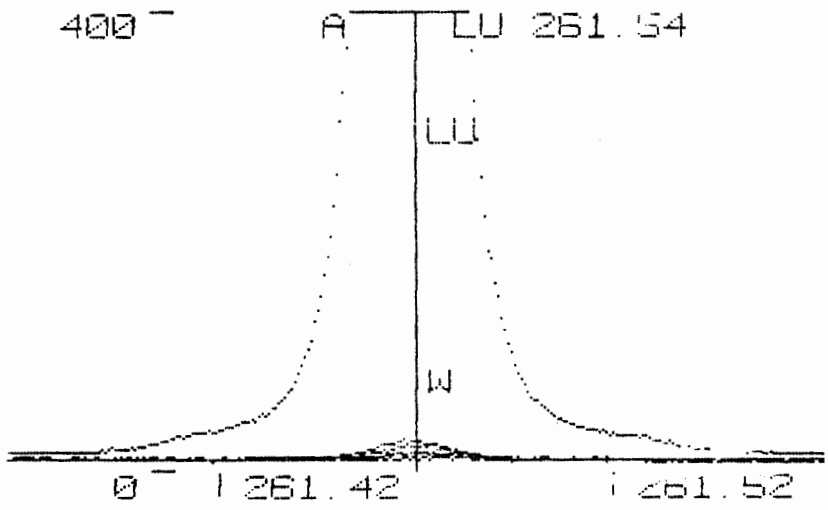

INTERFERENCES FROM NON-REE ON LU

LUTETIUM 219.55 nm

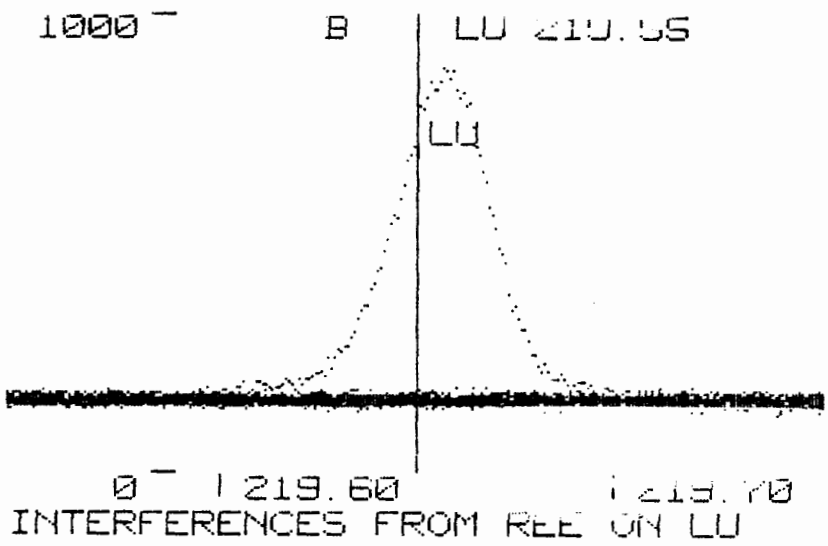

INTERFERENCES FROM REE ON LU.

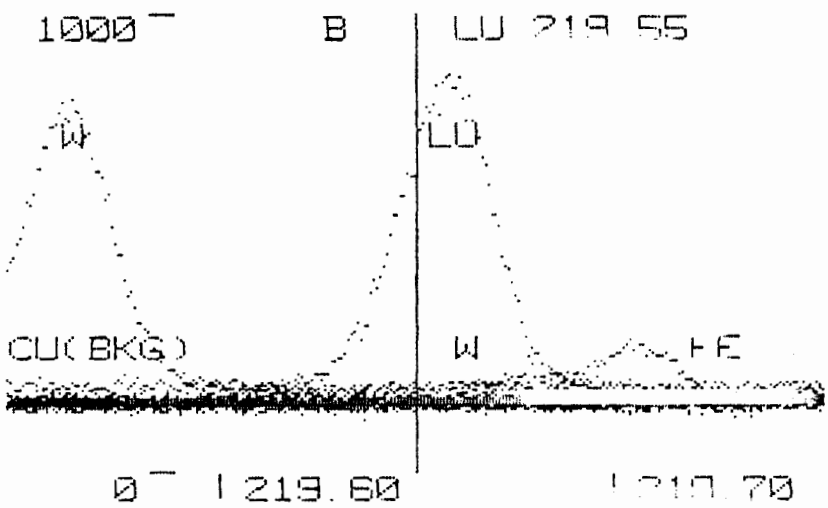

INTERFERENCES FROM NON-REE ON LU.

LUTETIUM 291.14 nm

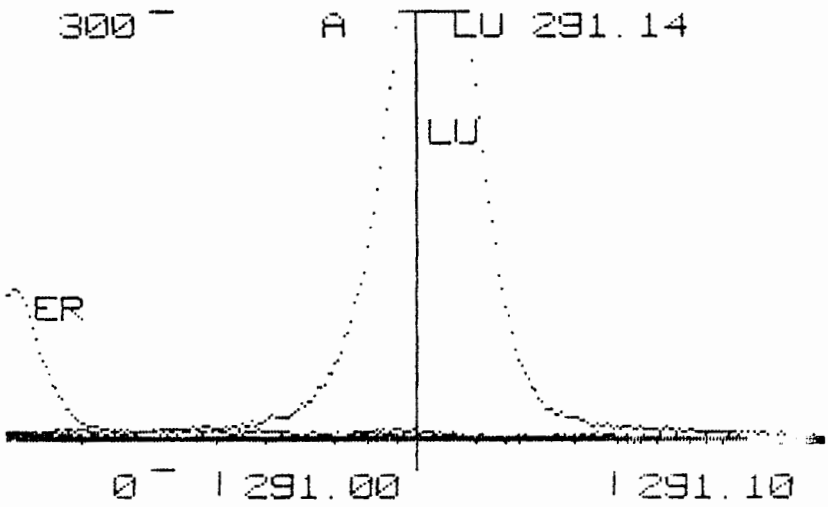

INTERFERENCES FROM REE ON LU.

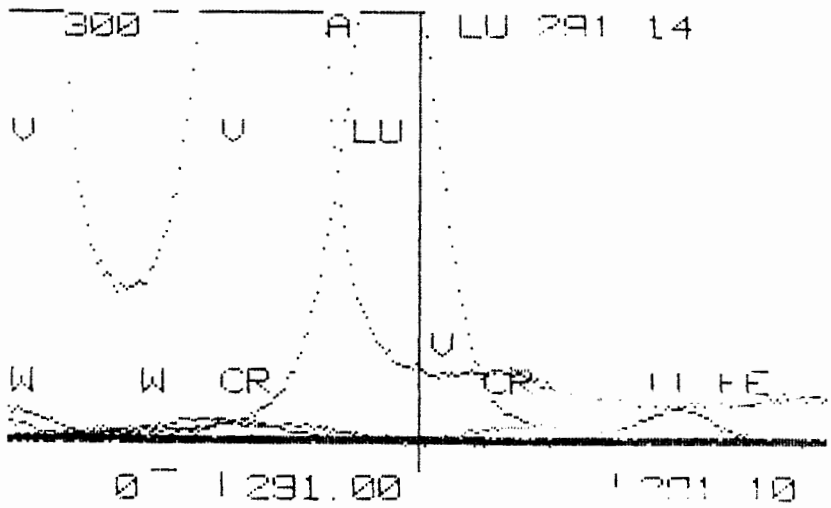

INTERFERENCES FROM NON-REE ON LU.